

AD _____

Grant Number DAMD17-96-1-6189

TITLE: Biology of Somatostatin and Somatostatin Receptors in
Breast Cancer

PRINCIPAL INVESTIGATOR: Dr. Yogesh C. Patel

CONTRACTING ORGANIZATION: McGill University
Montreal, Quebec, Canada H3A1A1

REPORT DATE: September 1998

TYPE OF REPORT: Annual

PREPARED FOR: U.S. Army Medical Research and Materiel Command
Fort Detrick, Maryland 21702-5012

DISTRIBUTION STATEMENT: Approved for public release;
distribution unlimited

The views, opinions and/or findings contained in this report are those of the author(s) and should not be construed as an official Department of the Army position, policy or decision unless so designated by other documentation.

**Reproduced From
Best Available Copy**

DTIC QUALITY INSPECTED 4

REPORT DOCUMENTATION PAGE

Form Approved
OMB No. 0704-0188

Public reporting burden for this collection of information is estimated to average 1 hour per response, including the time for reviewing instructions, searching existing data sources, gathering and maintaining the data needed, and completing and reviewing the collection of information. Send comments regarding this burden estimate or any other aspect of this collection of information, including suggestions for reducing this burden, to Washington Headquarters Services, Directorate for Information Operations and Reports, 1215 Jefferson Davis Highway, Suite 1204, Arlington, VA 22202-4302, and to the Office of Management and Budget, Paperwork Reduction Project (0704-0188), Washington, DC 20503.

1. AGENCY USE ONLY (Leave blank)		2. REPORT DATE September 1998	3. REPORT TYPE AND DATES COVERED Annual (12 Aug 97 - 11 Aug 98)	
4. TITLE AND SUBTITLE Biology of Somatostatin and Somatostatin Receptors in Breast Cancer			5. FUNDING NUMBERS DAMD17-96-1-6189	
6. AUTHOR(S) Dr. Yogesh C. Patel				
7. PERFORMING ORGANIZATION NAME(S) AND ADDRESS(ES) McGill University Montreal, Quebec, Canada H3A1A1			8. PERFORMING ORGANIZATION REPORT NUMBER	
9. SPONSORING/MONITORING AGENCY NAME(S) AND ADDRESS(ES) U.S. Army Medical Research and Materiel Command Fort Detrick, Maryland 21702-5012			10. SPONSORING/MONITORING AGENCY REPORT NUMBER	
11. SUPPLEMENTARY NOTES			19981210 113	
12a. DISTRIBUTION / AVAILABILITY STATEMENT Approved for public release; distribution unlimited			12b. DISTRIBUTION CODE	
13. ABSTRACT (Maximum 200) Fifty additional primary human breast tumor samples were analysed for SSTR1-5 mRNA and shown to be all receptor positive. Mean SSTR mRNA level was the highest for SSTR3 followed by SSTR1, SSTR2, SSTR5, and SSTR4. Statistical analysis showed a negative correlation between SSTR2 and tumor size, a positive correlation between SSTR2 and estrogen receptors (ER), and a trend towards a positive correlation between SSTR2 and progesterone receptor, SSTR1 and ER, SSTR1 and lymph node status, and SSTR3 and tumor grade. Breast cancer cell lines also expressed multiple SSTR subtypes but the level of receptor expression was less than that in solid tumors. A panel of antibodies against hSSTR1-5 was produced which detected all five SSTR antigens by Western blots and immunocytochemistry. Both analyses showed a correlation between receptor subtype expression at the protein level with SSTR mRNA levels. All five SSTRs inhibited tumor cell growth, SSTR3 by triggering apoptosis, and the remaining four subtypes by inducing cytostasis (SSTR5 > SSTR2 > SSTR4 = SSTR1). Both cytostatic and cytotoxic signalling were dependent on G protein-linked activation of phospho-tyrosine phosphatase (SHP1). SSTR3-induced apoptosis led to induction of wt p53, an increase in Bax, and activation of a cation insensitive acidic endonuclease. Cytostasis involved dephosphorylation and activation of pRb and activation of the CDK inhibitor p21. The C-terminal domain of hSSTR5 is crucial for its cytostatic signalling.				
14. SUBJECT TERMS Breast Cancer			15. NUMBER OF PAGES 185	
			16. PRICE CODE	
17. SECURITY CLASSIFICATION OF REPORT Unclassified	18. SECURITY CLASSIFICATION OF THIS PAGE Unclassified	19. SECURITY CLASSIFICATION OF ABSTRACT Unclassified	20. LIMITATION OF ABSTRACT Unlimited	

FOREWORD

Opinions, interpretations, conclusions and recommendations are those of the author and are not necessarily endorsed by the U.S. Army.

____ Where copyrighted material is quoted, permission has been obtained to use such material.

____ Where material from documents designated for limited distribution is quoted, permission has been obtained to use the material.

____ Citations of commercial organizations and trade names in this report do not constitute an official Department of Army endorsement or approval of the products or services of these organizations.


____ In conducting research using animals, the investigator(s) adhered to the "Guide for the Care and Use of Laboratory Animals," prepared by the Committee on Care and use of Laboratory Animals of the Institute of Laboratory Resources, national Research Council (NIH Publication No. 86-23, Revised 1985).

____ For the protection of human subjects, the investigator(s) adhered to policies of applicable Federal Law 45 CFR 46.

____ In conducting research utilizing recombinant DNA technology, the investigator(s) adhered to current guidelines promulgated by the National Institutes of Health.

____ In the conduct of research utilizing recombinant DNA, the investigator(s) adhered to the NIH Guidelines for Research Involving Recombinant DNA Molecules.

____ In the conduct of research involving hazardous organisms, the investigator(s) adhered to the CDC-NIH Guide for Biosafety in Microbiological and Biomedical Laboratories.



PI - Signature

9/10/98

Date

TABLE OF CONTENTS

Front Cover	Page 1
Report Documentation Page SF 298	Page 2
Foreword	Page 3
Table of Contents	Page 4
Introduction	Page 5
Longterm Objectives	Page 6
Details of Progress	Pages 6-12
Conclusions	Page 12-15
Tables	Pages 16-18
Figure Legends	Pages 19-20
Appendix	Page 21

INTRODUCTION

Somatostatin (SST) a peptide hormone is widely produced in the body and acts as an inhibitory regulator of such important cellular functions as neurotransmission, secretion of hormones and growth factors, and cell proliferation (1,2). These actions are mediated by a family of G protein coupled receptors with currently five members termed SSTR1-5. The ability of SST to block hormone secretion led to the application of long acting analogs such as Octreotide (OCT) in the early 1980s, for the treatment of hormone hypersecretion from pancreatic, intestinal, and pituitary tumors. A number of subsequent developments followed which suggested that SST not only inhibited hormone hypersecretion from these tumors, but also caused their shrinkage through an additional antiproliferative effect. The antiproliferative effects of SST have since been demonstrated experimentally both in vivo in DMBA-induced or transplanted rat mammary carcinomas, as well as in cultured cells derived from both endocrine and non-endocrine tumors (pituitary, thyroid, breast, prostate, colon, pancreas, lung, and brain) (1,2). These effects involve cytostatic (cell growth inhibition) and cytotoxic (apoptotic) actions, and are mediated (1) directly by SSTRs present on tumors cells and (2) indirectly via SSTRs present on non-tumor cell targets, to inhibit the secretion of hormones and growth factors which promote tumor growth, inhibit angiogenesis, promote vasoconstriction, and modulate immune cell function. These observations have generated great interest in the oncological properties of SST and led to the approval of multi-center clinical trials by the NSABP (Pittsburgh), and the NCI Canada, to look at the effects of SST with or without tamoxifen (TAM), in stage 1 and stage 2 breast cancer. Patient accrual for these trials began earlier this year, and whilst their outcome will take many years, expectations have already been raised to the point of hysteria in some countries such as Italy over the potential cancer curing properties of drug mixes containing SST (3).

Several SSTR subtypes and signal transduction pathways have been implicated in SST antiproliferation (1,2). A SST sensitive 66 kDa SH2-domain containing protein tyrosine phosphatase (PTP), called SHP-1 (formerly called PTP-1C/HCP/SHP/HCP) which dephosphorylates and inactivates growth factor receptor kinases has been shown to translocate from the cytosol to the plasma membrane upon receptor activation, and to associate with SSTRs. SST also inhibits MAP kinase (MAPK) activity, via PTP-dependent inactivation of raf-1, or through inhibition of guanylate cyclase. Our earlier studies have shown that PTP dependent antiproliferation by SST involves both cytostatic and cytotoxic (apoptosis) actions, and is dose-dependent and subtype-selective (4). Apoptosis occurs only in cycling cells, uniquely via the SSTR3 subtype, and is associated with induction of wild-type p53 and Bax (4). The remaining four SSTRs elicit a cytostatic response by inducing G1 cell cycle arrest due to activation of the retinoblastoma gene product pRb and the cyclin-dependent kinase inhibitor p21 (5). Our studies have shown that whereas apoptosis is triggered at low agonist concentration, (≤ 10 nM), cytostasis is induced at much higher (≥ 25 nM) agonist concentrations. Overall this means that acting via SSTR3, SST will induce apoptosis even when present at low physiological concentrations, whereas it will attenuate the mitogenic signal and trigger growth arrest via SSTR1, 2, 4, 5, only at pharmacological concentrations. The molecular signal in SSTR3, that confers subtype selectivity for apoptosis as well as the downstream pathways for both the cytostatic and cytotoxic actions of SST, are under active investigation in our laboratory

and could involve phosphorylation-dependent modulation of p53, raf-1, MAPK, and other substrates implicated in regulating cell proliferation.

LONG TERM OBJECTIVES

The long term goal of our work remains unchanged from that defined in the original proposal, and will be to **elicit the pattern of expression of the five individual SSTR subtypes in breast tumor, to determine whether their pattern of expression can provide an independent prognostic marker, and whether the SSTRs are modulated by estrogens and antiestrogens . In addition we wish to determine the subtype-selectivity for the antiproliferative effects of SST, as well as the role of PTP, p53, and other downstream effectors, in mediating the cytostatic and cytotoxic effects of SST.** Towards these goals we have made further progress during the second year of the project.

SPECIFIC TASKS PROPOSED FOR YEAR 2:

Dr. Y. C. Patel

- 1) RT-PCR analysis of SSTR1-5 in breast tumor
- 2) *In situ* hybridization analysis of SSTR1-5 mRNA in breast tumor
- 3) Immunocytochemical analysis of SSTR1-5 in tumor samples
- 4) Anti receptor blockade experiments
- 5) Antisense knockout experiments
- 6) Regulation of SSTR1-5 by estrogens/tamoxifen

Dr. C. B. Srikant

- 1) Studies correlating SSTR binding with PTP-1C regulation and growth inhibition
- 2) Studies of subtype selectivity for PTP-1C association in CHO-K1 and COS-7 cells
- 3) Studies of subtype selectivity for apoptosis in CHO-K and COS-7 cells
- 4) PTP-1C involvement in apoptosis

DETAILS OF PROGRESS

Expression of SSTR1-5 mRNA in Human Breast Cancer

Since there are 5 known SSTR subtypes, and since drugs like OCT target only three of these (SSTR2,3,5), there is great interest in knowing the pattern of expression of SSTRs in tumors such as breast cancer, which subtypes mediate the antiproliferative responses, whether they involve cytostatic or cytotoxic effects, whether receptor expression correlates with known tumor markers, or whether it can provide an independent prognostic index. 15-66% of primary human breast tumors

have been reported to be SSTR positive by in vitro binding analysis, and 75% to be positive by in vivo receptor imaging with an indium labelled OCT analog (6-8). Since there are no pure SST agonists currently available for any of the individual SSTR subtypes however, such binding analyses using standard radioligands do not tell us about the pattern of expression of the separate SSTR subtypes. Expression of SSTRs at the mRNA level has been reported by three different groups (including our own) with results that are widely divergent probably because of methodological differences (9-11). For instance, Vikić-Topić et al., used RT-PCR (without southern blots) for analysing SSTR1-4 (but not SSTR5) in 44 primary breast cancers (9). They found SSTR2 in all but one sample, with lesser expression of transcripts for SSTR1 > SSTR3 > SSTR4 (9). Evans et al., analysed 51 breast carcinomas, also by RT-PCR, but with southern blots and found ubiquitous expression of SSTR2 (11). SSTR5 was expressed in 30% of tumors but there was negligible expression of SSTR1, 3, 4, (2-12% of tumors). The pattern of SSTR expression in both studies was independent of patient age, histological grade and levels of estrogen (ER) and progesterone receptors (PR).

During the year we completed a detailed quantitative analysis of SSTR1-5 mRNA by RT-PCR in an additional batch of 50 breast tumor samples obtained from the Manitoba, Breast Tumor Bank. All were ductal NOS carcinomas of mixed grades and different levels of ER and PR. We processed these samples as a single batch immediately upon receipt, with minimal storage time using quantitative RT-PCR methodology, that we have modified and improved during the past year. The data were accordingly analysed separately and not pooled with our earlier analyses of 90 tumors which had been processed in several batches over a period of time with methodology that was still evolving. As in our previous analysis as well as in the published reports, all samples were positive for SSTR mRNA (Figure 1 and Table 1). 33% were positive for all five SSTR mRNA, 19% expressed four subtypes, 41% expressed three SSTR subtypes, and 7% were positive for two subtypes (Table 1). Thus all tumors in this series expressed more than one SSTR isoform. Of the individual subtypes, SSTR2 was ubiquitously expressed, SSTR3 occurred in 92% of tumors, SSTR1 in 81%, SSTR5 in 58%, and SSTR4 in 50 % of samples. Mean SSTR mRNA level (relative to actin mRNA), was the highest for SSTR3 (2.29 ± 0.33), followed by SSTR1 (0.97 ± 0.14), SSTR2 (0.56 ± 0.06), SSTR5 (0.43 ± 0.06), SSTR4 (0.39 ± 0.06). The finding of high level expression of SSTR3 in breast tumors is exciting, since we have shown earlier that this subtype uniquely mediates SST induced apoptotic cell death in SSTRs transfected CHO-K1 cells (4). The results were statistically analysed by Dr. Michael Edwards, Department of Epidemiology and Biostatistics, McGill University, who found several potential pairwise Pearson correlations as follows (Fig. 2):

- 1) A positive correlation between SSTR2 and ER ($r, 0.31, p < 0.05$).
- 2) A negative correlation between SSTR2 and tumor size ($r, -0.33, p < 0.04$).
- 3) A trend towards a positive correlation between SSTR2 and PR ($r, 0.28, p < 0.07$).
- 4) A trend towards a positive correlation between SSTR1 and ER ($r, 0.26, p < 0.08$).
- 5) A trend towards a negative correlation between SSTR1 and lymph node status (yes or no), ($r, -0.27, p < 0.07$).
- 6) A positive trend between SSTR3 and tumor grade ($r, 0.24, p < 0.1$).

Transformation of the variables to natural logarithms and squares, strengthened the correlations and helped to further define these relationships (Fig. 2). The positive trend between SSTR2 and ER was also noted in the 90 samples that we had analysed previously, but the other relationships were new. The results from the present samples also differed in other regards from our earlier analyses especially in the incidence and level of expression of SSTR5. Whilst our improved RT-PCR methodology is one explanation for these differences, another and more important one comes from recently acquired evidence, that some of the earlier batches shipped from Manitoba, may not have been optimally preserved, leading to RNA degradation. The storage time of the samples as well as their processing in several different batches may also have contributed to the variance. Rather than waste time to sort out the reliability of SSTR mRNA analyses in the different previous batches, we have decided to keep the earlier results separate from those of the recent batch to maintain statistical purity. In general, the trends that we are seeing now between SSTR expression and the various tumor markers are exciting and need to be confirmed with a larger sample size. Towards this end, we have already begun an analysis of an additional 50 samples that are being processed exactly like the previous batch which should be completed over the next three months and which will provide the necessary statistical power to complete this task.

Expression of SSTR 1-5 mRNA in Breast Cancer Cell Lines

Using the identical quantitative RT-PCR methodology for characterizing SSTR expression in human breast tumor samples, we analysed ER⁺, and ER⁻, human breast cancer cell lines for SSTR mRNA expression. Like the solid tumors, the cell lines express multiple SSTR subtypes, with no obvious distinction between ER⁺, and ER⁻ cell lines (Fig. 1, Table 2). There were however, interesting differences in that the overall level of SSTR expression in cell lines was less than that in the solid tumors. SSTR3, the subtype which uniquely induces apoptosis, was well expressed in the solid tumors, but relatively poorly expressed in the cell lines. SSTR5, a weak subtype in solid tumors was relatively better expressed in the cell lines. These results indicate that the various breast cancer cell lines, although useful for studying SSTR biology, do not necessarily reflect endogenous tumor SSTR expression or function. A likely explanation for the difference is the probable induction of SSTR expression in solid tumors by circulating hormones, or locally by growth factors, cytokines, and other mediators produced from peritumoral structures, eg. stroma, blood vessels and immune cells. This is an important new lead which we are pursuing further.

Expression of SSTR1-5 Protein by Immunohistochemistry

A prime target of our work has been to characterize receptor subtype expression directly at the protein level and towards this goal we have made a major investment in raising subtype-selective antibodies suitable for immunohistochemistry, and Western blots (12). At the time of submission of this proposal, we had produced a panel of anti-peptide rabbit polyclonal antibodies which detected both rat and human receptors. These antibodies worked well and continue to work well in immunocytochemistry, but were of low titre and except for one (SSTR2), did not work in Western blots which, limited their usefulness (13-15). Because of this, we have generated a second panel of antibodies, to common rat and human sequences which are of higher titre and suitable for both immunocytochemistry and Western blot analysis (12). These antibodies were affinity purified and shown to detect predominant, single, SSTR protein bands of 44-60 kDa, by Western blots of rat

brain cortex (Fig. 3), and human fetal brain (Fig. 4). The affinity purified antibodies were also characterized for immunohistochemistry by confocal immunofluorescence, and immunoperoxidase in normal human islet cells and rat aorta (12,15). We have completed immunoperoxidase immunohistochemistry of all five receptors in 20 of the recent 50 Manitoba Breast Tumor Bank samples that we have processed concurrently for mRNA by RT-PCR (eg. Figs. 5, 6). In general, there is a correlation between receptor subtype expression at the mRNA and protein levels, although the relationship is not an absolute one. Tumor sections, display receptor immunoreactivity both in tumor cells and in peritumoral structures, especially blood vessels, where we have found a rich expression of SSTR2 and SSTR1. Dr. Peter Watson, Pathologist, University of Manitoba, is critically examining immunohistochemical sections for SSTR1-5, in the twenty tumor samples. Frozen fixed section were received from Winnipeg, processed for immunocytochemistry in Montreal, and returned blinded to Dr. Watson. In this way, we hope to have an objective back to back comparison of immunohistochemistry with mRNA. These studies are still ongoing, having been delayed on account of our long distance pathology collaboration. While we await the results of the precise immunohistochemical analysis, we have begun Western blots of breast tumor cell lines, for a more quantitative assessment of receptor subtype protein expression (Fig. 7). Because of differences in the level of SSTR expression in tumor cell lines, and solid tumors, we plan to analyse 5-10 tumors by Western blots and will need to collect separate large tumor samples within our Hospital for this purpose, since the amount of tissue available from the Manitoba, Breast Tumor Bank, will not be sufficient for these analyses. Finally, our originally proposed plan to study SSTR mRNA expression by *in situ* hybridization, has been cancelled (as indicated in our year 1 report) in view of our success with immunocytochemistry, which will be a more direct approach for delineating the cellular expression of SSTRs in tumor and peritumoral structures.

Antisense and Immunoneutralization Experiments

We have already made substantial progress in elucidating subtype-selectivity for antiproliferation using CHO-K1 cells individually transfected with the five receptor subtypes. We have shown that all five subtypes are capable of inhibiting cell growth, SSTR1, 2, 4, 5, being cytostatic whereas, SSTR3 uniquely induces apoptosis (1,2,4,5). As planned for year two, we have now begun experiments with MCF-7 (and other breast cancer cell lines), which express several endogenous SSTR subtypes to look at the effect of individual antisense receptor knockout on cell growth. In preliminary experiments, we have shown a significant decrease in membrane SSTR1 and SSTR2 expression (by binding analysis and immunocytochemistry) in MCF-7 cells, treated with 10-20 μ M antisense oligonucleotides. The effect on cell proliferation however, has been variable. These are difficult experiments which we will have to carefully master in year three and year four as planned. The variable effects of SST on cell proliferation of MCF-7, and several other cell lines tested is a significant problem in our hands at the moment. Another difficulty is, that although MCF-7 cells display SST induced apoptosis, they show negligible expression of SSTR3 in the basal state. Whether SSTR3 is induced in these cells by SST, or whether these cells express another as yet unknown SSTR subtype which triggers apoptosis, are questions that we are actively pursuing.

Regulation of SSTR1-5 by Estrogen/Tamoxifen

The original experiments proposed for this task, were to look at SSTR1-5 mRNA regulation

by estrogens and TAM, in several ER⁺ cell lines. We have already shown that E2 (10^{-7} - 10^{-9} M), produces dose dependent downregulation of SSTR1 mRNA and upregulation of SSTR3 mRNA in MCF7 cells. In the course of these studies however, 3 recent reports described the effect of E2 on SSTR mRNA regulation in human breast cancer cells, and in rat pituitary with results there are contradictory (16-18). Using ribonuclease protection assay for mRNA measurement, Xu et al studied five different breast cancer cell lines and found SSTR2 expression in three, SSTR5 expression in one, but no other subtypes in any of the cell lines (16). This differs markedly from our findings by RT-PCR in the same cell lines (Table 2). E2 treatment upregulated SSTR2 expression (16). In contrast, in transplantable rat prolactin secreting pituitary tumor cells, SSTR2, and SSTR3 expression are both induced *in vitro* by E2 treatment (17), and in the rat pituitary which expresses all five SSTRs, E2 upregulates SSTR2 mRNA and downregulates SSTR5 mRNA (18). These reports have created enormous confusion with respect to E2 regulation of SSTR subtypes. Accordingly, we have extended our original plans to investigate E2 regulation of SSTR mRNA in breast cancer cell lines by RT-PCR analysis alone, to a more complete study of the *in vivo* and *in vitro* effects of E2 on SSTR1-5 regulation in normal tissues and in breast tumor cell lines as determined, both by mRNA (RT-PCR) and protein (Western blots, binding assays) analysis.

Structure Function and Regulation of SSTR3

These are new experiments not originally proposed which we have initiated because they are important to our longterm objectives. They arose from our observation that SSTR3 is a prominent subtype in primary breast tumor samples and that it is the only subtype which mediates apoptosis (4). It is thus important in the context of our program to characterize the regulation of SSTR3 gene and the molecular signals in the receptor responsible for triggering apoptosis. To get a handle on the regulation of SSTR3, we cloned and sequenced the 5' flanking promoter region of this gene. We previously screened a human λ EML3 library and isolated a λ phage containing the hSSTR3 coding region. We performed restriction mapping analysis of the clone, subcloned various genomic DNA fragments and sequenced a 5 kb DNA sequence, 5' to the ATG codon (Fig. 8). Promoter scan analysis showed that the hSSTR3 gene, like the other four hSSTR genes which have been sequenced so far is a TATA-less gene. Several potential cis regulatory elements for SP1, Ebox, NF κ B, IRF2, Pit-1, SRF, and CRE elements were identified (Fig. 8). The sequence has been deposited in Genbank (accession # AF068757). Studies are underway to map the transcription start site and to investigate promoter function with promoter-CAT constructs. Our second project with hSSTR3 is aimed at investigating the role of the cytoplasmic C-tail of the receptor in inducing apoptosis. Interestingly, SSTR3 is the only member of this family whose cytoplasmic tail does not possess a palmitoylation anchor, shown in other receptors to be important in receptor function (1). We have created by PCR three receptor mutants as follow:

- 1) Deletion of hSSTR3 C-tail to see if it blocks apoptosis.
- 2) Introduction of a palmitoylation motif in the hSSTR3 C-tail to see whether it attenuates apoptosis.
- 3) Chimeric hSSTR3/hSSTR5 receptors substituting the C-tail, TM domains 6 and 7 and the third intracellular loop of hSSTR5 with the corresponding region of hSSTR3, to see if such a swap will confer the ability to induce apoptosis by hSSTR5.

These three mutants have been stably transfected in HEK cells and will be tested with respect to their ability to induce apoptosis with SST application. If it turns out that the C-tail confers apoptosis then we will conduct detailed mutagenesis experiments to identify the specific residues involved.

SSTR Subtype Selectivity For Antiproliferation: The Role of SHP1 and Other Downstream Effectors in Mediating Cytotoxic and Cytostatic Signalling

We have investigated the mechanism and the nature of the antiproliferative signalling of SST leading to cytostasis (cell cycle arrest) or apoptosis using as models breast cancer cell lines and heterologous cells expressing each of the five hSSTR subtypes. Earlier studies had reported that OCT inhibits the growth of MCF-7 cells by inducing either apoptosis or growth arrest. Since these cells express several SSTR subtypes, we set out to resolve these contradictory responses and specifically to determine whether receptor subtype selectivity could account for either apoptosis or cell cycle arrest. We demonstrated that OCT elicits cytotoxic responses in these cells leading to apoptosis in a SHP1 dependent manner (19). This was associated with a rapid, time-dependent induction of *wt p53* and an increase in Bax. These changes coupled with the lack of induction of pRb and p21 (which negatively regulates G1-s transition) suggested that its cytotoxic action occurs in cycling cells. Additionally, we demonstrated that OCT-induced DNA fragmentation in this cell line is due to selective activation of a cation insensitive acidic endonuclease (19).

Using CHO-K1 cells individually expressing the five hSSTR subtypes, we had earlier reported that cytotoxicity is induced solely via SSTR3 (4). In a follow-up study, we reported that OCT-induced apoptosis is associated with intracellular acidification and activation of a divalent cation insensitive acidic endonuclease (20). The intracellular pH of cells undergoing apoptosis was 0.9 pH units lower than that of control cells (20). The effect of OCT on endonuclease and pH was inhibited by orthovanadate as well as by pretreatment with pertussis toxin suggesting that hSSTR3 initiated cytotoxic signalling is PTP-mediated and is G-protein dependent. These findings indicate that intracellular acidification and activation of acidic endonuclease mediate *wt p53* associated apoptosis signalled by hormones acting via G protein coupled receptors. We have now completed studies demonstrating that unlike hSSTR3, the remaining four hSSTR subtypes induce cytostatic signalling that triggers growth inhibition (5). In CHO-K1 cells stably expressing hSSTR1,2,4 and 5, we showed that SST triggers G1 cell cycle arrest. This effect was preceded by the induction of pRb and the cyclin-dependent kinase inhibitor p21^{waf1/cip1}. The relative efficacy of the receptors to initiate cytostatic signalling was hSSTR5 > hSSTR2 > hSSTR4 = hSSTR1. Western blot analysis of hSSTR5 expressing cells revealed an increase in the hypophosphorylated form of Rb following agonist treatment. hSSTR initiated induction of Rb and G_i arrest was inhibited by pertussis toxin pretreatment of the cells and by sodium orthovanadate suggesting that hSSTR5 initiated cytostatic signalling is G-protein-dependent and PTP-mediated. OCT did not stimulate membrane associated PTP activity *in vitro* in hSSTR5 expressing cells but induced the translocation of cytosolic PTP to the membrane in cells pretreated with the peptide (5). Finally, in structure-function studies of the cytoplasmic C-tail of hSSTR5, we showed that progressive deletion of the C-tail of this receptor leads to a progressive loss of its capacity for antiproliferative signalling providing the first evidence that the C-terminal domain of hSSTR5 is crucial for its cytostatic signalling (5).

In order to definitively establish the requirement of SHP1 in subtype selective SSTR-mediated antiproliferative signalling, we have stably overexpressed wild type SHP1 or its catalytically inactive mutant SHP1C455S in CHO-K1 cells expressing either hSSTR3 or hSSTR5. The transfected cells were selected on the basis of resistance to hygromycin in G418 containing medium. The overexpression of SHP1 and its mutant protein has been confirmed by immunoblot analysis and measurement of phosphatase activity. We have shown that hSSTR3 induced apoptosis is increased in cells overexpressing the active SHP1 and is abolished in cells expressing the inactive mutant protein (Fig. 9). Detailed studies are underway to delineate the temporal sequence of events in SHP1-dependent signalling of apoptosis via hSSTR3. Likewise the cytostatic signalling mediated through hSSTR5 was also found to be SHP1-dependent (Fig. 10). hSSTR5 signalled increase in Rb was greater in SHP1 transfected cells compared to control cells. SST was unable to induce Rb in cells expressing hSSTR5 and SHP-1C455S.

These results further confirm the potential therapeutic utility of SST analogs in oncology and have taken us a step further towards the possible treatment of SSTR positive breast cancer cells expressing *wt p53*. Our finding that cytotoxic signalling occurs only via hSSTR3 at low agonist doses compared to cytostatic signalling through other subtypes at higher agonist concentrations, coupled with the finding of a variable pattern of expression of the different hSSTR subtypes in breast tumors predict a varied outcome to SST pharmacotherapy depending on the relative abundance of SSTRs and of the various mediators of apoptosis and cell cycle progression.

CONCLUSIONS:

- 1) Further analysis of primary human breast tumor samples for SSTR mRNA expression by a modified quantitative RT-PCR method confirms SSTR positivity for all tumors in this additional series. Mean SSTR mRNA level was the highest for SSTR3 followed by SSTR1, SSTR2, SSTR5, and SSTR4. Primary tumors thus display good expression of the SSTR subtypes, e.g. SSTR3, SSTR2 which bind the octapeptide SST analog OCT that is currently used in breast cancer trials. The finding of high level expression of SSTR3 in primary tumors is exciting since this is the subtype which has been previously shown by us to uniquely induce apoptotic cell death.
- 2) Statistical analysis shows a positive correlation between SSTR2 and ER, a negative correlation between SSTR2 and tumor size, a trend towards a positive correlation between SSTR2 and PR, a trend towards a positive correlation between SSTR1 and ER, a trend towards a negative correlation between SSTR1 and lymph node status, and a positive trend between SSTR3 and tumor grade.
- 3) Like solid tumors, breast cancer cell lines express multiple SSTR subtypes with no obvious distinction between ER⁺ and ER⁻ cell lines. The overall level of SSTR expression in cell lines is less than that in solid tumors. A likely explanation for this difference is the probable induction of SSTR expression in solid tumors by circulating hormones or locally by growth factors, cytokines, and other mediators produced from peritumoral structures, e.g. stroma, blood vessels and immune cells).

- 4) Western blot analysis of tumor cell lines for SSTR1-5 protein expression shows predominant single bands ranging in size from 48-60 kDa whose presence correlates with SSTR expression by mRNA analysis. Immunocytochemical analysis of primary tumor samples also shows a correlation between receptor subtype expression at the mRNA and protein levels although the relationship is not an absolute one. Tumor sections display SSTR immunoreactivity both in tumor cells and in peritumoral structures especially blood vessels which are rich in SSTR2 and SSTR5.
- 5) Sequence analysis of the hSSTR3 promoter region reveals a TATA less gene containing several potential consensus sites for SP1, Ebox, and NFKappa E2, IRF2, Pit-1, SRF and CRE elements.
- 6) SST induces a cytotoxic response in MCF-7 cells leading to apoptosis in a SHP1-dependent manner associated with rapid time-dependent induction of *wt p53* and an increase in Bax. SST-induced DNA fragmentation in this cell line is due to selective activation of a cation insensitive acidic endonuclease. Likewise, the SST-induced apoptosis which occurs in CHO-K1 cells transfected with the SSTR3 subtype is associated with intracellular acidification and activation of a divalent cation insensitive acidic endonuclease. This effect is PTP-mediated and is G protein dependent. Whilst SSTR3 is the only subtype that induces apoptosis, the remaining four SSTRs induce cytostatic signalling by triggering G1 cell cycle arrest with relative potency SSTR5 > SSTR2 > SSTR4 = SSTR1. Like apoptosis, this effect is also G-protein dependent and PTP-mediated. It involves the dephosphorylation and activation of pRb and the activation of the cyclin-dependent kinase inhibitor p21.
- 7) SST activates PTP in CHO-K1 cells expressing SSTR5 by inducing the translocation of cytosolic enzyme to the membrane rather than direct activation of membrane associated PTP. Progressive deletion of the C-tail of hSSTR5 in structure-function studies has shown that the C-terminal domain of this receptor is crucial for its cytostatic signalling.
- 8) Overexpression of wild type SHP1 or its catalytically inactive mutant in CHO-K1 cells expressing either hSSTR3 or hSSTR5 has shown that apoptosis via hSSTR3 as well as cytostatic signalling mediated through hSSTR5 are both SHP1-dependent.

REFERENCES:

- 1) Patel, Y.C. and C.B. Srikant. Somatostatin receptors. Trends in Endocrinology and Metabolism 8:398-405, 1997.
- 2) Patel, Y.C. Basic aspects of somatostatin receptors. In: Advances in Molecular and Cellular Endocrinology, D. LeRoith (ed), JAI Press, Greenwich, CT., 1998 (in press).
- 3) Editorial: Controversial cancer drug wins local approval in Italy. Nature 391:217, 1998.
- 4) Sharma, K., Y.C. Patel, and C.B. Srikant. Subtype selective induction of p53-dependent apoptosis but not cell cycle arrest by human somatostatin receptor 3. Molecular Endocrinology 10:1688-1696, 1996.
- 5) Sharma, K., Y.C. Patel, and C.B. Srikant. C-terminal region of human somatostatin receptor 5 is required for induction of Rb and G1 cell cycle arrest. Molecular Endocrinology 1998 (in press).

- 6) Foekens, J.A., H. Portengen, W.L.J. van Putten, A.M.A.C. Trapman, J-C Reubi, J. Alexieva-Figusch, and J.G.M. Klijn. Prognostic value of receptors for insulin-like growth factor 1, somatostatin, and epidermal growth factor in human breast cancer. *Cancer Research* 49:7002-7009, 1989.
- 7) Fekete, M., A. Wittliff, and A.V. Schally. Characteristics and distribution of receptors for (D-Trp6)-luteinizing-releasing hormone, somatostatin, epidermal growth factor, and sex steroids in 500 biopsy samples of human breast cancer. *J. Clin. Lab. Anal.* 3:137-147, 1989.
- 8) Van Eijck, C.H., E.P. Krenning, A. Bootsma, J. Lindemans, J. Jeekel, J-C Reubi, and S.W.J. Lamberts. Somatostatin-receptor scintigraphy in primary breast cancer. *Lancet* 343:640-643, 1994.
- 9) Vikić-Topić, S., K.P. Raisch, L.K. Kvols, and S. Vuk-Pavlović. Expression of somatostatin receptor subtypes in breast carcinoma, carcinoid tumor, and renal cell carcinoma. *J. Clin. Endocrinol. Metab.* 80:2974-2979, 1995.
- 10) Patel, Y.C., M.T. Greenwood, R. Panetta, N. Hukovic, S. Grigorakis, L.-A. Robertson, and C.B. Srikant. Molecular biology of somatostatin receptor subtypes. *Metabolism* 45 (#8):31-38, 1996.
- 11) Evans, A.A., T. Crook, S.A.M. Laws, A.C. Gough, G.T. Royle, and J.N. Primrose. Analysis of somatostatin receptor subtype mRNA expression in human breast cancer. *Br. J. Cancer* 75 (6):798-803, 1997.
- 12) Kumar, U., R. Sasi, S. Suresh, A. Patel, M. Thangaraju, P. Metrakos, S.C. Patel, and Y.C. Patel. Subtype selective expression of the five somatostatin receptors (hSSTR1-5) in human pancreatic islet cells: A quantitative double-label immunohistochemical analysis. *Diabetes* 1998 (in press).
- 13) Patel, Y.C., R. Panetta, E. Escher, M. Greenwood, and C.B. Srikant. Expression of multiple somatostatin receptor genes in AtT-20 cells: evidence for a novel somatostatin-28 selective receptor subtype. *J. Biol. Chem.* 269:1506-1509, 1994.
- 14) Kumar, U., D. Laird, C.B. Srikant, E. Escher, and Y.C. Patel. Expression of the five somatostatin receptor (SSTR1-5) subtypes in rat pituitary somatotrophs: quantitative analysis by double-label immunofluorescence confocal microscopy. *Endocrinology* 138:4473-4476, 1997.
- 15) Khare, S., U. Kumar, R. Sasi, L. Puebla, L. Calderon, K. Lemstrom, P. Hayry, and Y.C. Patel. Differential regulation of somatostatin receptor types 1-5 in rat aorta after angioplasty. *FASEB J.* 1998 (submitted).
- 16) Xu, Y., J. Song, M. Berelowitz, and J.F. Bruno. Estrogen regulates somatostatin receptor subtype 2 messenger ribonucleic acid expression in human breast cancer cells. *Endocrinology* 137:5634-5640, 1996.
- 17) Visser-Visselaar, H.A., C.J.C. van Uffelen, P.M. van Koesveld, E.G.R. Lichtenauer-Kaligis, A.M. Waaijers, P. Uitterlinden, D.M. Mooy, S.W. Lamberts, and L.J. Hofland. 17- β -estradiol-dependent regulation of somatostatin receptor subtype expression in the 7315b prolactin secreting rat pituitary tumor *in vitro* and *in vivo*. *Endocrinology* 138:1180-1189, 1997.
- 18) Kimura, N., S. Tomizawa, K. Nakata Arai, and N. Kimura. Chronic treatment with estrogen upregulates expression of sst₂ messenger ribonucleic acid (mRNA) but down-regulates expression of sst₅ mRNA in rat pituitaries. *Endocrinology* 139:1573-1580, 1998.

- 19) Sharma, K. and C.B. Srikant. Induction of wild-type p53, Bax, and acidic endonuclease during somatostatin-signaled apoptosis in MCF-7 human breast cancer cells. *Int. J. Cancer* 76:259-266, 1998.
- 20) Sharma, K. and C.B. Srikant. G protein coupled receptor signaled apoptosis is associated with activation of a cation insensitive acidic endonuclease and intracellular acidification. *Biochem. Biophys. Res. Commun.* 242:134-140, 1998.

Table 1: Quantitative analysis of SSTR1-5 mRNA in primary ductal NOS breast cancer samples in relation to tumor histology and ER/PR status

TB#	sstr1	sstr2	sstr3	sstr4	sstr5	GR	IV	STR	FAT	ER	PR	SIZE	LN	LN+
10796	0.83	nd	1.12	0.11	0.52	7	30	45	25	136	8.2	1.3	13	2
10870	0.4	0.73	0.31	0.07	0.12	4	50	0	0	42	100	2.1	6	0
11517	0.36	0.45	3.24	0.03	0.03	9				1	2	99		+
10969	0.08	0.4	0.08	0.12	0.1	8	50	50	0	1.8	18	1.9	5	0
10991	0.15	nd	1.68	0.12	0.13	7	70	20	10	1.5	3.4	4	98	0
11069	0.08	0.71	0.6	0.18	0.14	9	50	50	0	0.6	0	6	19	0
11109	0.05	0.35	1.61	0	0.1	9	55	40	0	0	5.9	2.3	17	0
11129	0.51	0.86	1.21	0	0.08	7	25	50	20	9.1	56	1.5	11	0
11188	0.37	0.71	1.38	0.3	0.05	7	25	25	50	68	22	2.5	5	0
11225	0.15	0.85	0.43	0.04	0.07	5	30	35	25	10.4	101	2	17	0
11280	0.04	0.77	0.04	0.7	0.09	6	40	40	20	36	182	1.6	5	0
11287	0.28	0.14	0.9	0.26	0.34	7	30	50	15	1.5	10.2	4.5	7	0
11364	0.89	0.42	0.33	0.1	0.07	5	60	0	0	143	134	4.9	12	0
11416	0.73	nd	2.68	0.23	0.06	8	50	45	0	76	86	2.5	23	0
11465	0.4	nd	1.26	0.57	0.14	5	60	0	0	88	42	3	5	0
11492	0.69	0.45	0.66	0.05	0.07	8	50	30	20	2.1	8.1	3.2	9	0
11522	5.16	2.51	11.6	0.47	0.34	7	60	40	0	175	53	1.3	8	0
11562	0.37	0.88	4.82	0.19	0.21	7	30	35	35	32	136	1.2	12	0
11629	1.04	0.82	0.85	0.03	0.04	6	40	50	10	29	54	3.5	98	0
11644	0.24	0.34	0.4	0.04	0.04	6	30	60	10	37	38	1.2	16	0
11652	0.87	0.47	0.12	0.07	0.06	6	50	15	35	164	4.9	1.6	9	0
11806	0.13	1.01	1.02	0.09	0.5	8	20	10	60	32	386	1.9	17	3
11831	0.8	0.27	1.74	0.42	0.32	6	30	60	10	16.6	48	3.5	19	9
11833	1.46	0.44	3.61	2.0	1.32	7	40	55	5	90	12.4	3	10	0
11927	0.46	0.2	1.42	0.3	0.1	8	55	40	5	1.6	4.2	99.8	11	0
10800	0.12	0.26	0.29	0.03	0.22	6	60	40	0	105	136	5.6	7	0
11751	0.17	0.52	1.12	0.09	0.04	8	20	30	50	1.4	1.7	2	1	1
10936	0.79	0.91	0.15	0.39	0.1	6	40	0	0	60	197	4	6	6
10937	0.07	0.52	0.07	0.06	0.53	7	70	20	10	18.7	4.4	0	1	1
11051	0.1	0.4	2.06	0.06	0.05	8	20	30	50	0	5	3	14	1
11090	0.15	0.42	0.61	0.09	0.11	8	20	60	10	0.2	16.1	3.7	17	4
11332	0.07	nd	0.07	0.1	0.07	5	40	55	5	143	44	2.5	15	3
11673	0.64	0.57	4.1	0.84	0.11	7	20	60	10	0.4	8	5	12	2
11756	1.36	0.55	0.19	0.07	0.31	6	30	60	20	63	3.9	2.7	15	0

11022	0.24	0.54	0.61	0.05	0.04	8	35	40	25	1.8	2.9	4.9	18	13
11894	0.23	0.16	0.1	0.07	0.05	7	25	50	25	2	14.8	99.9	15	3
11209	2.37	0.31	7.18	1.4	0.89	7	20	40	40	51	37	99.9	22	0
11217	0.46	0.14	1.33	0.47	0.14	7	50	45	0	72	38	99.8	21	17
11662	0.22	nd	0.25	0.02	0.03	6	25	25	50	115	115	99.8	10	1
11727	0.88	0.48	0.32	0.07	0.05	5	30	60	10	48	5.5	99.8	6	0
11869	0.85	0.54	2.3	0.6	0.51	6	40	40	20	60	288	99.8	15	0
10903	0.67	0.39	3.5	0.03	0.13	8	20	70	0	1.6	5.7	3	6	3
10963	4.27	0.64	8.37	0.95	2.62	8	30	60	0	7	9	99.9	98	0
11110	0.04	0.45	2.38	0.1	0.05	8	40	30	30	1	3.8	99.9	9	8
11125	0.43	0.59	0.66	0.53	0.81	7	40	30	30	196	224	99.9	4	3
11772	0.07	0.43	0.36	0.05	0.05	7	20	40	30	175	8.8	99.8	6	0
10994	0.05	0.51	0.39	0.07	0.1	9	50	50	1	1.9	4.2	99.9	14	1
11818	0.61	0.46	2.97	0.6	0.34	8	40	40	20	1.4	6.1	99.9	6	1

SSTR1-5 = SSTR-1-5 mRNA expressed as fold increase compared to actin mRNA

GR = tumor grade (Nottingham scale)

IV = % invasiveness

STR = % stroma

Fat = % fat

ER = estrogen receptor levels

PR = progesterone receptor levels

Size = tumor size in centimeters, 99.9, size unknown; 99.8, multi-focal

LN+ = number of positive lymph nodes

Table 2: Expression of mRNA for different SSTR subtypes in breast cancer cell lines*

Cell line	ER status	SSTR 1	SSTR 2	SSTR 3	SSTR 4	SSTR 5
MCF-7	+	0.9 (+++)	0.33 (+)	0.07 (+/-)	0.05 (-)	0.91 (++)
MB 231	-	0.04 (+/-)	0.42 (+)	0.06 (+/-)	0.08 (+/-)	0.14 (+)
T47D	+	0.04 (+/-)	0.88 (++)	0.04 (-)	0.05 (-)	0.17 (+)
ZR75-1	+	0.1 (+)	0.9 (++)	0.08 (+/-)	0.11 (+/-)	0.06 (+/-)

+/- indicates weakly positive, if at all

* normalized values for SSTR mRNA expression against actin control

FIGURE LEGENDS

FIGURE 1: Representative Southern blots of hSSTR1-5 obtained by RT-PCR analysis of mRNA from 14 human ductal NOS tumor samples (lanes 1-14) to show the pattern of expression and relative abundance (compared to β -actin mRNA) of each subtype. Quantitative data obtained in this way for 48 samples is summarized in Table 1. The lane numbers (1-14) correspond to the tumor samples shown in Table 1 as follows: (1) 11364; (2) 11332; (3) 11280; (4) 10969; (5) 11806; (6) 10994; (7) 11225; (8) 10931; (9) 10870; (10) 11110; (11) 11069; (12) 11225; (13) 11109; (14) 11129. A comparison of hSSTR1-5 mRNA in four human breast cancer cell lines is represented by lanes A-D. (A) MCF-7; (B) MB231; (C) T47D; (D) ZR75-1.

FIGURE 2: Box-whisker plots correlating log SSTR1 mRNA with estrogen receptor (ER) levels (top left panel), log SSTR2 mRNA and ER (middle left panel), log SSTR2 mRNA and progesterone receptor (bottom left panel), log SSTR3 mRNA and tumor grade (top right panel) and log SSTR2 mRNA and tumor size (middle right panel). The inset in the bottom right panel tabulates the pair wise Pearson correlation (r) and P values for the nontransformed SSTR mRNA data against the different variables shown.

FIGURE 3: Western blot analysis of SSTR1-5 in rat brain membranes. 35 μ g membrane protein was fractionated by SDS-PAGE and probed with immunoaffinity purified SSTR antisera (lane A of each pair) or antigen preabsorbed antibody (lane B of each pair). Major protein bands of 53 kDa (SSTR1), 57 kDa (SSTR2), 60 kDa (SSTR3), 44 kDa (SSTR4), and 58 kDa (SSTR5) were obtained. The bands were specific and were inhibited in the presence of antigen absorbed antibody. 10 kDa protein ladder standards were used for molecular weight estimates.

FIGURE 4: Western blots of human fetal brain probed with hSSTR1-5 antisera. Major immunoreactive bands of 48-50 kDa (SSTR1), 46-50 kDa (SSTR2), 52-55 kDa (SSTR3), 52-55 kDa (SSTR4), and 50-52 kDa (SSTR5) were obtained. 35 μ g human fetal brain membranes were analysed by SDS-PAGE as described for rat brain (Fig. 3).

FIGURE 5: Adjacent sections from two ductal NOS primary breast cancer samples (tumor # 11629 /11110) analysed by peroxidase immunohistochemistry for SSTR1-5 antigens using affinity purified SSTR antibodies. Note the rich expression of SSTR1 and SSTR2 in most tumor cells in tumor #11629 (left hand panels). In tumor #11110, SSTR1 and SSTR3 are abundantly expressed with moderate expression of SSTR2 and SSTR4. In both tumors SSTR5 is poorly localized. Magnification x 400.

FIGURE 6: Adjacent sections from two ductal NOS primary breast cancer samples (tumor # 10870/10937) analysed by peroxidase immunohistochemistry for SSTR1-5 antigens using affinity purified SSTR antibodies. Tumor #10870 (left hand panels) shows strong localization of SSTR1 and SSTR2 in tumor cells with relatively poor expression of the other three SSTR subtypes. The right hand panels from tumor #10937 display an arteriole showing strong expression of SSTR2 and SSTR5 in the vessel wall especially in smooth muscle cells. Magnification x 400.

FIGURE 7: Western blot analysis of SSTR1-5 in human breast tumor cell lines MCF-7 and MB231. 35 µg membrane proteins were analysed by SDS-PAGE with affinity purified SSTR antisera as described for Fig. 3. Both cell lines displayed a major 55-60 kDa band for SSTR1 and a 48-52 kDa band for SSTR2. SSTR5 showed a major 50-52 kDa band and a minor band at 65-68 kDa. The intensity of SSTR5 expression was considerably weaker in MB231 cells compared to MCF-7 cells. No immunoreactivity corresponding to SSTR3 or SSTR4 was observed in either cell line. These results are in agreement with SSTR mRNA expression by RT-PCR in these cells (Table 2).

FIGURE 8: hSSTR3 promoter sequence analysis showing putative *cis* regulatory elements for SP1, Ebox, NFKappa E2, IRF2, Pit-1, SRF, and CRE elements.

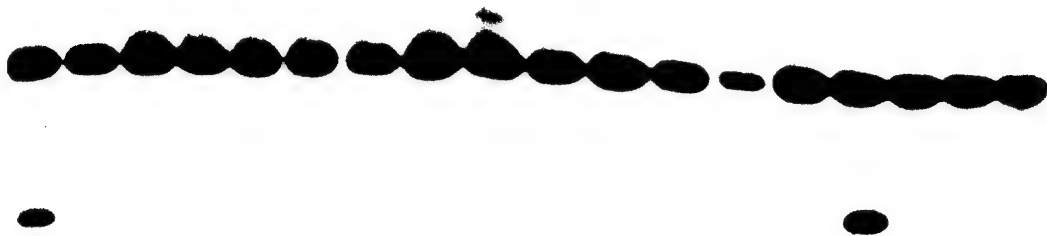
FIGURE 9: See Figure.

FIGURE 10: See Figure.

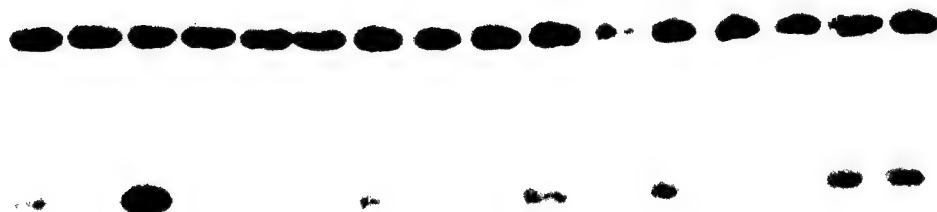
APPENDIX

- 1) Patel, Y.C. and C.B. Srikant. Somatostatin receptors. *Trends in Endocrinology and Metabolism* 8:398-405, 1997.
- 2) Patel, Y.C. Basic aspects of somatostatin receptors. In: *Advances in Molecular and Cellular Endocrinology*, D. LeRoith (ed), JAI Press, Greenwich, CT., 1998 (in press).
- 3) Sharma, K., Y.C. Patel, and C.B. Srikant. C-terminal region of human somatostatin receptor 5 is required for induction of Rb and G1 cell cycle arrest. *Molecular Endocrinology* 1998 (in press).
- 4) Kumar, U., R. Sasi, S. Suresh, A. Patel, M. Thangaraju, P. Metrakos, S.C. Patel, and Y.C. Patel. Subtype selective expression of the five somatostatin receptors (hSSTR1-5) in human pancreatic islet cells: A quantitative double-label immunohistochemical analysis. *Diabetes* 1998 (in press).
- 5) Sharma, K. and C.B. Srikant. Induction of wild-type p53, Bax, and acidic endonuclease during somatostatin-signaled apoptosis in MCF-7 human breast cancer cells. *Int. J. Cancer* 76:259-266, 1998.
- 6) Sharma, K. and C.B. Srikant. G protein coupled receptor signaled apoptosis is associated with activation of a cation insensitive acidic endonuclease and intracellular acidification. *Biochem. Biophys. Res. Commun.* 242:134-140, 1998.
- 7) Hukovic, N., R. Panetta, U. Kumar, M. Rocheville, and Y.C. Patel. The cytoplasmic tail of the human somatostatin receptor type 5 is crucial for interaction with adenylyl cyclase and in mediating desensitization and internalization. *J. Biol. Chem.* 273:21416-21422, 1998.
- 8) Patel, Y.C., K. Sharma, U. Kumar, S. Grigorakis, P. Watson, and C.B. Srikant. Expression and antiproliferative functions of somatostatin receptors in breast cancer. *Proceedings Department of Defense U.S. Army Medical Research and Material Command Breast Cancer Research Program: An Era of Hope*, Washington, D.C., October 31-November 4, 1997.

R1 1 2 3 4 5 6 7 8 9 10 11 12 13 14 A B C D



R2 3 4 5 6 7 8 9 10 11 12 13 14 A B C D



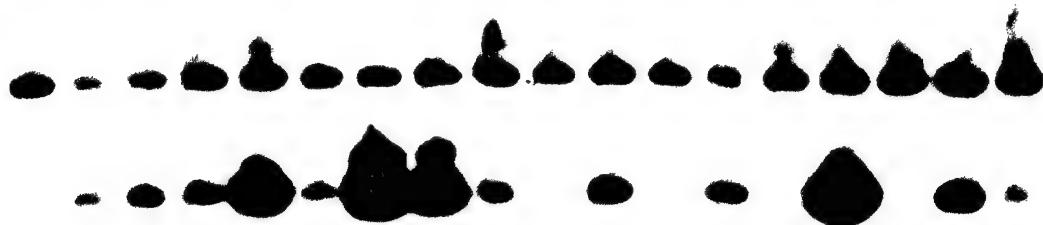
R3 1 2 3 4 5 6 7 8 9 10 11 12 13 14 A B C D

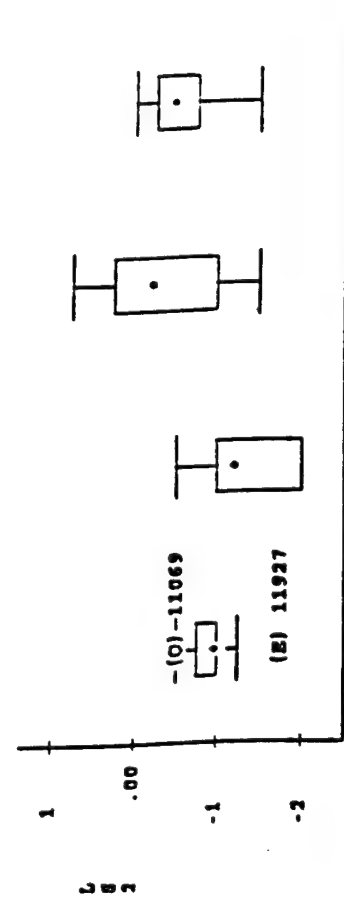
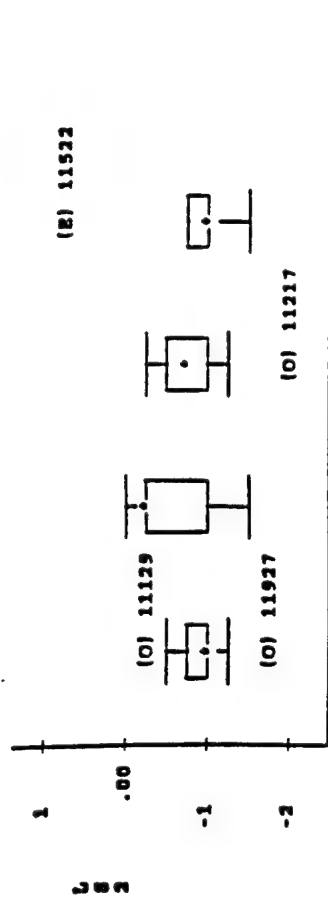
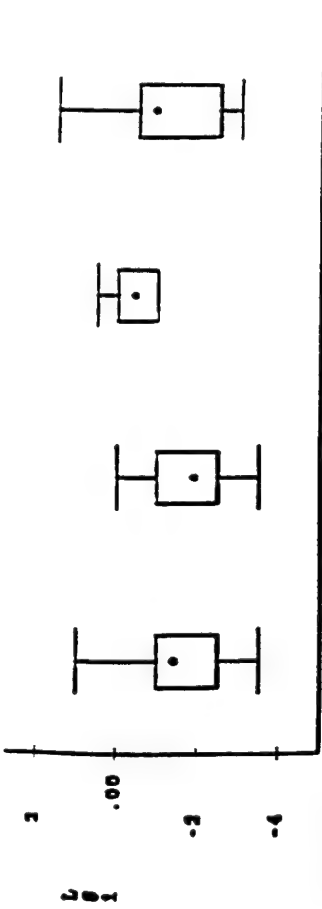


R4 1 2 3 4 5 6 7 8 9 10 11 12 13 14 A B C D

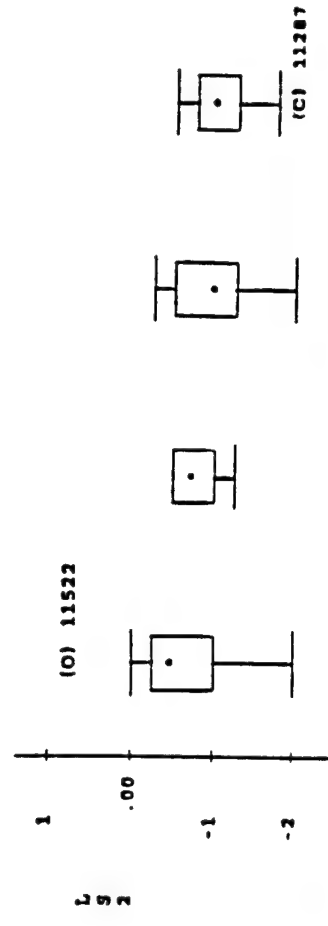
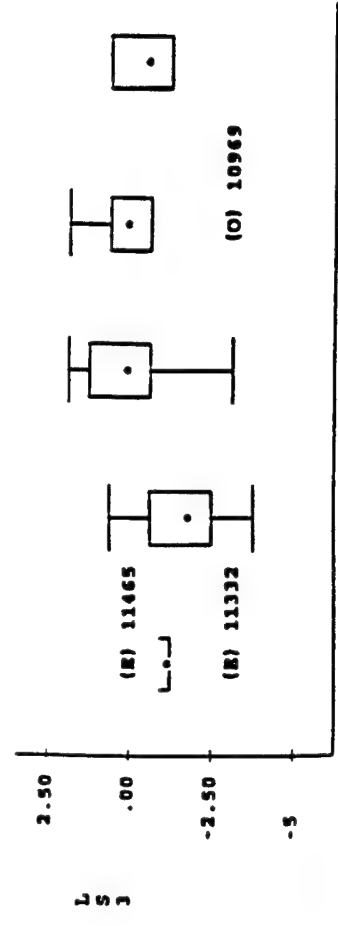


R5 1 2 3 4 5 6 7 8 9 10 11 12 13 14 A B C D





Symbol Key: • - Median (O) - Outlier (E) - Extreme



	r	P
SSTR1 vs ER	0,26	0,08
SSTR2 vs ER	0,31	0,05
SSTR2 vs PR	0,28	0,07
SSTR3 vs grade	0,24	0,1
SSTR2 vs size	-0,33	0,04
SSTR1 vs lymph node	-0,27	0,07

SSTR1

KDa a b

110 -
100 -
90 -
70 -
60 -
50 -
40 -

SSTR2

KDa a b

110 -
100 -
80 -
60 -
50 -
40 -

SSTR3

KDa a b

116 -
66.4 -
55.6 -
42.7 -
36.5 -

SSTR4

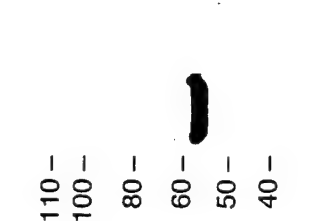
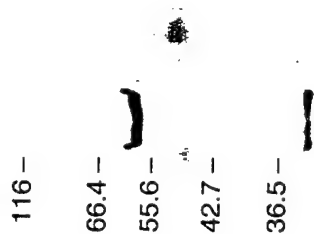
KDa a b

158 -
116 -
66.4 -
55.6 -
42.7 -

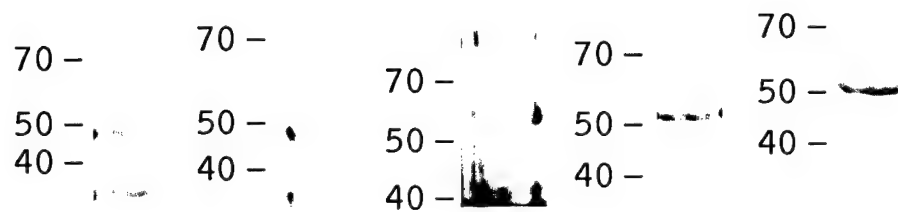
SSTR5

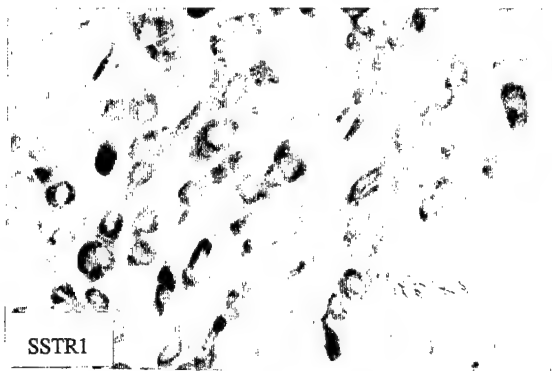
KDa a b

158 -
66.4 -
55.6 -
42.7 -
36.5 -

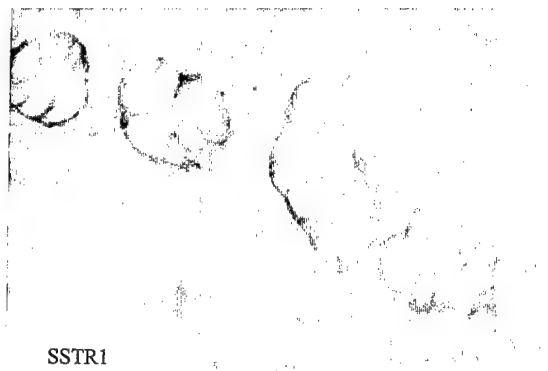


SSTR1 SSTR2 SSTR3 SSTR4 SSTR5

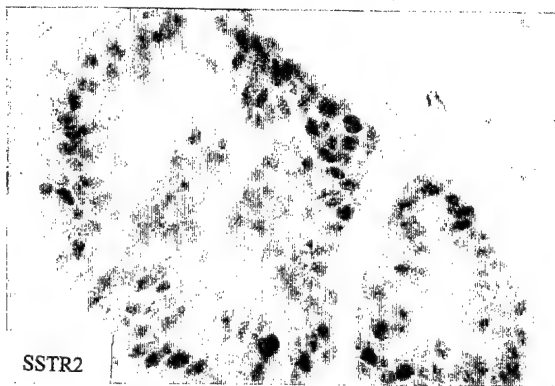




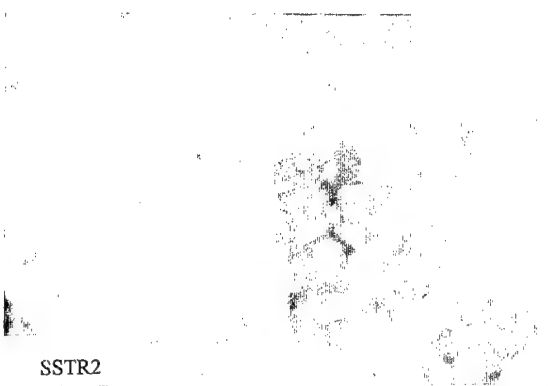
SSTR1



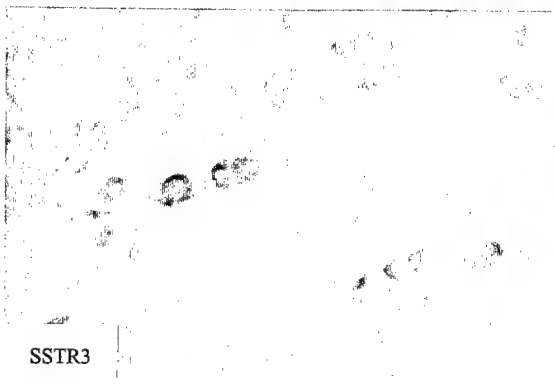
SSTR1



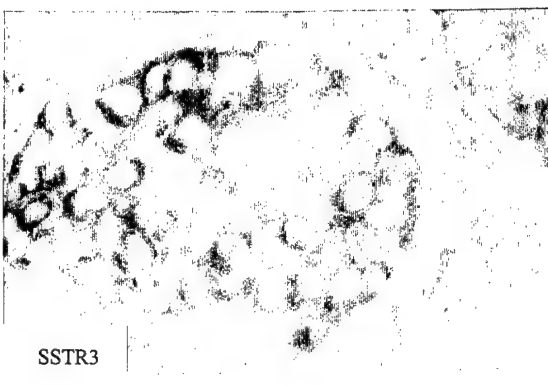
SSTR2



SSTR2



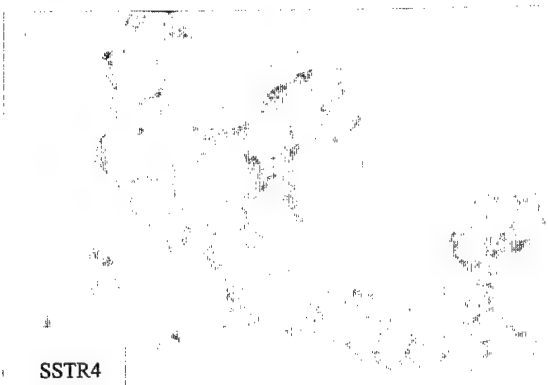
SSTR3



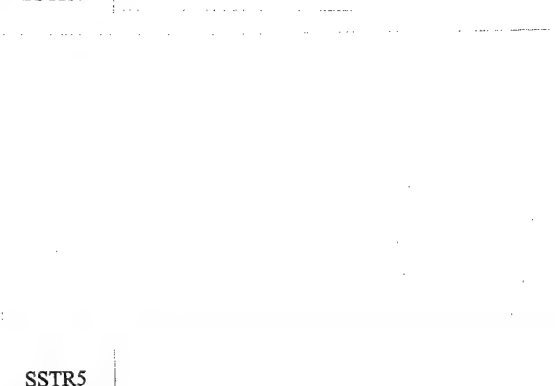
SSTR3



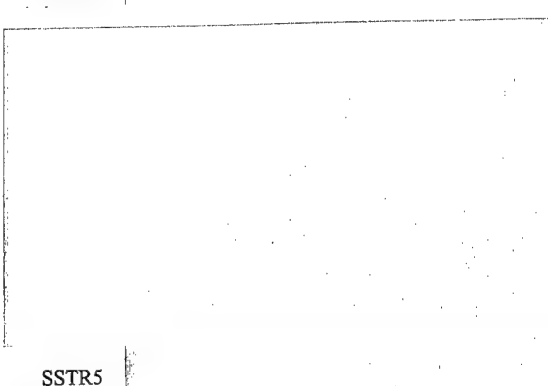
SSTR4



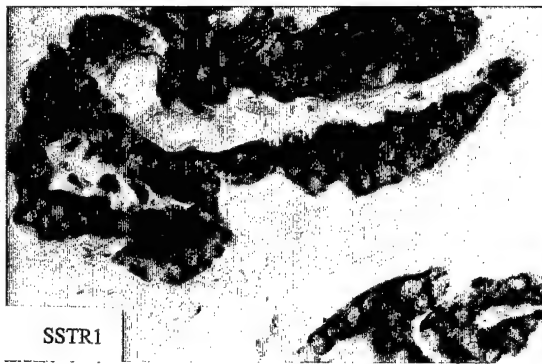
SSTR4



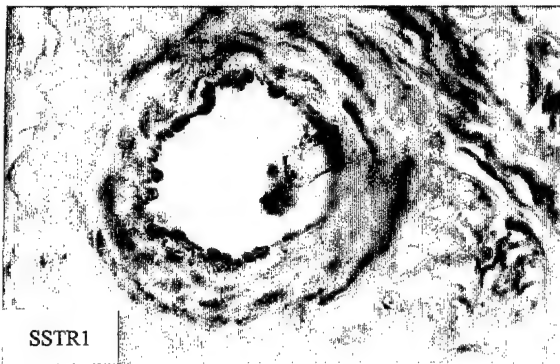
SSTR5



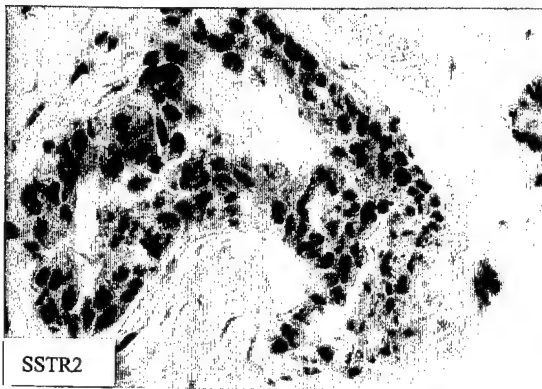
SSTR5



SSTR1



SSTR1



SSTR2



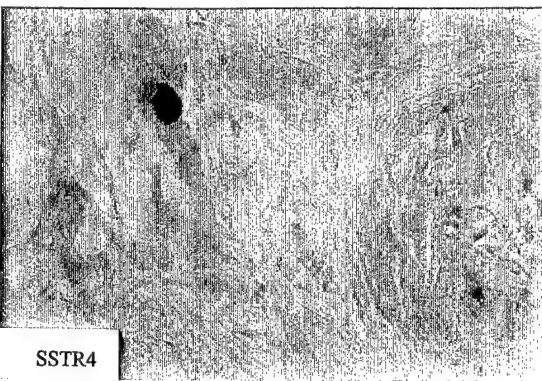
SSTR2



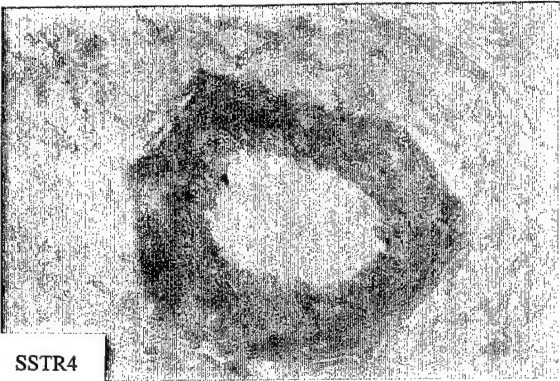
SSTR3



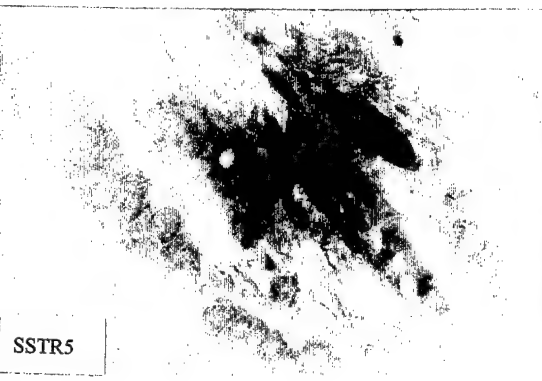
SSTR3



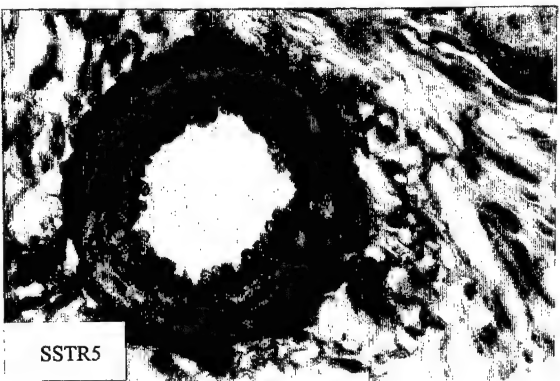
SSTR4



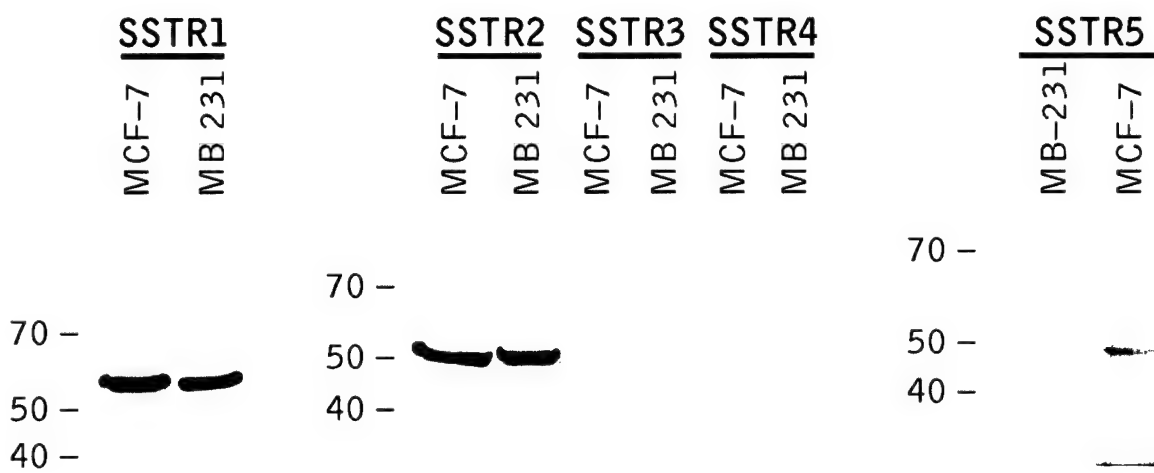
SSTR4



SSTR5



SSTR5



[illegible]

GGGCTCTCCAGATGTAACCAATCCAGAGACTAATGACCCCAACCGGCTCCCCGTGGTCCGTGGCCCGGTGGCCCGACTGCAGGGCTGGACT -5053
GTGACTCCCGGGCTGGCCAGCCCAACACAGCCCTTGCTTGGACACAGCTGCTGCCCGGGGACCCTGTGCCGCAATGGCCCTCACGAGCTGCTCTGG -4953
CTACTGGCTGGCAGCCTCGGCTCCCTGAGCACTGACACATTTCTCTCCAACTCCCTGGAGAGCCAGGCCAGCGGGCTGGGTGGCTGAAATCTC -4853
CCGGTAACAAGGTCTGGCCCCCTCTGCTCCCTCTCGGGCTTAACTGACCCCGGCCCCACCCCCACACACCCTGCTCTCCGGCCCTCAGC -4753
CCCTCCCTGCTTACTCCCTCTTACGGGCTCCATGTCACCATCTGTGGCAGTCCCTCTGTCACTCTCCCTGCCACCCCTCATCTCTCTTCTCTCC -4653
CTCTGCTCTCTCTGCTATCTCTCCCTCTCACCCGTGTCT -4553
TTCTGCCCTTCT -4453
CCCTTCCCT -4353
CAGATGTCTCTGGAGATGGGGGCTGACCTACAGGCTCTGTGGGAGTCAAGGCGGAGACAGATGGGAGAGGCTCTGTGGACAGCCGTGGCCGA -4253
GGCCCTGGGAGGGAACTGAGCCCGCAAGCGGTCTAGAGTGGGTGCTTGTGGGAGCCCTAGTTAGGAATGGCCCTGGGGGCACTGGGGGCTGGGCAGG -4153
GAGAGGGGACAGCAGAAATGATAACAGCCCTGGGCGAAGGAGGGAAGCCCTCACCCCATGGGCAAGTAAAGAGGCTGGGGCCCGGATGATGCTCCGAAGG -4053
GTGGGGTCTCTGGAAGCCCATCTCTGCCCCAGGATGAATTTGGGAGGCTGGGGTGGGGAGAGAGGGTGGGGACTCCACAGGAGGCAAGAGGGAGGCCCT -3953
TCCTGTGACCTTCCCGCTCGGCTGAGGGGCAGGGGCTTAGTCTCAGAACTCTAGGATCTCTAGGATCTCTAGGATCTCTAGGATCTCTAGGATCTCTAG -3853
GGCTGGAGGGAGCCAGATGATATCATCTCTGTTGGCTTCCCCAGCTCACTGGCAGCTCTCTGAGCTCTCTCTCTCTCTCTCTCTCTCTCTCTCTCTCT -3753

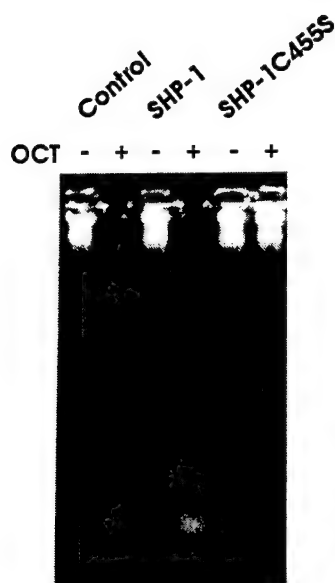


Fig. 9

SST-induced apoptosis in CHO-K1 cells is SHP-1-dependent. Cells were incubated in the absence or presence of 100 nM OCT for 24 h and the cellular DNA extracted and analysed for the presence of DNA fragmentation by agarose gel electrophoresis and ethidium bromide staining. DNA degradation caused by OCT was higher in cells overexpressing SHP-1 and was absent in cells overexpressing its catalytically inactive mutant SHP-1C455S.

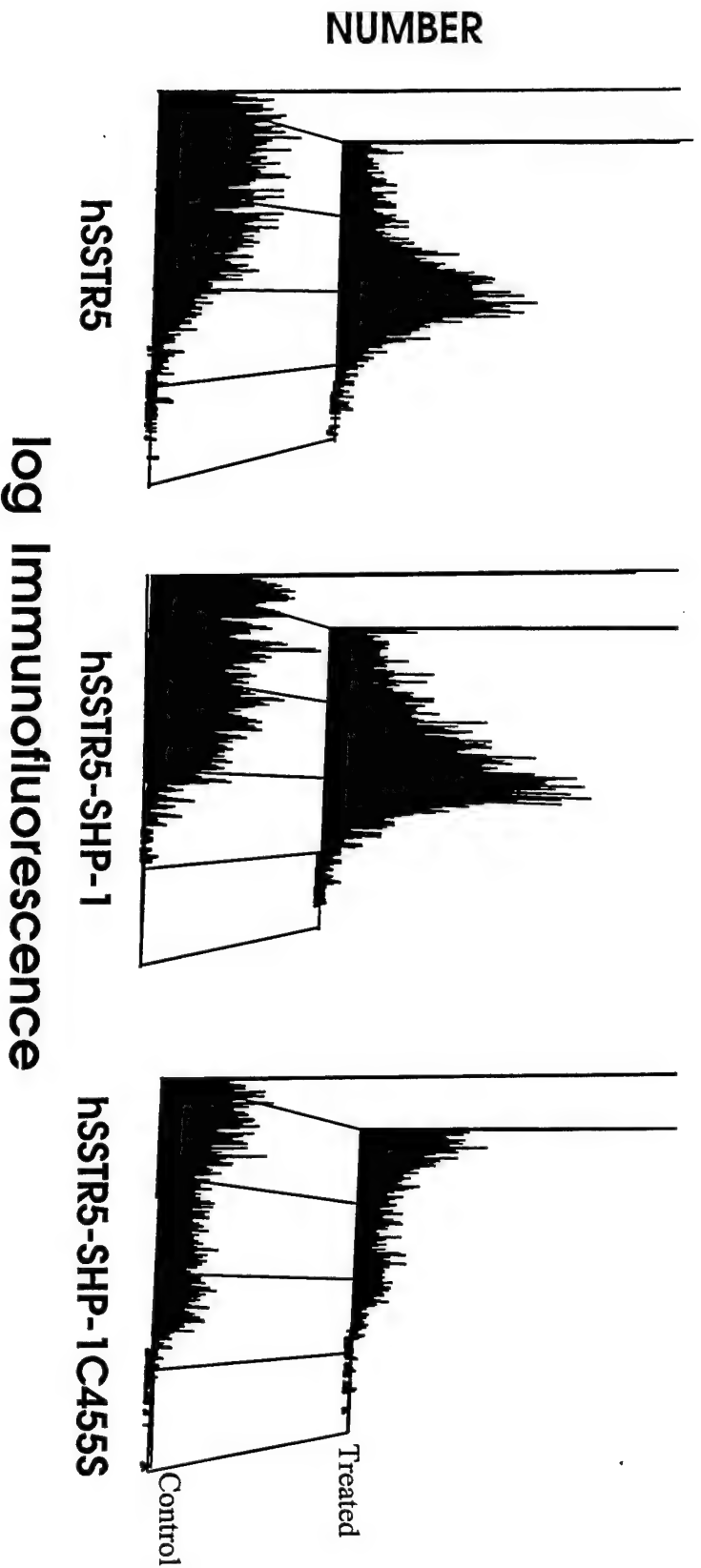


Fig. 10

Induction of Rb by SST in CHO-K1/hSSTR5 cells is SHP-1-dependent. Overexpression of SHP-1 (middle panel) enhanced the increase in Rb compared to untransfected cells (left panel). Induction of Rb by SST was prevented by the catalytically inactive mutant SHP-1C455 (right panel). Rb was immunostained with anti-Rb antibody (Santa Cruz Biotechnology), counter stained with FITC-conjugated secondary antibody and quantitated by flow cytometry.

Somatostatin Receptors

Yogesh C. Patel and Coimbatore B. Srikant

The diverse biological effects of somatostatin (SRIF) are mediated by a family of G protein-coupled receptors (termed sst) that are encoded by five nonallelic genes located on separate chromosomes. The receptors can be further divided into two subfamilies: sst_{2,3,5} react with octapeptide and hexapeptide SRIF analogues and belong to one subclass; sst_{1,4} react poorly with these compounds and fall into another subclass. This review focuses on the molecular pharmacology and function of these receptors, with particular emphasis on the ligand-binding domain, subtype-selective analogues, agonist-dependent receptor regulation and desensitization responses, subtype-specific effector coupling, and signal transduction pathways responsible for inhibiting cell secretion and cell growth or induction of apoptosis. (Trends Endocrinol Metab 1997;8: 398–405). © 1998, Elsevier Science Inc.

• The Somatostatin Receptor Family

Somatostatin (SRIF) is synthesized as the bioactive peptides, SRIF-14 and SRIF-28, which act on multiple targets, including the brain, gut, pituitary, endocrine and exocrine pancreas, adrenals, thyroid, kidneys, and immune cells (Reichlin 1983). The actions of SRIF include inhibition of virtually every known endocrine and exocrine secretion; motor, sensory, behavioral, cognitive and autonomic effects; as well as effects on intestinal motility, vascular contractility, cell proliferation, and intestinal absorption of nutrients and ions. These pleiotropic effects can be resolved into three cellular processes that are modulated by SRIF—neurotransmission, secretion, and cell proliferation—and are mediated via high-affinity plasma membrane receptors termed sst receptors (Patel et al. 1995, Reisine and Bell 1995, Lamberts et al. 1996, Patel 1997). Beginning in 1992,

the structure of sst receptors was elucidated by molecular cloning (Yamada et al. 1992a). Five individual subtypes were rapidly identified and shown to consist of a family of heptahelical G protein-coupled receptors (GPCR) (Yamada et al. 1992a and b, Bruno et al. 1992, O'Carroll et al. 1992, Rohrer et al. 1993, Panetta et al. 1994, Patel et al. 1995, Reisine and Bell 1995, Patel 1997). Human sst receptors (hsst) are encoded by a family of five nonallelic genes located on separate chromosomes (Table 1). Four of the genes are intronless, the exception being sst₂, which gives rise to spliced variants sst_{2A} and sst_{2B}, which differ only in the length of the cytoplasmic C-tail (Figure 1) (Patel et al. 1995, Reisine and Bell 1995). There are thus six putative sst subtypes of closely related size, each displaying a seven transmembrane domain (TM) topology. All sst isoforms that have been cloned so far from humans as well as from other species possess a highly conserved sequence motif YANSCANPI/VLY in the VIIth TM, which serves as a signature sequence for this receptor family (Figure 1) (Patel et al. 1995, Reisine and Bell 1995). Overall, there is 39%–57% sequence identity among the various members of this fam-

ily, with sst₁ and sst₄ showing the highest sequence identity. The individual subtypes display a remarkable degree of structural conservation across species. Thus there is 94%–98% sequence identity between the human, rat, and mouse isoforms of sst₁; 93%–96% sequence identity between human, rat, mouse, porcine, and bovine isoforms of sst₂; and 88% sequence identity between the rat and human isoforms of sst₄; sst₃ and sst₅ are somewhat less conserved, showing 82%–83% sequence identity between the human and rodent homologues. The nearest relatives of the sst receptors are the opioid receptors, whose δ subtype displays 37% sequence similarity to mouse sst₁.

• Binding Affinity of Natural and Synthetic Somatostatin Ligands

Over the years, many different analogues of SRIF have been synthesized for investigational and clinical use (Figure 2). Structure-function studies have shown that amino acid residues Phe⁷, Trp⁸, Lys⁹, and Thr¹⁰, which comprise a β turn, are necessary for biological activity, with residues Trp⁸ and Lys⁹ being crucial. The general strategy for designing SRIF analogues has been to retain the Phe⁷, Trp⁸, Lys⁹, and Thr¹⁰ segment and to incorporate a variety of cyclic and bicyclic restraints to stabilize the β turn around the conserved residues. In this way, a library of short synthetic compounds has been synthesized, several of which show greater metabolic stability and some pharmacological selectivity compared with SRIF-14 (Patel and Srikant 1994, Patel et al. 1995, Reisine and Bell 1995, Bruns et al. 1996, Shimon et al. 1997). All five sst subtypes bind SRIF-14 and SRIF-28 with high affinity (Table 2). sst_{1–4} bind SRIF-14 \geq SRIF-28, whereas sst₅ exhibits weak selectivity for SRIF-28 compared with SRIF-14. The octapeptide analogues SMS201-995 (SMS, Octreotide) and BIM23014 (Lanreotide) that are in clinical use, as well as the octapeptide RC160 (Vapreotide) and the hexapeptide MK678 (Seglitide), bind to only three of the hsst subtypes, displaying high affinity for subtypes 2 and 5 and moderate affinity for type 3 (Table 2). Based on structural similarity and reactivity for octapeptide and hexapeptide SRIF analogues, the receptor family can be divided into two

Yogesh C. Patel and Coimbatore B. Srikant are at the Fraser Laboratories, McGill University, Departments of Medicine and Neurology and Neurosurgery, Royal Victoria Hospital and the Montreal Neurological Institute, Montreal, Quebec H3A 1A1, Canada.

Table 1. Characteristics of the cloned subtypes of human somatostatin receptors^a

	<i>sst</i> ₁	<i>sst</i> _{2A}	<i>sst</i> ₃	<i>sst</i> ₄	<i>sst</i> ₅
Chromosomal localization	14q13	17q24	22q13.1	20p11.2	16p13.3
Amino acids	391	369	418	388	363
mRNA (kb)	4.8	8.5 (?)	5.0	4.0	4.0
G-protein coupling	+	+	+	+	+
Effector coupling					
Adenylyl cyclase activity	↓	↓	↓	↓	↓
Tyrosine phosphatase activity	↑	↑	↑	↑	
Ca ²⁺ channels		↓			
Na ⁺ /H ⁺ exchanger	↑				
Phospholipase C/IP ₃ activity		↑			↓↑
Phospholipase A2 activity				↑	
MAP kinase activity			↓	↑	↓
Tissue distribution ^b	Brain, pituitary, stomach, liver, pancreas, kidneys	Brain, pituitary, stomach, pancreas, kidneys	Brain, pituitary, stomach	Brain, stomach, pancreas, lungs, stomach	Brain, pituitary, stomach

^aModified from Patel (1997), Patel et al. (1995), and Reisine and Bell (1995).

^bBased on Lamberts et al. (1996) and Patel (1997). Not all tissues have been tested simultaneously. IP₃, inositol triphosphate; MAP kinase, mitogen-activated protein kinase.

subclasses: *sst*_{2,3,5} react with these analogues and constitute members of one subgroup; *sst*_{1,4} react poorly with these compounds and fall into another subgroup. The analogue Des-AA_{1,2,5} [D-Trp⁸ IAMP⁹] SRIF (CH275) has been recently reported as an *sst*₁ selective compound (Liapakis et al. 1996). In our hands, CH275 also binds to *sst*₄ and appears to be a prototypic agonist for the *sst*_{1,4} subclass (Table 2) (Patel 1997). Several other SRIF analogues have been similarly reported to be selective for one *sst* subtype, for example, *sst*₂ (MK678), *sst*₃ (BIM23056), and *sst*₅ (BIM23052, L362855) (Reisine and Bell 1995). Because of methodological variations, however, such claims of subtype selectivity of these and other analogues have not been substantiated by others and should be interpreted with caution (Patel and Srikanth 1994, Bruns et al. 1996). More recent binding analyses of these compounds using the human *sst* clones have identified only BIM23268 with modest selectivity for *hsst*₅ (Table 2). L362855 binds well to *sst*₅ and *sst*₂ and is only weakly selective for *sst*₅. Likewise, MK678 displays good binding affinity

for both *sst*₂ and *sst*₅ subtypes. Overall then, these results suggest that the binding selectivity of currently available SRIF analogues for the human *sst* subtypes is relative rather than absolute and that there are no pure agonists available for the individual subtypes. Very recently, the first potential *sst* peptide antagonists have been described (Bass et al. 1996, Wilkinson et al. 1997). One such compound [Ac-4-NO₂-Phe-c(D-Cys-Tyr-D-Trp-Lys-Thr-Cys)-D-Tyr-NH₂] binds to *hsst*₂ and *hsst*₅ with nM affinity, but antagonizes receptor effector coupling to adenylyl cyclase (Bass et al. 1996). A second peptide, BIM23056, appears to be an antagonist at the *sst*₅ receptor (Wilkinson et al. 1997).

• Ligand-Binding Domain

The ligand-binding site of peptide agonists comparable to SRIF typically involves residues in the extracellular loops (ECLs) or both the ECLs and the TMs (Schwartz and Rosenkilde 1996). By exploiting the differential ability of SMS to bind to *hsst*₂ but not to *hsst*₁, Kaupman et al. (1995) systematically

mutated *hsst*₁ to resemble *hsst*₂. They found two crucial residues, Gln₂₉₁ and Ser₃₀₅, in TMs VI and VII, respectively, of *hsst*₁, substitution of which for the corresponding residues Asn²⁷⁶ and Phe²⁹⁴ in *hsst*₂ increased the affinity of *hsst*₁ for SMS and other octapeptide analogues 1000-fold (Figure 1). Based on these results, Kaupman et al. (1995) have postulated a binding cavity for SMS involving hydrophobic and charged residues located exclusively within TMs III–VII. Their findings predict that the core residues Phe⁷, Trp⁸, Lys⁹, and Thr¹⁰ of SMS interact with Asn²⁷⁶ and Phe²⁹⁴ located at the outer end of TMs VI and VII, respectively (present in *sst*₂ but not in *sst*₁), which provide a hydrophobic environment for lipophilic interactions with Phe⁷, Trp⁸, Thr¹⁰, and Asp¹³⁷ in TM III, which anchors the ligand by an electrostatic interaction with Lys⁹ (Figure 1) (Nehring et al. 1995). SMS binds poorly to *hsst*₁ because of the presence of residues Gln²⁹¹ and Ser³⁰⁵ located close to the extracellular rims of TM helices VI and VII which prevent the short peptide from reaching deep within the pocket, whereas the corresponding residues Asn²⁷⁶ and Phe²⁹⁴ in *sst*₂ provide for a stable interaction with the disulfide bridge of SMS. Because of their greater length and flexibility, the natural ligands SRIF-14 and SRIF-28 can presumably adopt a conformation that allows their entry into the binding pocket of all five *sst* receptors. The involvement of the extracellular domains for binding SRIF ligands has been investigated by Greenwood et al. (1977), who used amino terminal deletion mutants or conservative segment exchange mutagenesis for the three ECLs of *hsst*₅. Their results predict a potential contribution of ECL2 (but not of ECL1, ECL3, or the amino terminal segment) to binding of the natural SRIF ligands (SRIF-14, SRIF-28), as well as SMS. The overall model that emerges from these studies suggests a binding domain for SRIF ligands made up of residues within TMs III–VII, with a potential contribution by ECL2, and is consistent with other peptide-binding GPCRs, for example, neurokinin I, angiotensin II, GnRH receptors, which interact with residues in both ECLs, and TMs (Schwartz and Rosenkilde 1996).

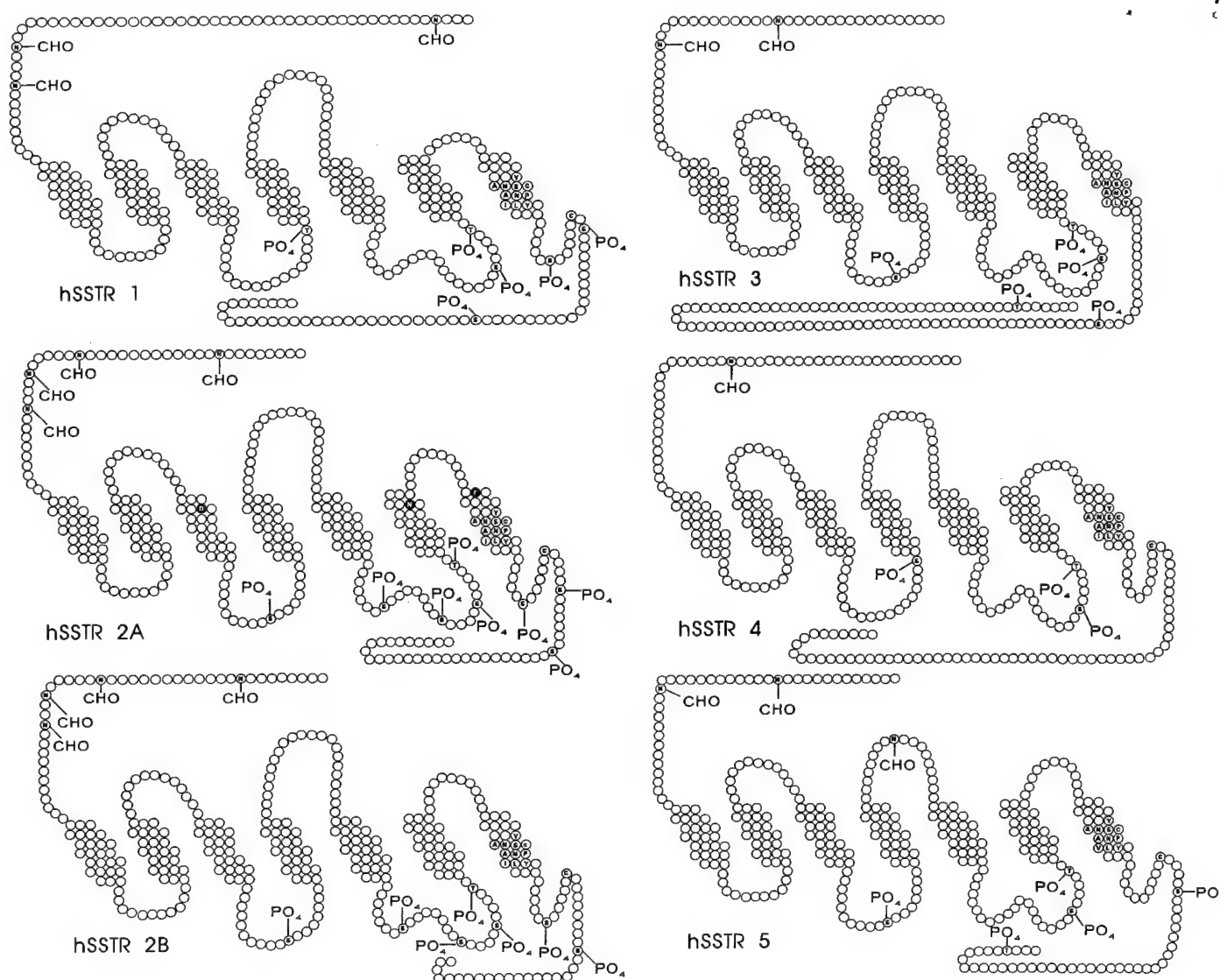


Figure 1. Schematic depiction of the seven-transmembrane topology of the human *sst*₁₋₅ receptors. CHO are the potential sites for N-linked glycosylation within the amino terminal segment and second extracellular loops (ECL); PO₄ are the putative sites for phosphorylation by protein kinase A, protein kinase C, and casein kinase. The cysteine residue 12 amino acids downstream from the VIIth TM is conserved in *sst*_{1,2,4,5} and may be the site of a potential palmitoyl membrane anchor. The YANSCAN PIVLY sequence in the VIIth TM is highly conserved in all members of the *sst* family. Residues Asp¹²², Asn²⁷⁶, and Phe²⁹⁴ in TMs III, VI, and VII, respectively, of *sst*_{2A} have been proposed to form part of a ligand-binding pocket for Octreotide and are shown by the closed circles. (From Patel 1997).

• G-Protein Coupling and Signal Transduction

Ligand activation of endogenous *sst* receptors is associated with a reduction in intracellular cAMP and Ca²⁺ and stimulation of protein phosphatases because of receptor activation of four major effector pathways, each involving a pertussis toxin-sensitive GTP-binding protein: (a) adenylyl cyclase, (b) K⁺ channels, (c) Ca²⁺ channels, and (d) protein phosphatases (Figure 3) (Patel et al. 1995, Reisine and Bell 1995, Lamberts et al. 1996,

Patel 1997). Receptor activation inhibits adenylyl cyclase, leading to a fall in intracellular cAMP. *Sst* receptors are coupled to several subsets of K⁺ channels (delayed rectifier, inward rectifier, ATP-sensitive K⁺ channels, and large conductance Ca²⁺-activated BK channels). Receptor activation of K⁺ channels causes reversible hyperpolarization of the membrane, leading to the cessation of spontaneous action potential activity and secondary reduction in intracellular Ca²⁺, because of inhibition of the normal depolarization induced Ca²⁺ influx via voltage sensitive Ca²⁺ channels. In

addition to this indirect effect on Ca²⁺ entry, *sst* receptors act directly on high-voltage-dependent Ca²⁺ channels to block Ca²⁺ currents. Stimulation of both K⁺ and Ca²⁺ channels may also occur through dephosphorylation of the channel proteins secondary to *sst* activation of a serine threonine phosphatase. Furthermore, *sst* receptors may inhibit Ca²⁺ currents through induction of cGMP, which activates cGMP protein kinase with further phosphorylation-dependent inhibition of Ca²⁺ channels. *Sst* receptors activate a number of phosphatases such as serine threonine phosphatases (White et al. 1991), the Ca²⁺-dependent phosphatase calcineurin (Renstrom et al. 1996), and protein tyrosine phosphatases (PTP) (Florino et al. 1994 and 1996, Buscail et al. 1995, Reardon et al. 1996). This action is dependent on activation of pertussis toxin-sensitive G proteins, but the nature of the G proteins involved and whether

SRIF-28	Ser-Ala-Asn-Ser-Asn-Pro-Ala-Met-Ala-Pro-Arg Glu-Arg-Lys-Ala-Gly-Cys-Lys-Asn-Phe- Phe -Trp Cys-Ser-Thr-Phe-Thr-Lys
SRIF-14	Ala-Gly-Cys-Lys-Asn-Phe- Phe -Trp Cys-Ser-Thr-Phe-Thr-Lys
SMS 201-995 octreotide	D ¹ Phe-Cys- Phe -D ¹ Trp Thr(al)-Cys-Thr-Lys
BIM23014 lanreotide	D ¹ Nal-Cys-Tyr-D ¹ Trp Thr-Cys-Val-Lys
RC-160 vapreotide	D ¹ Phe-Cys-Tyr-D ¹ Trp Trp-Cys-Val-Lys
MK678 seglitide	(N-Me)-Ala-Tyr-D ¹ Trp Phe-Val-Lys

Figure 2. Natural and synthetic peptide agonists of the sst receptor family.

they couple sst receptors directly or indirectly to phosphatases is unknown.

Several laboratories have investigated the coupling of individually expressed sst subtypes to G proteins and various effectors. Despite initial controversy, there is now a growing consensus that all five sst subtypes, and certainly the human isoforms, are functionally coupled to inhibition of adenylyl cyclase (Table 1) (Patel et al. 1994). sst_{1,2,3,4} also stimulate PTP (Table 1). sst₁ stimulates a Na⁺/H⁺ exchanger via a pertussis toxin-insensitive mechanism (Hou et al. 1994). sst₂ suppresses voltage-dependent Ca²⁺ channels in islet RIN M5f cells and N- and P/Q-type Ca²⁺ channels in cultured rat amygdaloid neurons (Viana and Hille 1996). sst₄ activates PLA2-dependent arachidonate production as well as mi-

togen-activated protein kinase (MAPK) in CHO-K1 cells, both via a pertussis toxin-sensitive G protein (Bito et al. 1994, Patel et al. 1995, Reisine and Bell 1995). Acting through sst₃ and sst₅, however, SRIF also inhibits the MAPK signaling cascade (Reardon et al. 1996, Cordelier et al. 1997). Sst modulation of the PLC-IP₃ pathway remains controversial (Patel 1997). In transfected CHO-K1 cells, sst₅ inhibits IP₃-mediated Ca²⁺ mobilization, whereas sst₄ is without effect. By contrast, in COS-7 cells, sst₅ and sst_{2A} both stimulate IP₃ production, albeit only at high agonist concentrations. Major voids still remain in our understanding of sst subtype-selectivity for ion channel coupling and of the molecular signals in the receptors responsible for activation of various phosphatases. Much of our current knowledge on subtype-selectivity for signaling is based on transfected cells and should be interpreted with caution, given the limitations of these systems. The emergence of selective agonists and antagonists should greatly facilitate the study of subtype-selective effector coupling of endogenous sst receptors in normal cells.

• Signal Transduction Pathways for Inhibition of Secretion and Cell Proliferation

Blockade of secretion by SRIF is in part mediated through inhibition of Ca²⁺ and cAMP. Additionally, however, SRIF can inhibit hormone secretion stimulated by cAMP, Ca²⁺, and other second messengers, as well as in permeabilized cells (in

which membrane ion channels are short circuited) through a distal effect, which is believed to be mediated via a G-protein-dependent mechanism linking the receptor to exocytotic vesicles (Figure 3). Such direct inhibition of exocytosis is induced through SRIF-dependent activation of the protein phosphatase calcineurin (Rensstrom et al. 1996). The profound ability of sst and other inhibitory receptors, for example, α -adrenergic and galanin receptors, to block secretion via this distal mechanism suggests that phosphorylation-dephosphorylation events rather than the Ca²⁺ signal play a key role in the distal steps of exocytosis. The specific sst subtypes involved in this process remain to be determined. The antiproliferative effects of SRIF are mediated both indirectly through inhibition of hormones and growth factors that promote cell growth, and directly via sst receptors present on target cells, leading to growth arrest and induction of apoptosis (Srikant 1995, Patel 1997). Several sst subtypes and signal transduction pathways have been implicated. A SRIF-sensitive 66-kD SH2 domain containing PTP called PTP-1C, which dephosphorylates and inactivates growth factor receptor kinases, has been shown to translocate from the cytosol to the plasma membrane upon receptor activation and to associate with sst receptors (Zeggari et al. 1994, Srikant and Shen 1996). SRIF also inhibits MAPK activity via PTP-dependent inactivation of Raf-1 or through inhibition of guanylate cyclase (Reardon et al. 1996, Cordelier et al. 1997). PTP-dependent antiproliferation by SRIF involves both cytostatic and cytotoxic (apoptosis) actions and is dose-dependent and subtype-selective. Apoptosis occurs only in cycling cells, uniquely via the sst₃ subtype, and is associated with induction of wild-type p53 and Bax (Sharma et al. 1996). The remaining four sst subtypes elicit a cytostatic response by inducing G₁ cell cycle arrest associated with activation of the retinoblastoma gene product pRb and the cyclin-dependent kinase inhibitor p21. Whereas apoptosis is triggered at low agonist concentration (≥ 0.1 nM), cytostasis is induced at much higher (≥ 50 nM) agonist concentrations. Overall, this means that acting via sst₃, SRIF will induce apoptosis even when present at low physiological concentrations, whereas it will attenuate the mitogenic signal and trigger growth arrest via sst_{1,2,4,5} only at pharmacological concen-

Table 2. Ligand selectivity of cloned human somatostatin receptors^a

	IC ₅₀ (nM) ^b				
	sst ₁	sst _{2A}	sst ₃	sst ₄	sst ₅
SRIF-14	0.1–2.26	0.2–1.3	0.3–1.6	0.3–1.8	0.2–0.9
SRIF-28	0.1–2.2	0.2–4.1	0.3–6.1	0.3–7.9	0.05–0.4
Octreotide	290–1140	0.4–2.1	4.4–34.5	> 1000	5.6–32
Lanreotide	500–2330	0.5–1.8	43–107	66–2100	0.6–14
Vapreotide	> 1000	5.4	31	45	0.7
Seglitide	> 1000	0.1–1.5	27–36	127– > 1000	2–23
BIM 23052	6.3–100	10–13.5	2.1–5.6	16–141	1.2–7.3
BIM 23056	110– > 1000	132– > 1000	10.8–177	17–234	5.7–14.1
BIM 23268	18.4	15.1	61.6	16.3	0.37
L 362855	> 1000	1	6.2	63– > 1000	0.1–0.016
CH 275 ^c	3.2–4.3	>1000	>1000	4.3–874	>1000

^aBased on Patel and Srikant (1994), Reisine and Bell (1995), Bruns et al. (1996), and Shimon et al. (1997).

^bData of Patel and Srikant (1994) expressed as K_i.

^cFrom Liapakis et al. (1996) and Patel (1997).

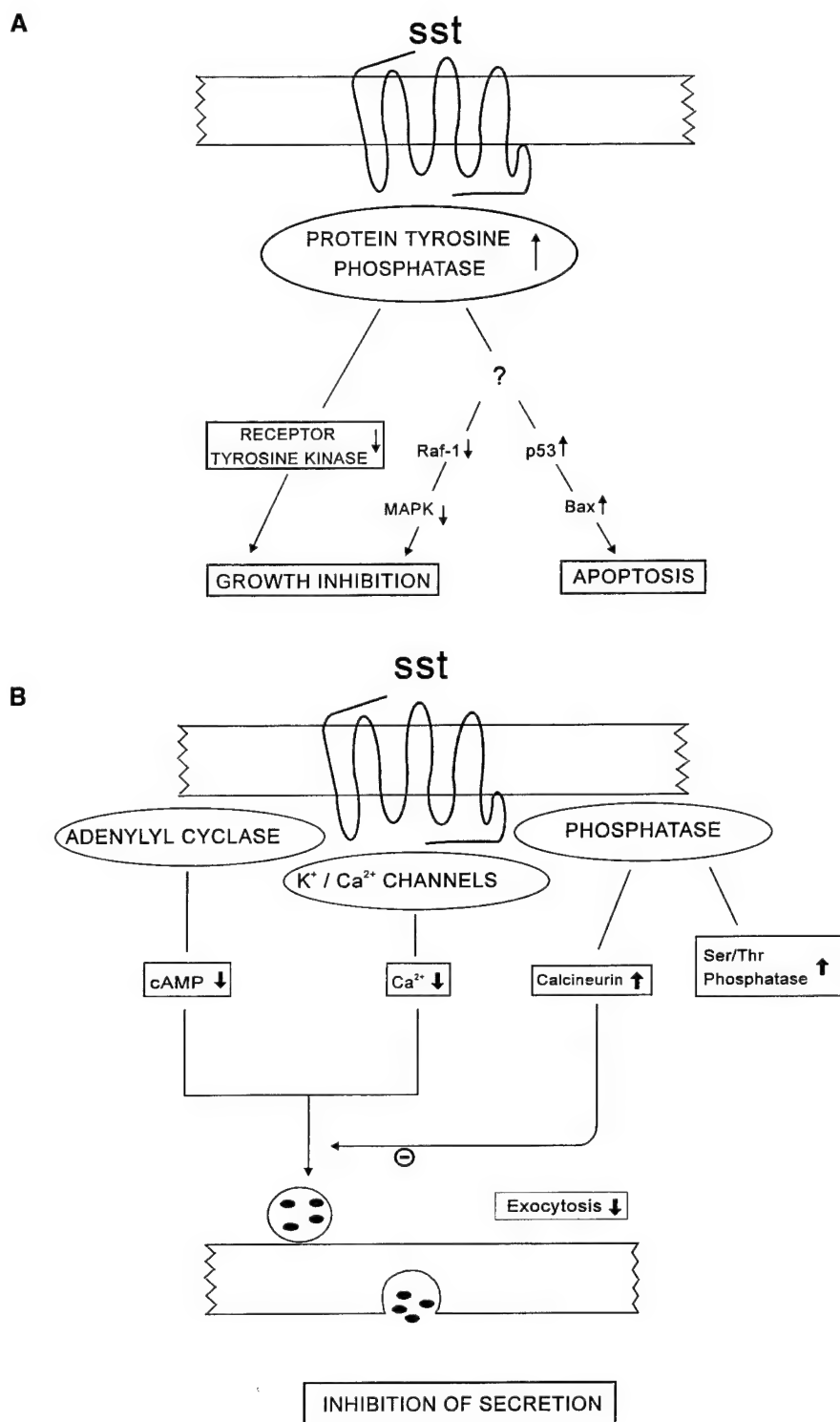


Figure 3. Schematic depiction of the key second-messenger systems involved in somatostatin (SRIF) modulation of cell secretion, cell proliferation, and apoptosis. **(A)** Receptor activation leads to a fall in intracellular cAMP (because of inhibition of adenylyl cyclase), a fall in Ca²⁺ influx (because of activation of K⁺ and Ca²⁺ ion channels) and stimulation of phosphatases such as calcineurin (which inhibits exocytosis), and serine threonine phosphatases (which dephosphorylate and activate Ca²⁺ and K⁺ channel proteins). Blockade of secretion by SRIF is in part mediated through inhibition of Ca²⁺ and cAMP (proximal effect) and through a more potent distal effect involving direct inhibition of exocytosis via SRIF-dependent activation of calcineurin. **(B)** Induction of protein tyrosine phosphatase by SRIF plays a key role in mediating the antiproliferative response by dephosphorylating growth factor receptor kinases and other putative substrates such as p53, Raf-1 and mitogen-activated protein kinase (MAPK) implicated in regulating cell proliferation and apoptosis.

trations. The molecular signal in sst₃ that confers subtype selectivity for apoptosis as well as the downstream pathways for both the cytostatic and cytotoxic actions of SRIF remains to be unraveled but could involve phosphorylation-dependent modulation of p53, Raf-1, MAPK, and other substrates implicated in regulating cell proliferation.

• Subtype-Selective Biological Responses

In view of the many biological actions of SRIF, an important question that arises is whether these effects are subtype-selective or whether multiple subtypes are involved in mediating a given response. The lack of suitable subtype-selective SRIF antagonists has so far proved to be a major impediment in elucidating subtype-specific tissue effects. Based on the pattern of expression of sst receptors in individual target cells as determined by double-label immunocytochemistry or in situ hybridization, there is growing evidence that single cells express several sst subtypes in varying densities (Day et al. 1995, O'Carroll and Krempels 1995, Kumar et al. 1997). For instance, rat somatotrophs feature all five sst isoforms, with sst₅ being the preponderant species (Day et al. 1995, Kumar et al. 1997). On the basis of the differential effects of various SRIF agonists on pituitary, islet, and intestinal responses, several studies have suggested sst₂ selectivity for inhibition of GH, glucagon, and gastric acid secretion in the rat; sst₅ selectivity for insulin inhibition in the rat; and sst₃ selectivity for gastric smooth muscle contractility in the guinea pig (Rossowski and Coy 1994, Wyatt et al. 1996, Gu et al. 1995). Unfortunately, because of questions concerning the subtype monoselectivity of the SRIF analogues used in these studies, these findings remain inconclusive (Patel and Srikant 1994, Bruns et al. 1996). Using a slightly different approach, Shimon et al. (1997) have proposed the mediation of both sst₂ and sst₅ in regulating GH and TSH secretion from the human fetal pituitary. A sst₂-deficient knockout mouse has been recently generated by Zheng et al. (1997) in which sst₂ receptors in arcuate GHRH neurons were found to be solely responsible for mediating GH-induced feedback inhibition of GH. Nonetheless, the animals grew normally and appeared healthy up to 15 months of age, excluding an essential role for sst₂ in embryogenesis

or postnatal growth and development. Although further work is required with this model, the findings so far do not support a preferential role of the sst₂ subtype in the pituitary or other peripheral targets in the rodent.

• Agonist-Dependent Regulation and Desensitization Responses

Although the acute administration of SRIF-14 or SMS produces a diverse range of biological effects, the initial response diminishes with continued exposure to the peptides because of the development of tolerance (Lamberts et al. 1996). Patients with SRIF-producing tumors display sustained hypersomatostatinemia, which, however, causes minimal symptomatology, notably mild steatorrhea, diabetes mellitus, and cholelithiasis secondary to inhibition of pancreatic exocrine secretion, insulin release, and gallbladder contraction. Long-term therapy with SMS is remarkably free of side effects (Lamberts et al. 1996). Most patients develop mild steatorrhea to which they become tolerant after 10–14 days. Likewise, they adapt rapidly to some of the other effects of SMS, for example, inhibition of insulin and TSH secretion, and thereby develop minimal signs of carbohydrate intolerance or hypothyroidism. Some effects, however, do persist, for example, inhibition of gallbladder emptying, which gives rise to a significant increase in the incidence of cholesterol gallstones (Lamberts et al. 1996). What is most interesting is that hormone-producing tumors such as GH adenomas, carcinoids, and VIPomas continue to respond to SMS injections with persistent suppression of hormone secretion, frequently for several years. This suggests a differential regulation of sst receptors in normal tissues and in tumors. Agonist-mediated receptor downregulation could explain the desensitization responses of insulin, TSH, and pancreatic exocrine secretion. The sst receptors involved in modulating biliary function are clearly different, because they do not appear to downregulate with continued SRIF treatment. The ability of hormone-secreting tumors to withstand desensitization may be due to several factors. Tumors express a high density of sst receptors compared with surrounding normal tissues (Lamberts et al. 1996). Conceivably, sst receptors in tumors behave differently owing to a loss of normal

receptor regulatory function or to an alteration in the pattern and composition of the various subtypes expressed or because of abnormal receptor signaling.

Agonist-specific desensitization is common to many GPCRs and is associated with receptor phosphorylation, uncoupling of the receptor from G proteins, receptor internalization, and receptor degradation. Short-term exposure to SRIF has been shown to induce G-protein uncoupling and sst receptor internalization in pituitary and islet cells. Prolonged agonist exposure (24–48 h) upregulates sst receptors in GH₄C₁ and RIN M5f cells (Presky and Schonbrunn 1988). Because normal pituitary and islet cells or their tumor cell derivatives express multiple sst subtypes, it has been necessary to study host cells stably transfected with each sst subtype in order to characterize the response of individual SSTR isotypes. hsst_{2,3,4,5} undergo rapid internalization in a time- and temperature-dependent manner over 60 min in CHO-K1 cells upon agonist activation (Hukovic et al. 1996). Maximum internalization occurs with sst₃ (78%), followed by sst₅ (66%), sst₄ (29%), and sst₂ (20%). In contrast, hsst₁ fails to be internalized. Prolonged agonist treatment for 22 h upregulates hsst₁ at the membrane by 110%, hsst₂ and hsst₄ by 26% and 22%, respectively, whereas hsst_{3,5} show no change (Hukovic et al. 1996). Agonist-promoted receptor upregulation also occurs with other receptors, for example, those for GnRH and dopamine 2, and involves the surface recruitment of preexisting pools of receptors (Ng et al. 1997). The underlying molecular signals remain to be identified. Desensitization and internalization of sst_{2A} and sst₃ receptors are associated with phosphorylation of cytoplasmic residues, especially in the carboxyl terminal segment (Hipkin et al. 1997, Roth et al. 1997). The ability of SRIF to regulate its receptors may provide a mechanism for targeting selective subtypes for diagnosis and therapy. For instance, upregulation of sst₁ and sst₂ by appropriate agonist treatment could be used for enhancing sst receptor expression for receptor scans. Subtypes such as sst₃ and sst₅, which are extensively internalized, could be targeted with selective α - or β -emitting sst radioligands for radiotherapy of certain sst-receptor-positive human cancers.

• Concluding Remarks

During the 6 years since the first sst receptor was cloned, great progress has been made toward characterizing the structure and molecular pharmacology of this receptor family, which now has five members. The rich pattern of expression of sst receptors throughout the brain and in peripheral tissues, coupled with the potent biological effects that they elicit, clearly suggests that sst receptors represent a major class of inhibitory receptors that play an important role in modulating higher brain function, the secretory process, cell proliferation, and apoptosis. Synthetic agonists of SRIF have been in clinical use for over 10 years and now occupy an important therapeutic niche both in the diagnosis and treatment of tumors. These are, however, first-generation compounds that interact with only three of the five sst subtypes. The development of other more selective agonists, as well as subtype-specific antagonists, should greatly expand the scope of SRIF pharmacotherapy. Future studies will need to define the function of individual subtypes, the role of multiple subtypes in the same cell, the downstream signaling pathways responsible for growth arrest and apoptosis, the molecular basis of receptor upregulation, and the mechanisms underlying differential desensitization responses in tumor cells compared with normal cells. Finally, a great deal needs to be learned about the biology of sst receptor dysfunction in neurological, gastroenterological, and immunological disorders.

• Acknowledgments

The work cited from the authors' laboratory was supported by grants from the Canadian Medical Research Council (MT-10411, MT-6011, MT-12603), the National Institutes of Health (NS32160), the U.S. Department of Defense, and the National Cancer Institute of Canada. The expert secretarial help of Maria Correia and Tracy Wilson is gratefully acknowledged.

References

- Bass RT, Buckwalter BL, et al.: 1996. Identification and characterization of novel somatostatin antagonists. *Mol Pharmacol* 50: 709–715.
- Bito H, Mori M, Sakanaka C, et al.: 1994. Functional coupling of SSTR4, a major hip-

- pocampal somatostatin receptor, to adenylylate cyclase inhibition, arachidonate release and activation of the mitogen-activated protein kinase cascade. *J Biol Chem* 269:12,722-12,730.
- Bruno JF, Xu Y, Song J, Berelowitz M: 1992. Molecular cloning and functional expression of a brain-specific somatostatin receptor. *Proc Natl Acad Sci USA* 89:11,151-11,155.
- Bruns C, Raulf F, Hoyer D, Schloos J, Lubbert H, Weckbecker G: 1996. Binding properties of somatostatin receptor subtypes. *Metabolism* 45(Suppl 1):17-20.
- Buscail L, Esteve J-P, Saint-Laurent N, et al.: 1995. Inhibition of cell proliferation by the somatostatin analogue RC-160 is mediated by somatostatin receptor subtypes SSTR2 and SSTR5 through different mechanisms. *Proc Natl Acad Sci USA* 92:1580-1584.
- Cordelier P, Esteve J-P, Bousquet C, et al.: 1997. Characterization of the antiproliferative signal mediated by the somatostatin receptor subtype sst₅. *Proc Natl Acad Sci USA* 94:9343-9348.
- Day R, Dong W, Panetta R, Kraicer J, Greenwood MT, Patel YC: 1995. Expression of mRNA for somatostatin receptor (sstr) types 2 and 5 in individual rat pituitary cells: a double labeling in situ hybridization analysis. *Endocrinology* 136:5232-5235.
- Florio T, Rim C, Hersherberger RE, Loda M, Stork PJ: 1994. The somatostatin receptor SSTR1 is coupled to phosphotyrosine phosphatase activity in CHO-K1 cells. *Mol Endocrinol* 8:1289-1297.
- Florio T, Scarziello A, Fattore M, et al.: 1996. Somatostatin inhibits PC C13 thyroid cell proliferation through the modulation of phosphotyrosine phosphatase activity-impairment of the somatostatinergic effects by stable expression of EIA viral oncogene. *J Biol Chem* 271:6129-6136.
- Greenwood MT, Hukovic N, Kumar U, et al.: 1997. Ligand binding pocket of the human somatostatin receptor 5 (hSSTR5): mutational analysis of the extracellular domains. *Mol Pharmacol* 52:807-814.
- Gu ZF, Corleio VD, Mantey SA, et al.: 1995. Somatostatin receptor subtype 3 mediates the inhibitory action of somatostatin on gastric smooth muscle cells. *Am J Physiol* 268:G739-G748.
- Hipkin RW, Friedman J, Clark RB, et al.: 1997. Agonist-induced desensitization, internalization and phosphorylation of the sst_{2A} somatostatin receptor. *J Biol Chem* 272:13,869-13,876.
- Hou C, Gilbert RL, Barber DL: 1994. Subtype-specific signaling mechanisms of somatostatin receptors SSTR1 and SSTR2. *J Biol Chem* 269:10,357-10,362.
- Hukovic N, Panetta R, Kumar U, Patel YC: 1996. Agonist-dependent regulation of cloned human somatostatin receptor types 1-5 (hSSTR1-5): subtype selective internalization or upregulation. *Endocrinology* 137:4046-4049.
- Kaupman K, Bruns C, Raulf F, Weber HP, Mattes H, Lubbert H: 1995. Two amino acids, located in transmembrane domains VI and VII, determine the selectivity of the peptide agonist SMS201-995 for the SSTR2 somatostatin receptor. *EMBO J* 14:727-735.
- Kumar U, Laird Dd, Srikant CB, Escher E, Patel YC: 1997. Expression of the five somatostatin receptor (SSTR1-5) subtypes in rat pituitary somatotrophs: quantitative analysis by double-label immunofluorescence confocal microscopy. *Endocrinology* 138:4473-4476.
- Lamberts SWJ, Van Der Lely AJ, de Herder WW: 1996. Drug therapy: octreotide. *N Engl J Med* 334:246-254.
- Liapakis G, Haeger C, Rivier J, Reisine T: 1996. Development of a selective agonist at the somatostatin receptor subtype SSTR1. *J Pharmacol Exp Ther* 276:1089-1094.
- Nehring RB, Meyerhof W, Richter D: 1995. Aspartic acid residue 124 in the third transmembrane domain of the somatostatin receptor subtype 3 is essential for somatostatin-14 binding. *DNA Cell Biol* 14:939-944.
- Ng GYK, Varghese G, Chung HT, et al.: 1997. Resistance of the dopamine D_{2L} receptor to desensitization accompanies the upregulation of receptors onto the surface of Sf9 cells. *Endocrinology* 138:4199-4206.
- O'Carroll AM, Krempels K: 1995. Widespread distribution of somatostatin receptor messenger ribonucleic acids in rat pituitary. *Endocrinology* 136:5224-5227.
- O'Carroll AM, Lolait SJ, Konig M, Mahan LC: 1992. Molecular cloning and expression of a pituitary somatostatin receptor with preferential affinity for somatostatin-28. *Mol Pharmacol* 42:939-946.
- Panetta R, Greenwood MT, Warszynska A, et al.: 1994. Molecular cloning, functional characterization, and chromosomal localization of a human somatostatin receptor (somatostatin receptor type 5) with preferential affinity for somatostatin-28. *Mol Pharmacol* 45:417-427.
- Patel YC: 1997. Molecular pharmacology of somatostatin receptor subtypes. *J Endocrinol Invest* 20:348-367.
- Patel YC, Srikant CB: 1994. Subtype selectivity of peptide analogs for all five cloned human somatostatin receptors (hSSTR1-5). *Endocrinology* 135:2814-2817.
- Patel YC, Greenwood MT, Warszynska A, Panetta R, Srikant CB: 1994. All five cloned human somatostatin receptors (hSSTR1-5) are functionally coupled to adenylyl cyclase. *Biochem Biophys Res Commun* 198:605-612.
- Patel YC, Greenwood MT, Panetta R, Demchishyn LL, Niznik HB, Srikant CB: 1995. The somatostatin receptor family. *Life Sci* 57:1249-1265.
- Presky DH, Schonbrunn A: 1988. Somatostatin pretreatment increases the number of somatostatin receptors in GH4C1 pituitary cells and does not reduce cellular responsiveness to somatostatin. *J Biol Chem* 263:714-721.
- Reardon DB, Wood SL, Brautigan DL, Bell GI, Dent P, Sturgill TW: 1996. Activation of a protein tyrosine phosphatase and inactivation of Raf-1 by somatostatin. *Biochem J* 314:401-404.
- Reichlin S: 1983. Somatostatin. *N Engl J Med* 309:1495-1501, 1556-1563.
- Reisine T, Bell GI: 1995. Molecular biology of somatostatin receptors. *Endocr Rev* 16:427-442.
- Renstrom E, Ding WG, Bokvist K, Rorsman P: 1996. Neurotransmitter-induced inhibition of exocytosis in insulin-secreting β cells by activation of calcineurin. *Neuron* 17:513-522.
- Rohrer L, Raulf F, Bruns C, Buettner R, Hofstaedter F, Schule R: 1993. Cloning and characterization of a fourth human somatostatin receptor. *Proc Natl Acad Sci USA* 90:4196-4200.
- Rossowski WJ, Coy DH: 1994. Specific inhibition of rat pancreatic insulin or glucagon release by receptor-selective somatostatin analogs. *Biochem Biophys Res Commun* 205:341-346.
- Roth A, Kreienkamp H-J, Meyerhof W, et al.: 1997. Phosphorylation of four amino acid residues in the carboxyl terminus of the rat somatostatin receptor subtype 3 is crucial for its desensitization and internalization. *J Biol Chem* 272:23,769-23,774.
- Schwartz TW, Rosenkilde MM: 1996. Is there a lock for all agonist keys in 7 TM receptors? *Trends Pharmacol Sci* 17:213-216.
- Sharma K, Patel YC, Srikant CB: 1996. Subtype selective induction of p53-dependent apoptosis but not cell cycle arrest by human somatostatin receptor 3. *Mol Endocrinol* 10:1688-1696.
- Shimon I, Taylor JE, Dong JZ, et al.: 1997. Somatostatin receptor subtype specificity in human fetal pituitary culture. *J Clin Invest* 99:789-798.
- Srikant CB: 1995. Cell cycle dependent induction of apoptosis by somatostatin analog SMS201-995 in AtT-20 mouse pituitary tumor cells. *Biochem Biophys Res Commun* 209:400-407.
- Srikant CB, Shen SH: 1996. Octapeptide somatostatin analog SMS 201-995 induces translocation of intracellular PTP1C to membranes in MCF-7 human breast cancer adenocarcinoma cells. *Endocrinology* 137:3461-3468.

- Viana F, Hille B: 1996. Modulation of high voltage-activated calcium channels by somatostatin in acutely isolated rat amygdaloid neurons. *J Neurosci* 16:6000-6011.
- White RE, Schonbrunn A, Armstrong DL: 1991. Somatostatin stimulates Ca^{2+} -activated K^{+} channels through protein dephosphorylation. *Nature* 351:570-573.
- Wilkinson GF, Feniuk W, Humphrey PPA: 1997. Characterization of human recombinant somatostatin sst_5 receptors mediating activation of phosphoinositide metabolism. *Br J Pharmacol* 121:91-96.
- Wyatt MA, Jarvie E, Feniuk W, Humphrey PPA: 1996. Somatostatin sst_2 receptor-mediated inhibition of parietal cell function in rat isolated gastric mucosa. *Br J Pharmacol* 119:905-910.
- Yamada Y, Post SR, Wang K, et al.: 1992a. Cloning and functional characterization of a family of human and mouse somatostatin receptors expressed in brain, gastrointestinal tract, and kidney. *Proc Natl Acad Sci USA* 89:251-255.
- Yamada Y, Reisine T, Law SF, et al.: 1992b. Somatostatin receptors, an expanding gene family: cloning and functional characterization of human SSTR3, a protein coupled to adenylate cyclase. *Mol Endocrinol* 6:2136-2142.
- Zeggari M, Esteve JP, Raully I, et al.: 1994. Copurification of a protein tyrosine phosphatase with activated somatostatin receptors from rat pancreatic acinar membranes. *Biochem J* 303:441-448.
- Zheng H, Bailey A, Jiang M-H, et al.: 1997. Somatostatin receptor subtype 2 knock-out mice are refractory to growth hormone negative feedback on arcuate neurons. *Mol Endocrinol* 11:1709-1717.

TEM

SOMATOSTATIN AND ITS RECEPTORS

Yogesh C. Patel and Coimbatore B. Srikant

Fraser Laboratories, Departments of Medicine and Neurology and Neurosurgery, Royal Victoria Hospital and Montreal Neurological Institute, Montreal, Quebec, Canada H3A 1A1.

Abbreviated Title: Somatostatin and Its Receptors

Address for correspondence:

Dr. Y.C. Patel

Room M3-15, Royal Victoria Hospital

687 Pine Avenue West

Montreal, Quebec H3A 1A1

CANADA

Tele: (514) 842-1231 ext. 5042

Fax: (514) 849-3681

TABLE OF CONTENTS

Somatostatin distribution and actions	Pg 3
Somatostatin genes, gene productions and regulation of gene expression	Pg 4
Identification of somatostatin receptors (SSTRs)	Pg 7
Molecular cloning of somatostatin receptors	Pg 9
Somatostatin agonists and antagonists	Pg 12
Ligand binding domain	Pg 14
Expression of SSTR Subtypes	Pg 16
G protein coupling and signal transduction	Pg 20
SSTR mediated inhibition of secretion and cell proliferation	Pg 23
Regulation of SSTRs	Pg 27
Regulation of SSTR gene expression	Pg 29
Acknowledgements	Pg 31
References	Pg 32
Figure legends	Pg 49
Tables	Pg51-52

SOMATOSTATIN DISTRIBUTION AND ACTIONS

Somatostatin (SST) a tetradecapeptide was first isolated in 1973 from the hypothalamus as a growth hormone inhibitory substance (Brazeau et al., 1973). Subsequent studies revealed that SST is not only produced in the hypothalamus, but also occurs widely throughout the central nervous system and in the periphery (Hokfelt et al., 1975; Patel and Reichlin, 1978; Reichlin, 1983). Indeed, SST-like immunoreactivity has been found in many tissues in both vertebrate and invertebrate species as well as in the plant kingdom. In mammals, SST producing cells occur at high densities throughout the central and peripheral nervous systems, in the endocrine pancreas and in the gut, and in small numbers in the thyroid, adrenals, submandibular glands, kidneys, prostate, placenta, and lymphoid tissue (Hokfelt et al., 1975; Reichlin, 1983; Patel, 1992). Somatostatin-containing nerve fibers have been detected in the heart. The typical morphological appearance of a SST- producing cell is that of a neuron with multiple branching processes, or a secretory cell often with short cytoplasmic extensions (δ cells) (Finley et al., 1981; Larsson et al., 1979). Brain regions rich in SST producing cells include the hypothalamus, the deeper layers of the cortex, all limbic structures, the striatum, the periaqueductal central grey and all levels of the major sensory pathways (Finley et al., 1981; Patel, 1992). Gut SST cells are of two types: δ cells in the mucosa, and neurons that are intrinsic to the submucous and myenteric plexuses (Hokfelt et al., 1975; Larsson et al., 1979). Somatostatin cells in the pancreas are confined to the islet where they occur as δ cells in close proximity to the insulin, glucagon, and pancreatic polypeptide producing cells (Dubois, 1975). Within the thyroid, SST coexists with calcitonin in a subpopulation of C cells (Reichlin, 1983). In the rat, the gut accounts for ~ 65% of total body SST-like immunoreactivity, the brain for ~ 25%, the pancreas for ~ 5%, and the remaining organs for ~ 5% (Patel and Reichlin, 1978).

Along with its extensive tissue distribution, SST acts on multiple targets to produce a broad range of biological effects (Reichlin, 1983; Patel, 1992). It functions as a neurotransmitter in the brain, with effects on cognitive, locomotor, sensory, and autonomic functions. It inhibits both the basal and stimulated secretion of pituitary, islet, and gastrointestinal hormones, and suppresses TSH-stimulated release of thyroid hormones, calcitonin release, angiotensin II stimulated aldosterone secretion, and acetylcholine stimulated adrenal catecholamine release (Reichlin, 1983; Patel, 1992). Furthermore, it has been shown to regulate the release of growth factors (IGF1, EGF, PDGF) and cytokines (IL-6, $\text{If-}\gamma$) (Hayry et al., 1993). It inhibits gut exocrine secretion and suppresses motor activity generally, as well as through inhibition of gastric emptying, gallbladder contraction, and small intestinal segmentation (Reichlin, 1983; Patel, 1992). Other effects of SST include vasoconstriction especially in the splanchnic circulation, and inhibition of proliferation of intestinal mucosal cells and lymphocytes (Reichlin, 1983; Patel, 1992). The cellular actions of SST which account for these diverse effects consist of the modulation of secretion, cell proliferation, and neurotransmission.

SOMATOSTATIN GENES, GENE PRODUCTS AND REGULATION OF GENE EXPRESSION

Like other protein hormones, SST is synthesized from a large preprosomatostatin (prepro SST) precursor molecule that is processed enzymatically to yield several mature products (reviewed in Patel et al., 1998, in press). cDNAs for several preproSST molecules were first identified in 1980 followed by the elucidation of the structure of the rat and human SST genes in 1984 (Montminy et al., 1984; Shen and Rutter, 1984). The human gene maps to the long arm of chromosome 3. Mammalian proSST consists of a 92 amino acid protein which is processed predominantly at the C-terminal segment to generate two bioactive forms SST-14 and its NH_2 terminally extended form,

SST-28 (Patel et al., 1998, in press) . The two peptides are synthesized in variable amounts by different SST producing cells due to differential precursor processing. SST-14 predominates in pancreatic islets, stomach, and in neural tissues and is virtually the only form in retina, peripheral nerves and enteric neurons. SST-28 accounts for 20-30% of total immunoreactive SST in brain but it is not clear whether it is cosynthesized with SST-14 or whether it is produced in separate neurons. SST-28 is synthesized as a terminal product of proSST processing in intestinal mucosal cells which constitute the largest peripheral source of the peptide. Several genes encoding SST-like peptides have been identified (Montminy et al., 1984; Shen and Rutter, 1984; Hobart et al., 1980; Tostivini et al., 1996; Patel et al., 1998, in press). The various forms of SST observed in mammals are all derived from differential processing of a common precursor, preproSST-I. In the fish, however, there are two separate genes, one corresponding to mammalian preproSST-I which gives rise to only SST-14, and another preproSST-II which generates NH₂-terminally extended forms of SST such as anglerfish 28, a homolog of mammalian SST-28, and catfish 22. The SST-14 sequence is totally conserved between fish and mammals whereas mammalian SST-28 shares only 40-66% homology with its fish counterparts. Interestingly, expression of the SST-28 encoding genes in fish is restricted to the pancreatic islets whereas the SST-14 encoding gene, like its mammalian counterpart, is widely expressed in many body cells including the pancreas. Recently, a novel second SST-like gene called cortistatin (CST) has been described in humans and rat which gives rise to two putative cleavage products comparable to SST-14 and SST-28 (De Lecea et al., 1996). These consist of human CST-17 and its rat homolog CST-14, and human and rat CST-29. Unlike the broad distribution of the preproSST I gene, gene expression of CST is restricted to the cerebral cortex. The human CST gene is distinct from the preproSST II gene and appears to be the homolog of a recently described novel

SST-like gene in the frog whose expression is also restricted to the brain (Tostivini et al., 1996). Based on nucleotide sequence homologies, the picture that emerges suggests that the preproSST I gene of the fish is the common ancestral gene which has evolved into the human preproSST gene. The preproSST II gene of teleosts arose from a gene duplication event. A separate duplication event in the tetrapod lineage ~ 400 million years ago gave rise to the CST gene which has been carried through from amphibians to man (Tostivini et al., 1996).

The transcriptional unit of the rat SST gene consists of exons of 238 and 367 bp separated by an intron of 621 bp (Montminy et al., 1984; Patel et al., 1998, in press) (INSERT FIGURE 1 ABOUT HERE). The 5' upstream region contains a number of regulatory elements: a variant of the TATA box at -26 bp, a cAMP response element (CRE) at -48 to -41 bp, two nonconsensus glucocorticoid response elements (GREs) at -167 and -219 bp, and a consensus insulin response element CGGA activated by an ETS-related transcription factor in the 5' UT at +43 to +46 bp. In addition, tissue-specific promoter elements consisting of TAAT motifs that operate in concert with CRE to provide high level constitutive activity are reiterated three times over a 500 nucleotide region (Patel et al., 1998, in press). Steady state SST mRNA levels are stimulated by various members of the growth factor-cytokine family (GH, IGF-1, IL-1, TNF α , and IL-6), glucocorticoids, testosterone, estradiol, and NMDA receptor agonists, and inhibited by glucocorticoids and insulin (Patel et al., 1998, in press). Among the intracellular mediators known to modulate SST gene expression are Ca²⁺, cAMP, cGMP, and nitric oxide (NO). cAMP is a potent activator of both gene transcription and secretion of SST and has emerged as the most prominent signalling pathway for regulating SST function. cAMP induces transcription of the SST gene via CRE which binds a 43 kDa nuclear protein

CREB (cAMP response element binding protein) whose transcriptional efficacy is regulated through phosphorylation by the cAMP-dependent protein kinase A (Montminy et al., 1995). cAMP-inducible transcriptional activation in turn requires the recruitment of a 265 kDa CREB binding protein (CBP) which acts as an adaptor molecule linking CREB to the polymerase II complex (Kowk et al., 1994; Montminy et al., 1995). Ca^{2+} -dependent induction of the SST gene occurs through phosphorylation of CREB by the Ca^{2+} -dependent protein kinases I and II. Induction of the SST gene by GH is transcriptionally induced through promoter interaction at the -71 to -44 bp region (Patel et al., 1998, in press). IGF-1 and IGF-2 also stimulate SST gene transcription in promoter transfection studies although the nature of the promoter interaction remain unknown. Likewise, the molecular mechanisms underlying the potent stimulation of SST mRNA levels by cytokines remains to be clarified. Glucocorticoids exert a dual effect on the SST gene involving both transcriptional activation through interaction between the glucocorticoid receptor and SST promoter elements between -250 and -71 bp, as well as through accelerated SST mRNA degradation (Patel et al., 1998, in press). Finally, estrogens, testosterone, cGMP, and NO all augment steady state SST mRNA levels but the direct or indirect bases as well as the molecular mechanisms underlying the effects of these agents remain to be determined.

IDENTIFICATION OF SOMATOSTATIN RECEPTORS (SSTRs)

The actions of SST are mediated through high affinity plasma membrane receptors (termed SST receptors, SSTRs) which were first described in the pituitary GH_4C_1 cell line by Schonbrunn and Tashjian using whole cell binding analyses (Schonbrunn and Tashjian, 1978). Subsequent studies using a variety of other techniques such as membrane binding analyses, *in vivo* and *in vitro*

autoradiography, covalent crosslinking, and purification of the solubilized receptor, showed the occurrence of SSTRs in varying densities in brain, gut, pituitary, endocrine and exocrine pancreas, adrenals, thyroid, kidneys, and immune cells (reviewed in Patel et al., 1995; Reisine and Bell, 1995; Patel et al., 1997). SSTRs have also been localized in a number of other cell lines, e.g. AtT-20 pituitary tumor cells, hamster insulinoma and Rin m5f islet tumor cells, AR42J and Mia PaCa pancreatic tumor cells, and in human breast cancer, neuroblastoma, glioma, and leukemic and myeloma cell lines (reviewed in Patel et al., 1995; Reisine and Bell, 1995; Patel et al., 1997). The existence of more than one SSTR subclass was first proposed based on differential receptor binding potencies and actions of SST-14 and SST-28 in brain, pituitary, and islet cells (Mandarino et al., 1981; Srikant and Patel, 1981). Subsequent studies confirmed and extended these observations towards the realization that not only were there distinct SST-14 and SST-28 selective receptors but that the SST-14 binding site itself was heterogeneous and could be further distinguished into two subclasses that are differentially sensitive to the octapeptide SST analog SMS201995 (Tran et al., 1985). Identical findings were reported with the hexapeptide SST analog MK678 and led to the classification of SSTRs into two subtypes, SRIF I which bound octapeptide and hexapeptide analogs and SRIF II which was insensitive to these compounds (Reisine and Bell, 1995). Attempts to characterize the molecular properties of SSTRs by chemical crosslinking of receptor bound radioligands have yielded widely divergent size estimates ranging from 21-228 kDa (Patel et al., 1995; Reisine and Bell, 1995; Patel et al., 1997). Much of this discrepancy may be explained by differential glycosylation of the receptor proteins and by the use of different ligands, different crosslinking conditions, and possibly receptor degradation. Photoaffinity labelling and purification studies, which are much more specific, have provided evidence for the existence of several molecular species of

SSTR proteins of 32-85 kDa which are expressed in a tissue-specific manner, and some which exhibit selective agonism for SST-14 or SST-28. In the rat, these include a 58 kDa form found in most tissues and additional 32 kDa and 80 kDa receptor proteins unique to the brain and pituitary respectively (Srikant et al., 1992). Photoaffinity labelled bands of 72, 75, 82, and 85 kDa have been identified respectively in H1T insulinoma, AR42J pancreatic and AtT-20 and GH₄C₁ pituitary tumor cells (Brown et al., 1990).

MOLECULAR CLONING OF SOMATOSTATIN RECEPTORS

Proof of the existence of more than one subtype of the SSTR came in 1992 with molecular cloning which revealed a more extensive receptor family than previously suspected from pharmacological and biochemical criteria (Patel et al., 1995; Reisine and Bell, 1995; Patel, 1997). To date five distinct SSTR genes have been identified (INSERT TABLE 1 ABOUT HERE). Yamada et al (1992) cloned the first two SSTRs (SSTR1 and SSTR2) in early 1992 as the human and mouse homolog of SSTR1 and SSTR2. The rat SSTR2 gene was identified simultaneously by Kluxen et al (1992). The success of these two laboratories was rapidly followed by the cloning of rat SSTR1, bovine and porcine SSTR2, mouse, rat and human SSTR3, rat, mouse and human SSTR4, and rat, mouse, and human SSTR5 (Patel et al., 1995; Reisine and Bell, 1995; Patel, 1997). Genes for four of the receptors (SSTR1,3,4,5) lack classical introns. The SSTR2 gene displays a cryptic intron at the 3' end of the coding segment which gives rise to two separate isoforms, a long (SSTR2A) and a short (SSTR2B) variant through alternate mRNA splicing (Vanetti et al., 1992; Patel et al., 1993). In the human gene, the spliced exon encodes for 25 amino acid residues compared to 38 residues in the unspliced form (Patel et al., 1993). The 2A and 2B variants differ only in the

length of the cytoplasmic C-tail. There are thus six putative SSTR subtypes of closely related size, each displaying a 7 transmembrane domain (TM) topology typical of G-protein coupled receptors (GPCR) (INSERT FIGURE 2 ABOUT HERE). In humans, the five SSTR genes localize on separate chromosomes (Table 1). The encoded receptor proteins range in size from 356-391 amino acid residues and show the greatest sequence similarity in the putative TMs (55-70% sequence identity), and diverge the most at their amino and carboxy terminal segments (Patel et al., 1995; Reisine and Bell, 1995; Patel, 1997). Overall, there is 39-57% sequence identity among the various members of the SSTR family. All SSTR isoforms that have been cloned so far from humans as well as other species possess a highly conserved sequence motif YANSCANPI/VLY in the VIIth TM which serves as a signature sequence for this receptor family (Fig. 2). The five hSSTRs display 1-4 sites for N-linked glycosylation within the amino terminal segment and second extracellular loop (ECL) (subtype 5). All of the hSSTRs feature 3-8 putative recognition motifs for protein phosphorylation by protein kinase A, protein kinase C, and calmodulin kinase II in the cytoplasmic C-terminal segment and within the second and third intracellular loops. hSSTR1, 2, 4, 5 display a conserved cysteine residue 12 amino acids downstream from the VIIth TM which may be the site of a potential palmitoyl membrane anchor as observed in several other members of the GPCR superfamily. Covalent attachment of palmitic acid in this position likely creates a fourth cytoplasmic loop. Interestingly, hSSTR3 which uniquely lacks the cysteine palmitoylation membrane anchor features a much longer C-tail than the other four members of the family. Using polyclonal antipeptide receptor antibodies, Western blot analysis of the five hSSTR subtypes individually expressed in mammalian cell lines has revealed size estimates of 53-72 kDa for hSSTR1, 71-95 kDa for hSSTR2, 65-85 kDa for hSSTR3, 45 kDa for hSSTR4, and 52-66 kDa for hSSTR5 (Patel et al., 1994; Helboe et al., 1997) (Table 1). Enzymatic

deglycosylation reduces the size of hSSTR1, 2, 3, and 5 to that of the core protein confirming N-linked glycosylation of these four subtypes (Helboe et al., 1997). hSSTR4 on the other hand does not appear to be glycosylated at its single putative glycosylation site (Helboe et al., 1997). The size of the native rat SSTR2 receptor has been determined by Western blot analysis of brain and pancreatic membranes as well as by purification of the receptor from GH₄C₁ cells to be in the range of 72-90 kDa, comparable to that of the human homolog (Patel et al., 1994; Dournaud et al., 1996; Mezey et al., 1998). The five SSTR subtypes display a remarkable degree of structural conservation across species. For instance, there is 94-99% sequence identity between the human rat and mouse isoforms of SSTR1, 93-96% sequence identity between human, rat, mouse, porcine, and bovine isoforms of SSTR2, and 88% sequence identity between the rat and human isoforms of SSTR4. SSTR3 and SSTR5 are somewhat less conserved showing 82-83% sequence identity between the human and rodent homolog. The nearest relatives of the SSTRs are the opioid receptors whose δ subtype displays a 37% sequence similarity to the mouse SSTR1. The question of whether there are additional members of the SSTR family still waiting to be cloned, remains open. There is some evidence for a variant form of SSTR5 (Patel et al., 1994). Cortistatin which is capable of interacting with the five known SSTR subtypes, nonetheless possesses unique neuronal depressant and sleep modulating properties that are not present in SST, suggesting a separate CST receptor which may be related to the SSTR family (De Lecea et al., 1996; Patel, 1997). Several novel genes with sequence similarity to the SSTR family have been recently described. Two of these (SLC-1/GPR-24, GPR-25) display 34-40% sequence homology with the TMs of SSTRs but do not contain the YANSCANPI/VLY motif (Kolakowski et al., 1996; Jung et al., 1997). These receptors do not bind SST or any other known ligand and therefore currently remain as orphan receptors which probably

belong to a related family.

SOMATOSTATIN AGONISTS AND ANTAGONISTS

Like other transmitter substances, endogenous SST is thought to be produced mainly at local sites of action and is rapidly inactivated following release by peptidases in tissue and blood, thereby minimizing unwanted systemic effects. Injections of synthetic SST, however, produce a wide array of effects due to simultaneous activation of multiple target sites. Thus, for effective pharmacotherapy with SST, it is necessary to design analogs with more selective actions and with greater metabolic stability than the naturally occurring peptides (INSERT FIGURE 3 ABOUT HERE). Structure-activity studies of SST-14 have shown that amino acid residues Phe⁷, Trp⁸, Lys⁹ and Thr¹⁰ which comprise a β turn are necessary for biological activity with residues Trp⁸ and Lys⁹ being essential, whereas Phe⁷ and Thr¹⁰ can undergo minor substitutions, e.g. Phe \rightarrow Tyr and Thr \rightarrow Ser or Val. The general strategy for designing SST analogs has been to retain the crucial Phe⁷, Trp⁸, Lys⁹, Thr¹⁰ segment and to incorporate a variety of cyclic and bicyclic restraints through either a disulphide bond or amide linkage to stabilize the β turn around the conserved residues. In this way, a library of short synthetic compounds have been synthesized, several of which show greater metabolic stability and subtype selectivity compared to SST-14 (INSERT TABLE 2 ABOUT HERE). The five hSSTR subtypes bind SST-14 and SST-28 with nanomolar affinity. hSSTR1-4 bind SST-14 \geq SST-28 whereas hSSTR5 exhibits 10-15 fold selectivity for SST-28 compared to SST-14 (Patel and Srikant, 1994; Patel et al., 1995; Patel, 1997). The putative mature products of the CST precursor hCST-17 and rCST-14 display nanomolar affinity for the five hSSTRs. Synthetic rCST-29 binds to hSSTR1, 3, 4 with comparable affinity to SST-14. Its affinity for SSTR2 and SSTR5 is 5-100 fold lower than

that of SST-14 and SST-28 (Patel, 1997). The two octapeptide analogs SMS201995 (SMS, Octreotide), and BIM23014 (Lanreotide) that are in clinical use, as well as the octapeptide RC160 (Vapreotide) and the hexapeptide MK678 (Seglitide) bind to only three of the five hSSTR subtypes, displaying high affinity for subtypes 2 and 5 and moderate affinity for subtype 3 (Patel et al., 1995; Reisine and Bell, 1995; Patel, 1997; Patel and Srikant, 1994; Bruns et al., 1996; Shimon et al., 1997). It should be noted that the binding affinity of SMS, BIM23014, RC160, and MK678 for subtypes 2 and 5 is comparable to that of SST-14 indicating that they are neither selective for these subtypes nor more potent than the endogenous ligands (Patel and Srikant, 1994). The striking low affinity interaction of hSSTR1 and 4 with the conformationally restricted analogs, coupled with their high degree of amino acid identity has led to the subdivision of these two receptors into a distinct SSTR subclass (Hoyer et al., 1995). SSTR2, 3, and 5 react with these analogs and fall into another subgroup. These two subclasses correspond to the previously described SRIF II and SRIF I receptor subtypes respectively. Other than SST-14 and SST-28 and some of their immediate structural derivatives, there are no current SST compounds capable of binding to all five subtypes (Patel and Srikant, 1994). The analog Des AA_{1,2,5} [D-Trp⁸ IAMP⁹] SST (CH275) has been recently described as a SSTR1 selective compound (Liapakis et al., 1996). In our hands, CH275 also binds to SSTR4 and appears to be a prototypic agonist for the SSTR1,4 subclass (Patel, 1997). Several other SST analogs have been similarly reported to be selective for one SSTR subtype, e.g. BIM23056 (SSTR3), and BIM23052 and L362-855 (SSTR5) (Reisine and Bell, 1995). Because of methodological variations in the binding analyses, such claims of subtype selectivity of these and other analogs have not been confirmed by others and remain disputed (Patel and Srikant, 1994; Bruns et al., 1996). To resolve these discrepancies, several groups have analysed these and other SST analogs under uniform

binding conditions using only the human SST clones (Patel and Srikant, 1994; Bruns et al., 1996; Shimon et al., 1997). On the basis of these results, BIM23268 displays modest selectivity for hSSTR5 and appears to be the only currently available subtype monospecific analog. L362855 binds well to SSTR5 and SSTR2, being only weakly selective for SSTR5. NC8-12 displays modest 20-50 fold selectivity for hSSTR2 and 3; DC2360, EC5-21, and BIM23197 exhibit 19-50 fold selectivity for hSSTR2 although these compounds also bind well to hSSTR5. Overall then these results suggest that the binding selectivity of the present generation of SST analogs for the human SSTR subtypes is relative rather than absolute; except for BIM23268 which displays some monospecificity for hSSTR5, there are no other pure agonists available for any of the individual subtypes. Very recently, the first potential SST peptide antagonists have been described (Bass et al., 1996). One such compound [Ac-4-NO₂ - Phe-c (D-Cys-Tyr-D-Trp-Lys-Thr-Cys) -D-Tyr-NH₂] binds to hSSTR2 and hSSTR5 with nM affinity but antagonizes receptor-effector coupling to adenylyl cyclase (Bass et al., 1996). A second peptide BIM23056 also blocks hSSTR5 signalling and appears to be an antagonist for this subtype (Wilkinson et al., 1997).

LIGAND BINDING DOMAIN

Because of the difficulty in crystalizing GPCRs, attempts to elucidate the ligand binding domain of these molecules have resorted to indirect methods such as site-directed mutagenesis and receptor chimeras. Such studies from other GPCR systems have suggested that the ligand binding domain is made of a number of noncontiguous amino acid residues which form a binding pocket within the folded 3 dimensional structure of the receptor (Baldwin, 1994). An alternative view proposes that there is no binding cavity as such, but that agonists interact with crucial residues in the

extracellular and/or TM domains to stabilize preformed active receptor conformations ((Schwartz and Rosenkilde, 1996). In the case of very large protein ligands such as glycoprotein hormones, the interacting residues appear to be exclusively located in the amino terminal segment. Biogenic amines interact with residues exclusively within the TMs. In contrast, the ligand binding site of peptide agonists comparable to SST typically involves residues in the ECLs or both the ECLs and the TMs. By taking advantage of the binding selectivity of ligands such as SMS for hSSTR2 but not hSSTR1, Kaupman et al (1995) systematically mutated hSSTR1 to resemble hSSTR2. They identified two crucial residues Gln²⁹¹ and Ser³⁰⁵ in TMs VI and VII respectively of hSSTR1 substitution of which for the corresponding residues Asn²⁷⁶ and Phe²⁹⁴ in hSSTR2 increased the affinity of hSSTR1 for SMS and other octapeptide analogs 1000 fold. By molecular modelling using these identified residues as well as the known structure of SMS, Kaupman et al have postulated a binding cavity for SMS involving hydrophobic and charged residues located exclusively within TMs III-VII. Their model predicts that the core residues Phe⁷, Trp⁸, Lys⁹ and Thr¹⁰ of SMS interact with Asn²⁷⁶ and Phe²⁹⁴ located at the outer end of TMs VI and VII respectively (present in hSSTR2 but not in hSSTR1) which provide a hydrophobic environment for lipophilic interactions with Phe⁷, Trp⁸ and Thr¹⁰, whereas Asp¹³⁷ in TM III anchors the ligand by an electrostatic interaction with Lys⁹. SMS binds poorly to hSSTR1 because of the presence of residues Gln²⁹¹ and Ser³⁰⁵ located close to the extracellular rims of TM helices VI and VII which prevent the short peptide from reaching deep within the pocket whereas the corresponding residues Asn²⁷⁶ and Phe²⁹⁴ in hSSTR2 provide for a stable interaction with the disulphide bridge of SMS. Because of their greater length and flexibility, the natural ligands SST-14 and SST-28 can presumably adopt a conformation that allows their entry into the binding pocket of all five SSTRs. Such a model is consistent with mutational studies of the

Asp residue in TM III which abolishes ligand binding although it is not known whether this is due to a direct interaction of the residue with SST ligands or to an allosteric alteration in receptor structure (Nehring et al., 1995). Using chimeric mouse SSTR1/SSTR2 receptors, Fitz-Patrick and Vandlen have confirmed the importance of residues in the upper segments of TMs VI and VII for binding the hexapeptide MK678 (Fitz-Patrick and Vandlen, 1994). It should be noted that the residues identified by mutagenesis so far to be important in recognizing SMS and MK678 have not been shown directly to be critical for binding the natural ligands SST-14 and SST-28. Furthermore, the assumption that the hSSTR2 ligand binding pocket may be common for the other SSTR subtypes may not be valid since closely related GPCRs feature different sets of epitopes for binding of a common ligand. The involvement of the extracellular domains for binding SST ligands has been investigated by Greenwood et al (Greenwood et al., 1997). Their results predict a potential contribution of ECL2 (but not of ECL1, ECL3 or the amino terminal segment) to binding of the natural SST ligands (SST-14, SST-28) as well as SMS. The overall model that emerges from these studies suggests a binding domain for SST ligands made up of residues within TMs III-VII, with a potential contribution by ECL2, and is consistent with other peptide binding GPCRs such as neurokinin I, angiotensin II, and GnRH receptors which also interact with residues in both ECLs and TMs.

EXPRESSION OF SSTR SUBTYPES

The cellular expression of SSTR subtypes has been characterized in rodent and human tissues as well as various tumors and tumor cell lines by mRNA analysis using Northern blots, reverse transcriptase-PCR, ribonuclease protection assay, and *in situ* hybridization. With the recent development of subtype selective SSTR antibodies, several laboratories have additionally begun to

localize the individual SSTR proteins by immunocytochemistry. These studies have revealed expression of multiple SSTR mRNAs in brain and peripheral organs with an overlapping but characteristic pattern that is subtype-selective, tissue-specific, and species-specific (Patel et al., 1995; Reisine and Bell, 1995; Patel, 1997). In the rat, mRNA for SSTR1-5 has been localized in cerebral cortex, striatum, hippocampus, amygdala, olfactory bulb, and preoptic area (reviewed in Bruno et al., 1993). Areas rich in expression of individual subtype genes are cerebral cortex for types 1 and 2, amygdala for types 1 and 3, and the hypothalamus and preoptic area for type 5. SSTR4 is the least well expressed subtype in brain compared to the other four isoforms. In contrast to the rat, there is negligible expression of SSTR5 mRNA in the human brain (Thoss et al., 1996). The distribution of SSTR2 in rat brain by immunohistochemistry shows a rich expression of receptors in neuronal perikarya, dendrites, and axon terminals in cerebral cortex and limbic structures (Dournaud et al., 1997). Furthermore, double labelling studies have suggested that a subset of SSTR2 receptors consist of autoreceptors on SST immunopositive neurons (Dournaud et al., 1998). Adult rat pituitary features all five SSTR genes whereas the adult human pituitary expresses four of the subtypes 1, 2, 3, and 5 (Bruno et al., 1993; Panetta and Patel, 1994; Day et al., 1995; O'Carroll and Krempels, 1995). hSSTR4 is transiently expressed during development but is absent in the adult (Panetta and Patel, 1994). Colocalization of the SSTRs in pituitary cell subsets in the rat has revealed expression of one or more subtypes in all of the major pituitary cell types including corticotrophes and gonadotrophes, previously thought to be SSTR negative (Day et al., 1995; O'Carroll and Krempels, 1995). SSTR5 is the principal subtype expressed throughout the pituitary followed by SSTR2 (Day et al., 1995). Immunohistochemical colocalization has demonstrated SSTR5 as the predominant subtype in rat somatotrophes being expressed in 86% of cells (Kumar et al., 1997). The

preponderance of SSTR5, the only SST-28 preferring subtype, correlates with the reported higher potency of SST-28 than SST-14 for inhibiting GH secretion in the rat. A proportion of somatotrophs colocalize both SSTR5 and SSTR2 providing proof for the expression of more than one SSTR subtype in individual target cells (Mezey et al., 1998). Although there are no direct data on the pattern of expression of SSTRs in the human pituitary, SSTR5 and SSTR2 appear to be the principal subtypes mediating GH suppression in the human based on pharmacological evidence correlating the preferential agonist binding properties of some SST analogs for SSTR2 and SSTR5 with their ability to regulate GH secretion from human fetal pituitary cultures (Shimon et al., 1997).

Previous studies using autoradiography have described SST-14 selective binding sites on rat islet α cells and SST-28 preferring sites on β cells which may account for the selective suppression of glucagon by SST-14 and of insulin by SST-28 in this species (Amherdt et al., 1987). Rat islets have been found to express all five SSTR mRNA species (Patel et al., 1995). In the case of human islets, immunohistochemical colocalization of SSTR1-5 with insulin, glucagon, and SST has revealed predominant expression of SSTR1, 2, and 5 (Kumar et al., 1998). Like pituitary cells, islet β , α , and δ cells each express multiple SSTR isoforms. Although there is no absolute specificity of any SSTR for an islet cell type, SSTR1 is preferentially expressed in β cells, SSTR2 in α cells, and SSTR5 in β and δ cells. Such selectivity could form the basis for preferential insulin suppression by SSTR5 specific ligands and of glucagon inhibition by SSTR2 selective compounds. Human stomach expresses all five SSTR subtypes (LeRomancer et al., 1996). Rat small intestine displays moderate levels of SSTR1 and 5, low levels of SSTR3 and 4, but no expression of SSTR2 mRNA (Bruno et al., 1993). The adrenals, a known target of SST action, display a rich concentration of SSTR2 and

modest levels of SSTR1 and 3 (Bruno et al., 1993; Patel et al., 1995). A number of peripheral organs exhibit a surprising level of expression of some SSTR subtypes, e.g. SSTR3 in the liver and spleen, SSTR4 in the lung, heart, and placenta, and SSTR1, 2, and 3 in spermatocytes and Sertoli cells in the testis (Bruno et al., 1993; Patel et al., 1995; Zhu et al., 1998).

In addition to normal tissues, many tumor cell lines of pituitary (AtT-20, GH₄C₁), islet (Rin m5f, HIT), pancreatic (AR42J), breast (MCF7) and neural (LA-N-2 neuroblastoma) origin are rich in SSTRs that are typically expressed as multiple SSTR mRNA subtypes (Patel et al., 1995; Reisine and Bell, 1995; Patel, 1997). Likewise, the majority of human tumors either benign or malignant are generally positive for SSTRs featuring more than one isotype (Patel, 1997). These include functioning and nonfunctioning pituitary tumors, carcinoid tumors, insulinomas, glucagonomas, pheochromocytoma, breast carcinoma, renal carcinoma, prostate carcinoma, meningioma, and glioma. The general pattern of SSTR expression in these tumors suggests a very high frequency of SSTR2 mRNA in all tumors. mRNA for SSTR1 is the next most common, followed by SSTR3 and 4. SSTR5 expression appears to be tumor-specific being 100% positive in some tumors, e.g. breast, but absent in others, e.g. islet cell tumors (Patel, 1997). It should be noted that all analyses of SSTR subtypes in tumors carried out so far are based on mRNA expression which may not necessarily reflect functional receptor levels. Future studies will need to correlate mRNA expression with receptor protein expression by immunocytochemistry or binding analyses with subtype selective analogs.

G PROTEIN COUPLING AND SIGNAL TRANSDUCTION

Somatostatin receptors elicit their cellular responses through G protein-linked activation of multiple second messenger systems including adenylyl cyclase, Ca^{2+} and K^+ ion channels, a Na^+/H^+ antiporter, guanylate cyclase, phospholipase C, phospholipase A_2 , MAP kinase (MAPK), and serine threonine, and phosphotyrosyl protein phosphatase (PTP) (Patel et al, 1995; Reisine and Bell, 1995; Patel, 1997) (Table 1). Inhibition of adenylyl cyclase and cAMP formation is a key event in SSTR signalling. Based on the ability of antiserum to G_i or antisense G_i plasmids to block SSTR inhibition of adenylyl cyclase in AtT-20 and GH_4C_1 cells, all three $\text{G}_{i\alpha}$ subunits, $\text{G}_{i\alpha 1}$, $\text{G}_{i\alpha 2}$, and $\text{G}_{i\alpha 3}$ have been shown to mediate SSTR coupling to adenylyl cyclase (Tallent and Reisine, 1992; Liu et al, 1994; Zhu et al, 1998). SSTRs are coupled to several subsets of K^+ channels including delayed rectifier, inward rectifier, ATP-sensitive K^+ channels, and large conductance Ca^{2+} activated BK channels (Patel et al, 1995; Reisine and Bell, 1995; Patel, 1997). $\text{G}_{i\alpha 3}$, and $\beta\gamma$ dimers which associate with $\text{G}_{i\alpha 3}$ appear to be responsible for transducing SSTR activation of the inwardly rectifying K^+ current. G protein mediation of the other K^+ channel subsets remains to be determined. Receptor activation of K^+ channels induces hyperpolarization of the membrane, rendering it refractory to spontaneous action potential activity leading to a secondary reduction in intracellular Ca^{2+} due to inhibition of the normal depolarization induced Ca^{2+} influx via voltage sensitive Ca^{2+} channels. In addition to this indirect effect on Ca^{2+} entry, SSTRs act directly on high voltage-dependent Ca^{2+} channels via $\text{G}_{o\alpha 2}$ protein to block Ca^{2+} currents. Stimulation of both K^+ and Ca^{2+} channels can additionally occur through dephosphorylation of the channel proteins secondary to SSTR activation of a serine threonine phosphatase (White et al, 1991). Furthermore, SSTRs may inhibit Ca^{2+} currents through induction of cGMP which activates cGMP protein kinase with further phosphorylation-dependent inhibition of

Ca^{2+} channels (Meriney et al, 1994). SSTRs activate a number of phosphatases such as serine threonine phosphatases, the Ca^{2+} -dependent phosphatase calcineurin, and PTP (White et al., 1991; Renstrom et al., 1996; Florio et al, 1994; Buscail et al., 1995; Reardon et al., 1996; Florio et al., 1996). These actions are dependent on stimulation of pertussis toxin-sensitive G proteins but the specific G proteins involved and whether they couple SSTRs directly or indirectly to phosphatases is unknown. SSTRs in colon carcinoma cells are coupled to a Na^+/H^+ exchanger via a pertussis toxin insensitive mechanism (Barber et al., 1989). Other signalling pathways for endogenous SSTRs that are somewhat less well characterized include phospholipase A_2 -dependent stimulation of arachidonate production in hippocampal neurons and phospholipase C-mediated stimulation of IP_3 formation in intestinal smooth muscle cells (Schweitzer et al., 1990; Murthy et al., 1996).

A key issue concerning the signalling specificity of a family of receptor isotypes such as the SSTRs is whether a given subtype activates only one or several G protein linked effector pathways. Several laboratories have begun to address this question using SSTR subtypes individually expressed in various host cells. A putative BBxB (where B is a basic residue) consensus sequence for G protein coupling exists in the third cytoplasmic loop of SSTR2,3,4,5 but not SSTR1. SSTR2A purified from GH_4C_1 cells or expressed in CHO cells is capable of associating with $\text{G}_{i\alpha 1}$, $\text{G}_{i\alpha 2}$, $\text{G}_{i\alpha 3}$ and $\text{G}_{\alpha 2}$ (Luthin et al., 1993; Gu and Schonbrunn, 1997). SSTR3 couples to both $\text{G}_{i\alpha 1}$ and $\text{G}_{i\alpha 3}$ (Law et al., 1994). The specific G proteins which associate with the other SSTR subtypes have not been determined. Although there were conflicting data from different laboratories initially, there is now general agreement that all five SSTR subtypes and especially the human isoforms are functionally coupled to inhibition of the adenylyl cyclase-cAMP pathway via pertussis toxin sensitive G proteins

(Patel et al., 1994) (Table 1). Four of the subtypes (SSTR1,2,3,4) also stimulate PTP, once again through pertussis toxin sensitive pathways (Florio et al., 1994; Buscail et al., 1995; Reardon et al., 1996; Florio et al., 1996). However, the nature of the G proteins involved and whether they couple the receptor directly or indirectly to PTP remain unclear. SSTR1 stimulates a Na^+/H^+ exchanger via a pertussis toxin insensitive mechanism (Hou et al., 1994). SSTR2 does not activate the antiporter and coupling of SSTR3,4,5 to this pathway remains to be investigated. In Rin m5F cells and in rat amygdaloid neurons SSTRs with the pharmacological profile of the type 2 isoform inhibit voltage-dependent Ca^{2+} channels (Fujii et al., 1994; Viana and Hille, 1996). SSTR4 activates PLA-2 dependent arachidonate production via a pertussis toxin sensitive G protein in transfected CHO-K1 cells (Bito et al., 1994). Three of the SSTR subtypes inhibit the MAPK signalling cascade : SSTR2 in SY-5Y neuroblastoma cells, SSTR3 in NIH3T3 cells and in mouse insulinoma cells, and SSTR5 in transfected CHO-K1 cells (Cattaneo et al., 1996; Yoshitomi et al., 1997; Cordelier et al., 1997). In contrast, SSTR4 has been reported to stimulate MAPK in transfected CHO-K1 cells (Bito et al., 1994). Despite earlier claims for a lack of effect of SSTRs on PLC- IP_3 signalling, several recent reports have described SSTR modulation of this pathway. For instance, the endogenous SSTR in intestinal smooth muscle cells which displays the pharmacological properties of SSTR3 signals through activation of PLC β 3 and Ca^{2+} mobilization, and SSTR2A and SSTR5 both stimulate PLC-dependent IP_3 production in transfected COS-7 and F4C1 pituitary cells (Akbar et al., 1994; Murthy et al., 1996). SSTR5 has also been reported to inhibit IP_3 -mediated Ca^{2+} mobilization in transfected CHO-K1 cells whereas SSTR4 is without effect (Bito et al., 1994). These results clearly suggest that individual SSTR subtypes can activate more than one G protein and G protein-linked signalling cascades. Since all five SSTRs bind the natural ligands SST-14 and SST-28 with nanomolar affinity,

and share common signalling pathways such as adenylyl cyclase, and since single cells express more than one SSTR subtype, the question arises whether multiple SSTRs in the same cell are redundant or whether they interact functionally for greater signalling diversity. There is some evidence to suggest that SSTRs, like several other GPCRs, are capable of functional interaction as homo- and heterodimers (Rocheville et al., 1998). Major voids still remain in our understanding of SSTR subtype selectivity for K^+ and Ca^{2+} channel coupling and of the molecular signals in the receptors responsible for activation of the various phosphatases and the MAPK pathway. Much of our current knowledge on subtype selectivity for signalling is based on transfected cells and should be interpreted with caution given the limitations of these systems. The future development of highly selective agonists and antagonists for each of the subtypes should greatly facilitate the study of subtype selective effector coupling of endogenous SSTRs in normal cells.

SSTR MEDIATED INHIBITION OF SECRETION AND CELL PROLIFERATION

The profound ability of SST to inhibit cell secretion so widely can be explained in part through SSTR-induced reductions in the two key intracellular mediators cAMP and Ca^{2+} due to effects on adenylyl cyclase and K^+ and Ca^{2+} ion channels (INSERT FIGURE 4A ABOUT HERE). In addition to this so-called proximal effect, however, SST can block secretion stimulated by cAMP, Ca^{2+} ionophores (A23187, ionomycin), the Ca^{2+} channel agonist BAYK8644, or by IP_3 , diacylglycerol and extracellular Ca^{2+} in permeabilized cells (reviewed in Patel, 1992; Patel et al., 1995). These observations clearly indicate that SST, independent of any effects on cAMP, Ca^{2+} or indeed any other known second messenger is able to inhibit secretion via this distal action. This effect appears to be mediated via a G protein-dependent inhibition of exocytosis and is induced through SST-dependent

activation of the protein phosphatase calcineurin (Renstrom et al., 1996). A similar distal effect on the secretory process has been shown for other inhibitory receptors, e.g. α -adrenergic and galanin receptors and suggests that phosphorylation-dephosphorylation events rather than the Ca^{2+} signal play a key role in the distal steps of exocytosis. The specific SSTR subtypes involved in this process as well as the signalling mechanisms leading to calcineurin activation remain to be determined. In addition to its effect on exocytotic secretion, SST is also capable of inhibiting the release of constitutively secreted proteins such as growth factors and cytokines by unknown mechanisms.

The ability of SST to block hormone secretion led to the application of long acting analogs such as Octreotide in the early 1980's for the treatment of hormone hypersecretion from pancreatic, intestinal, and pituitary tumors. A number of subsequent developments followed which suggested that SST not only inhibited hormone hypersecretion from these tumors but also caused their shrinkage through an additional antiproliferative effect. The antiproliferative effects of SST have since been demonstrated experimentally both *in vivo* in DMBA-induced or transplanted rat mammary carcinomas, as well as in cultured cells derived from both endocrine and nonendocrine tumors (pituitary, thyroid, breast, prostate, colon, pancreas, lung, and brain) (Weckbecker et al., 1993; Weckbecker et al., 1994). These effects involve cytostatic (growth arrest) and cytotoxic (apoptosis) actions and are mediated (i) directly by SSTRs present on tumor cells, and (ii) indirectly via SSTRs present on nontumor cell targets to inhibit the secretion of hormones and growth factors which promote tumor growth, inhibit angiogenesis, promote vasoconstriction, and modulate immune cell function. Several SSTR subtypes and signal transduction pathways have been implicated (INSERT FIGURE 4B ABOUT HERE). Each of the three key second messenger systems cAMP, Ca^{2+} , and

PTP modulated by SSTRs, could be involved (Weckbecker et al., 1993, Patel, 1997). Most interest is focused on protein phosphatases which dephosphorylate receptor tyrosine kinases or which inactivate the MAPK signalling cascade thereby attenuating mitogenic signal transduction. A SST-sensitive PTP capable of dephosphorylating and inactivating the EGF receptor kinase in Mia PaCa human pancreatic cancer cells was first described by Liebow et al (Liebow et al., 1989). This observation was confirmed in normal pancreatic acinar cells, in AR42J rat pancreatic tumor cells, GH₄C₁ cells, and MCF7 human breast cancer cells (Viguerie et al, 1989; Florio et al, 1994; Srikant and Shen, 1996). Several other GPCRs have since been shown to regulate cell proliferation through modulation of PTP, e.g. dopamine 2, angiotensin II, and α 2 adrenergic receptors. The dose-response for PTP activation parallels the concentration of SST ligand required for receptor activation. A 66 kDa PTP identified as SHP-1 (SHP/SHPTP-1, PTP-1C/HCP) copurifies with membrane SSTRs from AR42J pancreatic cells which are enriched in SSTR2 (Zeggari et al., 1994). SHP-1 is a cytosolic PTP containing two Src homolog 2 (SH2) domains which associates *in vivo* with activated receptor tyrosine kinases, cytokine receptors, and various antigen receptors, and may play a role in terminating growth factor mitogenic signals by dephosphorylating critical molecules (Imboden et al., 1995). It has been suggested that SHP-1 associates with SSTR2, based on its copurification with this subtype in AR42J cells and constitutive association of SSTR2 and SHP-1 coexpressed in CHO-K1 cells (Buscail et al., 1995; Zeggari et al., 1994). Receptor activation results in a rapid dissociation of SHP-1 from SSTR2, accompanied by an increase in PTP activity. Contrary findings in MCF7 cells, however, suggest that SSTR activation promotes translocation of cytosolic PTP to the membrane, with little direct stimulation of PTP by SST ligands in membrane preparations (Srikant and Shen, 1996). Besides SSTR2, three other subtypes SSTR1, 3, and 4 have also been shown to stimulate

PTP activity in various transfected cells (Florio et al., 1994; Reardon et al., 1996; Florio et al., 1996). Whilst there is ample evidence now for a key role of SHP-1 as the initial transducer of the antimitogenic signal transmitted by SSTR2, it remains to be determined whether SHP-1 or another PTP mediates the antiproliferative effects of SSTR1,3, and 4.

Several of the SSTRs have been reported to modulate MAPK activity (Reardon et al., 1996; Bito et al., 1994; Cattaneo et al., 1996; Yoshitomi et al., 1997; Cordelier et al., 1997). Acting through SSTR3, SST inhibits MAPK activity via PTP-dependent inactivation of Raf-1 in transfected NIH3T3 cells (Reardon et al., 1996). In MIN-6 mouse insulinoma cells, SSTR3 exerts a dual effect on MAPK activity characterized by a transient increase followed by a decrease (Yoshitomi et al., 1997). Acting through a putative SSTR2 in SY-5Y neuroblastoma cells, SST inhibits MAPK activity and cell proliferation induced by receptor tyrosine kinases (Cattaneo et al., 1996). This effect is blocked by orthovanadate suggesting dephosphorylation-dependent inactivation of MAPK through SST activation of PTP. SSTR5, the only subtype which does not induce PTP, inhibits MAPK activity through inhibition of guanylate cyclase and cGMP formation (Cordelier et al., 1997).

The ability of SST to induce apoptosis has been shown in AtT-20 cells treated with octreotide (Srikant, 1995). Apoptosis occurred in a dose-dependent manner over the concentration range 10^{-10} to 10^{-5} M in cells progressing through cell cycle division but not under cell cycle block. In MCF7 cells, octreotide induces marked apoptosis which, can be blocked by orthovanadate implicating PTP activation as a necessary step in SSTR-mediated apoptotic signalling (Sharma and Srikant, 1998). Since AtT-20 and MCF7 cells both express more than one octreotide sensitive SSTR subtype, it is

not possible to determine subtype selectivity for signalling apoptosis in these cells. In CHO-K1 cells individually expressing the five recombinant hSSTRs, apoptosis is triggered uniquely via the hSSTR3 subtype (Sharma et al., 1996). hSSTR3 promoted apoptosis is associated with activation of wild type (wt) tumor suppressor protein p53 and the proapoptotic protein Bax. wt p53 is believed to be in an inactive phosphorylated form and is activated by dephosphorylation of serine residues. Induction of wt p53 by hSSTR3 activation occurs rapidly in a time-dependent manner and precedes the activation of Bax and the onset of apoptosis. Furthermore, p53 exhibits perinuclear localization in untreated cells but displays preferential intranuclear accumulation concomitant with nuclear shrinkage, a characteristic feature of cells undergoing apoptosis. hSSTR3-induced apoptosis can be blocked by pretreatment with pertussis toxin or orthovanadate suggesting the mediation of pertussis toxin sensitive G proteins and PTP. hSSTR3 initiated increase in p53 occurs in all phases of the cell cycle and does not require G₁ cell cycle arrest as suggested by the lack of induction of the cyclin-dependent kinase inhibitor p21 which typifies cells undergoing G₁ arrest. More recently, hSSTR3 induced apoptotic signalling has been shown to involve the activation of a cation insensitive acidic endonuclease concomitant with intracellular acidification (Sharma and Srikant, 1998). In contrast to hSSTR3, the other subtypes initiate G₁ arrest in a p53 independent manner (hSSTR5 > hSSTR2 > hSSTR4 > hSSTR1) via the retinoblastoma protein PRB (Sharma et al., 1997).

REGULATION OF SSTRs

AGONIST-DEPENDENT REGULATION

Although the acute administration of SST produces a diverse range of biological effects, the initial response diminishes with continued exposure to the peptide as a result of receptor

desensitization (Patel et al., 1995; Reisine and Bell, 1995; Patel, 1997). Agonist-induced desensitization is common to many GPCRs and is associated with receptor phosphorylation, uncoupling of the receptor from G proteins, receptor internalization, and receptor downregulation due to lysosomal degradation. The cytoplasmic C-tail contains sites of phosphorylation on serine and threonine residues, as well as tyrosine and dileucine internalization signals and is critically important in these processes. Agonist-induced uncoupling of SSTRs from G proteins has been shown in AtT-20 cells (Reisine and Bell, 1995). Agonist-dependent internalization of SSTRs has been demonstrated in rat anterior pituitary cells, in rat islet cells, and in AtT-20 mouse and human pituitary tumor cells (Morel et al., 1985; Amherdt et al., 1989; Hofland et al., 1995). Prolonged agonist exposure for 24-48 h has been shown to upregulate SSTRs in GH₄C₁ and Rin m5f cells (Presky and Schonbrunn, 1988). Since normal pituitary and islet cells or their tumor cell derivatives express multiple SSTR subtypes, it has been necessary to study host cells stably transfected with each SSTR subtype in order to characterize the response of individual receptor isotypes. hSSTR2,3,4,5 undergo rapid internalization in a time- and temperature-dependent manner over 60 min in CHO-K1 cells upon agonist activation (Hukovic et al., 1996). Maximum internalization occurs with SSTR3 (78%) followed by SSTR5 (66%), SSTR4 (29%), and SSTR2 (20%). In contrast, hSSTR1 fails to be internalized. Similar results have been reported for hSSTR1 and mouse SSTR2 in transfected COS-7 cells or rat SSTR2 in transfected GH₄C₁ cells (Nouel et al., 1997). A different pattern of internalization has been described for the five rat SSTR subtypes in human embryonic kidney (HEK) cells in which SSTR1-3 are rapidly internalized in the presence of SST-14 or SST-28 whereas SSTR5 is internalized only in the presence of SST-28 and SSTR4 is not internalized by either natural SST ligand (Roth et al., 1997). The reason for this discrepancy is unclear but may be due in part to

structural differences between the rodent and human SST isoforms as well as the cell lines used for transfecting the SSTRs. Desensitization and internalization of rat SSTR2A and SSTR3 receptors as well as the human SSTR5 receptor is associated with phosphorylation of cytoplasmic residues especially in the carboxyl terminus (Hipkin et al., 1997; Roth et al., 1997). Prolonged exposure of SSTRs to agonist for 22 h upregulates hSSTR1 levels at the membrane by 110%, hSSTR2 and hSSTR4 by 26% and 22% respectively, whereas hSSTR3 and 5 show no change (Hukovic et al., 1996). Upregulation of SSTRs by longterm agonist treatment was described ten years ago in pituitary and islet tumor cells and is now being increasingly recognized for a number of other GPCRs, e.g. GnRH, dopamine 2, 5HT, and β 3-adrenergic receptor. In the case of SSTR1 and dopamine 2 receptors, upregulation does not require new protein synthesis and involves the surface recruitment of pre-existing pools of receptors (Ng et al., 1997; Hukovic et al., 1998). Deletion of the cytoplasmic C-tail of hSSTR1 abolishes upregulation and chimeric substitution of the C-tail of hSSTR5 with that of hSSTR1 confers the property of upregulation indicating the presence of molecular signals in the C-tail of hSSTR1 which specify upregulation (Hukovic et al., 1998).

REGULATION OF SSTR GENE EXPRESSION

SSTR genes are developmentally regulated in a time- and tissue-specific manner and are influenced by a variety of hormones and disease states in the adult. Starvation or insulin-deficiency diabetes is associated with decreased mRNA levels for SSTR1-3 in the pituitary and of SSTR5 in the hypothalamus (Bruno et al., 1994). The underlying mechanisms remain to be elucidated. Steady state SSTR mRNA levels are augmented in response to treatment with cAMP, gastrin or EGF, and SST itself (Patel et al., 1993; Vidal et al., 1994; Bruno et al., 1994). Glucocorticoids regulate SSTR gene

transcription in a time-dependent biphasic manner in GH₄C₁ cells (Xu et al., 1995). Short term exposure to glucocorticoids induces SSTR1 and SSTR2 mRNA, more prolonged treatment inhibits transcription of both genes. Estrogen induces SST binding sites in cultured rat pituitary cells and upregulates mRNA expression of SSTR2 and SSTR3 in rat prolactinomas and of SSTR2 mRNA in MCF7 breast cancer cells (Xu et al., 1996; Visser-Wisselaar et al., 1997). Thyroid hormone induces mRNA for SSTR1 and SSTR5 in mouse thyrotrophe tumor cells (James et al., 1997). To gain a better understanding of extracellular and tissue-specific factors regulating SSTR genes, a number of laboratories have begun to analyse promoter sequences. rSSTR1, hSSTR2, rSSTR4, and hSSTR5 and mSSTR5 feature TATA-less, G+C-rich promoters typical of tissue-specific housekeeping promoters (Greenwood et al., 1994; Hauser et al., 1994; Greenwood et al., 1995; Xu et al., 1995; Pscherer et al., 1996). In the case of hSSTR2, a novel initiator element SSTR2_{inr} located close to the mRNA initiation site confers gene expression in the absence of the TATA box by binding a helix loop helix transcription factor SEF-2 which interacts with the basal transcription machinery (Pscherer et al., 1996). The four SSTR promoters that have been characterized contain consensus sequences for a number of common transcription factors. rSSTR1 gene shows AP2 and Pit1 binding sites as well as the consensus TRE between -97 and -81 bp downstream from Pit1. hSSTR2 and rSSTR4 display multiple AP1 and AP2 sites which may confer cAMP responsiveness. The hSSTR5 promoter is also cAMP-inducible and additionally contains an Alu repeat sequence 1.2 Kb upstream of the ATG which is a site of DNA polymorphism. The functional significance of such polymorphism both with respect to the normal pattern of SSTR5 expression as well as disease susceptibility remain to be determined. A SSTR2-deficient knockout mouse has been recently generated in which SSTR2 receptors in arcuate GHRH neurons were found to be solely responsible for mediating GH-induced

feedback inhibition of GH (Zheng et al., 1997). Nonetheless, the animals appeared healthy and grew normally up to 15 months of age excluding an essential role for SSTR2 in embryogenesis or post-natal growth and development (Zheng et al., 1997). Additional gene knockouts of the remaining four SSTR subtypes are required to shed further light on subtype selective biological responses, if any, attributable to the individual members of the receptor family.

ACKNOWLEDGEMENTS

The work cited from the author's laboratory was supported by grants from the Canadian Medical Research Council (MT-10411, MT-6011, and MT-12603), the NIH (NS32160), the US Department of Defence, and the National Cancer Institute of Canada. The expert secretarial help of Maria Correia and Tracy Wilson is gratefully acknowledged.

REFERENCES

- Akbar, M., Okajima, F., Tomura, H., Majid, M.A., Yamada, Y., Seino, S., & Kondo, Y. (1994) Phospholipase C activation and Ca^{2+} mobilization by cloned human somatostatin receptor subtypes 1-5 in transfected COS-7 cells. *FEBS Lett* 348, 192-196.
- Amherdt, M., Patel, Y.C., & Orci, L. (1987). Selective binding of somatostatin-14 and somatostatin -28 to islet cells revealed by quantitative electron microscopic autoradiography. *J. Clin. Invest.* 80, 1455-1458.
- Amherdt, M., Patel, Y.C., & Orci, L. (1989) Binding and internalization of somatostatin, insulin, and glucagon by cultured rat islet cells. *J. Clin. Invest.* 84, 412-417.
- Baldwin, J.M. (1994). Structure and function of receptors coupled to G proteins. *Curr. Opin. In Cell Biol.* 6, 180-190
- Barber, D.L., McGuire, M.E. & Ganz, M.B. (1989) Beta-adrenergic and somatostatin receptors regulate Na-H exchange independent of cAMP. *J. Biol. Chem.* 264, 21038-21042.
- Bass, R.T., Buckwalter, B.L., Patel, B.P., Pausch, M.H., Price, L.A., Strnad, J. & Hadcock, J.R. (1996). Identification and characterization of novel somatostatin antagonists. *Mol. Pharmacol.* 50, 709-715.
- Bito, H., Mori, M., Sakanaka, C., Takano, T., Honda, Z., Gotoh, Y., Nishida, E. & Shimizu, T. (1994) Functional coupling of SSTR4, a major hippocampal somatostatin receptor, to adenylate cyclase inhibition, arachidonate release and activation of the mitogen-activated protein kinase cascade. *J. Biol. Chem.* 269, 12722-12730.
- Brassier, J. & Henske, E.P. (1997) Loss of the polycystic kidney (PKD1) region of chromosome 16p13 in renal cyst cells support a loss of function model for cyst pathogenesis. *J. Clin.*

Invest. 99, 194-199.

Brazeau, P., Vale, W.W., Burgus, R., Ling, N., Butcher, M., Rivier, J., & Guillemin, R. (1973).

Hypothalamic peptide that inhibits the secretion of immunoreactive pituitary growth hormone.

Science 179, 77-79.

Brown, P.J., Lee, A.B., Norman, M.G., Presky, D.H., & Schonbrunn, A. (1990). Identification of

somatostatin receptors by covalent labeling with a novel photoreactive somatostatin analog.

J. Biol. Chem. 265, 17995-18004.

Bruno, J.F., Xu, Y. & Berelowitz, M. (1994) Somatostatin regulates somatostatin receptor subtype

mRNA expression in GH₃ cells. *Biochem. Biophys. Res. Commun.* 202, 1738-1743.

Bruno, J.F., Xu, Y., Song, J., & Berelowitz, M. (1993). Tissue distribution of somatostatin receptor

subtype messenger ribonucleic acid in the rat. *Endocrinology* 133, 2561-2567.

Bruno, J.F., Xu, Y., Song, J. & Berelowitz, M. (1994) Pituitary and hypothalamic somatostatin

receptor subtype messenger ribonucleic acid expression in the food-deprived and diabetic rat.

Endocrinology 135, 1787-1792.

Bruns, C., Raulf, F., Hoyer, D., Schloos, J., Lubbert, H., & Weckbecker, G. (1996). Binding

properties of somatostatin receptor subtypes. *Metabolism* 45 (Suppl 1), 17-20.

Buscail, L., Esteve, J.-P., Saint-Laurent, N., Bertrand, V., Reisine, T., O'Carroll, A.-M., Bell, G.I.,

Schally, A.V., Vaysse, N. & Susini, C. (1995). Inhibition of cell proliferation by the

somatostatin analogue RC-160 is mediated by somatostatin receptor subtypes SSTR2 and

SSTR5 through different mechanisms. *Proc. Natl. Acad. Sci. (USA)* 92, 1580-1584.

Cattaneo, M.G., Amoroso, D., Gussoni, G., Sanguini, A.M. & Vincenti, L.M. (1996) A somatostatin

analogue inhibits MAP kinase activation and cell proliferation in human neuroblastoma and

- in human small cell lung carcinoma cell lines. *FEBS Lett* 397, 164-168
- Chen, L., Fitzpatrick, D., Vandlen, R.L. & Tashjian, A.H. (1997) Both overlapping and distinct signalling pathways for somatostatin receptor subtype SSTR1 and SSTR2 in pituitary cells. *J. Biol. Chem.* 272, 18666-18672.
- Cordelier, P., Esteve, J-P, Bousquet, C. (1997) Characterization of the antiproliferative signal mediated by the somatostatin receptor subtype sst5. *Proc. Natl. Acad. Sci. (USA)* 94, 9343-9348.
- Day, R., Dong, W., Panetta, R., Kraicer, J., Greenwood, M.T., & Patel, Y.C. (1995). Expression of mRNA for somatostatin receptor (sstr) types 2 and 5 in individual rat pituitary cells. A double labeling in situ hybridization analysis. *Endocrinology* 136, 5232-5235.
- De Lecea, L., Criado, J.R., Prospero-Garcia, O., Gautvik, K.M., Schweitzer, P., Danielson, P.E., Dunlop, C.L.M., Siggins, G.R., Henriksen, S.J., & Sutcliffe, J.G. (1996). A cortical neuropeptide with neuronal depressant and sleep-modulating properties. *Nature* 381, 242-245
- Dournaud, P., Boudin, H., Schonbrunn, A., Tannenbaum, G.S., & Beaudet, A. (1998) Interrelationships between somatostatin SST2A receptors and somatostatin-containing axons in rat brain. Evidence for regulation of cell surface receptors by endogenous somatostatin. *J. Neurosci.* 18, 1056-1071.
- Dournaud, P., Gu, Y.Z., Schonbrunn, A., Mazella, J., Tannenbaum, G.S., & Beaudet, A. (1996). Localization of the somatostatin receptor SST2A in rat brain using a specific antipeptide antibody. *J. Neurosci.* 16, 4468-4478.
- Dubois, M.P. (1975). Immunoreactive somatostatin is present in discrete cells of the endocrine

- pancreas. *Proc. Natl. Acad. Sci. (USA)* 72, 1340-1343.
- Finley, J.C.W., Maderdrut, J.L., Roger, L.J., & Petrusz, P. (1981). The immunocytochemical localization of somatostatin-containing neurons in the rat central nervous system. *Neurosci.* 6, 2173-92.
- Fitz-Patrick, V.D. & Vandlen, R.L. (1994). 6 agonist selectivity determinants in somatostatin receptor subtypes I and II. *J. Biol. Chem.* 269, 24621-24626.
- Florio, T., Rim, C., Hershberger, R.E., Loda, M., & Stork, P.J. (1994). The somatostatin receptor SSTR1 is coupled to phosphotyrosine phosphatase activity in CHO-K1 cells. *Mol. Endocrinol.* 8, 1289-1297.
- Florio, T., Scarziello, A., Fattore, M., Dalto, V., Salzano, S., Rossi, G., Berlingieri, M.T., Fusco, A., & Schettini, G. (1996) Somatostatin inhibits PC C13 thyroid cell proliferation through the modulation of phosphotyrosine phosphatase activity-impairment of the somatostatinergic effects by stable expression of EIA viral oncogene. *J. Biol. Chem.* 271, 6129-6136
- Fujii, Y., Gono, T., Yamada, Y., Chihara, K., Inagaki, N. & Seino, S. (1994) Somatostatin receptor subtype SSTR2 mediates the inhibition of high voltage activated calcium channels by somatostatin and its analogue SMS201-995. *FEBS Lett* 355, 117-120.
- Greenwood, M.T., Hukovic, N., Kumar, U., Panetta, R., Hjorth, S.A., Srikant, C.B., & Patel, Y.C. (1997). Ligand binding pocket of the human somatostatin receptor 5 (hsstr5): mutational analysis of the extracellular domains. *Mol. Pharmacol.* 52, 807-814.
- Greenwood, M.T., Panetta, R., Robertson, L.A., Liu, J-L & Patel, Y.C. (1994) Sequence analysis of the 5'-flanking promoter region of the human somatostatin receptor 5. *Biochem. Biophys. Res. Commun.* 205, 1883-1890.

- Greenwood, M.T., Robertson, L-A & Patel, Y.C. (1995) Cloning of the gene encoding the human somatostatin receptor 2: sequence analysis of the 5' flanking promoter region. *Gene* 159, 291-292.
- Gu, Y-Z & and Schonbrunn, A. (1997) Coupling specificity between somatostatin receptor sst2A and G proteins: isolation of the receptor-G protein complex with a receptor antibody. *Mol. Endocrinol.* 11 (5), 527-537.
- Hauser, F., Meyerhof, W., Wulfsen, I., Schonrock, C. & Richter, D. (1994) Sequence analysis of the promoter region of the rat somatostatin receptor subtype 1 gene . *FEBS Lett* 345, 225-228.
- Hayry, P., Raisanen, A., Ustinov, J., Mennander, A., Paavonen, T. (1993). Somatostatin analog Lanreotide inhibits myocyte replication and several growth factors in allograft arteriosclerosis. *FASEB J* 7, 1055-1060.
- Helboe, L., Moller, M., Novregaard, L., Schiodt, M., & Stidsen, C.E. (1997) Development of selective antibodies against the human somatostatin receptor subtypes SST1-SST5. *Mol. Br. Res.* 49, 82-88.
- Hipkin, R.W., Friedman, J., Clark, R.B. et al (1997) Agonist-induced desensitization, internalization and phosphorylation of the sst_{2A} somatostatin receptor. *J. Biol. Chem.* 27, 13869-13876.
- Hobart, P., Crawford, R., Shen, L-P., Pictet, R., & Rutter, W.J. (1980). Cloning and sequencing analysis of cDNAs encoding two distinct somatostatin precursors found in endocrine pancreas of anglerfish. *Nature* 288, 137-141.
- Hofland, L.J., Van Koetsveld, P.M., Waaijers, M., Zzuyderwijck, J., Breeman, W.A.P. & Lamberts, S.W.J. (1995) Internalization of the radioiodinated somatostatin analog [¹²⁵I-Tyr³] octreotide

- by mouse and human pituitary tumor cells: increase by unlabelled octreotide. *Endocrinology* 136, 3698-3706.
- Hokfelt, T., Effendic, S., Hellerstrom, C., Johansson, O., Luft, R., & Arimura, A. (1975). Cellular localization of somatostatin in endocrine-like cells and neurons of the rat with special references to the A₁ cells of the pancreatic islets and to the hypothalamus. *Acta. Endocrinol. (Kbh)* 80 (Suppl. 200), 5-41.
- Hou, C., Gilbert, R.L. & Barber, D.L. (1994) Subtype-specific signalling mechanisms of somatostatin receptors SSTR1 and SSTR2. *J. Biol. Chem.* 269, 10357-10362.
- Hoyer, D., Bell, G.I., Berelowitz, M., Epelbaum, J., Feniuk, W., Humphrey, P.P.A., O'Carroll, A.M., Patel, Y.C., Schonbrunn, A., Taylor, J.E., & Reisine, T. (1995). Classification and nomenclature of somatostatin receptors. *Trends in Pharmacol. Sci.* 16, 86-88.
- Hukovic, N., Kumar, U., Sasi, R., Khare, S., Rocheville, M., & Patel, Y.C. (1998) Agonist-dependent upregulation of human somatostatin receptor type 1 (hSSTR1) requires molecular signals in the cytoplasmic C-tail. Program Annual Meeting US Endocrine Society, New Orleans, June 24-27 (submitted).
- Hukovic, N., Panetta, R., Kumar, U. & Patel, Y.C. (1996) Agonist-dependent regulation of cloned human somatostatin receptor types 1-5 (hSSTR1-5): subtype selective internalization or upregulation. *Endocrinology* 137, 4046-4049.
- Imboden, J.B., & Koretsky, G.A. (1995). Intracellular signalling. Switching off signals. *Current Biology* 5:727-729.
- James, R.A., Sarapura, V.D., Bruns, C., Raulf, F., Dowding, J.M., Gordon, D.F., Wood, W.M. & Ridgway, E.C. (1997) Thyroid hormone induced expression of specific somatostatin receptor

- subtypes correlates with involution of the TtT-97 murine thyrotrope tumor. *Endocrinology* 138 (2), 719-724.
- Jung, B.P., T. Nguyen, L.F. Kolakowski Jr., K.R. Lynch, H.H.Q. Heng, S.R. George, and B.F. O'Dowd. Discovery of a novel human G protein coupled receptor gene (GPR25) located on chromosome 1. *Biochem. Biophys. Res. Commun.* 230, 69-72, 1997.
- Kaupman, K., Bruns, C., Raulf, F., Weber, H.P, Mattes, H., & Lubbert, H. (1995). Two amino acids, located in transmembrane domains VI and VII, determine the selectivity of the peptide agonist SMS201-995 for the SSTR2 somatostatin receptor. *EMBO J.* 14, 727-735.
- Kimura, N., Hayafiji, C., Konagaye, H. & Takahashi, K. (1986) 17 estradiol induces somatostatin (SRIF) inhibition of prolactin release and regulates SRIF receptors in rat anterior pituitary cells. *Endocrinology* 119, 1028-1036.
- Kluxen, F.W., Bruns, CH., & Lubbert, H. (1992). Expression cloning of a rata brain somatostatin receptor cDNA. *Proc. Natl. Acad. Sci. (USA)* 89, 4618-4622.
- Kolakowski, F.L., Jung, B.P., Nguyen, T., Johnson, M.P., Lynch, K.R., Cheng, R., Heng, H.H.Q., George, S.R., & O'Dowd, B.F. (1996). Characterization of a human gene related to genes encoding somatostatin receptors. *Febs. Lett.* 398, 253-258.
- Kowk, R.P.S., Lundblad, J.R., Chrivia, J.C., Richards, J.P., Bachinger, H.P., Brennan, R.G. Roberts, S.G.E., Green, M.R., & Goodma, R.H. (1994). Nuclear protein CBP is a coactivator for the transcription factor CREB. *Nature* 370, 223-6.
- Kumar, U., Laird, D., Srikant, C.B., Escher, E., & Patel, Y.C. (1997). Expression of the five somatostatin receptor (SSTR1-5) subtypes in rat pituitary somatotrophes: quantitative analysis by double-label immunofluorescence confocal microscopy. *Endocrinology* 138,

4473-4476.

- Kumar, U., Patel, A., Suresh, S., Metrakos, P., Patel, S.C., & Patel, Y.C. (1998). Immuno-histochemical colocalization of somatostatin receptors 1-5 (hSSTR1-5) with insulin, glucagon, and somatostatin in human islets. *Program Annual Meeting US Endocrine Society, New Orleans, USA, June 24-27*, (submitted).
- Larsson, L.I., Golterman, N., De Magistris, L., Rehfeld, J.F., & Schwartz, T.W. (1979). Somatostatin cell processes as pathways for paracrine secretion. *Science* 205, 1393-1395.
- Law, S., Zaina, S., Sweet, R., Yasuda, K., Bell, G.I., Stadel, J. & Reisine, T. (1994) $G_{i\alpha 1}$ selectivity couples the SRIF receptor subtype sstr3 to adenylyl cyclase: identification of the functional domains of this alpha subunit necessary for mediating SRIF's inhibition of cAMP formation. *Mol. Pharmacol.* 45, 587-590.
- Le Romancer, M., Cherifi, Y., Levasseur, S., Laigneau, J.P., Peranzi, G., Jois, P., Lewin, M. J., & Reyl-Desmars, F. (1996). Messenger RNA expression of somatostatin receptor subtypes in human and rat gastric mucosae. *Life Sci.* 58, 1091-1098
- Liapakis, G., Haeger, C., Rivier, J., & Reisine, T. (1996). Development of a selective agonist at the somatostatin receptor subtype SSTR1. *JPET* 276, 1089-1094.
- Liebow, C., Reilly, C., Serrano, M., et al. (1989). Somatostatin analogues inhibit growth of pancreatic cancer by stimulating tyrosine phosphatase. *Proc. Natl. Acad. Sci. (USA)* 86, 2003-2007.
- Liu, Y.F., Jacobs, K.H., Rosewick, M.M., & Albert, P.R. (1994). G protein specificity in receptor-effector coupling: analysis of the roles of G_o and G_i in GH_4C_1 pituitary cells. *J. Biol. Chem.* 269, 13880-13886

- Luthin, D.R., Eppler, C.M. & Linden, J. (1993) Identification and quantification of Gi-type GTP-binding proteins that copurify with a pituitary somatostatin receptor. *J. Biol. Chem.* 268, 5990-5996.
- Mandarino, L., Stenner, D., Blanchard, W., Nissen, S., Gerich, J., Ling, N., Brazeau, P., Bohlen, P., Esch, F. & Guillemin, R. (1981). Selective effects of somatostatin- 14, -25, and -28 on in vitro insulin and glucagon secretion. *Nature* 291, 76-77.
- Meriney, S.D., Gray, D.B., & Pilar, G.R. (1994). Somatostatin-induced inhibition of neuronal Ca^{2+} current modulated by cGMP-dependent protein kinase. *Nature* 336-339.
- Mezey, E., Hunyady, B., Mitra, S., Hayes, E., Liu, Q., Schaeffer, J., & Schonbrunn, A. (1998). Cell specific expression of the SSTR2A and SSTR5 somatostatin receptors in the rat anterior pituitary. *Endocrinology* 139, 414-419.
- Montminy, M., Brindle, P., Arias, J., Ferreri, K., & Armstrong, R. (1995). Regulation of somatostatin gene transcription by cAMP. In *Somatostatin and Its Receptors*, Ciba Foundation Symposium 190, John Wiley and Sons, West Sussex, pp. 7-20.
- Montminy, M.R., Goodman, R.H., Horovitch, S.J., & Habener, J.F. (1984). Primary structure of the gene encoding rat preprosomatostatin. *Proc. Natl. Acad. Sci. (USA)* 81, 3337-3340.
- Morel, G., Leroux, P. & Pelletier, G. (1985) Ultrastructural autoradiographic localization of somatostatin-28 in the rat pituitary gland. *Endocrinology* 116, 1615-1620.
- Murthy, K.S., Coy, D.H., & Makhlouf, G. (1996) Somatostatin receptor-mediated signalling in smooth muscle. *J. Biol. Chem.* 271, 23458-23463
- Nehring, R.B., Meyerhof, W., & Richter, D. (1995). Aspartic acid residue 124 in the third transmembrane domain of the somatostatin receptor subtype 3 is essential for somatostatin-14

- binding. *DNA and Cell Biol.* 14, 939-944.
- Ng, G.Y.K., Varghese, G., Chung, H.T. et al (1997) Resistance of the dopamine D_{2L} receptor to desensitization accompanies the upregulation of receptors onto the surface of Sf9 cells. *Endocrinology* 138, 4199-4206.
- Nouel, D., Gaudriault, G., Houle, M., Reisine, T., Vincent, J-P, Mazella, J. & Beaudet, A. (1997). Differential internalization of somatostatin in COS-7 cells transfected with SST1 and SST2 receptor subtypes: a confocal microscopic study using novel fluorescent somatostatin derivatives. *Endocrinology* 138, 296-306.
- O'Carroll, A. & Krempel, K. (1995). Widespread distribution of somatostatin receptor messenger ribonucleic acids in rat pituitary. *Endocrinology* 136, 5224-5227
- Panetta, R. & Patel, Y.C. (1994). Expression of mRNA for all 5 human somatostatin receptor (hSSTR1-5) in pituitary tumors. *Life Sci.* 56, :333-342
- Patel, Y.C. (1992). General aspects of the biology and function of somatostatin. In: Weil C, Muller EE, Thorner MO (eds) Basic and Clinical Aspects of Neuroscience. Springer-Verlag, Berlin, vol 4: 1-16.
- Patel, Y.C. (1997). Molecular pharmacology of somatostatin receptor subtypes. *J. Endocrinol. Invest.* 20, 348-367.
- Patel, Y.C., Greenwood, M.T., Kent, G., Panetta, R., & Srikant, C.B. (1993). Multiple gene transcripts of the somatostatin receptor SSTR2: tissue selective distribution and cAMP regulation. *Biochem. Biophys. Res. Commun.* 192, 288-294.
- Patel, Y.C., Greenwood, M.T., Panetta, R. et al (1995): Mini Review: The somatostatin receptor family. *Life Sciences* 57, 1249-1265.

- Patel, Y.C., Greenwood, M.T., Warszynska, A., Panetta, R. & Srikant, C.B. (1994) All five cloned human somatostatin receptors (hSSTR1-5) are functionally coupled to adenylyl cyclase. *Biochem. Biophys. Res. Commun.* 198, 605-612.
- Patel, Y.C., Liu, J-L., Galanopoulou, A.S., & Papachristou, D.N. (1998). Production, action, and degradation of somatostatin. In *The Handbook of Physiology, The Endocrine Pancreas and Regulation of Metabolism*, L.S. Jefferson and A.D. Cherrington (eds), Oxford University Press, N.Y. (in press).
- Patel, Y.C., Panetta, R., Escher, E., Greenwood, M., & Srikant, C.B. (1994). Expression of multiple somatostatin receptor genes in AtT-20 cells: evidence for a novel somatostatin-28 selective receptor subtype. *J. Biol. Chem.* 269, 1506-1509
- Patel, Y.C., & Reichlin, S. (1978). Somatostatin in hypothalamus, extrahypothalamic brain and peripheral tissues of the rat. *Endocrinology* 102, 523-530.
- Patel, Y.C., & Srikant, C.B. (1994). Subtype selectivity of peptide analogs for all five cloned human somatostatin receptors (hsstr1-5). *Endocrinology* 135, 2814-2817.
- Presky, D.H., & Schonbrunn, A. (1988) Somatostatin pretreatment increases the number of somatostatin receptors in GH4C1 pituitary cells and does not reduce cellular responsiveness to somatostatin. *J. Biol. Chem.* 263, 714-721.
- Pscherer, A., Dorflinger, U., Kirfel, J., Gawlas, K., Ruschoff, J., Buettner, R. & Schule, R. (1996) The helix-loop-helix transcription factor SEF2 regulates the activity of a novel initiator element in the promoter of the human somatostatin receptor II gene. *EMBO J.* 15, 6680-6690
- Reardon, D.B., Wood, S.L., Brautigan, D.L., Bell, G.I., Dent, P. and Sturgill, T.W. (1996)

Activation of a protein tyrosine phosphate and inactivation of Raf-1 by somatostatin.

Biochem. J. 314, 401-404.

Reichlin, S. (1983). Somatostatin. *N. Engl. J. Med.* 309, 1495-1501, 1556-1563.

Reisine, T., & Bell, G.I. (1995). Molecular biology of somatostatin receptors. *Endo. Rev.* 16, 427-442

Renstrom, E., Ding, W-G., Bokvist, K., & Rorsman, P. (1996). Neurotransmitter-induced inhibition of exocytosis in insulin-secreting β cells by activation of calcineurin. *Neuron* 17, 513-522

Rocheville, M., Hukovic, N. & Patel, Y.C. (1998) Functional dimerization of the human somatostatin receptor subtype 5 (hSSTR5). *Program Annual Meeting US Endocrine Society, New Orleans, USA, June 24-27*, (submitted).

Roth, A., Kreienkamp, H-J, Meyerhof, W. et al (1997) Phosphorylation of four amino acid residues in the carboxyl terminus of the rat somatostatin receptor subtype 3 is crucial for its desensitization and internalization. *J. Biol. Chem.* 38, 23769-23774.

Roth, A., Kreienkamp, H.J., Nehring, R.B., Roosterman, D., Meyerhof, W., & Richter, D. (1997) Endocytosis of the rat somatostatin receptors - subtype discrimination, ligand specificity and delineation of carboxyterminal positive and negative sequence motifs. *DNA and Cell Biology* 16, 111-119.

Sanford, R., Sgotto, B., Burn, T. & Brenner, S. (1996) The tuberlin (TSC2) autosomal dominant polycystic kidney disease (PKD1) and somatostatin type V receptor (SSTR5) genes form a synteny group in the fugu genome. *Genomics* 38, 84-86.

Schonbrunn, A. & Tashjian Jr, A.H. (1978). Characterization of functional receptors for somatostatin

- in rat pituitary cells in culture. *J. Biol. Chem.* 253, 6473-6483.
- Schwartz, T.W. & Rosenkilde, M.M. (1996). Is there a lock for all agonist keys in 7 TM receptors. *TIPS* 17, 213-216.
- Schweitzer, R., Madamba, S. & Siggins, G.R. (1990) Arachidonic acid metabolites as mediators of somatostatin-induced increase of neuronal M-current. *Nature* 346, 464-466.
- Senogles, S.E. (1994). The D2 dopamine receptor isoforms signal through distinct Gi alpha proteins to inhibit adenylyl cyclase. A study with site-directed mutant Gi alpha proteins. *J. Biol. Chem.* 269 (37), 23120-23127.
- Sharma, K., Patel, Y.C., & Srikant, C.B. (1996) Subtype selective induction of p53-dependent apoptosis but not cell cycle arrest by human somatostatin receptor 3. *Mol. Endocrinol.* 10, 1688-1696.
- Sharma, K., Patel, Y.C. & Srikant, C.B. (1997) Subtype selective human somatostatin receptor (hSSTR) mediated cytostatic and cytotoxic actions involve different signalling mechanisms. *Prog. US Endocrine Society Mtg.*, Minneapolis, June 11-14, Abstr. #P1-152.
- Sharma, K., & Srikant, C.B. (1998). G protein coupled receptor signaled apoptosis is associated with activation of a cation insensitive acidic endonuclease and intracellular acidification. *Biochem. Biophys. Res. Commun.* 242, 134-140.
- Sharma, K. & Srikant, C.B. (1998) Induction of wild type p53, bax and acidic endonuclease during somatostatin signaled apoptosis in MCF-7 human breast cancer cells. *Inter. J. Cancer* (in press).
- Shen, L.P., & Rutter, W.J. (1984). Sequence of the human somatostatin I gene. *Science* 224, 168-171.

- Shimon, I., Taylor, J.E., Dong, J.Z., Bitonte, R.A., Kim, S., Morgan, B., Coy, D.H., Culler, M.D., & Melmed, S. (1997). Somatostatin receptor subtype specificity in human fetal pituitary culture. *J. Clin. Invest.* 99, 789-798.
- Srikant, C.B. (1995) Cell cycle dependent induction of apoptosis by somatostatin analog SMS201-995 in AtT-20 mouse pituitary tumor cells. *Biochem. Biophys. Res. Commun.* 209, 400-407.
- Srikant, C.B., & Shen, S.H. (1996). Octapeptide somatostatin analog SMS 201-995 induces translocation of intracellular PTP1C to membranes in MCF-7 human breast cancer denocarcinoma cells. *Endocrinology* 137, 3461-3468.
- Srikant, C.B., Murthy, K.K., Escher, E., & Patel, Y.C. (1992). Photoaffinity labelling of the somatostatin receptor: Identification of molecular subtypes. *Endocrinology* 130, 2937-2946.
- Srikant, C.B., & Patel, Y.C. (1981). Receptor binding of somatostatin-28 is tissue specific. *Nature* 294, 259-260.
- Tallent, M., & Reisine, T. (1992). Gi alpha 1 selectively couples somatostatin receptors to adenylyl cyclase in pituitary-derived AtT-20 cells. *Mol. Pharmacol.* 41, 452-455.
- Taylor, J.E. & Coy, D.H. (1997). The receptor pharmacology of somatostatin agonists and antagonists: implications for clinical utility. *J. Endocrinol. Invest.* 20 (Suppl. 7), 8-10.
- Thoss, V.S., Perez, J., Probat, A., & Hoyer, D. (1996). Expression of five somatostatin receptor mRNAs in the human brain and pituitary. *Arch. Pharmacol.* 354, 411-419.
- Tostivini, H., Likrmann, I., Bucharles, C., Vieau, D., Coulouarn, Y., Fournier, A., Conlon, J. M., & Vaudry, H. (1996). Occurrence of two somatostatin variants in the frog brain: characterization of the cDNAs, distribution of the mRNAs, and receptor-binding affinities of the peptides. *Proc. Natl. Acad. Sci. (USA)* 93, 12605-12610.

- Tran, V.T., Beal, M.F., & Martin, J.B. (1985). Two types of somatostatin receptors differentiated by cyclic somatostatin analogs. *Science* 228, 492-495.
- Vanetti, M., Kouba, M., Wang, X., Vogt, G., & Holtt, V. (1992). Cloning and expression of a novel mouse somatostatin receptor (SSTR2B). *FEBS Letts* 311, 290-294.
- Viana, F. & Hille, B. (1996) Modulation of high voltage-activated calcium channels by somatostatin in acutely isolated rat amygdaloid neurons. *J. Neurosci.* 16, 6000-6011.
- Vidal, C., Raully, I., Zeggari, M., Delesque, N., Esteve, J-P, Saint-Laurent, N., Vaysse, N. & Susini, C. (1994) Up-regulation of somatostatin receptors by epidermal growth factor and gastrin in pancreatic cancer cells. *Mol. Pharmacol.* 46, 97-104.
- Viguerie, N., Tahiri-Jouti, N., Ayrat, A.M., Cambillau, C., Scemama, J.L., Bastie, M.J., Knuhtsen, S., Esteve, J.P., Pradayrol, L., Susini, C., & Vaysse, N. (1989). Direct inhibitory effects of a somatostatin analog, SMS 201-995, on AR4-2J cell proliferation via pertussis toxin-sensitive guanosine triphosphate-binding protein-independent mechanism. *Endocrinology* 124, 1017-1025.
- Visser-Wisselaar, H.A., Van Uffelen, C.J.C., Van Koetsveld, P.M., Lichtenauer-Kaligis, E.G.R., Waaijers, A.M., Uitterlinden, P., Movy, D.M., Lamberts, S.W.J. & Hofland, L.J. (1997) 17 estradiol dependent regulation of somatostatin receptor subtype expression in the 7315 b prolactin secreting rat pituitary tumor *in vitro* and *in vivo*. *Endocrinology* 138, 1180-1189.
- Weckbecker, G., Raulf, F., Stolz, B. & Bruns, C. (1993) Somatostatin analogs for diagnosis and treatment of cancer. *Pharmac. Ther.* 60, 245-264.
- Weckbecker, G., Tolcsvai, L., Stolz, B., Pollack, M. & Bruns, C. (1994). Somatostatin analogue octreotide enhances the antineoplastic effect of tamoxifen and ovariectomy on 7, 12-

- dimethylbenz(a)anthracene-induced rat mammary carcinomas. *Cancer Res.* 54, 6334-6337.
- White, R.E., Schonbrunn, A., & Armstrong, D.L. (1991). Somatostatin stimulates Ca^{2+} -activated K^{+} channels through protein dephosphorylation. *Nature* 351, 570-573.
- Wilkinson, G.F., Feniuk, W., & Humphrey, P.P.A. (1997). Characterization of human recombinant somatostatin sst5 receptors mediating activation of phosphoinositide metabolism. *Br. J. Pharmacol.* 121, 91-96.
- Xu, Y., Berelowitz, M. & Bruno, J.F. (1995) Dexamethasone regulates somatostatin receptor subtype messenger ribonucleic acid expression in rat pituitary GH_4C_1 cells. *Endocrinology* 136, 5070-5075.
- Xu, Y., Bruno, J.F. & Berelowitz, M. (1995) Characterization of the proximal region of the rat somatostatin receptor gene, SSTR4. *Biochem. Biophys. Res. Commun.* 206, 935-941.
- Xu, Y.X., Song, J., Berelowitz, M. & Bruno, J.F. (1996) Estrogen regulates somatostatin receptor subtype 2 messenger ribonucleic acid expression in human breast cancer cells. *Endocrinology* 5634-5640.
- Yamada, Y., Post, S.R., Wang, K., Tager, H.S., Bell, G.I., & Sein, S. (1992). Cloning and functional characterization of a family of human and mouse somatostatin receptors expressed in brain, gastrointestinal tract, and kidney. *Proc. Natl. Acad. Sci. (USA)* 89, 251-255.
- Yoshitomi, H., Fujii, Y., Miyazaki, M., Nakajima, M., Inagaki, N. & Seino, S. (1997) Involvement of MAP kinase and cfos signalling in the inhibition of cell growth by somatostatin. *Am. J. Physiol. Endocrinol. Metab.* 35, E769-E774.
- Zeggari, M., Esteve, J. P., Raully, I., Cambillau, C., Mazarguil, H., Dufresne, M., Pradayrol, L., Chayvialle, J-A., Vaaysse, N., & Susini, C. (1994). Copurification of a protein tyrosine

phosphatase with activated somatostatin receptors from rat pancreatic acinar membranes.

Biochem. J. 303, 441-448.

Zheng, H., Bailey, A., Jiang, M-H et al (1997) Somatostatin receptor subtype 2 knock out mice are refractory to growth hormone, negative feedback on arcuate neurons. *Mol. Endocrinol.* 11, 1709-1717.

Zhu, L-J, Krempels, K., Bardin, C.W., O'Carroll, A.M., & Mezey, E. (1998). The localization of messenger ribonucleic acids for somatostatin receptors 1, 2, and 3 in rat tissues. *Endocrinology* 139, 350-357

FIGURE LEGENDS

FIGURE 1. Schematic depiction of the rat SST gene and its regulatory domains. The messenger RNA coding region consists of two exons of 238 and 367 base pairs (bp) separated by an intron of 621 bp. Located upstream (i.e. 5' end) from the start site of mRNA transcription (arrow) are the regulatory elements TATA (-26 bp), cAMP response element, CRE (-48/-41 bp), atypical glucocorticoid response element a GRE (-250/-71 bp) and a somatostatin promoter silencer element, SMS-PS (-260/-189 bp). Tissue specific elements (TSE) consisting of TAAT motifs that operate in concert with CRE to provide high level constitutive activity are located within the TSE I (-104/-86 bp) and TSE II (-303/-286 bp) regions.

FIGURE 2. Schematic depiction of the structural domains of the 6 putative hSSTR proteins showing the 7 TM topology, the extracellular and intracellular loops and the amino- and carboxy terminal (C-tail) segments. CHO-potential sites for N-linked glycosylation within the amino terminal segment and second ECL; PO₄ - putative sites for phosphorylation by protein kinase A, protein kinase C, and casein kinase. The cysteine residue 12 amino acids downstream from the VIIth TM is conserved in SST1,2,4,5 and may be the site of a potential palmitoyl membrane anchor. The YANSCAN PI/VLY sequence in the VIIth TM is highly conserved in all members of the sst family. Residues Asp¹²², Asn²⁷⁶, and Phe²⁹⁴ in TMs III, VI, and VII respectively of SST2A have been proposed to form part of a ligand binding pocket for Octreotide and are shown by the closed circles.

FIGURE 3. Natural and synthetic peptide agonists of the SST receptor family.

FIGURE 4. Schematic depiction of SSTR signalling pathway leading to inhibition of secretion (4A) and cell proliferation and induction of apoptosis (4B). Receptor activation leads to a fall in intracellular cAMP (due to inhibition of adenylyl cyclase), a fall in Ca^{2+} influx (due to activation of K^+ and Ca^{2+} ion channels) and stimulation of phosphatases such as calcineurin (which inhibits exocytosis), and serine threonine phosphatases (which dephosphorylate and activate Ca^{2+} and K^+ channel proteins). Blockade of secretion by SST is in part mediated through inhibition of Ca^{2+} and cAMP (proximal effect) and through a more potent distal effect involving direct inhibition of exocytosis via SST-dependent activation of calcineurin. Induction of protein tyrosine phosphatase by SST plays a key role in mediating the antiproliferative response by dephosphorylating growth factor receptor kinases and other putative substances such as p53, Raf-1 and MAPK implicated in regulating cell proliferation and apoptosis.

TABLE 1.
CHARACTERISTICS OF THE CLONED SUBTYPES OF HUMAN SOMATOSTATIN
RECEPTORS[†]

	SSTR1	SSTR2A	SSTR3	SSTR4	SSTR5
Chromosomal localization	14q13	17q24	22q13.1	20p11.2	16p13.3
Molecular size (kDa)	53-72	71-95	65-85	45	52-66
Amino acids	391	369	418	388	363
mRNA (kb)	4.8	8.5 (?)	5.0	4.0	4.0
G protein coupling	+	+	+	+	+
Effector coupling					
adenylyl cyclase activity	↓	↓	↓	↓	↓
tyrosine phosphatase activity	↑	↑	↑	↑	
Ca ²⁺ channels		↓			
Na ⁺ /H ⁺ exchanger	↑				
Phospholipase C/IP ₃ activity		↑			↓↑
Phospholipase A2 activity				↑	
MAP kinase activity		↓	↓↑	↑	↓
Tissue distribution**	brain, pituitary, islet, stomach liver, kidneys	brain, pituitary islet, stomach kidneys	brain, pituitary islet, stomach	brain, stomach islet, lungs placenta	brain, pituitary islet, stomach

[†] Modified from Patel 1997, Patel and Srikant 1998 and Reisine and Bell 1995.

** Based on Lamberts et al 1996 and Patel 1997. Not all tissues have been tested simultaneously.

IP₃, inositol, triphosphate, MAP kinase, mitogen activated protein kinase.

TABLE 2.

LIGAND SELECTIVITY OF CLONED HUMAN SOMATOSTATIN RECEPTORS[†]

	IC ₅₀ (nM)*				
	SSTR1	SSTR2A	SSTR3	SSTR4	SSTR5
SRIF-14	0.1-2.26	0.2-1.3	0.3-1.6	0.3-1.8	0.2-0.9
SRIF-28	0.1-2.2	0.2-4.1	0.3-6.1	0.3-7.9	0.05-0.4
Octreotide	290-1140	0.4-2.1	4.4-34.5	>1000	5.6-32
Lanreotide	500-2330	0.5-1.8	43-107	66-2100	0.6-14
Vapreotide	>1000	5.4	31	45	0.7
Seglitide	>1000	0.1-1.5	27-36	127->1000	2-23
BIM 23052	6.3-100	10-13.5	2.1-5.6	16-141	1.2-7.3
BIM 23056	110->1000	132->1000	10.8-177	17-234	5.7-14.1
BIM 23268	18.4	15.1	61.6	16.3	0.37
L 362855	>1000	1	6.2	63->1000	0.1-0.016
CH 275**	3.2-4.3	>1000	>1000	4.3-874	>1000

† Based on Patel and Srikant 1998, Reisine and Bell 1995, Bruns et al 1996, Shimon et al 1997.

* Data of Patel and Srikant (1994) expressed as Ki

**From Liapakis et al (1996) and Patel 1997.

Schematic depiction of the rat SST gene and its regulatory domains

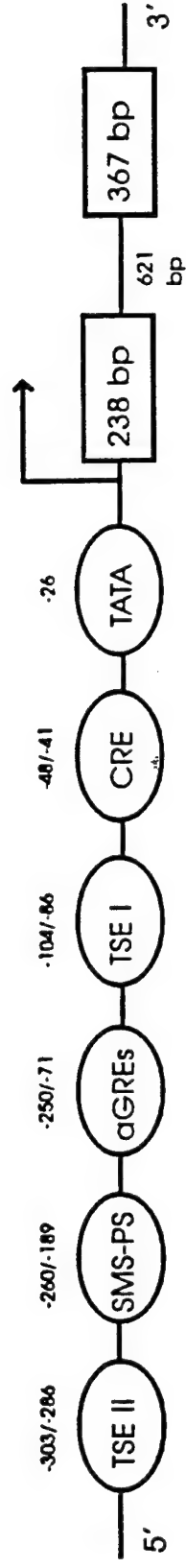


Figure 1

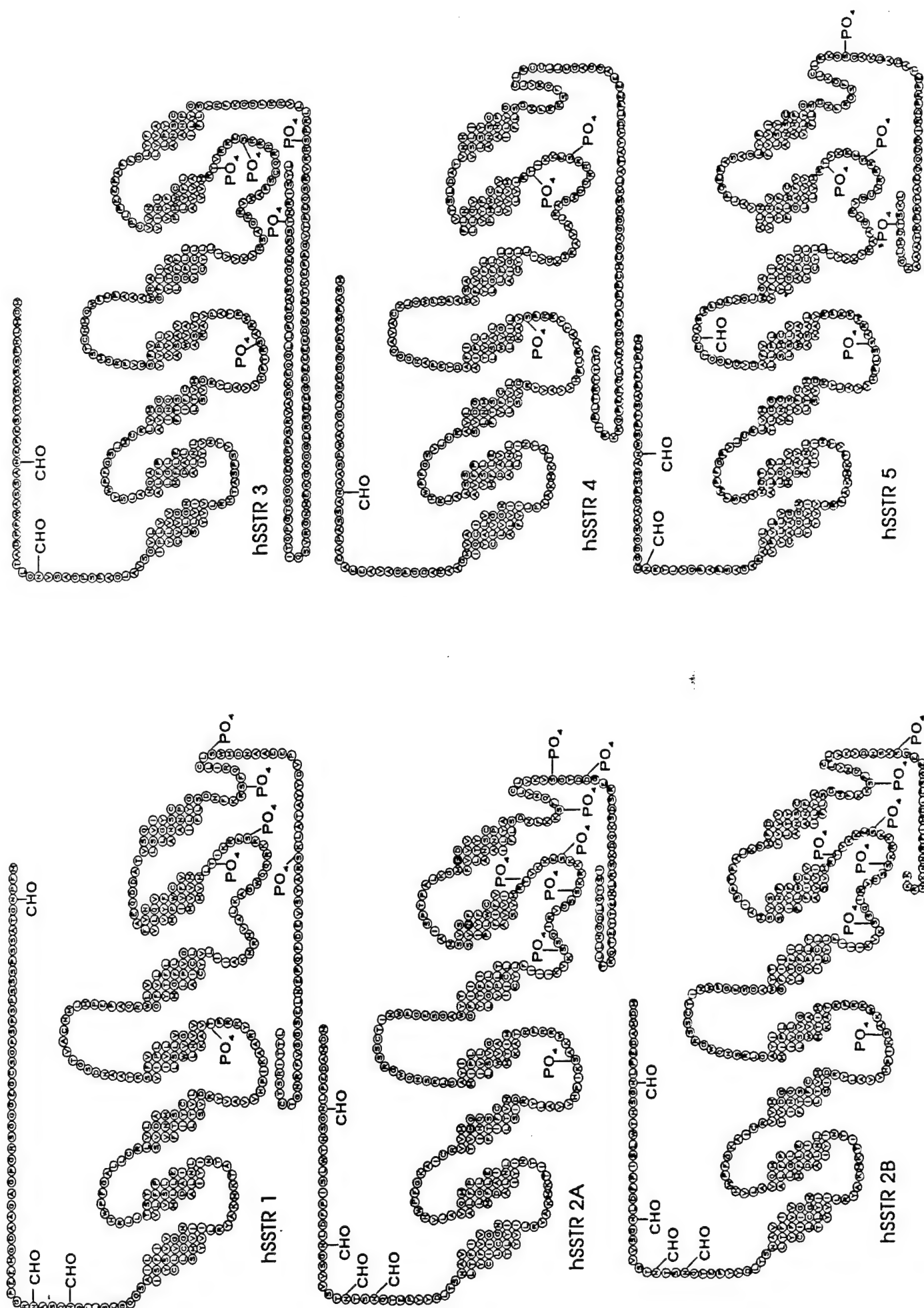


Figure 2.

Natural and synthetic peptide agonists of the sst receptor family

SST-28	Ser-Ala-Asn-Ser-Asn-Pro-Ala-Met-Ala-Pro-Arg Glu-Arg-Lys-Ala-Gly-Cys-Lys-Asn-Phe-Phe-Trp Cys-Ser-Thr-Phe-Thr-Lys
SST-14	Ala-Gly-Cys-Lys-Asn-Phe-Phe-Trp Cys-Ser-Thr-Phe-Thr-Lys
SMS 201-995 <i>octreotide</i>	DPhe-Cys-Phe-DTrp Thr(tol)-Cys-Thr-Lys
BIM23014 <i>lanreotide</i>	DAla-Cys-Tyr-DTrp Thr-Cys-Val-Lys
RC-160 <i>vapreotide</i>	DPhe-Cys-Tyr-DTrp Trp-Cys-Val-Lys
MK678 <i>seglitide</i>	(N-Me)-Ala-Tyr-DTrp Phe-Val-Lys
CH275	Cys-Lys-Phe-Phe-DTrp Cys-Ser-Thr-Phe-Thr-LAMP

Figure 3

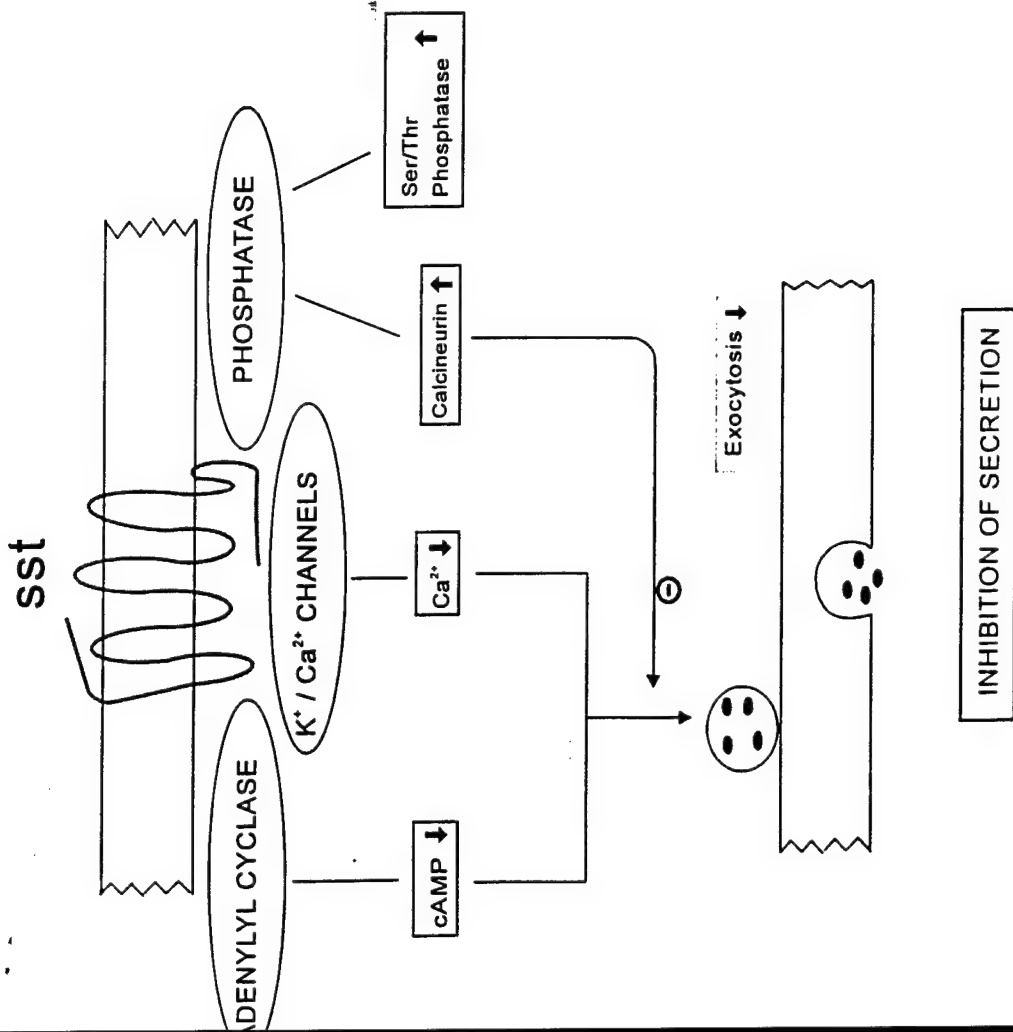


Figure 4A

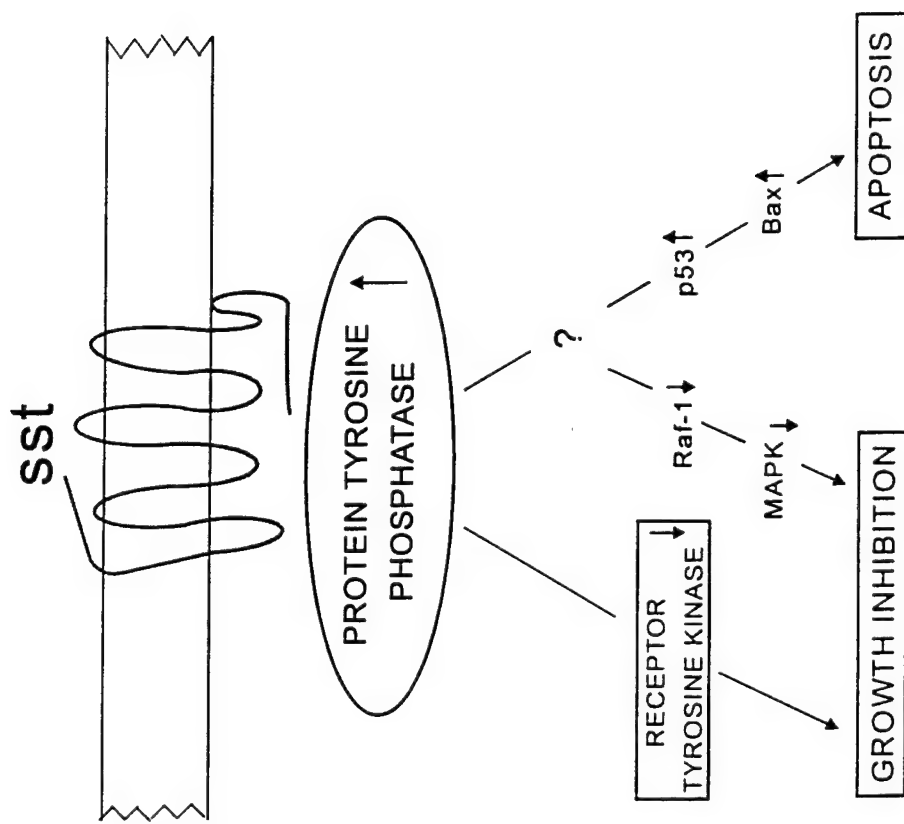


Figure 4B

**C-Terminal region of Human Somatostatin Receptor 5 is Required for Induction of Rb and
G₁ Cell Cycle Arrest**

Kamal Sharma, Yogesh C. Patel and Coimbatore B. Srikant*

Fraser Laboratories, Departments of Medicine, Neurology and Neurosurgery, McGill University
and Royal Victoria Hospital, Montreal, Quebec, Canada, H3A 1A1.

***Address for Correspondence:**

Dr. C.B. Srikant

M3.15, Royal Victoria Hospital

687, Pine Avenue West

Montreal, Quebec, Canada, H3A 1A1

Tel: 514 842 1231 ext. 5359

email: mdcs@musica.mcgill.ca

Running Title:

C-tail of hSSTR5 is required for cytostatic signaling

Ligand activated somatostatin receptors (SSTR) initiate cytotoxic or cytostatic antiproliferative signals. We have previously shown that cytotoxicity leading to apoptosis was signaled solely via human (h) SSTR subtype 3 whereas the other four hSSTR subtypes initiated a cytostatic response that led to growth inhibition. In the present study we characterized the antiproliferative signaling mediated by hSSTR subtypes 1,2,4 and 5 in CHO-K1 cells. We report here that cytostatic signaling via these subtypes results in induction of the retinoblastoma protein Rb and G₁ cell cycle arrest. Immunoblot analysis revealed an increase in hypophosphorylated form of Rb in agonist treated cells. The relative efficacy of these receptors to initiate cytostatic signaling was hSSTR5>hSSTR2>hSSTR4~hSSTR1. A Cytostatic signaling via hSSTR5 also induced a marginal increase in cyclin-dependent kinase inhibitor p21. hSSTR5 initiated cytostatic signaling was G protein-dependent and protein tyrosine phosphatase (PTP) mediated. OCT treatment induced a translocation of cytosolic PTP to the membrane whereas it did not stimulate PTP activity when added directly to the cell membranes. C-tail truncation mutants of hSSTR5 displayed progressive loss of antiproliferative signaling proportional to the length of deletion as reflected by the marked decrease in the effects of OCT on membrane translocation of cytosolic PTP, and induction of Rb and G₁ arrest. These data demonstrate that the C-terminal domain of hSSTR5 is required for cytostatic signaling which is PTP-dependent and leads to induction of hypophosphorylated Rb and G₁ arrest.

Introduction

The antiproliferative actions of somatostatin (SST) signaled via cell surface SST receptors (SSTR) regulate cellular protein phosphorylation and elicit cytostatic (growth arrest) and cytotoxic (apoptosis) responses in tumor cells. For instance, SST treatment causes apoptosis in MCF-7 and AtT-20 cells whereas it induces cell cycle arrest in GH₃ cells (1-5). Such discrepant findings may be due to the existence of five distinct SSTR subtypes and their differential expression in these tumor cells (6-10). We have reported that human (h) SSTR3 is the only subtype that is capable of cytotoxic signaling: upon ligand activation, cells transfected with hSSTR3 respond with induction of wild type (wt) tumor suppressor protein p53, the proapoptotic protein Bax and an acidic endonuclease and intracellular acidification, and undergo apoptosis (11, 12). The antiproliferative action of SST is also signaled via SSTRs 2,4 and 5. However, neither apoptosis nor changes in any of the above parameters were seen in cell lines stably expressing these subtypes (11, 13). While SST was shown to inhibit cell growth via hSSTRs 2,4 and 5 such a conclusion was based on measurement of thymidine incorporation or cell number at a single time point during SST treatment (14-17). Thus, the mechanism underlying the antiproliferative signaling mediated by the SSTR subtypes incapable of triggering apoptosis remained unknown. Since these SSTR subtypes do not initiate apoptotic signals, it appeared likely that they may transduce cytostatic signals leading to cell cycle arrest.

Cytostatic events leading to G₁ cell cycle arrest are associated with the induction of two proteins Rb (retinoblastoma tumor suppressor protein) and p21 (cyclin dependent kinase inhibitor, also called Waf-1/Cip1) (18). Rb is a phosphorylated protein: it remains hyperphosphorylated (ppRb) in S and G₂/M phases and becomes hypophosphorylated (pRb) in G₁. pRb nega-

tively regulates the G₁/S transition and promotes accumulation of cells in the G₁ phase (18, 19). Rapid phosphorylation of Rb occurs prior to entry of cells into S phase. While Rb functions independent of p53, p21 mediates p53-dependent G₁ arrest (18, 20). Nevertheless, overexpression of p21 can induce G₁ arrest in the absence of p53 induction (21). In order to determine whether the antiproliferative signaling via these hSSTRs causes cell cycle arrest and to identify the molecular mediators involved in this process, we evaluated the effect of SST in CHO-K1 cells expressing hSSTRs 1,2,4 and 5 on cell cycle progression and induction of Rb and p21. We report here that SST induced G₁ cell cycle arrest in these cells is due mainly to the induction of Rb. Maximal effect was exerted via hSSTR5 followed by hSSTR 2, 4 and 1. In hSSTR5 expressing cells, a major portion of SST-induced Rb was hypophosphorylated. SST-induced G₁ arrest and induction of Rb were pertussis toxin sensitive G protein dependent and protein tyrosine phosphatase (PTP) dependent. In OCT treated cells there was a redistribution of PTP activity from the cytosol to the membrane. Mutational analysis of the C-tail of this receptor revealed that the C-tail of the receptor is essential for PTP-dependent cytostatic signaling.

RESULTS

We first compared the effect of 100 nM peptide on cell cycle parameters in CHO-K1 cells expressing individual hSSTRs. Cells were incubated for 24 h in the absence or presence of 100 nM OCT (hSSTRs 2,3,5) or D-Trp⁸ SST-14 (hSSTRs 1,4) prior to analysis of DNA content by flow cytometry. Cells expressing hSSTRs 1,2,4 and 5 responded with a decrease in the rate of proliferation as evidenced by accumulation of cells in G₁ and a decrease in S (fig.1). The greatest cytostatic response was elicited through hSSTR 5 followed by hSSTR2> hSSTR4~ hSSTR1. The effect of agonist treatment on cell cycle parameters is shown in fig.2. In addition to the changes

in G₁ and S phases, a relative increase of cell number in G₂/M was also seen. The absence of oligonucleosomal DNA fragmentation even after treatment for 48 h indicated that SST-induced cell cycle arrest via hSSTR5 did not lead to apoptosis (data not shown).

Inhibition of cell cycle progression signaled via hSSTR 5 was associated with induction of Rb. The increase in intensity of fluorescence of immunolabeled Rb counterstained with FITC conjugated second antibody was seen in all phases of the cell cycle following OCT treatment. Dual label analysis of fluorescence emissions of PI and immunostained Rb revealed that the majority of cells were in G₀/G₁ phase (fig. 3A). Immunoblot analysis of cell extracts revealed that the level of Rb was low in untreated cells, and was present mainly as ppRb. OCT-induced increase in Rb was reflected in both hyper- and hypo-phosphorylated (ppRb and pRb) forms detectable by their differential electrophoretic mobility (fig. 3B). A marked enlargement of the nuclei in hSSTR5 expressing cells was observed in OCT treated cells (fig. 3C), a typical characteristic of G₁ arrested cells (22). OCT-induced increase in Rb was time-dependent and was detectable by 4 h (2.7 ± 0.9 fold) and was maximal at 24 h (8.1 ± 0.8 fold) (figure 4A). Induction of Rb preceded the onset of G₁ arrest since an increase in G₁/S ratio which is an index of inhibition of cell proliferation was detectable only by 8 h (figure 4B). The ability of OCT to induce Rb during 24 h incubation was dose-dependent and occurred over the concentration range 10-100 nM (figure 5A). Immunoblot analysis revealed a dose-dependent increase in both ppRb and pRb in OCT-treated cells (fig. 5B).

OCT treated hSSTR5 cells also displayed an increase in p21 (3 ± 0.6 fold over basal level) and was of much smaller magnitude compared to that of Rb. OCT-induced increase in Rb and p21 was abolished by pertussis toxin pretreatment (fig. 6). Sodium orthovanadate, an inhibi-

tor of PTP, also abrogated the inductive effect of OCT on Rb and p21^{Waf1} in these cells. To confirm that PTP activity is involved in the cytostatic signaling via hSSTR5, we measured PTP activity in extracts of cells before and after incubation with SST. In OCT treated cells there was a 40% increase in membrane-associated PTP while the cytosolic enzyme activity decreased by 20% (fig. 7). By contrast, when added to the membrane fractions at the time of enzyme assay, OCT failed to stimulate PTP activity (data not shown). While the maximal induction of Rb was hSSTR5 mediated, three other subtypes were also found to initiate cytostatic signals leading Rb induction (fig. 8). The rank order potency of these SSTRs for signaling the increase in Rb was hSSTR5>2>4>1, same as that observed for triggering G₁ arrest (fig. 1 and 2). By contrast, no increase in Rb occurred in hSSTR3 expressing cells, in agreement with our previously reported finding that OCT does not induce G₁ arrest via this subtype (11, 12).

The C-tail of several G protein coupled receptors have been implicated in G protein interaction and effector coupling (23, 24). To evaluate the importance of the C-tail of hSSTR5 in cytostatic signaling we investigated the effect of mutant hSSTR5 receptors with progressive truncation of the C-tail (fig. 9). These mutants have been previously reported to display binding characteristics and G protein coupling comparable to wild type hSSTR5 (25). Progressive truncation of the C-tail of hSSTR5 was associated with an impaired ability of OCT to signal activation of Rb and induce G₁. Compared to the wild type receptor which triggered 8.1 ± 0.8 fold increase in Rb in response to OCT, the $\Delta 347$ mutant displayed only a 6.1 ± 0.4 fold increase in Rb (fig. 10). The $\Delta 338$, $\Delta 328$ and $\Delta 318$ mutants displayed more marked loss in the ability to activate Rb in response to OCT (3.0 ± 0.9 fold for $\Delta 338$, 2.1 ± 0.7 fold for $\Delta 328$ and 1.3 ± 0.2 fold for $\Delta 318$). To determine if progressive loss of ability to induce Rb parallels the decrease in mem-

brane-associated PTP, we compared PTP activity in cytosolic and membrane fractions in cells incubated in the absence and presence of OCT. In contrast to the >2-fold increase induced by OCT pretreatment in cells expressing hSSTR5 only ~25% increase occurred with the mutant $\Delta 347$ and no change was seen with the shorter hSSTR5 mutants (fig. 11). Interestingly, the basal membrane-associated PTP activity was higher in untreated cells expressing each of the mutant receptors compared to wt hSSTR5.

DISCUSSION

The present study establishes that SSTR mediated antiproliferative signaling elicits subtype selective cytostatic effect via hSSTRs 1,2,4 and 5. In CHO-K1 cells expressing each of these four hSSTR subtypes, there was decreased proliferation due, in part, to a G_1 cell cycle arrest associated with an increase in Rb. The extent of Rb induction and inhibition of cell cycle progression was the greatest in CHO-K1 cells expressing hSSTR5, followed by hSSTR2>hSSTR4~hSSTR1. A significant proportion of Rb induced via hSSTR5 was present in a hypophosphorylated form as evident from its greater electrophoretic mobility. We show that OCT treatment caused nuclear enlargement in hSSTR5 expressing cells, a feature that is characteristic of cells in G_1 arrest (22). Additionally, hSSTR5 mediated cytostatic signaling did not lead to apoptosis. While the cytostatic action exerted through hSSTR5 by OCT was dose- and time-dependent, such an effect occurred with a relatively slow time course and could be seen only at concentrations >10 nM. This is in contrast to the greater sensitivity of hSSTR3 mediated induction of wt p53 which was clearly discernible within minutes and could be elicited at <10 nM concentration of OCT (11).

Pretreatment of cells with PTx abolished the induction of Rb, p21 and G₁ arrest, indicating that the cytostatic signaling by hSSTRs 1,2,4 and 5 is G protein dependent. Likewise, our finding that orthovanadate abolishes the effects of SST suggests a mediatory role for PTP in the cytostatic signaling initiated via hSSTRs 1,2 and 4 as well. PTP mediated antimitogenic effect of SST has previously been reported to be signaled through hSSTR1, mouse and human SSTR2, human and mouse SSTR3 and rat SSTR4 (11, 15, 16, 26-28). By contrast, rat SSTR5 initiated antiproliferative signaling was found to be PTP-independent (14, 17). The present findings suggest that the antiproliferative signaling via hSSTR 5 leading to growth inhibition is also PTP dependent and contradicts the reported inability of the rat homologue of SSTR5 to regulate PTP (14). Such a difference between the rat and human SSTR5 receptors is surprising given the high degree of C-terminal sequence identity between the two receptors. It remains to be seen whether structural differences in other regions of rat and human SSTR5 contribute to their divergent behavior.

The mechanism involved in SST induction of hypophosphorylated Rb remains to be elucidated. The concomitant, albeit smaller, induction of p21 raises the possibility that it may inhibit cyclin-dependent kinase mediated phosphorylation of Rb that is required for the cells to exit G₁. Alternatively, SST may activate phosphatase(s) that may dephosphorylate hyperphosphorylated Rb. Evidence for the existence of such a phosphatase comes from studies using anticancer drugs that promote p53-independent G₁ arrest in the absence of p21 induction (29). It remains to be tested whether hSSTR5 mediated increase in hypophosphorylated Rb is due to activation of Rb phosphatase alone or in conjunction with p21 mediated inhibition of Rb phosphorylation. Another possibility is that SST may inhibit Ca²⁺/calmodulin-mediated hyperphosphorylation of Rb

(30, 31). Cross-talk between SST-induced PTP and mitogenic signaling pathways involving MAP kinase may also contribute to the regulation of serine phosphorylation in Rb as well as cell cycle progression. It has been shown that cell cycle progression due to induction of cyclin dependent kinase and phosphorylation of Rb can occur following MAP kinase activation (32). It is likely that inhibition of MAP kinase activity by SST may be an additional factor involved in its cytostatic signaling. SSTR regulation of MAP kinase activation is, complex and involves inhibition by SSTR2 and SSTR5, stimulation through SSTR4 or a transient increase followed by subsequent decrease elicited by (murine) SSTR3 (33). $G_{\beta\gamma}$ subunit-mediated, activation of Ras is implicated in the induction of MAP kinase (34, 35). On the other hand, PTP dependent regulation of serine/threonine phosphorylation inactivates Raf-1 which functions downstream of Ras in the mitogenic signaling cascade (27, 36-39). Thus, regulation of MAPK cascade by SST may occur at two levels, activation of Ras by $\beta\gamma$ subunits of G protein and tyrosine phosphorylation-dependent inactivation of MAPK. Thus, it is plausible that activation of different phosphorylation/dephosphorylation mechanisms by SST elicited in a receptor subtype-specific or cell-specific manner may exert dual effects on cell growth and proliferation (40, 41). A direct correlation between subtype selective change(s) in MAP kinase and cell cycle arrest or apoptosis remains to be established.

Of the five hSSTRs only hSSTR3 induces cytotoxicity, the other four subtypes being cytostatic (11, 13, and the present study). We have previously reported that the $\Delta 347$, $\Delta 338$, $\Delta 328$ and $\Delta 318$ hSSTR5 mutants show progressive loss of the ability to inhibit forskolin-stimulated cAMP and variable impairment of agonist-dependent desensitization and internalization responses (25). This suggests a multifunctional role of the C-tail of hSSTR5 in mediating effector

coupling, desensitization and internalization (25). Here we have extended an analysis of these mutants to their ability to regulate membrane associated tyrosine phosphatase activity and to determine whether decreased potency to recruit cytosolic PTP to the membrane may account for their inability to initiate cytostatic signaling. Following OCT treatment, only 25% increase in PTP activity in the membrane fraction was seen in cells expressing hSSTR5 Δ 347, in contrast to the 100% increase detected in cells expressing the wild type receptor. Membrane-associated PTP activity did not increase in response to OCT in cells expressing Δ 338, Δ 328 and Δ 318 mutants. Surprisingly, however, the enzyme activity was 20-35% higher in the membrane fraction of these cells under basal conditions than in hSSTR5 expressing cells. We do not know the reason for this, but this observation raises the intriguing possibility that in the absence of ligand activation, the C-tail of the wild type receptor may inhibit the association of PTP with the membrane. Such a phenomenon has not previously been described. However, chronic association of the tyrosine phosphatase SHP-1 to the killer cell inhibitory receptor in natural killer cells has been reported to tonically inhibit the function of the receptor in the inactivated state: dissociation of SHP-1 upon receptor ligation restores its function (42). Despite its inability to recruit cytosolic PTP to the membrane in cells expressing these mutants, OCT was still capable of inducing Rb, albeit with progressively less efficiency paralleling the length of C-tail deletion. While this raises the possibility that OCT may be able to elicit cytostatic signaling through the PTP already present at the membrane, alternate, PTP-independent, mechanism may also contribute to hSSTR5-initiated antiproliferative signaling. For instance hSSTR5 can decrease intracellular Ca^{2+} thereby inhibiting cell growth (14, 43). While the nature of SST-induced, Ca^{2+} -sensitive, growth inhibition was not

established in these studies, it may invoke hypophosphorylation of Rb. Indeed, Ca^{2+} /calmodulin-dependent Rb hyperphosphorylation occurs during cell proliferation (30, 31).

In summary, the present findings demonstrate that SST peptides exert a cytostatic action via SSTR 1,2,4,5. Such subtype specific cytostatic signals target Rb and p21 leading to G_1 cell cycle arrest (hSSTR5>hSSTR2> hSSTR4~hSSTR1). These effects are pertussis toxin dependent G protein dependent and are PTP mediated. The marked decrease in the ability of C-tail mutants of hSSTR5 to induce Rb and G_1 cell cycle arrest suggests that the C-terminal domain of hSSTR5 is involved in cytostatic antiproliferative signaling.

MATERIALS AND METHODS

Materials

The SST analog SMS 201-995 (octreotide, OCT) was obtained from Sandoz Pharma, Basel, Switzerland. Propidium iodide (PI) was purchased from Sigma Chemical Co. (St. Louis, MO). Rabbit polyclonal antibodies against p21 (C-19) and Rb (C-15) were purchased from Santa Cruz Biotechnology (Santa Cruz, CA). FITC conjugated goat anti-mouse and anti-rabbit IgG antibodies were supplied by Zymed Laboratories (San Francisco, CA). All other reagents were obtained from local commercial sources and were of analytical quality.

CHO-K1 cells stably expressing hSSTR1-5 and mutant hSSTR5

Genomic fragments of hSSTR 2,3 and 5 or cDNA clones for hSSTR 1 and 2A containing the entire coding sequences were subcloned into the polylinker region of the mammalian expression vector pRc/CMV (Invitrogen). Mutant hSSTR5 receptors with progressive truncation of the C-tail ($\Delta 347$, $\Delta 338$, $\Delta 328$ and $\Delta 318$) were created by introducing stop codons at positions 347, 338, 328 and 318 of a cassette cDNA construct using the PCR overlap extension technique (25);

the mutant cDNAs were cloned into the mammalian expression vector PTEJ8 (25). Wild type hSSTRs and the mutant hSSTR5 receptors were stably transfected in CHO-K1 cells maintained under G418 selection (11, 44, 45). The expression and binding characteristics of the different hSSTRs and the hSSTR5 C-tail deletion mutants have previously been reported (25, 44, 45). Cells were grown in T75 flasks in Hams F-12 medium containing 5% fetal calf serum (Life Technologies) and 400 U/ml G-418 and cultured for 3-5 days at 37°C in a humidified atmosphere with 5% CO₂. When the cells had reached 60-70% confluency, medium was replaced with fresh medium containing 100 nM of either OCT (hSSTRs 2,3,5) or D-Trp⁸ SST-14 (hSSTR 1,4 which do not bind OCT (11,44)). After 24 h. Incubation, the cells were then washed in PBS, scraped, fixed sequentially in 1% paraformaldehyde and 70% ethanol. Cellular DNA was labeled with the intercalating dye PI (50 µg/ml) in PBS and incubated at 37° C for 5 min in presence of RNase A (50 µg/ml). Rb and p21 were immunolabeled with their respective antibodies, followed by counterstaining with FITC conjugated secondary antibodies as previously described (11).

Flow cytometry

Flow cytometry was carried out in an EPICS 750 series flow cytometer (Coulter Electronics, Hialeah, FL). Fluorescence was excited by a 5W argon laser generating light at 351-363 nm. PI emission was detected through a 610 nm long pass filter and FITC fluorescence was detected with a 560 nm short pass dichroic filter. At least 10,000 gated events were recorded for each sample and the data analyzed by Winlist software (Verity Software House, ME).

Analysis of nuclear morphology

Aliquots of cells stained with PI for analysis by flow cytometry were cytospun onto microscope slides, mounted using Immunomount (Shandon, Pittsburgh, PA), viewed, and photographed through a Reichert Polyvar 2 fluorescence microscope (original magnification x 400).

Western Blot Analysis

Cells were lysed in Tris-HCl buffer (100 mM, pH 7.2) containing 300 mM NaCl, 2% Nonidet P-40, 20% glycerol and 2mM ZnCl₂, 10 mg/ml pepstatin and 0.2 mM pefabloc (Boehringer Mannheim, Canada). Protein measurement was performed using the Bio-Rad protein assay kit. 30 µg aliquots were electrophoresed in 10% SDS-polyacrylamide gel in Running Buffer (50 mM Tris-HCl, 60 mM Boric acid, 1 mM EDTA, 0.1% SDS), transferred onto Protran plus membranes electrophoretically in a buffer containing 25 mM Tris, 192 mM glycine and 15% methanol. Blots were probed with anti--RB antibody (Pharmlngen) and visualized with alkaline phosphatase conjugate detection kit (Bio-Rad, Hercules, CA). Molecular size was determined using 10 kDa protein ladder (Life Technologies, Grand Island, NY) and staining with Ponceau S (46).

Measurement of PTP Activity

Phosphatase activity in whole cell extracts or membrane and cytosolic fractions was determined using pNPP as the substrate as described previously (47).

Acknowledgments

This work was supported by grants from the Medical Research Council of Canada (MT 12603 and MT 10411) and the U.S. Department of Defense. K.S. is a recipient of a studentship award of the Fonds de la Recherche en Sante du Quebec. We thank Jun Cai for technical assistance with cell culture and Dr. Halwani and S. Schiller for assistance with flow cytometry.

FIGURE LEGENDS

Figure 1

Effect of peptide treatment on cell cycle parameters in CHO-K1 cells expressing hSSTR1-5. Representative plots showing the phase distribution of cells incubated for 24 h in the absence (top panel) or presence (bottom panel) of 100 nM OCT (hSSTRs 2,3,5) or D-Trp8 SST-14 (hSSTRs 1,4). Cellular DNA was stained with PI and analyzed by flow cytometry. An increase in G₁ peak can be seen in cells expressing four of the five hSSTR subtypes (hSSTR5>hSSTR2>hSSTR4~ hSSTR1). This contrasts with the decrease in G₁ peak and the appearance of a hypodiploid peak in the region A₀ seen following peptide treatment in cells expressing hSSTR3.

Figure 2

Effect of agonist treatment on cell cycle parameters in CHO-K1 cells expressing individual hSSTR subtypes. The distribution of cells in G₀/G₁ (top panel), S (middle panel) and G₂/M (bottom panel) were quantitated by analysis of PI stained cells by flow cytometry. Increase in the number of cells G₀/G₁ was accompanied by a decrease in cell number in S phase. A small increase in G₂/M was also evident in agonist treated cells (mean \pm SE, n=4). * p< 0.005; ** p< 0.05

Figure 3

hSSTR5 mediated antiproliferative signaling in CHO-K1 cells causes G₁ cell cycle arrest associated with induction of Rb. **A.** Flow cytometric analysis of hSSTR5 expressing cells incubated in the absence and presence of 100 nM OCT for 24h. Scattergram represents dual label plot of FITC fluorescence of immunostained Rb measured on a log scale against PI fluorescence meas-

ured on a linear scale. In addition, PI fluorescence depicting the cell cycle distribution is shown on the top and the FITC fluorescence of immunostained Rb fluorescence is shown on the right of the scattergram. OCT induced increase in Rb occurred in all phases of the cell cycle and was associated with an increase in the number of cells in G₁. Data representative of 3 separate experiments. **B.** Western blot analysis of Rb in CHO-K1 cells. In addition to the total increase in Rb in OCT treated cells, a significant portion was in the hypophosphorylated form (pRb) that could be distinguished from the hyperphosphorylated form (ppRb) on the basis of differential electrophoretic mobility. **C.** Nuclear morphology of PI stained cells revealed nuclear enlargement, a feature that is characteristic of G₁ arrested cells.

Figure 4

Time dependency of hSSTR5 mediated induction of Rb and inhibition of cell cycle progression. Following incubation in presence of 100 nM OCT for the indicated time, Rb and DNA were quantitated in the same cell populations by dual label flow cytometry (mean \pm SE, n=3; *, p<0.05; **, p<0.005). **A.** Change in Rb is expressed as fold increase in the fluorescence intensity compared to that in untreated cells taken as 1. **B.** Inhibition of cell proliferation by OCT is reflected in the increase in the ratio of cells in G₁ and S phases is evident by 8h and was maximal at 24 h.

Figure 5

A. Dose-dependent induction of Rb by OCT via hSSTR5. Rb was measured following immunofluorescent staining in cells incubated with the indicated concentrations of the peptide for 24 h (mean \pm SE, n=3). **B.** Immunoblot demonstrating that OCT-induced augmentation in Rb is associated with a dose-dependent increase in hypophosphorylated form of Rb (pRb).

Figure 6

hSSTR5 mediated cytostatic signaling is pertussis toxin sensitive G protein mediated and PTP dependent. OCT treated cells displayed an increase in p21 in addition to Rb. The increase in p21 in cells incubated with 100 nM OCT was less than that of Rb (3.0 ± 0.8 vs. 8.1 ± 0.8 fold respectively). hSSTR5 signaled induction of these proteins was abolished by pretreatment of the cells with 100 ng pertussis toxin for 18 h prior to incubation with the peptide. Na orthovanadate (10 μ g/ml) present during the incubation with the peptide also inhibited the action of OCT (mean \pm SE, n=4, *, $p < 0.005$; **, $p < 0.05$).

Figure 7

Effect of OCT on PTP activity in CHO-K1 cells expressing hSSTR5. PTP activity was measured in membrane and cytosolic fractions prepared from cells incubated in the absence or presence of 100 nM OCT for 24h. The enzyme activity was measured using pNPP as the substrate (mean \pm SE, n=3). By contrast, OCT did not stimulate PTP activity of the membrane fractions when added at the time of enzyme assay (not shown).

Figure 8

hSSTR subtype selectivity for induction of Rb. Maximum induction of Rb was seen in cells expressing hSSTR5, followed by hSSTR2>hSSTR4>hSSTR1. The fluorescence intensity of immunostained Rb was measured in cells incubated with 100 nM OCT (hSSTRs 2,3,5) or D-Trp⁸ SST-14 (hSSTRs 1,4) for 24 h. The relative increase in fluorescence intensity in peptide treated cells is expressed as a ratio compared to that in the respective untreated cells taken as 1 (mean \pm SE, n=3; *, $p < 0.05$; **, $p < 0.005$).

Figure 9

Topographical arrangement of primary aminoacid sequence of hSSTR5 showing the N-glycosylation sites (CHO), S/T phosphorylation sites (dark circles) and palmitoylation site (ζ). C-tail truncation mutants of this receptor were generated by inserting stop codons at sites indicated by solid lines.

Figure 10

Effect of C-tail deletion mutations on hSSTR5 initiated Rb induction. Values represent fold change in fluorescence intensity compared to that in the respective untreated controls taken as 1 (mean \pm SE, n=3, *, p<0.01; **, p<0.0001).

Figure 11

Effect of C-tail truncation on hSSTR5 signaled change in cellular distribution of PTP activity in CHO-K1 cells. PTP activity was measured using pNPP as the substrate in membrane and cytosolic fractions of cells incubated for 2 h in the absence and presence of 100 nM OCT (mean \pm SE, n=3; *, p<0.0001; **, p<0.005).

REFERENCES

1. Cheung NW, Boyages SC 1995 Somatostatin-14 and its analog octreotide exert a cytostatic effect on GH3 rat pituitary tumor cell proliferation via a transient G0/G1 cell cycle block. *Endocrinology* 136: 4174-4181.
2. Candi E, Melino G, De Laurenzi V, Piacentini M, Guerreri P, Spinedi A, Knight RA 1995 Tamoxifen and somatostatin affect tumors by inducing apoptosis. *Cancer Lett* 96: 141-145.
3. Pagliacci MC, Tognellini R, Grignani F, Nicoletti I 1991 Inhibition of human breast cancer cell (MCF-7) growth in vitro by the somatostatin analog SMS 201-995: effects on cell cycle parameters and apoptotic cell death. *Endocrinology* 129: 2555-2562.
4. Sharma K, Srikant CB 1998 Induction of wild type p53, Bax and a cation-insensitive acidic endonuclease during somatostatin signaled apoptosis in MCF-7 human breast cancer cells. *Int J Canc* 76: 259-266.
5. Srikant CB 1995 Cell cycle dependent induction of apoptosis by somatostatin analog SMS 201-995 in AtT-20 mouse pituitary cells. *Biochem Biophys Res Commun* 209: 400-406.
6. Patel YC, Greenwood MT, Panetta R, Demchyshyn L, Niznik H, Srikant CB 1995 The somatostatin receptor family. *Life Sci* 57: 1249-1265.
7. Patel YC, Greenwood M, Panetta R, Hukovic N, Grigorakis S, Robertson LA, Srikant CB 1996 Molecular biology of somatostatin receptor subtypes. *Metabolism* 45: 31-38.
8. Bruno JF, Xu Y, Berelowitz M 1994 Somatostatin regulates somatostatin receptor subtype mRNA expression in GH3 cells. *Biochem Biophys Res Commun* 202: 1738-1743.

9. Patel YC, Panetta R, Escher E, Greenwood M, Srikant CB 1994 Expression of multiple somatostatin receptor genes in AtT-20 cells. Evidence for a novel somatostatin-28 selective receptor subtype. *J Biol Chem* 269: 1506-1509.
10. Xu Y, Song J, Berelowitz M, Bruno JF 1996 Estrogen regulates somatostatin receptor subtype 2 messenger ribonucleic acid expression in human breast cancer cells. *Endocrinology* 137: 5634-5640.
11. Sharma K, Patel YC, Srikant CB 1996 Subtype-Selective Induction of Wild-Type P53 and Apoptosis, But Not Cell Cycle Arrest, By Human Somatostatin Receptor 3. *Mol Endocrinol* 10: 1688-1696.
12. Sharma K, Srikant CB 1998 G protein-coupled receptor signaled apoptosis is associated with induction of a cation-insensitive acidic endonuclease and intracellular acidification. *Biochem Biophys Res Commun* 242: 134-140.
13. Sharma K, Patel YC, Srikant CB, 1997 Subtype selective human somatostatin receptor (hSSTR) mediated cytostatic and cytotoxic actions involve different signaling mechanisms. In: *77th Annual Meeting of the Endocrine Society, Minneapolis, MN*, pp. Abstract #P-152, p.172.
14. Buscail L, Esteve JP, Saint-Laurent N, Bertrand V, Reisine T, AM OC, Bell GI, Schally AV, Vaysse N, Susini C 1995 Inhibition of cell proliferation by the somatostatin analogue RC-160 is mediated by somatostatin receptor subtypes SSTR2 and SSTR5 through different mechanisms. *Proc Natl Acad Sci U S A* 92: 1580-1584.

15. Buscail L, Delesque N, Esteve JP, Saint-Laurent N, Prats H, Clerc P, Robberecht P, Bell GI, Liebow C, Schally AV, Vaysse N, Susini C 1994 Stimulation of tyrosine phosphatase and inhibition of cell proliferation by somatostatin analogues: mediation by human somatostatin receptor subtypes SSTR1 and SSTR2. *Proc Natl Acad Sci USA* 91: 2315-2319.
16. Florio T, Scorizello A, Fattore M, V DA, Salzano S, Rossi G, Berlingieri MT, Fusco A, Schettini G 1996 Somatostatin inhibits PC Cl3 thyroid cell proliferation through the modulation of phosphotyrosine activity. Impairment of the somatostatinergic effects by stable expression of E1A viral oncogene. *J Biol Chem* 271: 6129-6136.
17. Lopez F, Esteve JP, Buscail L, Delesque N, Saint-Laurent N, Vaysse N, Susini C 1996 Molecular mechanisms of antiproliferative effect of somatostatin: involvement of a tyrosine phosphatase. *Metabolism* 45: 14-16.
18. Weinberg RA 1995 The retinoblastoma protein and cell cycle control. *Cell* 81: 323-330.
19. Sherr CJ 1993 Mammalian G1 cyclins. *Cell* 73: 1059-1065.
20. Hermeking H, Funk JO, Reichert M, Ellwart JW, Eick D 1995 Abrogation of p53-induced cell cycle arrest by c-Myc. Evidence for an inhibitor of p21(WAF1/CIP1/SDI1). *Oncogene* 11: 1409-1415.
21. Michieli P, Chedid M, Lin D, Pierce JH, Mercer We, Givol D 1994 Induction of WAF1/CIP1 by a p53-independent pathway. *Cancer Res.* 54: 3391-3395.
22. Ookawa K, Tsuchida S, Adachi J, Yokota J 1997 Differentiation induced by RB expression and apoptosis induced by p53 expression in an osteosarcoma cell line. *Oncogene* 14: 1389-1396.

23. Baldwin JM 1994 Structure and function of receptors coupled to G proteins. *Curr Opin Cell Biol* 6: 180-190.
24. Dohlman HG, Thorner J, Caron MG, Lefkowitz RJ 1991 Model systems for the study of seven-transmembrane-segment receptors. *Annu Rev Biochem* 60: 653-688.
25. Hukovic N, Panetta R, Kumar U, Rocheville M, Patel YC 1998 The cytoplasmic tail of the human somatostatin receptor type 5 is crucial for interaction with adenylyl cyclase, and in mediating desensitization and internalization. *J. Biol. Chem.* :273: 21416-21422.
26. Yoshitomi Y, Fujii Y, Miyazaki M, Nakajima N, Inagaki N, Seino S 1997 Involvement of MAP kinase and c-fos signaling in the inhibition of cell growth by somatostatin. *Am. J. Physiol.* 272 (Endocrinol. Metab. 35): E769-E774.
27. Reardon DB, Wood SL, Brautigan DL, Bell GI, Dent P, Sturgill TW 1996 Activation of a protein tyrosine phosphatase and inactivation of Raf-1 by somatostatin. *Biochem J* 314: 401-404.
28. Lopez F, Esteve JP, Buscail L, Delesque N, Saint-Laurent N, Theveniau M, Nahmias C, Vaysse N, Susini C 1997 The tyrosine phosphatase SHP-1 associates with the sst2 somatostatin receptor and is an essential component of sst2-mediated inhibitory growth signaling. *Journal of Biological Chemistry* 272: 24448-24454.
29. Dou QP, An B, Will PL 1995 Induction of a retinoblastoma phosphatase activity by anti-cancer drugs accompanies p53-independent G1 arrest and apoptosis. *Proceedings of the National Academy of Sciences of the United States of America* 92: 9019-9023.
30. Nie L, Oishi Y, Doi I, Shibata H, Kojima I 1997 Inhibition of proliferation of MCF-7 breast cancer cells by a blocker of Ca^{2+} -permeable channel. *Cell Calcium* 22: 75-82.

31. Takuwa N, Zhou W, Kumada M, Takuwa Y 1993 Ca^{2+} -dependent stimulation of retinoblastoma gene product phosphorylation and p34cdc2 kinase activation in serum-stimulated human fibroblasts. *J. Biol. Chem.* 268: 138-145.
32. Yatsunami J, Komori A, Ohta T, Suganuma M, Fujuki H 1993 Hyperphosphorylation of retinoblastoma protein and p53 by okadaic acid, a tumor promoter. *Cancer Res.* 53: 239-241.
33. Cordelier P, Esteve JP, Bousquet C, Delesque N, AM OC, Schally AV, Vaysse N, Susini C, Buscail L 1997 Characterization of the antiproliferative signal mediated by the somatostatin receptor subtype sst5. *Proc Natl Acad Sci U S A* 94: 9343-9348.
34. Crespo P, Xu N, Simonds WF, Gutkind JS 1994 Ras-dependent activation of MAP kinase pathway is mediated by G protein $\beta\gamma$ subunits. *Nature* 369: 418-420.
35. Koch WJ, Hawes BE, Allen LF, Lefkowitz RJ 1994 Direct evidence that Gi-coupled receptor stimulation of mitogen-activated protein kinase is mediated by G $\beta\gamma$ activation of p21^{ras}. *Proc. Natl. Acad. Sci. USA* 91: 12706-12710.
36. Marshall CJ 1994 MAP kinase kinase kinase, MAP kinase kinase and MAP kinase. *Curr. Opin. Genes Dev.* 4: 82-89.
37. Dent P, Reardon DB, Wood SL, Lindorfer MA, Graber SG, Garrison JC, Brautigan DL, Sturgill TW 1996 Inactivation of raf-1 by a protein-tyrosine phosphatase stimulated by GTP and reconstituted by Galphai/o subunits. *J Biol Chem* 271: 3119-3123.
38. Dent P, Reardon DB, Morrison DK, Sturgill TW 1995 Regulation of Raf-1 and raf-1 mutants by Ras-dependent and Ras-independent mechanisms in vitro. *Mol. Cell. Biol.* 15: 4125-4135.

39. Yao B, Zhang Y, Delikat S, Mathais S, Basu S, Kolesnick R 1995 Phosphorylation of Raf by ceramide-activated protein kinase. *Nature* 378: 307-310.
40. Cattaneo MG, Amoroso D, Gussoni G, Sanguini AM, Vicentini LM 1996 A somatostatin analogue inhibits MAP kinase activation and cell proliferation in human neuroblastoma and in human small cell lung carcinoma cell lines. *FEBS Letters* 397: 164-168.
41. Ruiz-Torres P, Lucio FJ, Gonzalez-Rubio M, Rodriguez-Puyol M, Rodriguez-Puyol D 1993 A dual effect of somatostatin on the proliferation of cultured rat mesangial cells. *Biochem. Biophys. Res. Commun.* 195: 1057-1062.
42. David M, Chen HE, Goelz S, Larner AC, Neel BG 1995 Differential regulation of the alpha/beta interferon-stimulated Jak/Stat pathway by the SH2 domain-containing tyrosine phosphatase SHPTP1. *Mol Cell Biol* 15: 7050-7058.
43. Wilkinson GF, Thurlow RJ, Sellers LA, Coote JE, Fenuik W, Humphrey PP 1996 Potent antagonism by BIM-23056 at the human recombinant somatostatin sst5 receptor. *Brit. J. Pharmacol.* 118: 445-447.
44. Patel YC, Srikant CB 1994 Subtype selectivity of peptide analogs for all five cloned human somatostatin receptors (hsstr1-5). *Endocrinology* 135: 2814-2817.
45. Patel YC, Greenwood MT, Warszynska A, Panetta RP, Srikant CB 1994 All five cloned human somatostatin receptors (hSSTR1-5) are functionally coupled to adenylylcyclase. *Biochem. Biophys. Res. Commun.* 198: 605-612.
46. Srikant CB, Shen SH 1996 Octapeptide somatostatin analog SMS 201-995 induces translocation of intracellular PTP1C to membranes in MCF-7 human breast adenocarcinoma cells. *Endocrinology* 137: 3461-3468.

47. Zhao Z, Bouchard P, Diltz CD, Shen SH, Fischer EH 1993 Purification and characterization of a protein tyrosine phosphatase containing SH2 domains. *J Biol Chem* 268: 2816-2820.

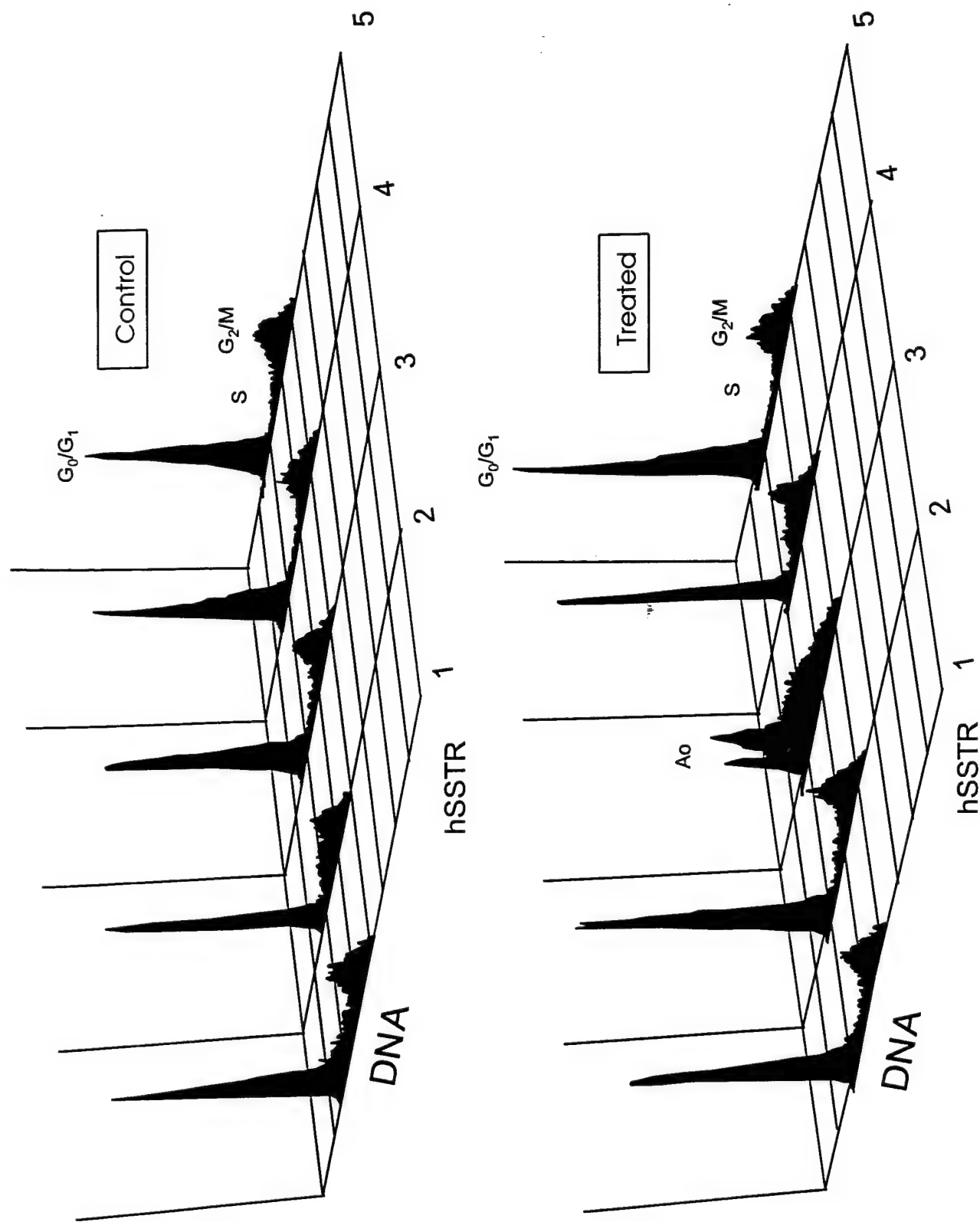


Figure 1

Sharma et al.

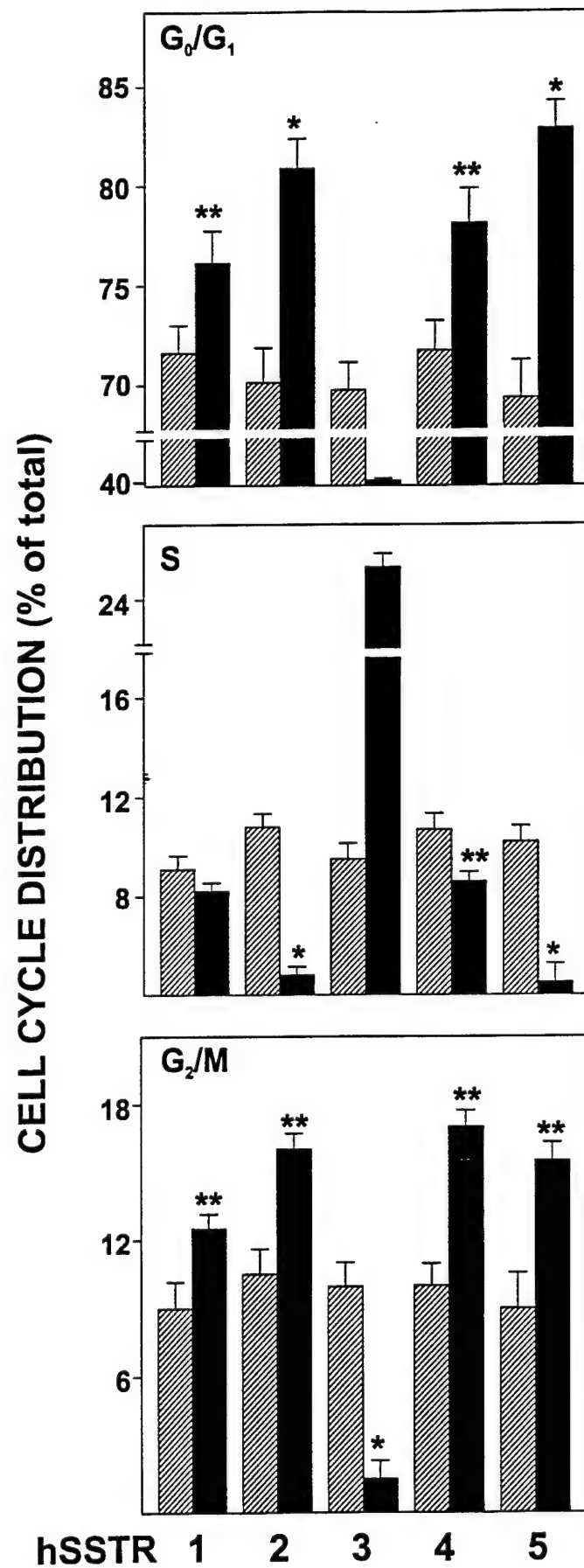
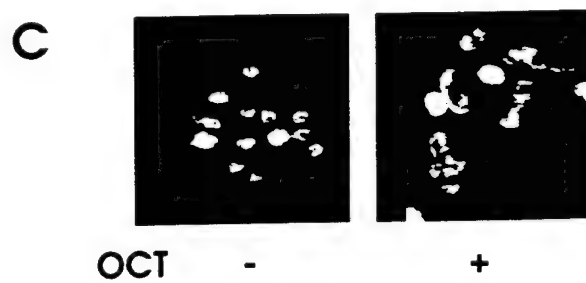
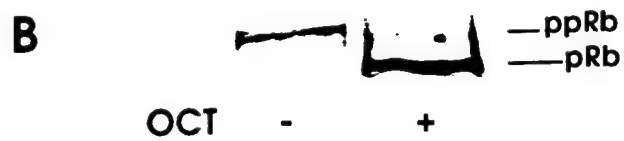
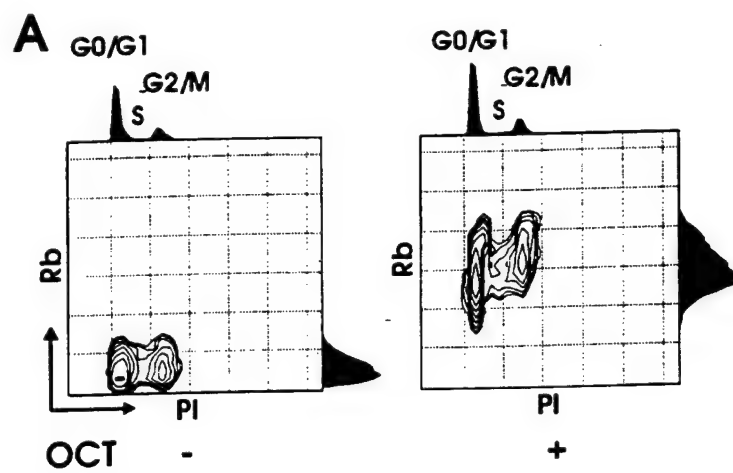


Figure 2
Sharma et al.



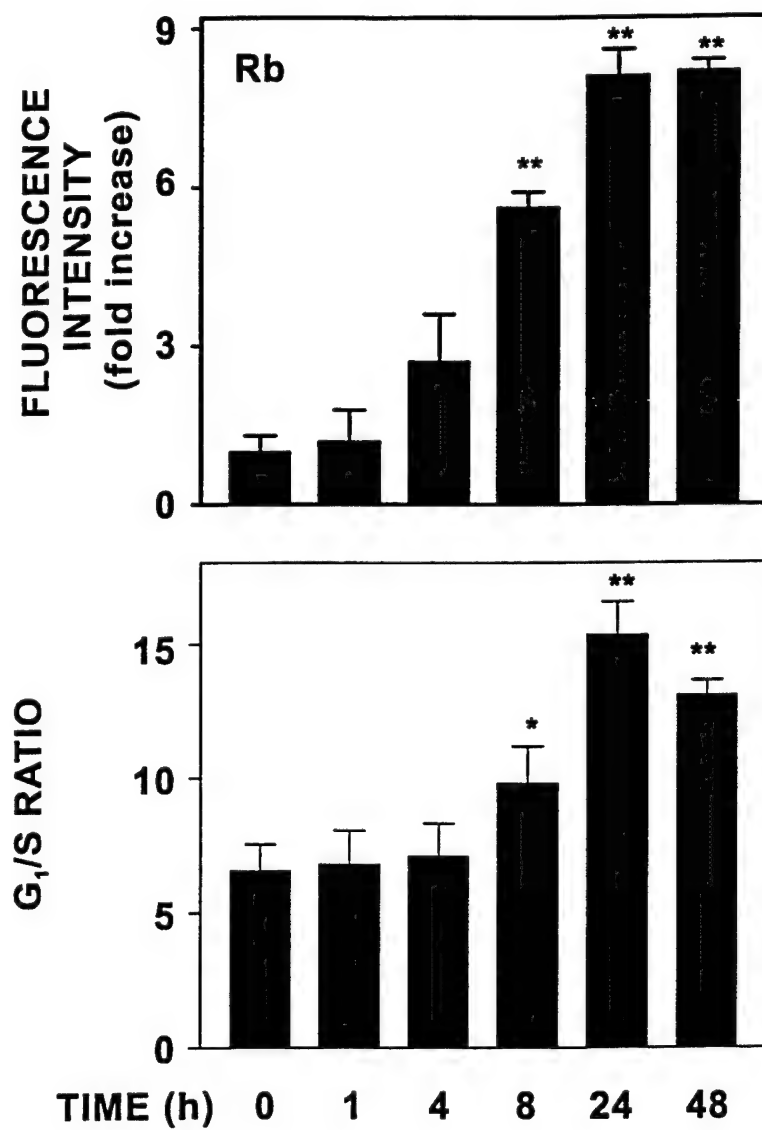


Figure 4
Sharma et al.

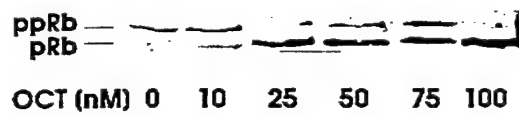
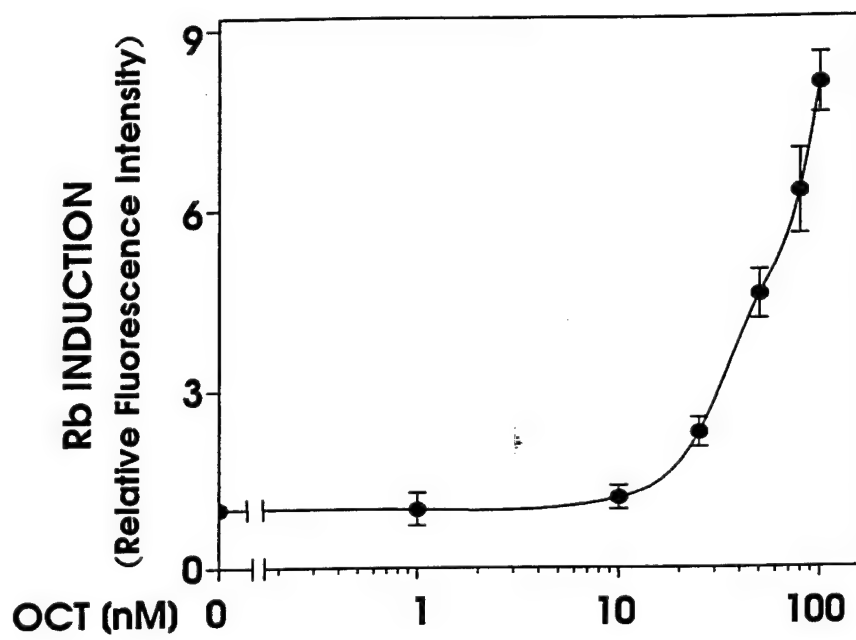


Figure 5A
Sharma et al.

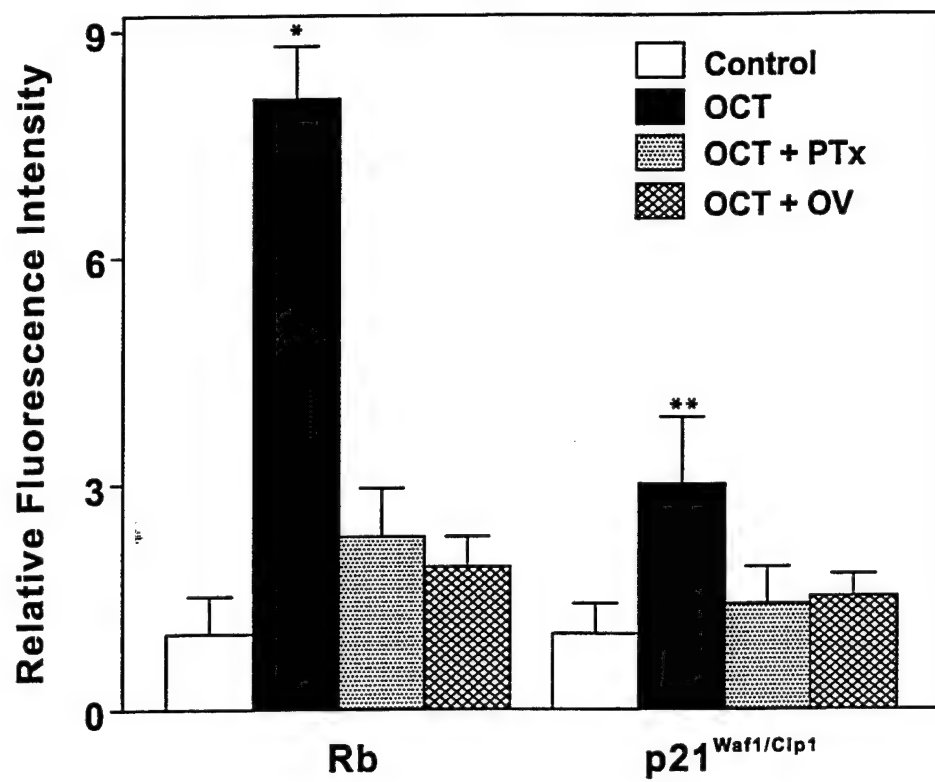


Figure 6

Sharma et al.

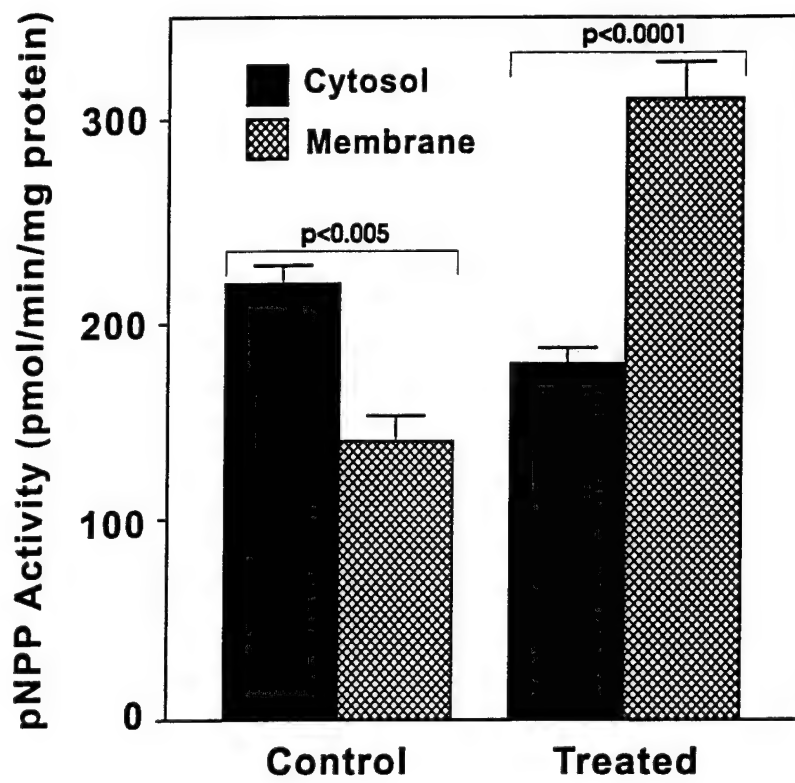


Figure 7
Sharma et al.

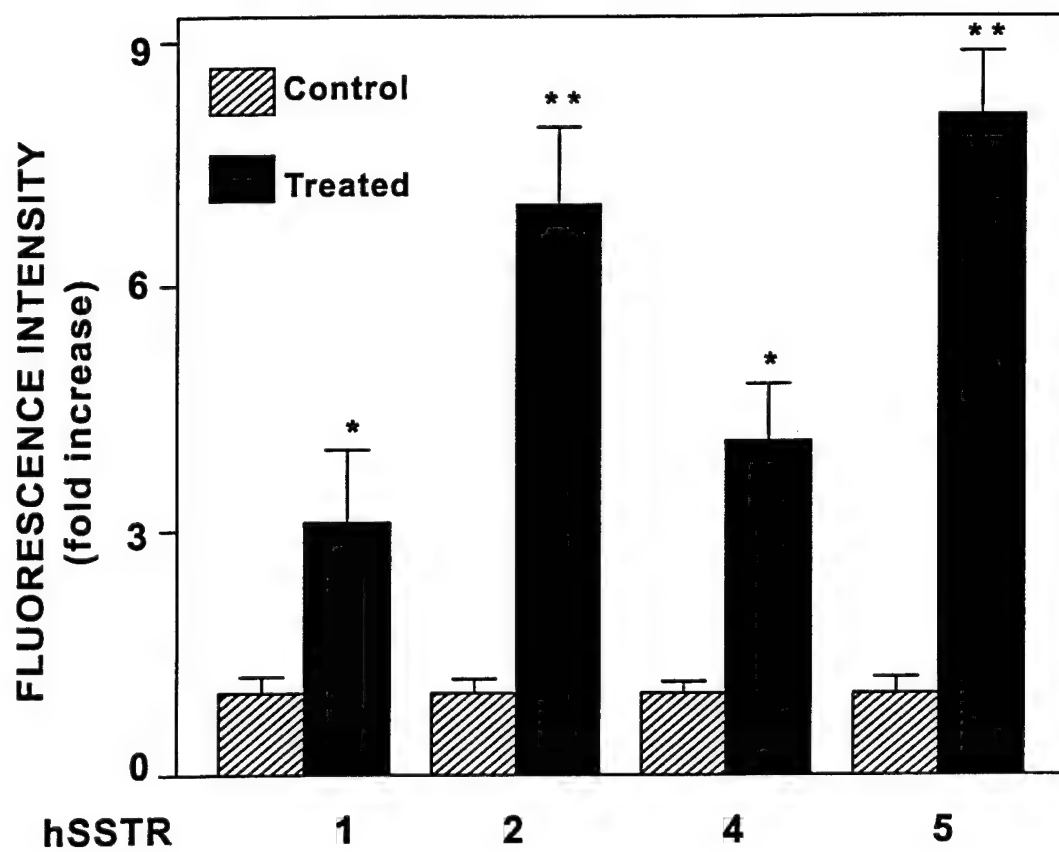
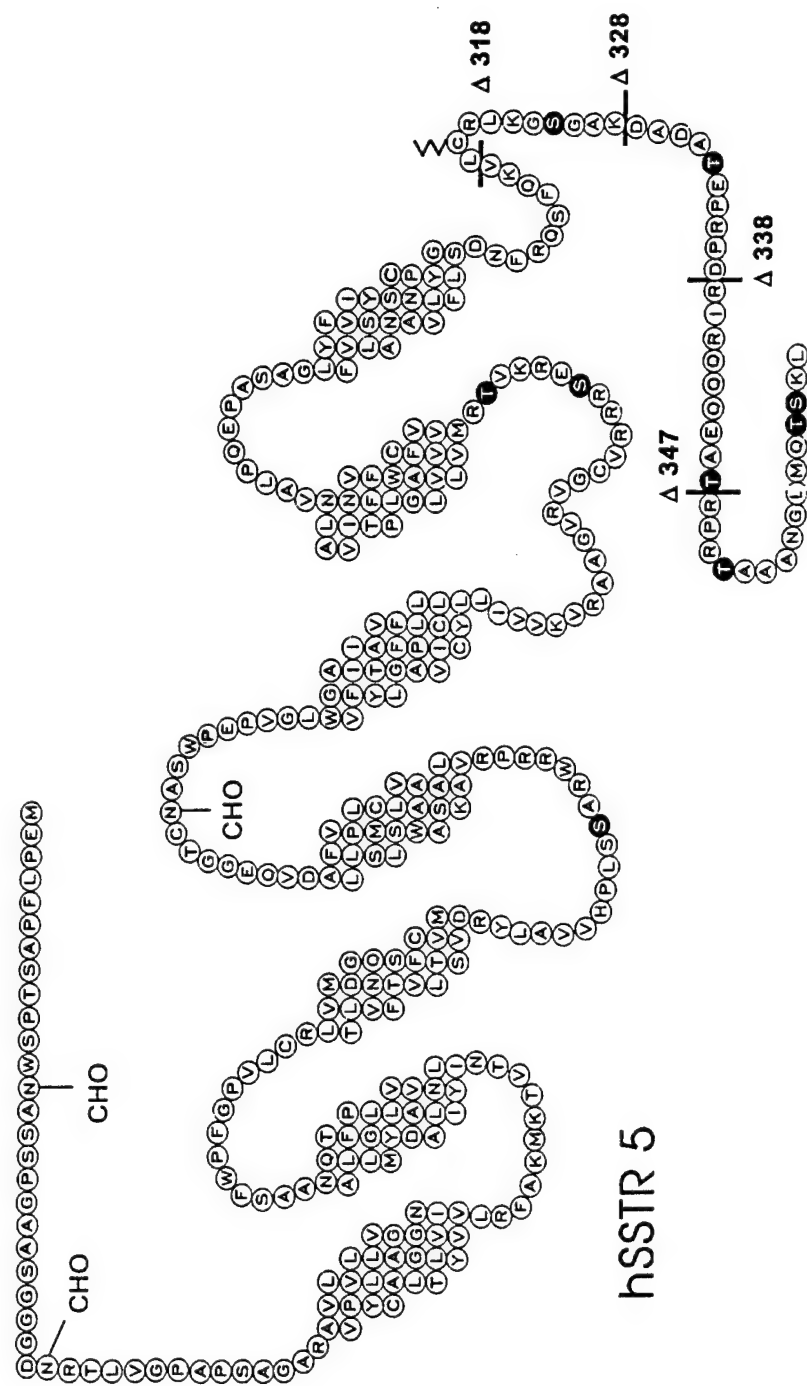


Figure 8
Sharma et al.

Figure 9
Kamal et al

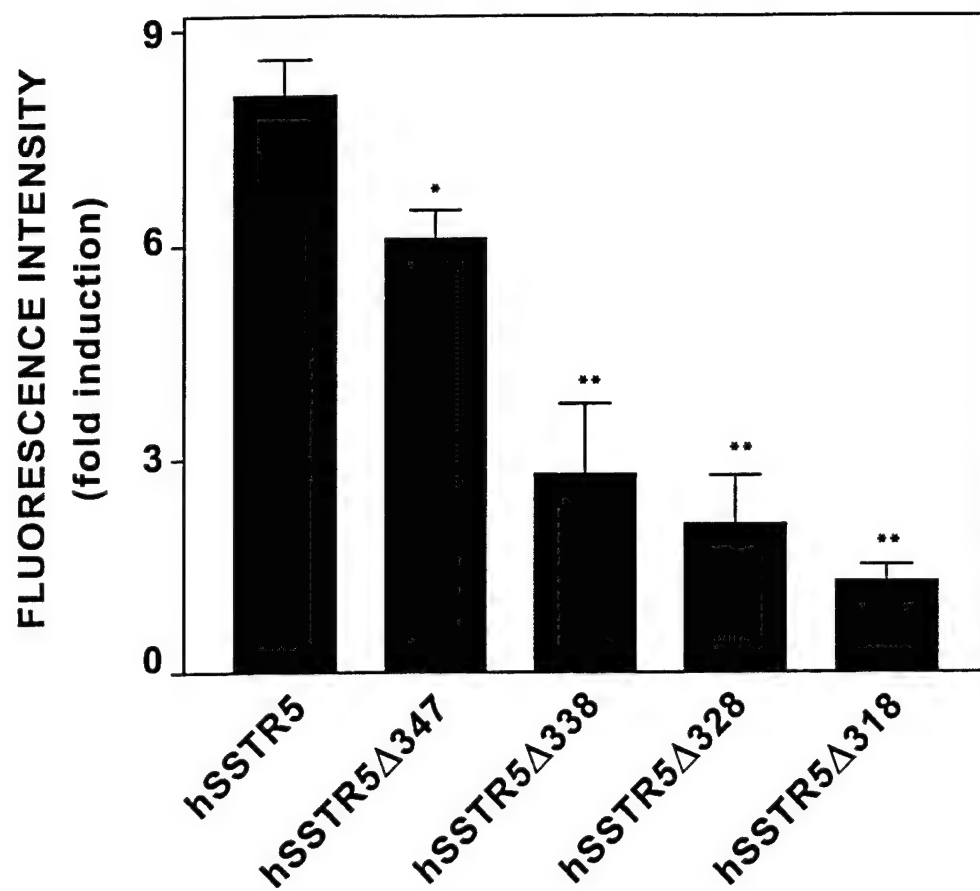


Figure 10
Sharma et al.

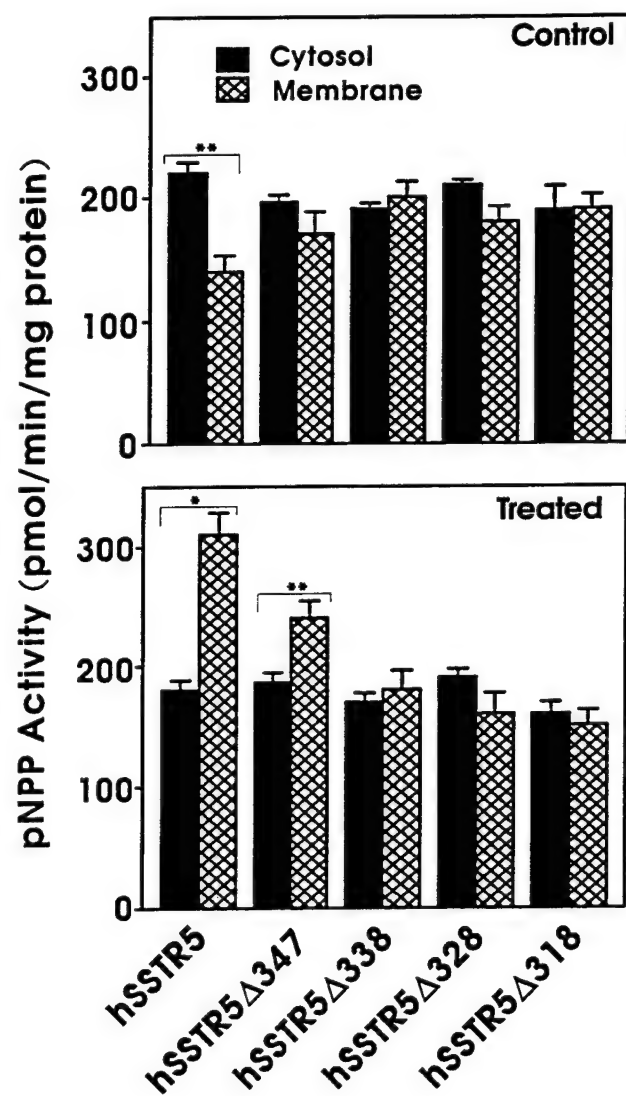


Figure 11
Sharma et al.

**SUBTYPE SELECTIVE EXPRESSION OF THE FIVE SOMATOSTATIN RECEPTORS
(hSSTR1-5) IN HUMAN PANCREATIC ISLET CELLS: A QUANTITATIVE DOUBLE-
LABEL IMMUNOHISTOCHEMICAL ANALYSIS**

Ujendra Kumar, Ramakrishnan Sasi, Sundar Suresh, Amit Patel, Muthusamy Thangaraju, Peter

Metrakos, Shutish C. Patel, and Yogesh C. Patel

Fraser Laboratories, Departments of Medicine and Neurology and Neurosurgery, and Surgery,

McGill University, Royal Victoria Hospital, and the Montreal Neurological Institute, Montreal,

Quebec H3A 1A1, Canada.

Running Title: Somatostatin Receptor Subtypes in Human Islet Cells

Address for correspondence: Dr. Y.C. Patel

Room M3-15, Royal Victoria Hospital

687 Pine Avenue West

Montreal, Quebec H3A 1A1

CANADA

TELE: (514) 842-1231 ext. 5042

FAX: (514) 849-3681

E-mail: patel@rvhmed.lan.mcgill.ca

Key Words: somatostatin, receptors, human, islet, immunohistochemistry

ABSTRACT

We have developed a panel of rabbit polyclonal antipeptide antibodies against the five somatostatin receptor subtypes (hSSTR1-5) and used them to analyse the pattern of expression of hSSTR1-5 in normal human islet cells by quantitative double label confocal fluorescence immunocytochemistry. All five hSSTR subtypes were variably expressed in islets. The number of SSTR immunopositive cells showed a rank order of SSTR1 > SSTR5 > SSTR2 > SSTR3 > SSTR4. SSTR1 was strongly colocalized with insulin in all β cells. SSTR5 was also an abundant isotype being colocalized in 87% of β cells. SSTR2 was found in 46% of β cells whereas SSTR3 and 4 were relatively poorly expressed. SSTR2 was strongly colocalized with glucagon with 89% of α cells whereas SSTR5 and SSTR1 colocalized with glucagon in 35% and 26% of α cells respectively. SSTR3 was detected in occasional α cells and SSTR4 was absent. SSTR5 was preferentially expressed in 75% of SST positive cells and was the principal δ cell SSTR subtype whereas SSTR1-3 were colocalized in only a few δ cells and SSTR4 was absent. These studies reveal predominant expression of SSTR1, 2, and 5 in human islets. β , α , and δ cells each express multiple SSTR isoforms, β cells being rich in SSTR1 and SSTR5, α cells in SSTR2, and δ cells in SSTR5. Although there is no absolute specificity of any SSTR for an islet cell type, SSTR1 is β cell selective, and SSTR2 α cell selective. SSTR5 is well expressed in β and δ cells, and moderately well expressed in α cells, and thereby lacks the islet cell selectivity displayed by SSTR1 and SSTR2. Subtype selective SSTR expression in islet cells could be the basis for preferential insulin suppression by SSTR1 specific ligands and of glucagon inhibition by SSTR2 selective compounds.

INTRODUCTION

Somatostatin (SST)¹, a multi-functional peptide, is produced in many cells throughout the body notably in the brain, gastrointestinal tract, and pancreas (1,2). There are two endogenous bioactive forms of SST, SST-14 and SST-28, which act on a diverse array of endocrine, exocrine, neuronal, and immune cell targets to inhibit secretion, modulate neurotransmission, and regulate cell division (1-4). These actions are mediated by a family of G protein coupled receptors with five known subtypes termed SSTR1-5 that are widely expressed in the brain and periphery in a tissue- and subtype-selective manner (3,4). All five SSTRs are functionally coupled to inhibition of adenylyl cyclase (3). Some of the receptor subtypes also signal through other effectors such as phosphotyrosine phosphatase, K^+ , and voltage-dependent Ca^{2+} ion channels, a Na^+ / H^+ exchanger, phospholipase C, phospholipase A_2 , and in vitro activated protein kinase (3). SST-14 and SST-28 bind to all five human (h) SSTR subtypes with nanomolar affinity (5). SSTR1-4 bind the two peptides approximately equally whereas SSTR5 displays weak selectivity for SST-28 (5). This is in contrast to the current generation of clinically used SST analogs, the octapeptides octreotide and lanreotide, which bind to only three SSTRs displaying high affinity for SSTR2 and 5 and moderate affinity for SSTR3 (3-5). SSTRs are dynamically regulated at the membrane in a time-dependent manner by agonist treatment (6-9). SSTR2,3,4, and 5 undergo acute desensitization and are variably internalized whereas SSTR1 is resistant to internalization (6-9). Furthermore, during longterm agonist treatment SSTR1, and to a lesser extent SSTR2 and 4 are upregulated at the membrane

¹**Abbreviations:** SST, somatostatin; SST-14, somatostatin-14; SST-28, somatostatin-28; SSTR, somatostatin receptor; ICL, intracellular loop; ECL, extracellular loop; BSA, bovine serum albumin; TBS, tris buffered saline; NGS, normal goat serum.

whereas there is no effect on SSTR3 and 5 (6).

The pancreas is an important target of SST action, and with increasing use of SST analogs for treating neuroendocrine tumors and various digestive disorders, a great deal of interest is currently focused on the effects of longterm SST pharmacotherapy on islet cell function and the nature of the SSTR subtypes expressed in islet cells (1,2,10,11). SST is produced in the pancreas in islet δ cells and acts directly on β and α cells to inhibit both the synthesis and secretion of insulin and glucagon (12-15). SST also inhibits pancreatic polypeptide as well as endogenous SST secretion from δ cells through an autofeedback mechanism (2,16,17). Specific high affinity binding sites for SST have been demonstrated in isolated rat islets, cultured islet cells, and hamster (HIT) and rat (Rin M5f) insulinoma cells (2, 18-24). By quantitative electron microscopic autoradiography, binding sites for SST have been identified in β , α , and δ cells in cultured rat islet preparations (18,21,22). Furthermore, using SST-14 and SST-28 selective radioligands, SS-28 preferring sites have been shown to predominate on β cells and SST-14 sites on α cells (21). At a molecular level, little progress has been made in characterizing the pattern of expression of the five cloned SSTR subtypes in individual islet cell subpopulations. Preliminary evidence based on reverse transcriptase polymerase chain reaction has shown expression of mRNA for each of the five SSTR subtypes in whole rat islets (25). By immunohistochemistry, SSTR2 has been recently reported to be localized in α and PP cells but not in β cells of rat islets (26). In contrast to the rat, nothing is currently known about the expression of SSTRs in human islets. Furthermore, because of known species-specific variations in SSTR expression, the results of rat islet SSTRs may not apply to human islets (2-4). Accordingly, in the present study, we have developed and characterized a panel of SSTR1-5

selective polyclonal antibodies and applied them to study the immunohistochemical colocalization of the receptor isotypes in human islet cells as a necessary step towards elucidating differential islet cell SSTR expression and subtype-specific regulation of individual pancreatic hormones.

METHODS

Reagents and Cell Lines Expressing SSTRs

Porcine monocomponent insulin and porcine glucagon were obtained from Novo Nordisk (Copenhagen, Denmark). Synthetic SST-14 was purchased from Bachem (Torrance, CA). Antisera to islet hormones were obtained as gifts as follows: guinea pig anti insulin serum (P. Wright, Indianapolis, IN); sheep antiglucagon serum (R.A. Donald, Christchurch, N.Z.); mouse monoclonal anti SST-14 (J.C. Brown, Vancouver, B.C.). Rhodamine conjugated goat anti-rabbit secondary antibody as well as anti-guinea pig, anti-sheep, and anti-mouse FITC conjugated secondary antibodies were obtained from Jackson Laboratory (Bar Harbor, Maine). Stable CHO-K1 transfectants individually expressing hSSTR1-5 were prepared as described and cultured in Ham's F12 medium containing 10% fetal calf serum and 400 µg/ml G418 (27).

Production and Characterization of SSTR Antibodies

Rabbit polyclonal antibodies were raised against synthetic oligopeptides of 13-22 mer corresponding to sequences in the C-tail, the third intracellular loop (ICL) or the second extracellular loop (ECL) of human or rat SSTR as shown below. The sequences selected were identical in the case of human and rat SSTR1 and SSTR2, or differed by a single amino acid residue in the case of SSTR4 (4). The rSSTR3 and rSSTR5 oligopeptides showed 50% and 70% sequence

identity with the corresponding regions of the human receptors (4).

hSSTR1 - C-tail	LKSRAYSVEDFQPENL
hSSTR2 - C-tail	DGERSDSKQDKSRLNETTETQR
rSSTR3 - 3rd ICL	RAPSCQWVQAPACQRRR
rSSTR4 - 2nd ECL	DTRPARGGEAVAC
rSSTR5 - C-tail	RRGYGMEDADAIEPRP

Peptides were conjugated to keyhole limpet hemocyanin and the complexes used for rabbit immunization (27). Anti SSTR activity in rabbit sera was screened by dot blot analysis against the peptide antigens. Antibodies identified in this way were purified from whole serum by immunoaffinity chromatography using the immunizing peptides crosslinked to activated agarose beads. Immunoaffinity purified SSTR antibodies were characterized by Western blots analysis and immunocytochemistry using CHO-K1 cells individually transfected with hSSTR1-5.

Western Blot Analysis

Brain membranes were prepared from cerebrocortical tissue freshly obtained from male Sprague-Dawley rats for analysis of SSTR proteins. 35 µg membrane protein was solubilized in sample buffer containing 62.5 mM Tris-HCl, pH 6.8, 2% SDS, 10% glycerol, and 50 mM dithiothreitol and fractionated by electrophoresis on 10% SDS polyacrylamide gels as described by Laemmli (28). The fractionated proteins were transferred by electrophoresis to 0.2 µm nitrocellulose membranes (Protran BA83, Schleicher & Schuell Inc.) in a transfer buffer containing 0.025 M Tris - 0.192 M glycine, 15% methanol. The membranes were blocked with 5% bovine serum albumin

(BSA) in Tris-buffered saline (50 mM Tris-HCl, pH 7.4, 1.5% NaCl) (TBS) containing 0.2% Tween 20 for 3 h at 20° C and subsequently incubated overnight at 4 ° C with affinity purified SSTR1-5 antisera or antigen preabsorbed antisera (2 µg/ul) each diluted 1:400 in TBS containing 0.2% Tween 20. Immunoreactive bands were detected by exposure to x-ray films processed for chemiluminescent detection (CSPD, Boehringer Mannheim). For molecular weight estimates, the 10 kDa protein ladder standard (Life Technologies, Bethesda, MD) was used.

Immunocytochemistry

CHO-K1 cells were fixed in 4% paraformaldehyde and processed for immunocytochemistry as previously described (27). Pancreata were freshly obtained from 3 accidentally deceased individuals (2 male, 1 female, age range 34-56) through the McGill Pancreas Transplantation Program. The pancreas was removed by dissection, perfused with University of Wisconsin solution, stored at 4°C for 8-12h (cold ischaemia time), prior to fixation in 4% formaldehyde for 2h at room temperature and embedding in paraffin. Five µm sections were deparaffinized, incubated in 1% BSA, and 5% normal goat serum (NGS) in TBS for 1 h at room temperature. Sections were then incubated with SSTR antibodies (affinity purified and diluted 1:500 - 1:700 in TBS) at 4° C overnight in a humid atmosphere. Following 3 successive washes in TBS, sections were incubated with rhodamine conjugated goat anti-rabbit IgG (diluted 1:100 in TBS) for 60 min at room temperature and after several additional washes in TBS, were mounted in Immunofluor mounting medium for visualization under a confocal microscope. For double immunofluorescence localization of SSTR1-5 with insulin, glucagon, and SST, sections were first immunostained for SSTR1-5 and then processed for islet hormone localization using a similar protocol to that for SSTR

immunohistochemistry. Sections were incubated overnight at 4° C with guinea pig anti-insulin serum (1:800), sheep anti-glucagon serum (1:1000), or anti-mouse monoclonal SST-14 (1:100) antibodies. After three washes in TBS, sections were incubated with FITC conjugated goat anti-guinea pig, goat anti-sheep, and goat anti-mouse secondary antibody to visualize insulin, glucagon, and SST respectively. Sections were then washed again in TBS and mounted in Immunofluor.

All fluorescent images were visualized on a Zeiss LSM 410 inverted confocal microscope equipped with an argon-krypton laser. Rhodamine signals for SSTR1-5 were imaged by exciting samples with a helium/neon (543 nM) laser. Fluorescein signals for insulin, glucagon, and SST in the same field were obtained by excitation with a 488 nM line from an argon/krypton laser. The images were overlapped for colocalization of SSTRs in insulin, glucagon, and SST immunoreactive cells. Images were obtained as single optical sections taken from the tissue and averaged over 32 scans per frame. All images were archived on Jaz Iomega disk and printed on a Kodak XLS8300 high resolution (300 dpr) color printer. To validate the specificity of SSTR immunoreactivity, the following controls were included: (a) preimmune serum in place of primary antibody; (b) primary antibody absorbed with excess antigen; (c) nontransfected CHO-K1 cells. Antigen absorbed antibody was used as control for insulin, glucagon, and SST immunofluorescence.

Quantitative Analysis

The three pancreases were subjected to quantitative analysis to determine the percent of insulin, glucagon, and SST positive cells which colocalized SSTR1-5. The mean percent of β , α , and δ cells coexpressing a given SSTR subtype was determined in 8-20 islets from each pancreas

and the results presented as mean \pm SE (n=3). Because islets in a given section varied in size, they were randomly selected to include both large and small islets. 1081 ± 80 insulin positive cells, 432 ± 28 glucagon positive cells, and 221 ± 12 SST positive cells were analysed for colocalization of each of the five SSTRs.

RESULTS

Specificity of SSTR1-5 Antibodies

Figure 1 illustrates Western blots of SSTR1-5 in rat brain membranes probed with immunoaffinity purified SSTR antisera. Major protein bands of 53 kDa (SSTR1), 57 kDa (SSTR2), 60 kDa (SSTR3), 44 kDa (SSTR4), and 58 kDa (SSTR5) were obtained. Additional minor bands of 43 kDa (SSTR1), 90 kDa (SSTR3) and 75 kDa (SSTR5) were observed in the case of three of the SSTRs. The bands were specific and were inhibited in the presence of antigen absorbed antibody. CHO-K1 cells stably transfected with individual hSSTR1-5 displayed positive fluorescence only when reacted with the corresponding SSTR primary antibody (data not shown). There was no crossreactivity of any of the five SSTR antisera with another (nonhomologous) subtype.

Distribution of SSTR1-5 in Pancreatic Islets

Figure 2 shows representative islets from different parts of the pancreas single stained with SSTR1-5. The five SSTRs were variably expressed in all islets examined (panels A-J). Rhodamine immunofluorescence was confined mainly to islet endocrine cells and to occasional nonislet cells and was distributed both on the cell surface as well as in cytoplasmic vesicular structures (Fig. 2, panels K-O). All islets displayed intense SSTR1 immunofluorescence in the majority of cells. In the case of SSTR2, two populations of islets of large and small size were identified with different patterns of expression of this subtype (panels B, G). Large islets expressed SSTR2 in many cells in the center as well as the periphery, whereas in smaller sized islets, SSTR2 positive cells were confined to the peripheral mantle zone. SSTR3 and SSTR4 were expressed in only a few islet cells whereas SSTR5 was localized in the majority of islet cells. Quantitative analysis of the total number

of SSTR immunopositive islet cells showed a rank order of $\text{SSTR1} > \text{SSTR5} > \text{SSTR2} > \text{SSTR3} > \text{SSTR4}$. Outside the islet, SSTR2 was readily identified in the walls of many small and medium sized arterioles; scattered nonislet cells with a neuronal appearance were positive for SSTR1, 2, and 3 (not shown).

Colocalization of SSTR1-5 With Insulin in Islet β Cells

To determine the pattern of expression of SSTR1-5 in individual islet cell subpopulations, we undertook a quantitative analysis by double-label immunofluorescence confocal microscopy of SSTR antigens with insulin, glucagon, and somatostatin. Figure 3 (panels A-E) shows rhodamine immunofluorescent localization of SSTR1-5 (in red) in representative islet samples. β cells were identified in the same sections by fluorescein immunofluorescence with insulin antibody (in green) and accounted for approximately 80% of the islet endocrine cells (Fig. 3, panels F-J). Overlapping the SSTR and insulin immunofluorescent images, revealed colocalization of SSTR1-5 with insulin (yellow-orange color) (Fig. 3, K-O). By quantitative analysis, SSTR1 colocalized strongly with all insulin positive cells and was the predominant β cell SSTR (Fig. 4, upper panel). SSTR2 colocalized with $46 \pm 9\%$ of insulin-producing cells whereas SSTR3 and SSTR4 were relatively poorly expressed in $28 \pm 8\%$ and $17 \pm 4\%$ of β cells respectively. SSTR5 was also an β -cell abundant isotype being colocalized in $87 \pm 10\%$ of cells. Overall, the relative frequency of SSTR expression in β cells was $\text{SSTR1} > \text{SSTR5} > \text{SSTR2} > \text{SSTR3} > \text{SSTR4}$.

Colocalization of SSTR1-5 With Glucagon in Islet α Cells

Figure 5 depicts representative islet sections processed for colocalization of SSTR1-5

(rhodamine fluorescence, red) with glucagon (fluorescein immunofluorescence, green). As expected, glucagon-producing α cells were much less numerous than β cells and were distributed both as scattered cells within the core region of the islet as well as around the islet mantle (Fig. 5, F-J). Colocalization of SSTR1-5 with glucagon (Fig. 5, K-O) showed a different profile of SSTR expression compared to β cells. SSTR1 positive cells colocalized with only $26 \pm 10\%$ of glucagon positive cells (Fig. 4, middle panel). SSTR2 was the predominant α cell subtype being colocalized in $89 \pm 11\%$ of glucagon positive cells. SSTR3 immunofluorescence was confined to a small subset, $14 \pm 6\%$ of glucagon positive cells, whereas SSTR4 was absent in α cells (Fig. 5, M-N). SSTR5 was moderately well colocalized with glucagon, being detected in $35 \pm 10\%$ of the α cells (Fig. 5, panel O and Fig. 4, middle panel).

Colocalization of SSTR1-5 With SST in δ Cells

Figure 6 shows the results of SSTR1-5 colocalization with SST in representative islet sections. SST-producing cells were identified as a sparse population of cells distributed both within the center and peripheral regions of the islet (Fig. 6, panels F-J). A distinctive pattern of SSTR1-5 expression in δ cells was observed which differed from that in β and α cells (Fig. 6, panels K-O). SSTR5 was preferentially expressed in $75 \pm 10\%$ of SST positive cells and was the predominant δ cell SSTR subtype (Fig. 6, panel O, Fig. 4, lower panel). In contrast, SSTR1-3 antigens were colocalized in only a few δ cells comprising $12 \pm 4\%$, $11 \pm 6\%$, and $14 \pm 6\%$ of the total SST positive cells respectively (Fig. 6, panels K-M and Fig. 4, lower panel). As in the case of α cells, SSTR4 was also absent from δ cells (Fig. 6N).

SSTR Subtype Selectivity For β -, α -, and δ - Cell Expression

A comparison of SSTR subtype selectivity for islet cell expression showed preferential expression of SSTR1 in β cells and of SSTR2 in α cells (Fig. 4). Such selectivity in the case of SSTR2 was relative rather than absolute since approximately half the β cells also expressed SSTR2. SSTR5 was well expressed in β and δ cells and moderately well expressed in α cells and thereby did not display the same degree of selectivity as SSTR1 and SSTR2. SSTR4, a weakly expressed islet subtype was nonetheless only found in β cells. SSTR3 was the the least distinctive subtype being constitutively expressed in 10-20% of all islet cells examined.

DISCUSSION

The present study represents the first description of the pattern of expression of the five SSTRs in normal human pancreas. All five SSTRs were detected in islets, with a rich expression of subtypes 1, 2, and 5 and relatively weak expression of SSTR3 and 4. The five SSTRs displayed a cell- and subtype-specific pattern of expression in β , α , and δ cells. All β cells expressed SSTR1 and the majority coexpressed SSTR5 making these two isoforms the predominant β cell SSTRs. α cells preferentially expressed SSTR2 and δ cells were selective for SSTR5. SSTR1 is thus β cell-selective and SSTR2 α cell-selective. SSTR5 was well expressed in β and δ cells and moderately well expressed in α cells and thereby lacked the islet cell selectivity displayed by SSTR1 and SSTR2.

Because there are no monospecific agonists or antagonists currently available for any of the individual SSTR subtypes (3), we developed a panel of rabbit polyclonal antipeptide SST antibodies

as tools for studying the cellular distribution of each individual SSTR protein. The specificity of our antibodies for the human receptors was validated by confocal immunofluorescence analysis of CHO-K1 cells individually transfected with hSSTR1-5. In addition, to reduce background immunoreactivity, we used only affinity purified antibodies for Western analysis and immunocytochemistry and confirmed specific labelling in each case by using optimally titrated antibody concentrations and by inhibition with antigen preabsorbed antibody controls. For colocalization experiments, we used primary antibodies against the SSTRs and islet hormones that were raised in different species. The antibodies were directed against both rat and human receptor sequences and by immunoblot analysis of rat brain membranes reacted in each case with a single predominant protein species. The size of rSSTR1 (53 kDa) is within the range reported for hSSTR1 expressed in BHK cells (53-72 kDa) (29). Likewise, the size of our rSSTR3 and rSSTR4 is similar or virtually identical to that described for the human isoforms of these two subtypes (29). Our estimate of the molecular mass of rSSTR5 (58 kDa) is comparable to that of the human receptor (52-66 kDa) although both are somewhat smaller than the receptor size recently described for pituitary rSSTR5 (29,30). In the case of SSTR2, our protein band of 57 kDa is within the range described previously for this subtype in rat brain and mouse AtT-20 cells, and for hSSTR2 in transfected HEK-293 cells (29,31). Others, however, have found a somewhat larger SSTR2 protein of 90 kDa by immunoblot analysis in rat brain and pancreas (26,32). These differences may be explained by variations in antibody specificity, the presence of multiple bands, and differential glycosylation of the receptor protein in the different transfected cell lines and tissues studied.

Human islets were rich in SSTRs, expressing all five subtypes. Islets thus join other tissues

such as the rat brain, and pituitary, which have also been shown to coexpress the full SSTR family (2-4, 26,33). SSTR1 was a major islet cell receptor and was expressed in all β cells. This contrasts with the poor expression of SSTR1 in the pituitary, especially in rat somatotrophes which are virtually devoid of this subtype (27). Since most β cells also expressed SSTR5, and half expressed SSTR2 as well, this means that individual β cells coexpress SSTR1 with SSTR5 and a small subpopulation features some of the remaining subtypes as well. Increasing evidence points to the occurrence of multiple SSTR subtypes in many different types of tumor cells as well as in normal cells such as the pituitary which have been characterized in detail (27,30,31,33). Since all five SSTR isoforms bind the natural ligands SST-14 and SST-28 with nanomolar affinity, and share common signalling pathways such as the inhibition of adenylyl cyclase, the functional significance of more than one SSTR subtype in the same cell remains unclear at the moment (3,4). Whether the different SSTRs subserve different biological roles in the same cell, or whether they cooperate through e.g. dimerization, to create greater signalling diversity remains to be determined (34,35).

Our findings suggest that SST regulation of β cell function is mediated via SSTR1 and SSTR5, the two predominant subtypes expressed in this cell. Binding studies using quantitative autoradiography have suggested a preponderance of SST-28 compared to SST-14 sites in rat β cells, presumably reflecting preferential expression of the SST-28 selective SSTR5 subtype, but whether this applies also to human islets will require additional quantitative studies with subtype selective ligands (21). The pattern of expression of SSTRs in α cells was much more selective than in β cells. Virtually all of these cells expressed SSTR2, whereas coexpression of the remaining subtypes was

restricted to 15-30% of cells. Our finding of the preferential expression of SSTR2 with glucagon is in agreement with similar results obtained by immunohistochemistry with SSTR2 antibody in the rat pancreas, and along with earlier autoradiographic data showing preferential labelling of α cells with SST-14 compared to SST-28 selective ligands, suggests that SSTR2 is the likely mediator of SST action in α cells (21,26). Like α cells, δ cells also displayed a subtype-selective pattern of SSTR expression with virtually exclusive expression of SSTR5. The presence of specific SSTRs on δ cells is consistent with the well known ability of synthetic analogs of SST to inhibit endogenous SST secretion by autocrine feedback (17). Furthermore, the finding of SSTR5 as the δ cell SSTR corroborates our earlier autoradiographic finding of mainly SST-28 selective binding sites on this cell type (20).

The present results have important functional and therapeutic implications. The predominant expression of SSTR1 and 5 in β cells and of SSTR2 in α cells helps to explain the differential sensitivity of human and monkey islets to insulin suppression by SST-14 and to glucagon inhibition by octreotide (36,37). It may also explain the relatively benign effect of octapeptide SST analogs like octreotide on carbohydrate tolerance during longterm therapy. This is because SSTR1, a major β cell SSTR does not bind octreotide, and SSTR5 in β cells would likely desensitize with time, whereas the α cell SSTR2 subtype would upregulate with continued SST treatment and remain responsive (5,6). Our finding of subtype selective expression of SSTRs in islet cells now provides a rational basis for the development of SSTR1 specific ligands for preferential insulin suppression and of SSTR2 selective compounds for glucagon inhibition.

ACKNOWLEDGEMENTS

The authors thank M. Correia for secretarial help. This work was supported by grants from the Canadian Medical Research Council, the NIH, and the US Department of Defence. YCP is a Distinguished Scientist of the Canadian Medical Research Council.

REFERENCES

1. Reichlin S: Somatostatin. *N. Engl. J. Med.* 309:1495 1501, 1556 1563, 1983.
2. Patel YC, Liu J-L, Galanopoulou AS, Papachristou DN: Production, action, and degradation of somatostatin. In *The Handbook of Physiology, The Endocrine Pancreas and Regulation of Metabolism*, Jefferson LS and Cherrington AD, Eds. Oxford University Press, N.Y. 1998 (in press).
3. Patel YC, Srikant CB: Somatostatin receptors. *Trends in Endocrinology and Metabolism* 8:398 405, 1997.
4. Reisine T, Bell GI: Molecular biology of somatostatin receptors. *Endo. Rev.* 16:427 442, 1995.
5. Patel YC, Srikant CB: Subtype selectivity of peptide analogs for all five cloned human somatostatin receptors (hsstr1-5). *Endocrinology* 135:2814 2817, 1994.
6. Hukovic N, Panetta R, Kumar U, Patel YC: Agonist-dependent regulation of cloned human somatostatin receptor types 1-5 (hSSTR1-5): subtype selective internalization or upregulation. *Endocrinology* 137:4046 4049, 1996.
7. Nouel D, Gaudriault G, Houle M, Reisine T, Vincent JP, Mazella J, Beaudet A: Differential internalization of somatostatin in COS-7 cells transfected with SST1 and SST2 receptor subtypes: a confocal microscopic study using novel fluorescent somatostatin derivatives. *Endocrinology* 138:296 306, 1997.
8. Hipkin RW, Friedman J, Clark RB et al: Agonist-induced desensitization, internalization and phosphorylation of the sst_{2A} somatostatin receptor. *J. Biol. Chem.* 27:13869 13876, 1997.
9. Roth A, Kreienkamp HJ, Meyerhof W et al: Phosphorylation of four amino acid residues in

- the carboxyl terminus of the rat somatostatin receptor subtype 3 is crucial for its desensitization and internalization. *J. Biol. Chem.* 38:23769 23774, 1997.
10. Lamberts SWJ, Van Der Lely AJ, de Herder WW: Drug therapy: octreotide. *N. Eng. J. Med.* 334:246 254, 1996.
 11. Koerker DJ, Ruch W, Chideckel E, Palmer J, Goodner CJ, Ensinnck J, Gale CC: Somatostatin: Hypothalamic inhibitor of the endocrine pancrea. *Science* 184:482 4843, 1974.
 12. Dubois M P: Immunoreactive somatostatin is present in discrete cells of the endocrine pancreas. *Proc. Natl. Acad. Sci. (USA)* 72:1340 1343, 1975.
 13. Mandarino L, Stenner D, Blanchard W, Nissen S, Gerich J, Ling N, Brazeau P, Bohlen P, Esch F, Guillemin R: Selective effects of somatostatin-14, -25, and -28 on in vitro insulin and glucagon secretion. *Nature* 291:76 77, 1981.
 14. Philippe J: Somatostatin inhibits insulin-gene expression through a posttranscriptional mechanism in a hamster islet cell line. *Diabetes* 42:244 249, 1993.
 15. Kendall DM, Poitout V, Olson LK, Sorenson RL, Robertson RP: Somatostatin coordinately regulates glucagon gene expression and exocytosis in HIT-15 cells. *J. Clin. Invest.* 96:2496 2502, 1995.
 16. Williams G, Fuessl H, Kraenzlin M, Bloom SR: Post prandial effects of SMS201-995 on gut hormones and glucose tolerance. *Scand. J. Gastroenterology* 21 (Suppl 119):73 83, 1985.
 17. Ipp E, Rivier J, Dobbs RE, Brown M, Vale W, Unger RH: Somatostatin analogs inhibits somatostatin release. *Endocrinology* 104:1270 1273, 1979.
 18. Patel YC, Amherdt M, Orci L: Quantitative electron microscopic autoradiography of insulin, glucagon and somatostatin binding sites on islets. *Science* 217:1155 1156, 1982.

19. Reubi JC., Rivier J, Perrin M, Brown M, Vale W: Specific high affinity binding sites for somatostatin-28 on pancreatic B-cells: differences with brain somatostatin receptors. *Endocrinology* 110:1049 1051, 1982.
20. Sullivan SJ, Schononbrunn A: Distribution of somatostatin receptors in RINm5F cells. *Endocrinology* 122:1137 1145, 1988.
21. Amherdt M, Patel YC, Orci L: Selective binding of somatostatin-14 and somatostatin-28 to islet cells revealed by quantitative electron microscopic autoradiography. *J. Clin. Invest.* 80:1455 1458, 1987.
22. Amherdt M, Patel YC, Orci L: Binding and internalization of somatostatin, insulin, and glucagon by cultured rat islet cells. *J. Clin. Invest.* 84:412 417, 1989.
23. Thermos K, Meglasson MD, Nelson J, Lounsbury KM, Reisine T: Pancreatic β -cell somatostatin receptors. *Am. J. Physiol.* 259:E216 E224, 1990.
24. Maletti M, Andersson M, Marie JC, Rosselin G, Mutt V: Solubilization and partial purification of somatostatin-28 preferring receptors from hamster pancreatic beta cells. *J. Biol. Chem.* 267:15620 15625, 1992.
25. Grigorakis SI, Panetta R, Patel YC: Expression of mRNA for somatostatin receptor (sstr) subtypes 1-5 in islets and differential downregulation of sstr2 mRNA by SST agonists. *Diabetes* 44 (Suppl. 1): 132A (Abstr. #485), 1995. .
26. Hunyady B, Hipkin RW, Schonbrunn A, Mezey E: Immunohistochemical localization of somatostatin receptor sst2A in the rat pancreas. *Endocrinology* 138:2632 2635, 1997.
27. Kumar U, Laird D, Srikant CB, Escher E, Patel YC: Expression of the five somatostatin receptor (SSTR1-5) subtypes in rat pituitary somatotrophes: quantitative analysis by double-

- label immunofluorescence confocal microscopy. *Endocrinology* 138:4473-4476, 1997.
28. Laemmli UK: Cleavage of structural proteins during the assembly of the head of bacteriophage T4. *Nature* 227:680-685, 1970.
 29. Helboe L, Moller M, Novregaard L, Schiodt M, Stidsen CE: Development of selective antibodies against the human somatostatin receptor subtypes SST1-SST5. *Mol. Br. Res.* 49:82-88, 1997.
 30. Mezey E, Hunyady B, Mitra S, Hayes E, Liu Q, Schaeffer J, Schonbrunn A: Cell specific expression of the SSTR2A and SSTR5 somatostatin receptors in the rat anterior pituitary. *Endocrinology* 139:414-419, 1998.
 31. Patel YC, Panetta R, Escher E, Greenwood MT, Srikant CB: Expression of multiple somatostatin receptor genes in AtT-20 cells: evidence for a novel somatostatin-28 selective receptor subtype. *J. Biol. Chem.* 269:1506-1509, 1994.
 32. Dournaud P, Gu YZ, Schonbrunn A, Marinella J, Tannenbaum GS, Beaudet A: Localization of the somatostatin receptor SST2A in rat brain using a specific antipeptide antibody. *J. Neurosci.* 16:4468-4478, 1996.
 33. O'Carroll A, Krempel K: Widespread distribution of somatostatin receptor messenger ribonucleic acids in rat pituitary. *Endocrinology* 136:5224-5227, 1995.
 34. Gouldson PR, Reynolds CA: Simulations on dimeric peptides: evidence for domain swapping in G-protein-coupled receptors? *Biochem. Soc. Trans.* 25 (3):1066-1071, 1997.
 35. Rocheville M, Hukovic N, Patel YC: Functional dimerization of the human somatostatin receptor subtype 5 (hSSTR5). Program 80th Annual Meeting US Endocrine Society, New Orleans, June 24-27, 1998 (abstract in press), 1998.

36. Skamene A, Patel YC: Infusions of graded concentrations of somatostatin-14 in man: Pharmacokinetics and differential inhibitory effects on pituitary and islet hormones. *Clin. Endocrinol.* 20:555 564, 1984.
37. Bauer W, Briner U, Doepfner W, Haller R, Huguenin R, Marbach P, Petcher IP, Pless J: SMS 201-995: a very potent and selective octapeptide analogue of somatostatin with prolonged action. *Life Sci.* 31:1133 1140, 1982.

FIGURE LEGENDS

Figure 1. Western blot analysis of SSTR1-5 in rat brain membranes. 35 μ g membrane protein was fractionated by SDS-PAGE and probed with immunoaffinity purified SSTR antisera (lane A of each pair) or antigen preabsorbed antibody (lane B of each pair). Major protein bands of 53 kDa (SSTR1), 57 kDa (SSTR2), 60 kDa (SSTR3), 44 kDa (SSTR4), and 58 kDa (SSTR5) were obtained. The bands were specific and were inhibited in the presence of antigen absorbed antibody. 10 kDa protein ladder standards were used for molecular weight estimates. Data are representative of 3 experiments.

Figure 2. Confocal images depicting the immunohistochemical localization of SSTR1-5 in representative islet sections. Sections were immunolabelled with anti-rabbit SSTR antibodies followed by rhodamine conjugated goat anti-rabbit IgG. All five SSTRs are localized in islet cells with a rich expression of subtypes 1,2, and 5 and relatively weak expression of subtypes 3 and 4. Note the differential expression of SSTR2 in large islets (many cells labelled) and small islets (peripheral cells labelled only). Panels K-O are high powered images showing SSTR immunoreactivity both as surface membrane as well as cytosolic immunofluorescence. Control sections in which the SSTR primary antibodies were replaced with antigen preabsorbed serum show no immunoreactivity (panels P-T). Scale bar in G = 10 μ m, K-O, 5 μ m and the remaining panels 25 μ m.

Figure 3. Confocal images of representative islets double labelled for immunofluorescence for SSTR1-5 and insulin. SSTR immunoreactivity is localized by rhodamine (red) fluorescence in the

left-hand panels. Insulin positive cells are identified by green immunofluorescence in the same sections (middle panels). Coexpression of SSTRs with insulin is indicated by a yellow-orange color (right-hand panels). These 1100 x 800 pixel images constructed in a single composite do not fully reflect the quality of the fields viewed through the microscope. Please refer to the Methods section for details of the primary antibodies and controls used for colocalization. Scale bar 25 μ m.

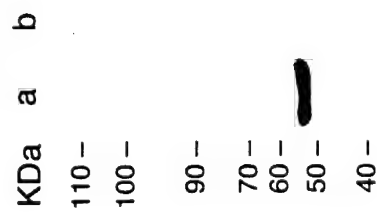
Figure 4. Quantitative analysis of the expression of SSTR1-5 in β , α , and δ cells. The bars represent the mean \pm SE ($n = 3$) percent of cells positive for a given SSTR subtype in 8-20 islets from each of the three pancreases. A mean of 1081 ± 80 β cells, 432 ± 28 α cells, and 221 ± 12 δ cells were analysed.

Figure 5. Confocal images of pancreatic islet cells double labelled for immunofluorescence for SSTR1-5 and glucagon. SSTR immunoreactivity is localized by rhodamine (red) fluorescence in the left-hand panels. Glucagon-positive cells are identified by green immunofluorescence in the same sections (middle panels). Coexpression of SSTRs with glucagon is indicated by a yellow-orange color (right-hand panels). For details of the primary antibodies and controls used for colocalization refer to the Methods section. See also legend to figure 3. Scale bar 25 μ m.

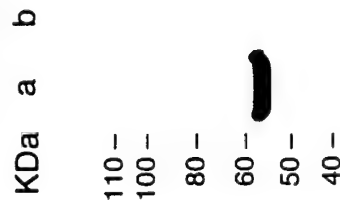
Figure 6. Confocal images of pancreatic islet cells double labelled for immunofluorescence for SSTR1-5 and SST. SSTR immunoreactivity is localized by rhodamine (red) fluorescence in the left-hand panels. SST-positive cells are identified by green immunofluorescence in the same sections (middle panels). Coexpression of SSTRs with SST is indicated by a yellow-orange color (right-hand

panels). For details of the primary antibodies and controls used for colocalization refer to the Methods section. See also legend to figure 3. Scale bar 25 μm .

SSTR1



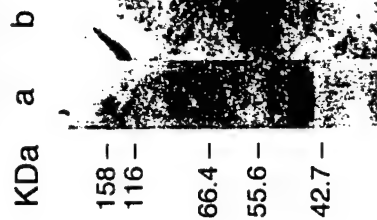
SSTR2



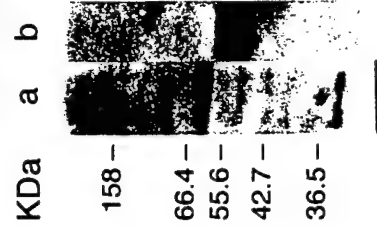
SSTR3

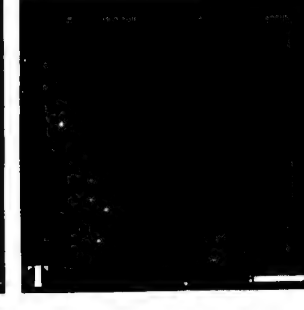
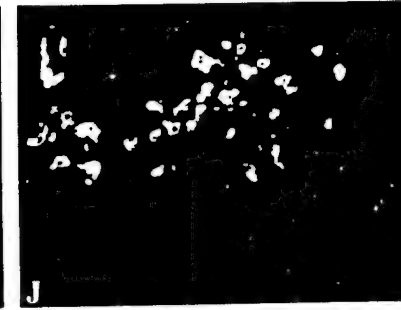
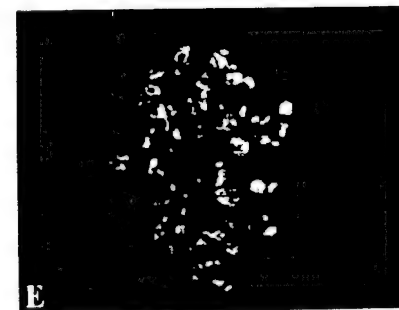
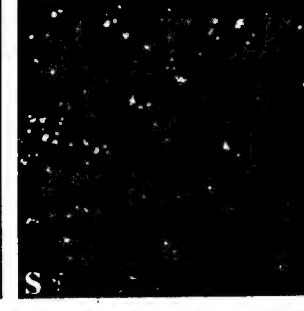
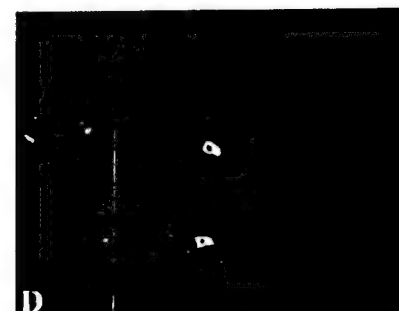
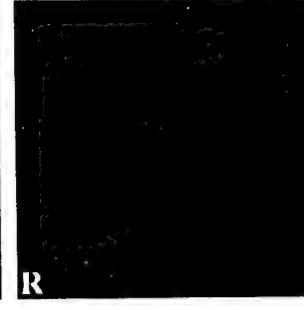
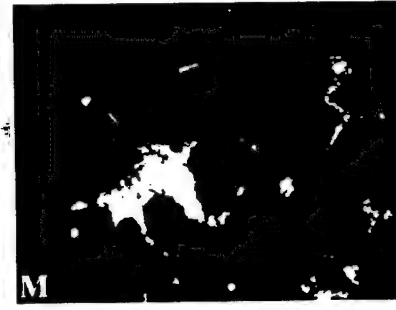
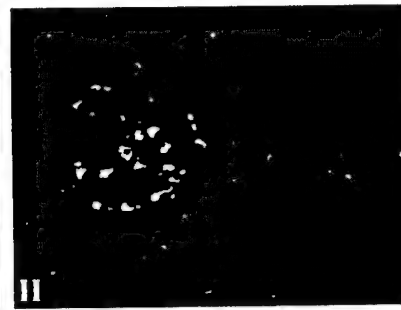
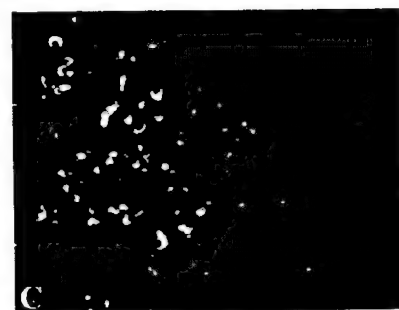
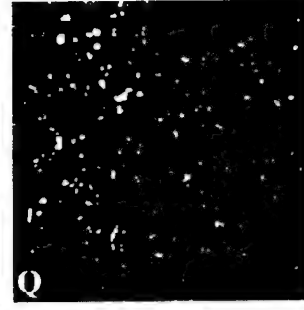
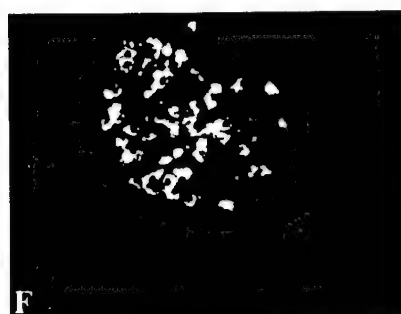
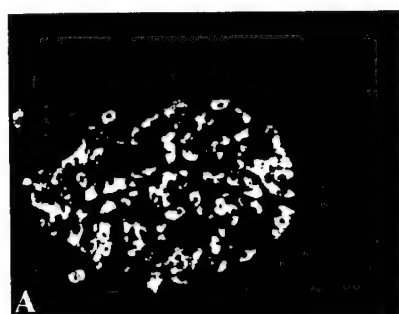


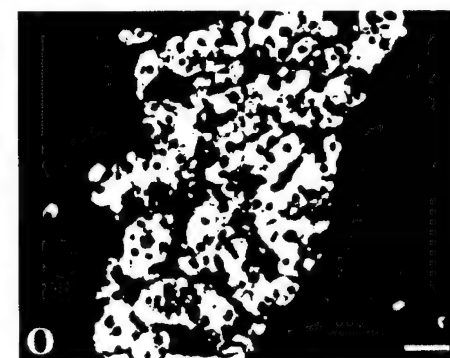
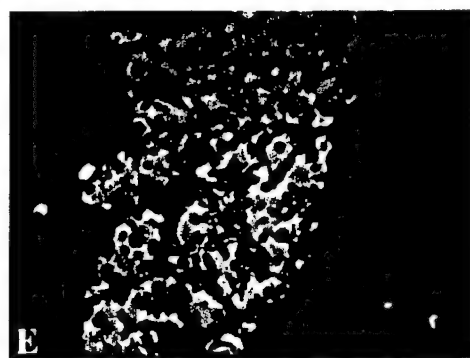
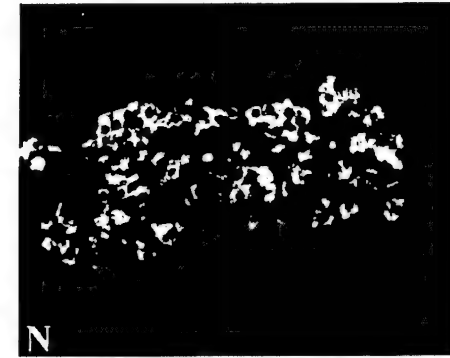
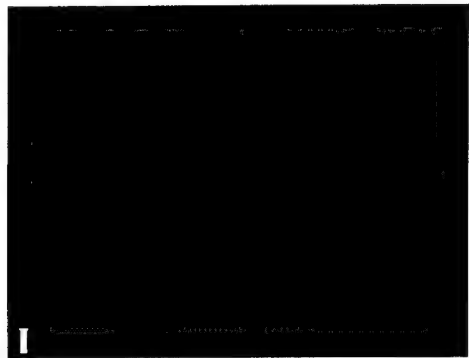
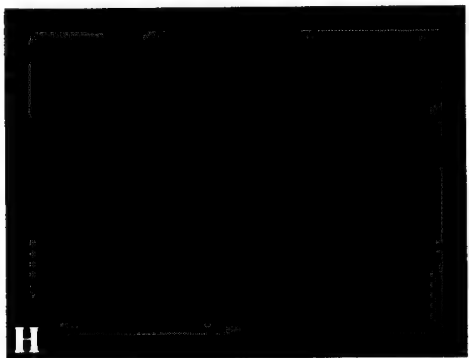
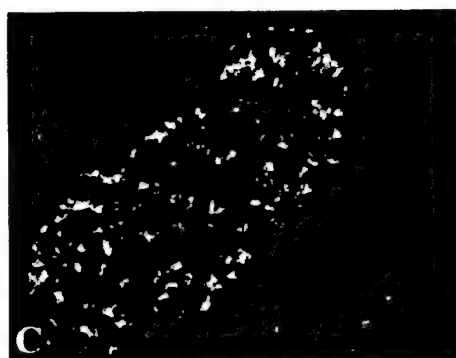
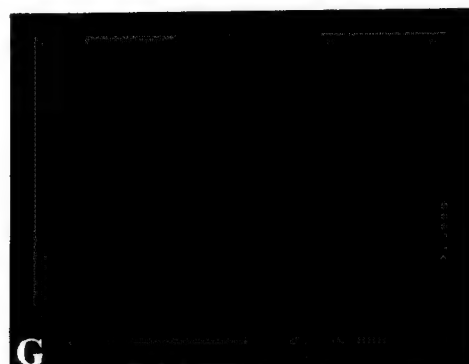
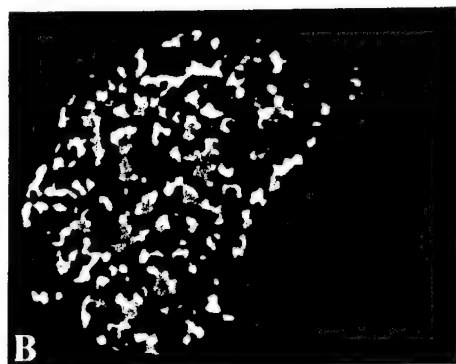
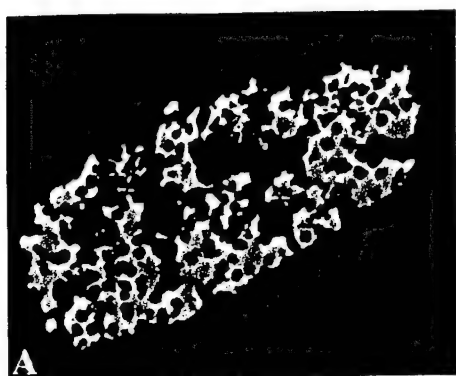
SSTR4



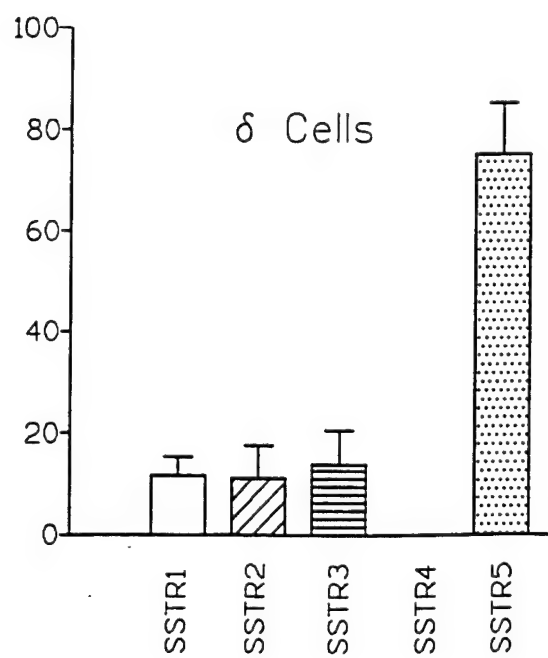
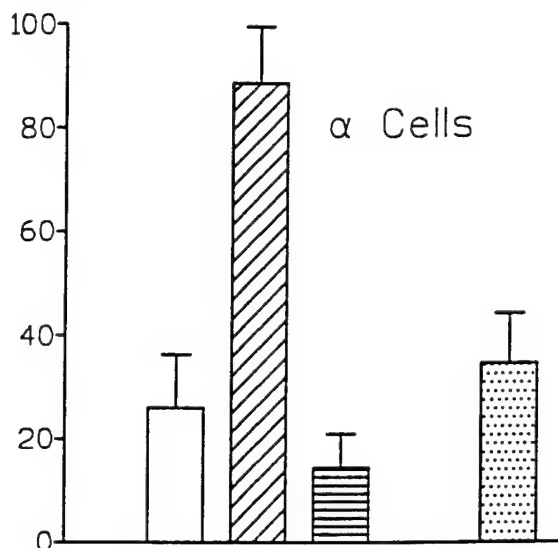
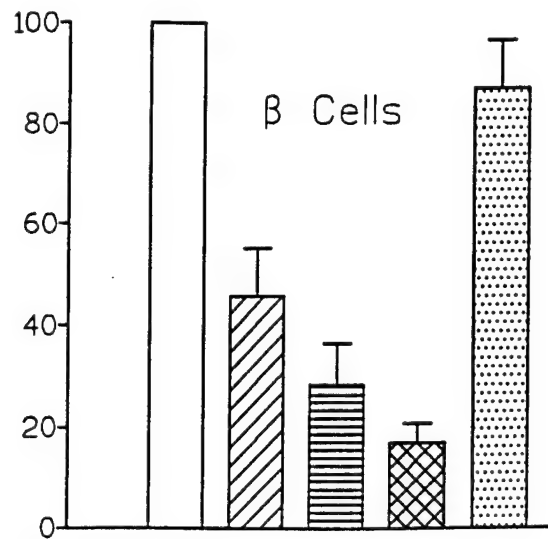
SSTR5

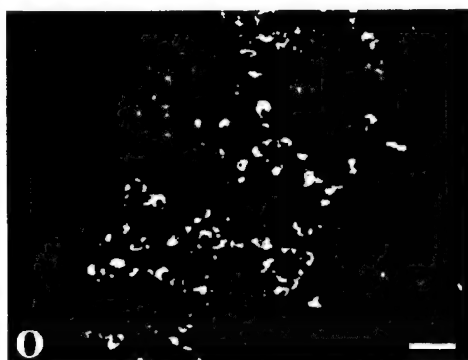
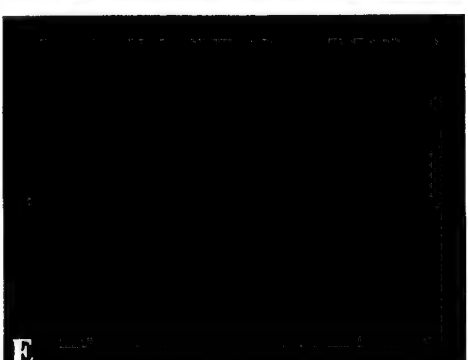
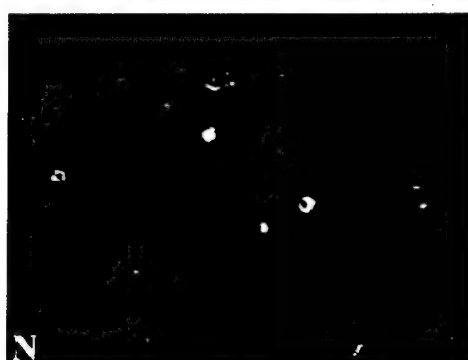
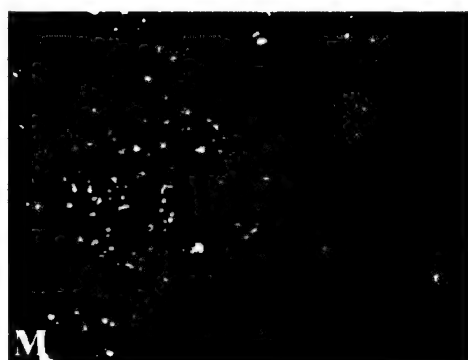
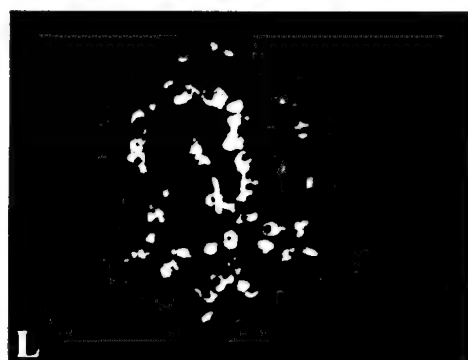


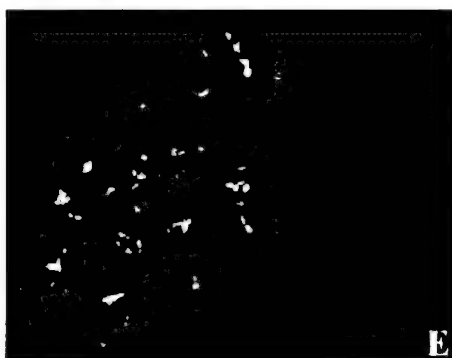
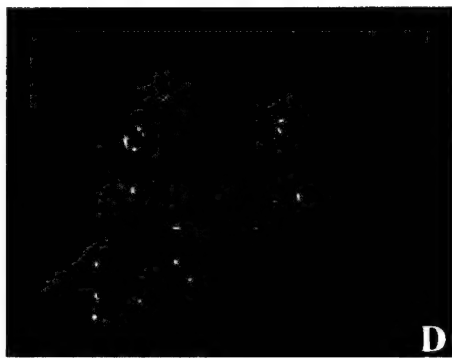
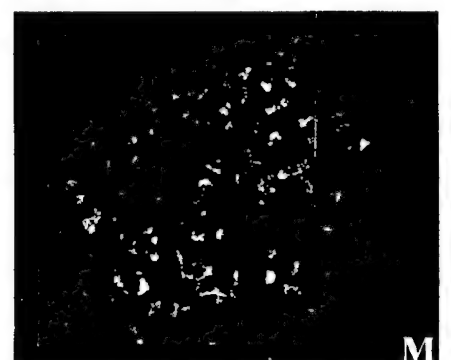
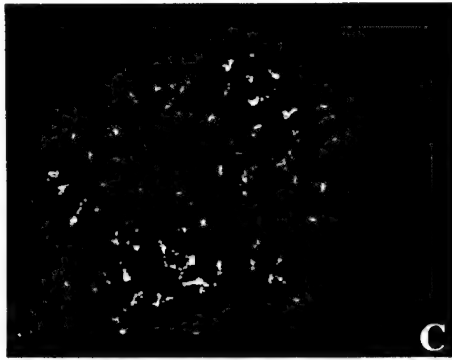
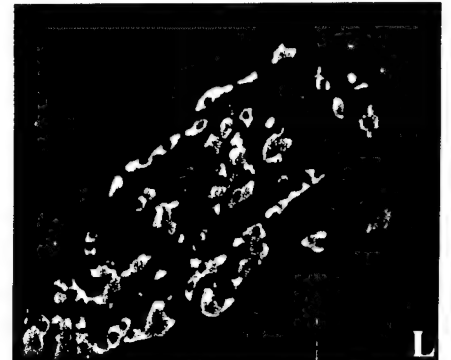
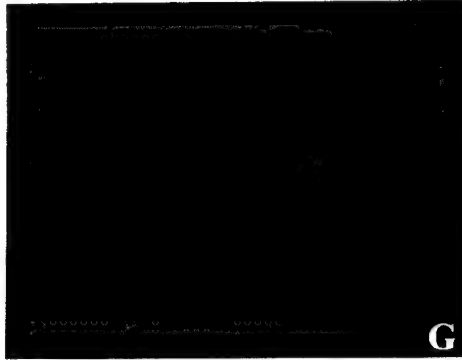
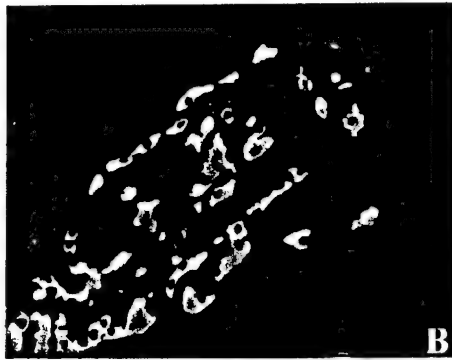
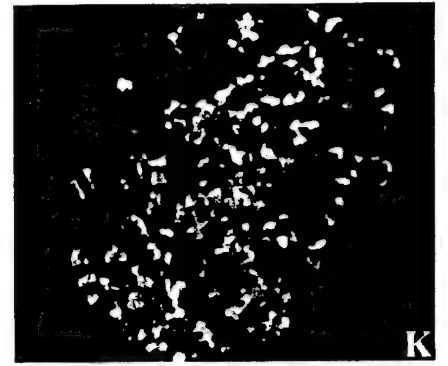
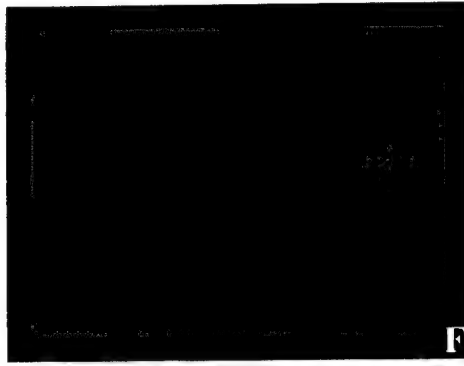
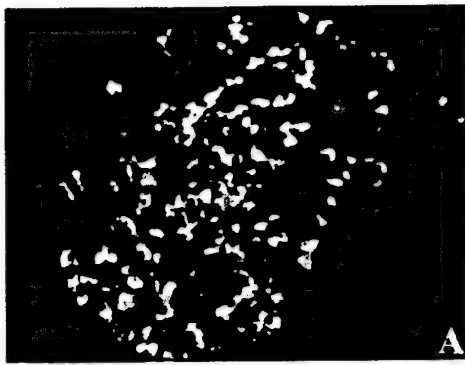




% of Islet cells Coexpressing SSTR







INDUCTION OF WILD-TYPE p53, BAX, AND ACIDIC ENDONUCLEASE DURING SOMATOSTATIN-SIGNALLED APOPTOSIS IN MCF-7 HUMAN BREAST CANCER CELLS

Kamal SHARMA and Coimbatore B. SRIKANT*

Fraser Laboratories for Diabetes Research, McGill University and Royal Victoria Hospital, Montreal, Quebec, Canada

Somatostatin (SST) analogs inhibit tumor cell growth by exerting direct anti-proliferative effects with cytostatic (growth arrest) or cytotoxic (apoptosis) consequences. The SST analog SMS 201-995 (octreotide, OCT) inhibits growth of MCF-7 human breast adenocarcinoma cells, which express multiple SSTRs. Its action has been reported to result in either apoptosis or growth arrest, but the underlying mechanisms have not been elucidated in this tumor cell model. Here, we report that OCT elicits cytotoxic response in these cells, leading to apoptosis, which is associated with a rapid, time-dependent induction of wild-type p53 and an increase in Bax. There was no G₁ cell-cycle arrest in these cells during OCT treatment as suggested by the decrease in G₁/S ratio and the lack of induction of pRb and p21. Additionally, we demonstrate that OCT-induced DNA fragmentation in this cell line is due to selective activation of a cation-insensitive acidic endonuclease. Our data provide a rationale for utilizing SST analogs to treat SSTR-positive breast cancer cells expressing wild-type p53. Int. J. Cancer 76:259–266, 1998.

© 1998 Wiley-Liss, Inc.

Somatostatin (SST) and its analogs regulate multiple cellular activities, such as secretion and proliferation through a family of 5 G protein-coupled receptor (SSTR) subtypes (Patel *et al.*, 1995). In tumor cells which express multiple SSTR subtypes, the growth-inhibitory action of SST can induce cell-cycle arrest and/or apoptosis (Patel *et al.*, 1994; Pagliacci *et al.*, 1991; Srikant, 1995; Candi *et al.*, 1995; Cheung and Boyages, 1995). We have demonstrated that SST induces apoptosis but not cell-cycle arrest selectively through human (h)SSTR3. This is associated with induction of the wild-type (wt) tumor-suppressor protein p53 and Bax (Sharma *et al.*, 1996). While hSSTR3-mediated cytotoxic signaling is agonist dose-dependent, we have determined that SST exerts cytostatic action *via* other hSSTR subtypes and induces a G₁ cell-cycle arrest but no apoptosis (Sharma *et al.*, 1996, 1997). Such cytostatic signaling occurs in a p53-independent manner. The octapeptide SST analog SMS 201-995 (octreotide, OCT) inhibits growth of MCF-7 human breast adenocarcinoma cells. We and others have shown that this is due to induction of apoptosis (Srikant, 1995; Candi *et al.*, 1995), contradicting a claim that it leads to transient cell-cycle arrest but no apoptosis (Pagliacci *et al.*, 1991). Since these effects are elicited by different SSTR subtypes, we examined the effect of OCT on wt p53, Bax, Bcl2, pRb, p21 and c-Myc in relation to changes in cell-cycle progression in MCF-7 cells as a model system which displays simultaneous expression of multiple SSTR subtypes. We report here that OCT activates wt p53 and Bax and triggers rapid apoptosis in these cells. Its cytotoxic action is elicited without altering cellular levels of p21, pRb, c-Myc or Bcl-2 and without imposing G₁ arrest. Additionally, we demonstrate that OCT-induced apoptosis is associated with selective activation of a Ca²⁺/Mg²⁺-insensitive endonuclease exhibiting an acidic pH optimum.

MATERIAL AND METHODS

MCF-7, a human breast adenocarcinoma cell line, was obtained from the ATCC (Bethesda, MD). The SST analog SMS 201-995

(OCT) was obtained from Sandoz (Basel, Switzerland). Propidium iodide (PI) was purchased from Sigma (St. Louis, MO). Monoclonal antibodies (MAbs) against wt specific anti-p53 antibody pAb 1801 and FITC-conjugated goat anti-mouse and anti-rabbit IgG antibodies were obtained from Zymed (San Francisco, CA). Anti-c-Myc antibody (Ab-2, MAb) and anti-Bcl-2 antibody (Ab-1, MAb) were purchased from Oncogene Science (Cambridge, MA). Antibodies against p21 (C-19, rabbit polyclonal) and anti-Bax (P-19, rabbit polyclonal) were from Santa Cruz Biotechnology (Santa Cruz, CA). The annexin V apoptosis detection kit was supplied by R&D Systems (Minneapolis, MN). All other chemicals used were of analytical grade and were obtained from regular commercial sources.

Cell culture

Cells were plated in 75-cm² culture flasks and grown in minimal essential medium containing non-essential amino acids and supplemented with 10% FBS and 10 mg · ml⁻¹ bovine insulin. Medium was changed every 2nd day until cells reached 60 to 70% confluence, after which cells were incubated in the presence or absence of 0.1 to 100 nM OCT for the indicated periods of time, with the medium containing fresh peptide being replenished every 24 hr during prolonged incubation.

At the end of the incubation, the medium was removed and cells were washed in PBS, scraped and fixed sequentially in 1% paraformaldehyde in PBS and in 70% ethanol. Cellular DNA was labeled with the intercalating dye PI (50 µg/ml) in PBS and incubated at 37°C for 5 min in the presence of RNase A (50 µg/ml). p53 was labeled with the anti-p53 MAb 1801. c-Myc, pRb, p21, Bax and Bcl-2 were labeled with the respective MAbs described above. Antigen-bound primary antibodies were then stained with FITC-conjugated goat anti-mouse or anti-rabbit IgGs and analyzed directly or after counterstaining with PI.

Detection of apoptosis by annexin V labeling

To establish that OCT induces apoptosis and not necrosis, unfixed cells were incubated with FITC-conjugated annexin V and PI using the apoptosis detection kit according to the manufacturer's instructions.

Flow cytometry

Flow cytometry was carried out with an EPICS 750 series flow cytometer (Coulter, Hialeah, FL). Fluorescence was excited by a 5W argon laser generating light at 351 to 363 nm, PI emission was detected through a 610-nm long-pass filter and FITC

Contract grant sponsor: Medical Research Council of Canada; Contract grant number: MT-12603.

*Correspondence to: M3.15, Royal Victoria Hospital, 687 Pine Avenue West, Montreal, P.Q. H3A 1A1, Canada. Fax: (514) 482-9124. E-mail: mdc@musica.mcgill.ca

Received 26 August 1997; Revised 28 November 1997

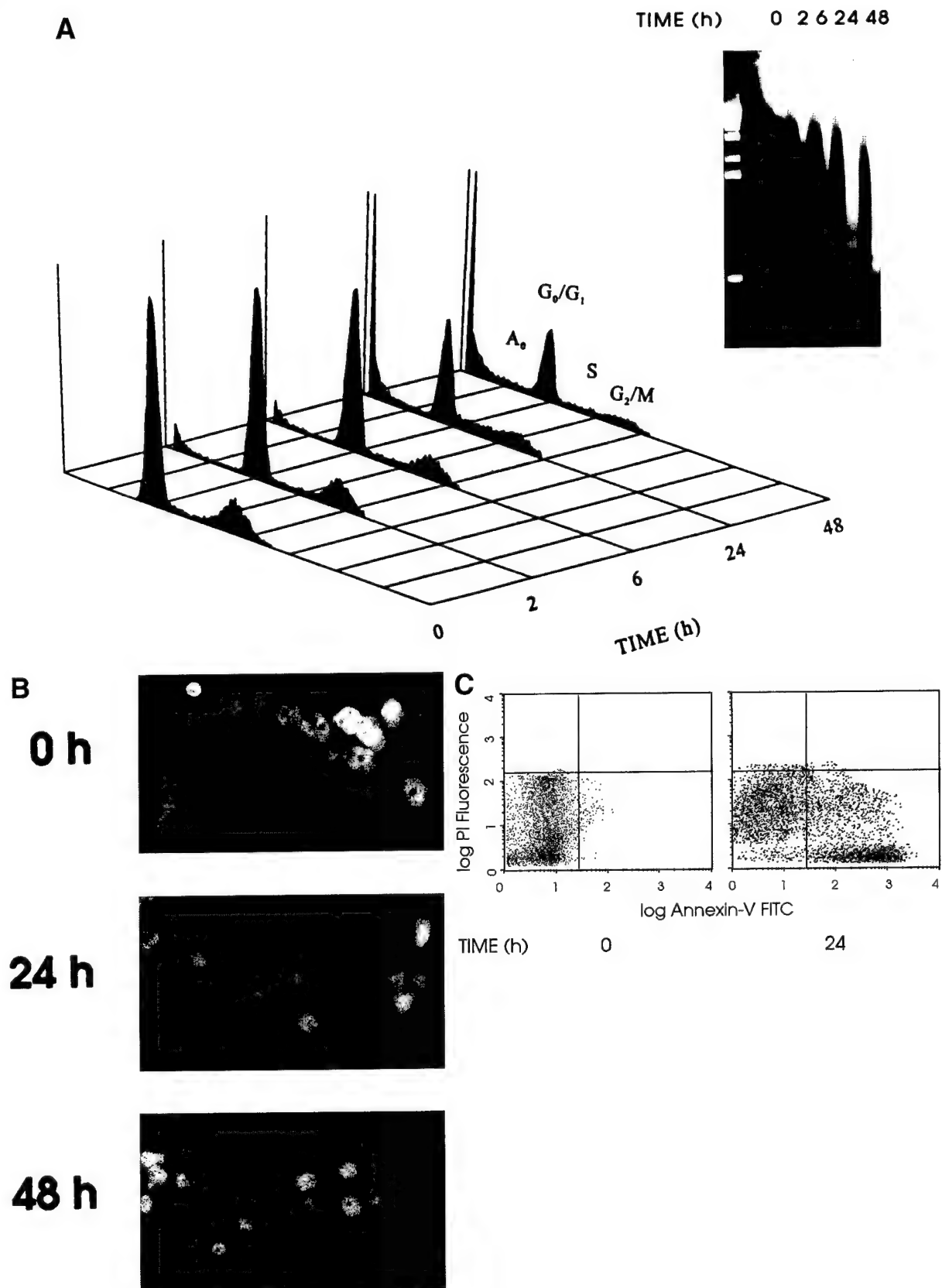


FIGURE 1

fluorescence was detected with a 560-nm short-pass dichroic filter. At least 10,000 gated events were recorded for each sample and the data analyzed by Winlist and Isocontour softwares (Verity Software House, Topsham, ME) and by WinMDI software.

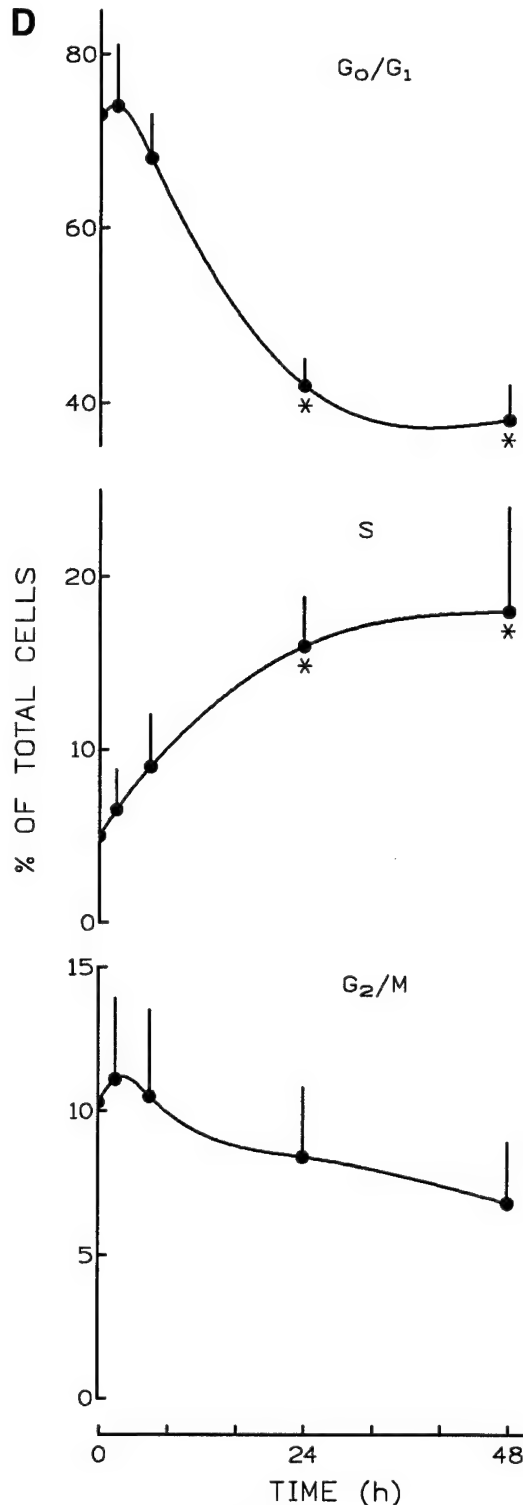


FIGURE 1

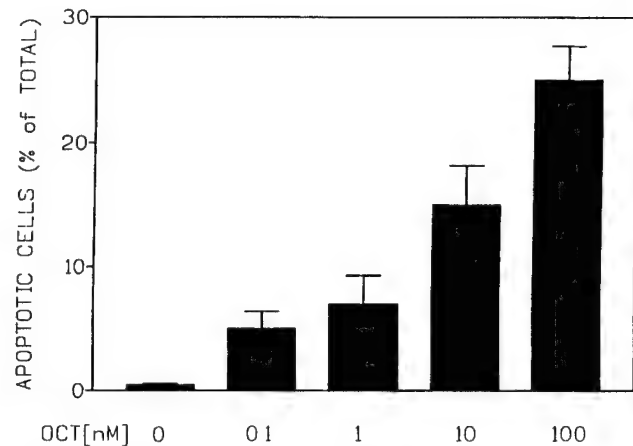


FIGURE 2—Dose dependence of OCT-induced apoptosis. MCF-7 cells were incubated with 0 to 100 nM peptide for 24 hr, and the percentage of cells exhibiting high annexin V-FITC fluorescence was determined by flow cytometry (mean \pm SE, $n = 4$).

Preparation of nuclear extract and determination of endonuclease activity

The nuclear protein extract containing endonuclease activity was prepared as described by Eastman (1995) from MCF-7 cells pre-incubated for 24 hr in the absence or presence of 100 nM OCT. Briefly, 2×10^6 cells were resuspended and allowed to swell for 20 min on ice in 20 mM Hepes-KOH buffer, pH 7.4, containing 0.75 mM spermidine, 0.15 mM spermine, 0.1 mM EDTA and 1 mM each of DTT and phenylmethylsulfonyl fluoride (PMSF, HSSE buffer). Cells were sonicated after adding sucrose to a final concentration of 0.5 M. This mixture was centrifuged for 10 min at 150 g, and the pellet was resuspended in 0.75 ml of the buffer containing 0.5 M sucrose, layered on 1.5 M sucrose/HSSE buffer and centrifuged for 20 min at 13,000 g. The nuclei were then resuspended in a buffer

FIGURE 1—Effect of OCT on cell-cycle parameters in MCF-7 cells. Data shown are representative of 4 experiments. (a) Representative plots depicting phase distribution of cells incubated with 100 nM OCT for the indicated periods of time. Cellular DNA was stained with PI and analyzed by flow cytometry. A rapid, time-dependent decrease in G_0/G_1 paralleled by the accumulation of cells with hypodiploid DNA content to the left of G_0/G_1 occurred during OCT treatment. A transient increase in S phase and a progressive decrease in G_2/M phase was also evident. Cells in the G_0/G_1 , S and G_2/M regions ranged $38 \pm 5\%$, $15 \pm 3\%$ and $9 \pm 2\%$, respectively, at 48 hr compared to $73.6 \pm 6\%$, $11.2 \pm 1.7\%$ and $16.4 \pm 2.7\%$, respectively, in the control (mean \pm SE, $n = 4$). *Inset*: Demonstration of time-dependent, OCT-induced increase in DNA fragmentation. DNA extracts were electrophoresed on 1.2% agarose gel, stained with ethidium bromide and visualized in UV light as described in "Material and Methods." (b) Morphological evidence for nuclear shrinking in OCT-treated cells. Cells labeled with PI for analysis by flow cytometry were cytopun onto microscope slides, mounted using immunomount (Shandon, Pittsburgh, PA), viewed and photographed through a Reichert (Vienna, Austria) Polyvar 2 fluorescence microscope. Bar: 25 μ m. (c) Dot-plot analysis of cells dual-labeled with annexin V-FITC and PI confirms the induction of apoptosis by OCT in MCF-7 cells. Annexin V-FITC labeling, but not PI labeling, is markedly enhanced following treatment with 100 nM OCT for 24 hr. The absence of necrosis is evident from the lack of dual-positive cells staining for both PI and annexin V-FITC (upper right quadrant). (d) Effect of OCT on cell-cycle distribution. The number of cells in G_0/G_1 , S and G_2/M phases is expressed as percent of total cells analyzed for PI staining at each time point. A statistically significant decrease in G_0/G_1 and an increase in S phase were observed at 24 and 48 hr (* $p < 0.01$, $n = 4$). A slight but non-significant decrease in G_2/M was also seen at these time points.

containing 10 mM sodium acetate, 10 mM sodium phosphate, 10 mM bistrispropane, 1 mM DTT and 1 mM PMSF (APB buffer) and recentrifuged to remove residual spermine and spermidine. Nuclear protein extracts were prepared by resuspending the nuclei in APB buffer (pH 7) containing 0.5 M NaCl. After 1-hr incubation on ice, the precipitated DNA was pelleted by centrifugation at 14,000 g for 10 min and the supernatant recovered. Genomic DNA was prepared from control, untreated MCF-7 cells as previously described (Sharma *et al.*, 1996). Endonuclease assay was performed by incubating 100 ng of genomic DNA (prepared from control, untreated MCF-7 cells) with 10 ng of nuclear protein extract in the absence or presence of $\text{Ca}^{2+}/\text{Mg}^{2+}$ in a buffer containing 10 mM sodium acetate, 10 mM sodium phosphate, 10 mM bistrispropane, 1 mM DTT and PMSF adjusted to pH 5.0, 7.0 or 8.0 (Eastman,

1995). This mixture was incubated at 37°C for 30 min, electrophoresed on a 1.2% agarose gel (w/v) containing ethidium bromide and visualized under UV light.

RESULTS

Analysis of DNA stained with the intercalating dye PI revealed that OCT (100 nM) induced a time-dependent decrease in the population of MCF-7 cells in G_1 phase and a transient increase in S phase, which was maximal by 24 hr (Fig. 1a). The progressive appearance of cells with hypodiploid DNA content suggested that OCT induces rapid apoptosis in these cells. This was confirmed by

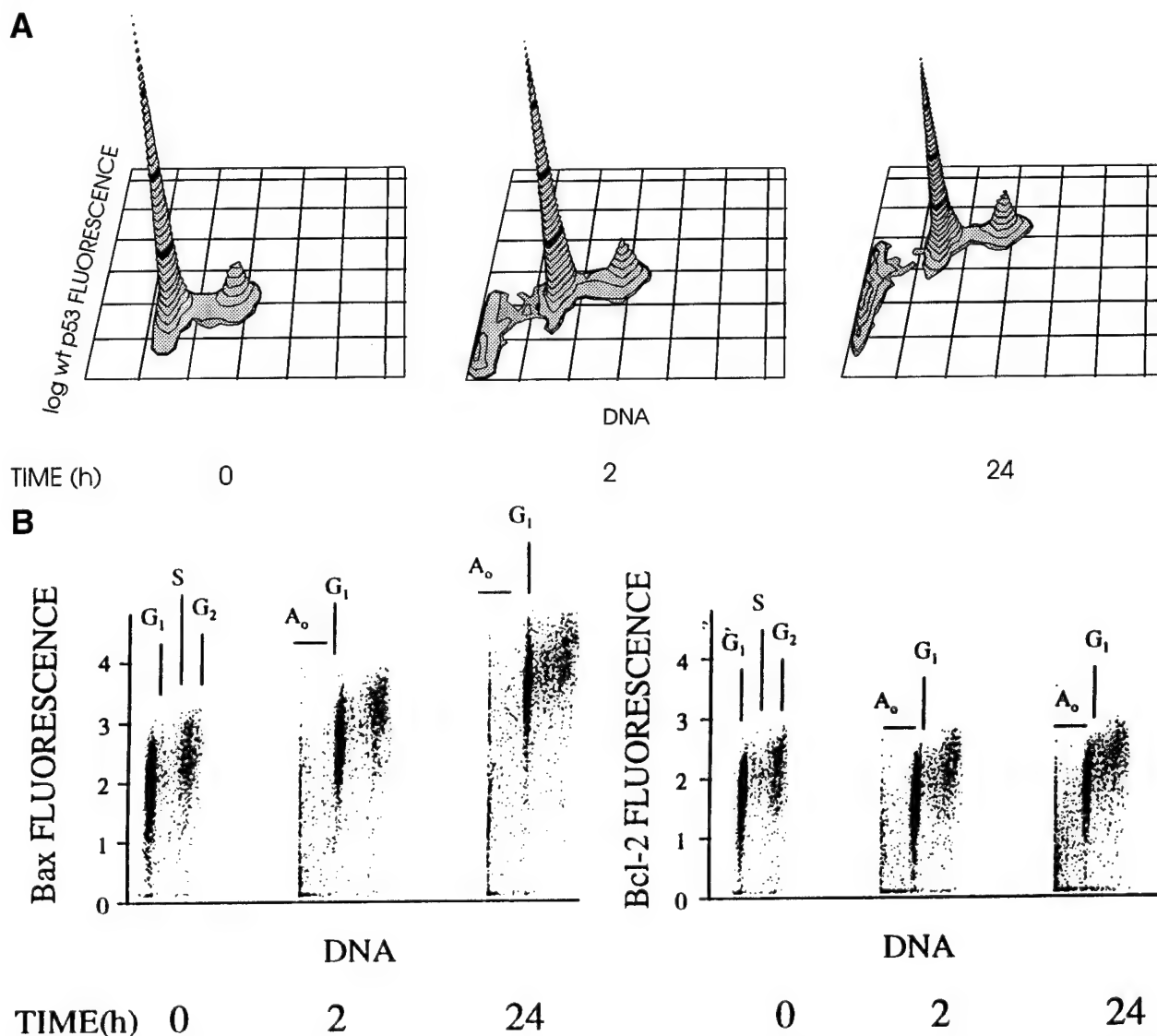


FIGURE 3 – OCT induced apoptosis in MCF-7 cells is associated with induction of wt p53 and Bax but not Bcl-2. Cells were labeled with the respective antibodies alone or with PI and analyzed by flow cytometry ($n = 4$). (a) Isocontour 3-D plots illustrating bivariate analysis of cells dual-labeled with wt-specific anti-p53 antibody pAb 1801 and PI. Increased labeling of p53 is seen in all phases of the cell cycle. The increase in p53 immunofluorescence averaged 7 ± 0.4 -fold in 4 separate experiments. During OCT treatment, apoptotic cells appear as a clearly defined population in the hypodiploid region by 2 hr and increase in number as well as p53 fluorescence by 24 hr. (b) Bivariate analysis of cells dual-labeled with anti-Bax or anti-Bcl-2 and PI. Selective, time-dependent increase in Bax occurs during OCT treatment, whereas Bcl-2 levels remain unaffected. As in the case of wt p53, OCT-induced increase in Bax is seen in all phases of the cell cycle and ranged 3- to 5-fold in 4 separate experiments. A time-dependent increase in Bax is also seen in apoptotic cells in the region designated A_0 .

the detection of oligonucleosome-sized DNA fragments in OCT-treated cells by pulse field electrophoresis (Fig. 1a, inset). DNA fragmentation was detectable by 2 hr of OCT treatment, increased with time and became massive by 48 hr. Another characteristic feature of OCT-induced apoptosis was the progressive shrinking of the nucleus in OCT-treated cells (24 and 48 hr compared to control, Fig. 1b). The incidence of apoptosis was further characterized by the presence of annexin V-positive cells following OCT treatment (Fig. 1c, lower right quadrant). Following OCT treatment, $38.6 \pm 6.3\%$ of the cells became annexin V FITC-positive (mean \pm SE, $n = 4$). The absence of cells dual-labeled with both annexin and PI suggests that OCT does not induce necrosis in these cells. Analysis of cell-cycle parameters revealed a progressive, time-dependent decrease in G_0/G_1 and an increase in S phase in cells treated with 100 nM OCT (Fig. 1d). A marginal, non-significant decrease in G_2/M was seen in OCT-treated cells. The G_1/S ratio in the control cells was 16 ± 4 and decreased to 9.6 ± 2.1 by 2 hr and to 2.6 ± 1.7 by 24 hr ($n = 4$). Induction of apoptosis in a 24-hr period in these cells was dependent on the concentration of OCT over a range of 0.1 to 100 nM (Fig. 2).

OCT-induced apoptosis was associated with induction of wt p53. This is illustrated by 3-D isocontour plots of cells dual-labeled with PI and wt-specific anti-p53 antibody pAb 1801, which recognizes both inactive and active conformations of wt p53. In Figure 3a, we compare the distribution of cells relative to both PI and p53 labeling at 0, 2 and 24 hr of incubation with 100 nM OCT. Increased immunostaining of cellular p53 is seen in all phases of the cell cycle (3 ± 1 - and 7 ± 1.9 -fold increase in fluorescence intensity by 2 and 24 hr, respectively, $n = 4$). No increase in p53 was detected with another p53 antibody, pAb 240, which reacts only with the inactive conformation of the molecule, as previously demonstrated in CHO-K1 cells expressing hSSTR3 (Sharma *et al.*, 1996; details not shown).

To determine if OCT-induced apoptosis is associated with an increase in Bax and/or suppression of Bcl-2, cells labeled with PI and anti-Bax or anti-Bcl-2 antibodies were analyzed by flow cytometry. Results from a representative experiment depicting the effect of OCT treatment are shown in Figure 3b. A rapid induction of Bax occurred in all phases of the cell cycle, as was seen in the case of wt p53 (1.5 ± 0.4 -fold by 2 hr and 3 ± 0.7 -fold by 24 hr, $n = 4$). By contrast, Bcl-2 levels remained unaffected.

We then investigated the nature of the endonuclease responsible for triggering OCT-induced DNA fragmentation. Nuclear protein extracts were prepared from MCF-7 cells incubated with OCT for 24 hr, and the endonuclease activity was assayed *in vitro* using DNA extracted from control MCF-7 cells as substrate at pH 5, 7 and 8 in the absence or presence of Ca^{2+}/Mg^{2+} , conditions under which various endonucleases associated with apoptosis have been

shown to be maximally active (Eastman, 1995). As illustrated in Figure 4, the nuclear protein extracts of OCT-treated cells displayed selective increases in the endonuclease active at pH 5. As shown in this figure, the activity of this endonuclease was not influenced by the addition of Ca^{2+}/Mg^{2+} . By contrast, OCT did not induce other endonucleases at neutral or alkaline pH in the absence or presence of Ca^{2+}/Mg^{2+} .

DISCUSSION

Our present results demonstrate that OCT inhibits MCF-7 cell growth by inducing apoptosis and provide insight into the molecular mediators involved in its cytotoxic signaling in this cell line. We have characterized OCT-induced apoptosis in MCF-7 cells using 4 distinct criteria: appearance of population of cells with hypodiploid DNA content by flow cytometry, selective labeling by

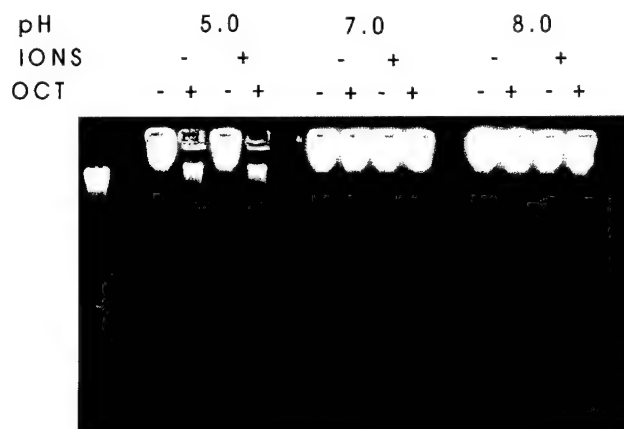


FIGURE 4 – OCT-induced apoptosis in MCF-7 cells involves selective activation of cation-insensitive acidic endonuclease. Endonuclease activity in nuclear extracts of cells treated with 100 nM OCT for 24 hr was assayed *in vitro* using DNA extracted from control cells and analyzed by electrophoresis on 1.2% agarose gel and visualized under UV light following staining with ethidium bromide. Incubations were carried out using nuclear protein extracts of control and OCT-treated cells at pH 5, 7 and 8 in the absence or presence of Ca^{2+}/Mg^{2+} , as described in "Material and Methods." DNA digestion occurred only at pH 5. This endonuclease activity was not influenced by the presence of Ca^{2+} and Mg^{2+} . By contrast, OCT did not induce either Ca^{2+}/Mg^{2+} -sensitive or Ca^{2+}/Mg^{2+} -insensitive endonuclease activity under neutral or alkaline conditions. The mobility of the 1-kb DNA ladder (Life Technologies, Gaithersburg, MD) is shown in lane 1. Data representative of 4 different experiments.

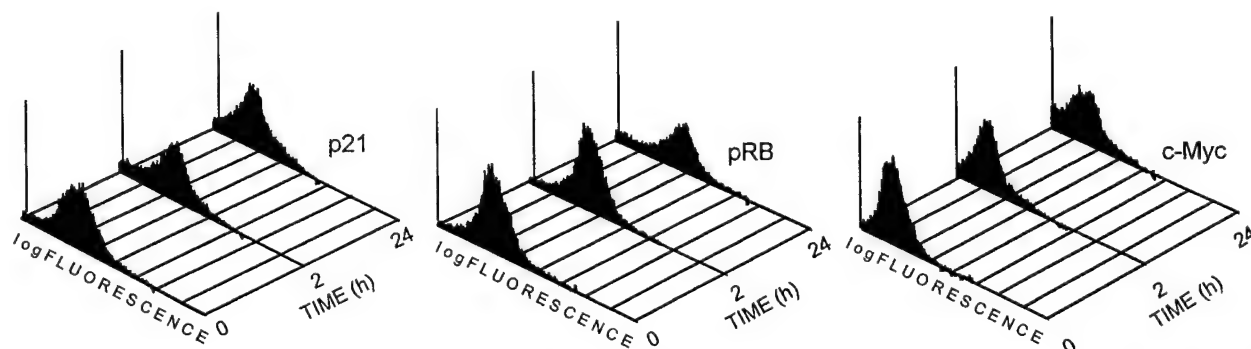


FIGURE 5 – OCT does not induce p21, pRb and c-Myc in MCF-7 cells. Following treatment with 100 nM peptide for the indicated times, cells were labeled with the respective antibodies and analyzed by flow cytometry. Data representative of 3 experiments.

annexin V but not PI in apoptotic cells, nuclear shrinking by morphological criteria and the presence of oligonucleosomal DNA fragments by electrophoresis. The absence of significantly high labeling of both annexin and PI suggests that OCT does not trigger events resulting in necrosis in MCF-7 cells. The cytotoxic signaling initiated by OCT is associated with the induction of wt p53 and Bax.

Several constitutive DNA-digesting enzymes (endonucleases) have been implicated in the DNA fragmentation associated with apoptosis. These include several $\text{Ca}^{2+}/\text{Mg}^{2+}$ -dependent endonucleases, including DNase I, Nuc 18 and endonuclease I (which possess an alkaline pH optimum), DNase γ (which has a neutral pH optimum) and an acidic endonuclease (active in the pH range of 6 to 7.5) (Walker and Sikorska 1994). In addition, a $\text{Ca}^{2+}/\text{Mg}^{2+}$ -insensitive endonuclease which has a pH optimum of 5 (endonuclease II) induces DNA degradation (Barry and Eastman, 1993; Eastman, 1995). By examining the *in vitro* endonuclease activity in the nuclear extracts of OCT-treated cells in the absence or presence of $\text{Ca}^{2+}/\text{Mg}^{2+}$ under different pH conditions, we demonstrate that OCT activates a pH-dependent, $\text{Ca}^{2+}/\text{Mg}^{2+}$ -insensitive endonuclease which appears to be similar to endonuclease II (Barry and Eastman, 1993; Eastman, 1995).

The decrease in the G_1/S ratio during OCT treatment suggests, but does not prove, that OCT-induced apoptosis occurs in the absence of G_1 cell-cycle arrest. This is in agreement with the findings that p53-signaled apoptosis occurs in the absence of G_1 arrest (Adachi *et al.*, 1995). Such a failure can be due to a lack of induction of pRb and/or p21, which have been implicated in the induction of G_1 arrest or a lack of c-Myc, which can abrogate p53-induced G_1 arrest (Hermeking *et al.*, 1995). No increase in p21, pRb or c-Myc was observed at 2 and 24 hr of OCT treatment (Fig. 5). In fact, the fluorescence intensity of immunolabeled p21 was found to decrease marginally in cells pretreated with OCT. Neither the peak size nor the fluorescence intensity of c-Myc was affected by OCT. The lack of induction of p21 by OCT is consistent with its ability to induce wt p53 and apoptosis but not G_1 arrest. In fact, p21 is induced only during p53-signaled G_1 arrest and is capable of protecting against p53-induced apoptosis (Chiarugi *et al.*, 1994; Gorospe *et al.*, 1997). No increase in G_2/M was observed in OCT-treated cells, a finding which contradicts a previous claim that it inhibits proliferation of MCF-7 cells by inducing a transient G_2/M arrest (Pagliacci *et al.*, 1991). These authors failed to substantiate their speculation that OCT-induced G_2/M arrest culminates in apoptosis (Pagliacci *et al.*, 1991).

We have shown that cytotoxic signaling of SST is receptor subtype-selective and is transduced uniquely through hSSTR3, leading to induction of wt p53, Bax and apoptosis in the absence of cell-cycle arrest (Sharma *et al.*, 1996). The other hSSTR subtypes signal in a different pathway, leading to induction of p53-independent G_1 arrest (Sharma *et al.*, 1997). This suggests that hSSTR3 may be the subtype which participates in the cytotoxic signaling in MCF-7 cells. However, such a conclusion is not supported by the reported absence of SSTR3 mRNA in MCF-7 cells (Xu *et al.*, 1996). We are currently analyzing the expression pattern of SSTRs in MCF-7 cells at both the mRNA and protein levels in order to resolve this discrepancy. It is of interest in this connection that significant expression of hSSTR3 was observed at the mRNA level in a screening of 46 malignant and 9 non-malignant human breast carcinoma samples, the relative expression of the subtypes being $\text{hSSTR2} > \text{hSSTR3} = \text{hSSTR1} > \text{hSSTR4}$ (Vikic-Topic *et al.*, 1995).

Adenovirus-based transfer of wt p53 sensitizes ovarian tumor radiation-induced apoptosis (Gallardo *et al.*, 1996). Overexpression of Bax can also sensitize tumor cells to radiation as well as chemotherapy-induced apoptosis (Sakakura *et al.*,

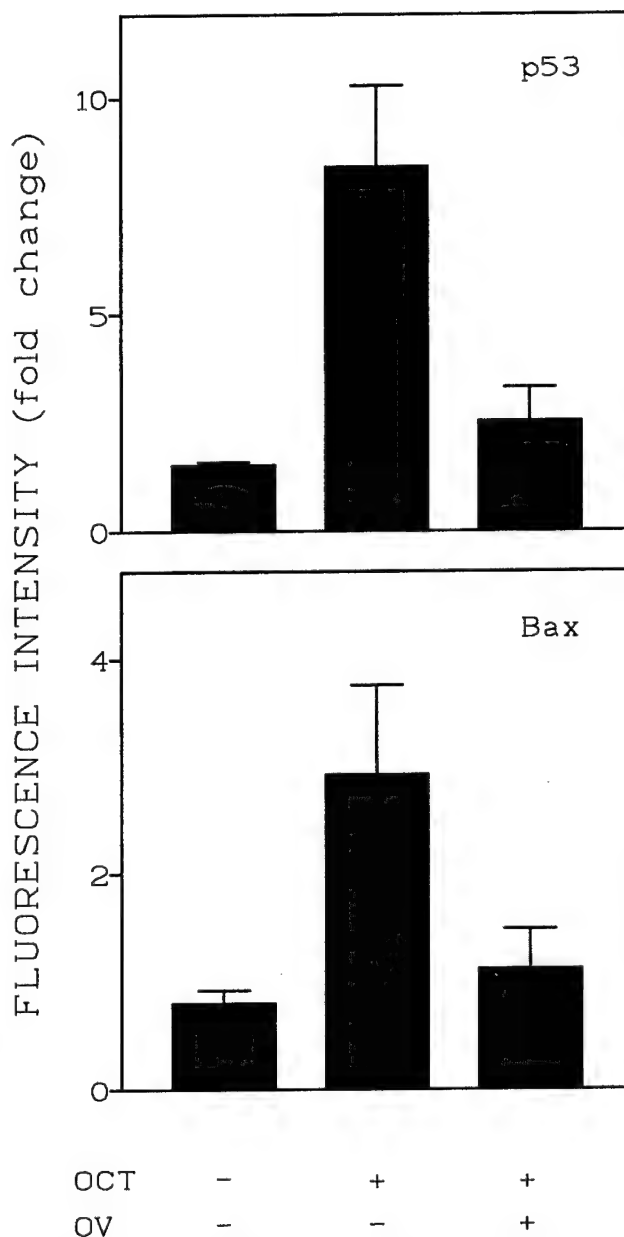


FIGURE 6 - Orthovanadate inhibits induction of wt p53 and Bax by OCT in MCF-7 cells. Cells were incubated for 24 hr with 100 nM OCT in the absence or presence of 50 μM orthovanadate (OV). Fluorescence intensity of cells labeled with anti p53 (pAb 1801) and anti-Bax (P-19) was determined by flow cytometry and expressed as fold change compared to the control values taken as 1 ($n = 3$).

1996; Wagner *et al.*, 1996). OCT induction of wt p53 and Bax should sensitize the responsiveness of these tumor cells to radiation and/or chemotherapy. Derivatives of OCT labeled with radionuclides such as ^{111}In and ^{99}Tc have been developed with a view to, not only label SSTR-positive tumors for diagnostic purposes, but also exploit the α or β emission from the tagged radionuclides at the tumor site for localized radiotherapy (Krenning *et al.*, 1992; Pearson *et al.*, 1996). Internalization of SSTR-bound [^{125}I -Tyr 3] OCT has been demonstrated in tumor cells (Hofland *et al.*, 1995). Therefore, the α - or β -emitting OCT-tagged radionu-

clides should elicit maximal cytotoxic response due not only to the triggering of apoptosis *via* induction of wt p53 and Bax by receptor-mediated signaling but also to the radiation induced damage following internalization. We predict that treatment with SST analogs alone or in combination with radiation and/or chemotherapy will be most effective in treating wt p53- and SSTR-expressing tumors not only of the breast but also of other organs.

We have shown that recruitment of the phosphotyrosine phosphatase (PTP) SHP1 (also called PTP1C/HCP/SHPTP1/SHP) to the cell membrane and not direct activation of membrane-associated PTP is an early event in OCT-induced anti-proliferative signaling in MCF-7 cells (Srikant and Shen, 1996). Orthovanadate, which inhibits PTP, blocks the ability of OCT to induce wt p53 and Bax in these cells (Fig. 6). The cytotoxic response to OCT treatment occurs faster in MCF-7 cells than in CHO-K1 cells, as reported earlier (Sharma *et al.*, 1996). This may be due to greater abundance of SHP1 in MCF-7 cells compared to CHO-K1 cells (data not shown). SST regulation of PTP is reported to occur *via* SSTRs 1, 2, 3 and 4 (Florio *et al.*, 1994, 1996; Buscail *et al.*, 1995; Reardon *et al.*, 1996). The fact that OCT does not bind to SSTRs 1 and 4 coupled with the fact that it signals apoptosis through hSSTR3, but not hSSTRs 2 and 5, raises the possibility that SHP1-mediated signaling may be SSTR3-selective. Such selectivity and the mechanistic sequence of events involved in hSSTR-mediated, dephosphorylation-dependent activation of p53 remain to be elucidated.

The cytotoxic action of OCT in MCF-7 cells contrasts with its reported cytostatic action in GH₃ rat pituitary tumor cells, in which it was observed to induce a transient G₀/G₁ cell-cycle block (Cheung and Boyages, 1995). Failure of SST to signal apoptosis in this cell line may be due to an inactivating mutation in p53 which renders the molecule incapable of attaining wt conformation or, alternatively, to a lack of PTP necessary for initiating SSTR-mediated apoptotic signals.

In summary, our present findings demonstrate that SSTR-signaled cytotoxic effects in MCF-7 cells involve induction of wt p53 and Bax and activation of a cation-insensitive, acidic endonuclease, leading to apoptosis.

ACKNOWLEDGEMENTS

We thank Ms. Jun Cai for assistance with cell culture and Dr. F. Halwani and Ms. S. Schiller for assistance with flow cytometry. This work was supported by a grant from the Medical Research Council of Canada (MT-12603).

NOTE ADDED IN PROOF:

Subsequent to submission of this manuscript we have reported the activation of a cation insensitive acidic endonuclease by OCT in CHO-K1 cells expressing hSSTR3 (Sharma and Srikant, 1998).

REFERENCES

- ADACHI, J., OOKAWA, K., SHISEKI, M., OKAZAKI, K., TSUCHIDA, S., MORISHITA, K. and YOKOTA, J., Induction of apoptosis but not G₁ arrest by expression of the wild type p53 gene in small cell lung carcinoma. *Cell Growth Differentiation*, **7**, 879–886 (1995).
- BARRY, A. and EASTMAN, A., Identification of deoxyribonuclease II as an endonuclease involved in apoptosis. *Arch. Biochem. Biophys.*, **300**, 440–450 (1993).
- BUSCAIL, L., ESTÉVE, J.-P., SAINT-LAURENT, N., BERTRAND, V., REISINE, T., O'CARROLL, A.-M., BELL, G.I., SCHALLY, A.V., VAYSSE, N. and SUSINI, C., Inhibition of cell proliferation by the somatostatin analog RC-160 is mediated by somatostatin receptor subtypes SSTR2 and SSTR5 through different mechanisms. *Proc. nat. Acad. Sci. (Wash.)*, **92**, 1580–1584 (1995).
- CANDI, E., MELINO, G., DE LAURENZA, V., PIACENTINI, M., GUERRERI, P., SPINEDI, A. and KNIGHT, R.A., Tamoxifen and somatostatin affect tumors by inducing apoptosis. *Cancer Lett.*, **96**, 141–145 (1995).
- CHEUNG, N.W. and BOYAGES, S.C., Somatostatin-14 and its analog octreotide exert a cytostatic effect on GH₃ rat pituitary tumor cell proliferation via a transient G₀/G₁ cell cycle block. *Endocrinology*, **136**, 4174–4181 (1995).
- CHIARUGI, V., MAGNELLI, L., CINELLI, M. and BASI, G., Apoptosis and the cell cycle. *Cell. mol. Biol. Res.*, **40**, 403–612 (1994).
- EASTMAN, A., Assays for DNA fragmentation, endonucleases, and intracellular pH and Ca²⁺ associated with apoptosis. *Methods Cell. Biol.*, **46**, 41–55 (1995).
- FLORIO, T., RIM, C., HERSHBERGER, R.E., LODA, M. and STORK, P.J.S., The somatostatin receptor SSTR1 is coupled to phosphotyrosine phosphatase activity in CHO-K1 cells. *Mol. Endocrinol.*, **8**, 1289–1297 (1994).
- FLORIO, T., SCORZIELLO, A., FATTORE, M., DALTO, V., SALZANO, S., ROSSI, G., BERLINGIERI, M.T., FUSCO, A. and SCETTINI, G., Somatostatin inhibits PC C13 thyroid cell proliferation through the modulation of phosphotyrosine phosphatase activity—impairment of the somatostatinergetic effects by stable expression of E1A viral oncogene. *J. biol. Chem.*, **271**, 6129–6136 (1996).
- GALLARDO, D., DRAZEN, K.E. and MCBRIDE, W.H., Adenovirus-based transfer of wild type p53 gene increases ovarian tumor radiosensitivity. *Cancer Res.*, **56**, 4891–4893 (1996).
- GOROSPE, M., CIRIELLI, C., WANG, X., SETH, P., CAPOGROSSI, M.C. and HOLBROOKE, N.J., p21 (Waf1/Cip1) protects against p53-mediated apoptosis of human melanoma cells. *Oncogene*, **14**, 929–935 (1997).
- HERMEKING, H., FUNK, J.O., REICHERT, M., ELLWART, J.W. and EICK, D., Abrogation of p53-induced cell cycle arrest by c-Myc. Evidence for an inhibitor of p21 (WAF1/CIP1/SDI1). *Oncogene*, **11**, 1409–1415 (1995).
- HOFLAND, L.J., VAN KOETSVELD, P.M., WAAJERS, M., ZUYDERWIJK, J., BREEMAN, W.A. and LAMBERTS, S.W.J., Internalization of the radioiodinated somatostatin analog [¹²⁵I-Tyr³] octreotide by mouse and human pituitary tumor cells: increase by unlabeled octreotide. *Endocrinology*, **136**, 3698–3706 (1995).
- KRENNING, E.P. and 13 OTHERS, Somatostatin receptor scintigraphy with [¹¹¹In-DTPA-D-Phe¹]-octreotide in man: metabolism, dosimetry and comparison with [¹²⁵I-Tyr³]-octreotide. *J. nucl. Med.*, **33**, 652–658 (1992).
- PAGLIACCI, M.C., TOGNELLINI, R., GRIGNANI, F. and NICOLETTI, I., Inhibition of human breast cancer cell (MCF-7) growth *in vitro* by the somatostatin analog SMS 201-995: effects on cell cycle parameters and apoptotic cell death. *Endocrinology*, **129**, 2555–2562 (1991).
- PATEL, Y.C., GREENWOOD, M.T., PANETTA, R., DEMCHYSHYN, L., NIZNIK, H.B. and SRIKANT, C.B., Mini review: The somatostatin receptor family. *Life Sci.*, **57**, 1249–1265 (1995).
- PATEL, Y.C., PANETTA, R., ESCHER, E.E., GREENWOOD, M.T. and SRIKANT, C.B., Expression of multiple somatostatin receptor genes in AtT-20 cells: evidence for a novel somatostatin-28 selective receptor subtype. *J. biol. Chem.*, **269**, 1506–1509 (1994).
- PEARSON, D.A., LISTER-JAMES, J., MCBRIDE, W.J., WILSON, D.M., MARTEL, L.J., CIVITELLO, E.R., TAYLOR, J.E., MOYER, B.R. and DEAN, R.T., Somatostatin receptor binding peptides labeled with technetium-99m: chemistry and initial biological studies. *J. Med. Chem.*, **39**, 1361–1371 (1996).
- REARDON, D.B., WOOD, S.L., BRAUTIGAN, D.L., BELL, G.I., DENT, P. and STURGILL, T.W., Activation of a protein tyrosine phosphatase and inactivation of Raf-1 by somatostatin. *Biochem. J.*, **314**, 401–404 (1996).
- SAKAKURA, C. and 14 OTHERS, Overexpression of Bax sensitizes human breast cancer MCF-7 cells to radiation-induced apoptosis. *Int. J. Cancer*, **67**, 101–105 (1996).
- SHARMA, K. and SRIKANT, C.B., G protein coupled receptor signaled apoptosis is associated with activation of a cation insensitive acidic endonuclease and intracellular acidification. *Biochem. Biophys. Res. Commun.*, **252**, 134–140 (1998).
- SHARMA, K., PATEL, Y.C. and SRIKANT, C.B., Subtype selective induction of wild-type p53 and apoptosis, but not cell cycle arrest, by human somatostatin receptor 3. *Mol. Endocrinol.*, **10**, 1688–1696 (1996).
- SHARMA, K., PATEL, Y.C. and SRIKANT, C.B., Subtype selective human somatostatin receptor (hSSTR) mediated cytostatic and cytotoxic actions

involve different signaling mechanisms. In: *Proc. of the 79th Annual Meeting of the Endocrine Society*, Minneapolis, June, 1997. Abstr. P1-152 (1997).

SRIKANT, C.B., Cell cycle dependent induction of apoptosis by somatostatin analog SMS 201-995 in AtT-20 mouse pituitary tumor cells. *Biochem. Biophys. Res. Comm.*, **209**, 400-407 (1995).

SRIKANT, C.B. and SHEN, S.-H., Octapeptide somatostatin analog SMS 201-995 induces translocation of intracellular PTP1C to membranes in MCF-7 human breast cancer adenocarcinoma cells. *Endocrinology*, **137**, 3461-3468 (1996).

VIKIC-TOPIĆ, S., RAISCH, K.-P., KVOLS, L.-K. and VUK-PAVLOVIC, S., Expression of somatostatin subtypes in breast carcinoma, carcinoid tumor,

and renal cell carcinoma. *J. clin. Endocrinol. Metab.*, **80**, 2974-2479 (1995).

WAGNER, C., BARGOU, R.C., DANIEL, P.T., BOMMERT, K., MAPARA, M.Y., ROYER, H.D. and DORKEN, B., Induction of the death-promoting gene Bax-alpha sensitizes cultured breast cancer cells to drug-induced apoptosis. *Int. J. Cancer*, **67**, 138-141 (1996).

WALKER, P.R. and SIKORSKA, M., Endonuclease activities, chromatin structure, and DNA degradation in apoptosis. *Biochem. Cell Biol.*, **72**, 615-623 (1994).

XU, Y., BRUNO, J.F. and BERELOWITZ, M., Estrogen regulates somatostatin receptor subtype 2 expression in human breast cancer cells. *Endocrinology*, **137**, 5634-5640 (1996).

G Protein Coupled Receptor Signaled Apoptosis Is Associated with Activation of a Cation Insensitive Acidic Endonuclease and Intracellular Acidification

Kamal Sharma and Coimbatore B. Srikant¹

Fraser Laboratories for Diabetes Research, Department of Medicine, McGill University and Royal Victoria Hospital, Montreal, Quebec, Canada, H3A 1A1

Received November 29, 1997

Apoptosis associated oligonucleosomal fragmentation of DNA can result from the activation of endonucleases that exhibit different pH optima and are either sensitive or insensitive to divalent cations. DNA fragmentation due to activation of cation sensitive endonucleases occurs in the absence of a change in intracellular pH whereas intracellular acidification is a feature of apoptosis characterized by activation of cation insensitive acidic endonuclease. We have reported earlier that somatostatin (SST) induced DNA fragmentation and apoptosis is signaled in a receptor subtype selective manner uniquely via human somatostatin receptor subtype 3 (hSSTR3). In the present study we investigated the pH dependence and cation sensitivity of endonuclease induced in hSSTR3 expressing CHO-K1 cells by the SST agonist octreotide (OCT) and its effect on intracellular pH. We show that OCT induced apoptosis is associated with selective stimulation of a divalent cation insensitive acidic endonuclease. The intracellular pH of cells undergoing OCT induced apoptosis was 0.9 pH units lower than that of control cells. The effect of OCT on endonuclease and pH was inhibited by orthovanadate as well as by pretreatment with pertussis toxin, suggesting that hSSTR3 initiated cytotoxic signaling is protein tyrosine phosphatase mediated and is G protein dependent. These findings suggest that intracellular acidification and activation of acidic endonuclease mediate wild type p53 associated apoptosis signaled by hormones acting via G protein coupled receptors. © 1998 Academic Press

Apoptosis constitutes a specific form of cell death characterized by cell shrinking, chromatin condensa-

tion and intranucleosomal digestion of genomic DNA (1). In apoptotic cells DNA fragmentation results from the action of DNA digesting enzymes (endonucleases) whose activity is modulated by molecular regulators of apoptosis including p53 and Bax (2). Two distinct sets of constitutive endonucleases which exhibit distinct pH optima under *in vitro* conditions have been implicated in this process. These include several Ca^{2+} and/or Mg^{2+} dependent endonucleases including DNase I, Nuc18 and endonuclease I which possess an alkaline pH optimum, DNase γ which has a neutral pH optimum, and an acidic endonuclease that is active in the pH range of 6–7.5 (3–7). In addition, a $\text{Ca}^{2+}/\text{Mg}^{2+}$ insensitive endonuclease (DNase II) which has a pH optimum of 5 has also been shown to induce DNA degradation (8,9). Cation sensitive endonuclease mediated DNA fragmentation leads to cell death in the absence of a change in intracellular pH. By contrast, in several cell types in which DNA fragmentation is caused by the activation of a pH dependent endonuclease, apoptosis is associated with intracellular acidification (7,9–11).

Somatostatin (SST¹), a G protein coupled receptor agonist, exerts cytotoxic effect triggering apoptosis as has been shown in tumor cells (12). Although SST acts via a family of five distinct human (h) SST receptor (SSTR) subtypes, cytotoxic signaling is transduced uniquely through hSSTR subtype 3 (13). We have shown that hSSTR3 signaled apoptosis in CHO-K1 cells is characterized by the appearance of oligonucleosomal DNA and is associated with the induction of the tumor suppressor protein wild type (wt) p53 and Bax (13). In order to determine which of the endonuclease(s) is/are activated during hSSTR3 mediated apoptosis and whether this is associated with intracellular acidification we investigated the effect of treatment with the somatostatin (SST) analog octreotide (OCT) on the endonuclease activity and intracellular pH in CHO-K1 cells stably transfected with hSSTR3. We report here that hSSTR3 signaled apoptosis in CHO-K1 cells is

¹ Address for correspondence: Dr. C.B. Srikant, M3.15, Royal Victoria Hospital, 687, Pine Avenue West, Montreal, Quebec, Canada, H3A 1A1. E-mail: mdc5@musica.mcgill.ca.

Abbreviations used: SST, somatostatin; SSTR, somatostatin receptor; OCT, octapeptide somatostatin analog octreotide; and PTx, pertussis toxin.

due to selective activation of a pH dependent, cation insensitive endonuclease which occurs concomitantly with intracellular acidification.

MATERIALS AND METHODS

Materials. The SST analog SMS 201-995 (octreotide, OCT) was obtained from Sandoz Pharma (Basel, Switzerland). D-Trp⁸ SST-14 was purchased from Bachem (Torrance, CA). Reagents required for cellular staining and flow cytometry were procured from the following sources: Propidium iodide (PI) from ICN Pharmaceuticals (Costa Mesa, CA), Hoechst 33342 from Calbiochem (San Diego, CA) and, carboxy SNARF-1 and its cell permeant derivative aminomethyl ester from Molecular Probes (Eugene, OR). All other reagents were obtained from local commercial sources and were of analytical quality.

Cell lines. Establishment and characterization of CHO-K1 cell lines stably expressing individual hSSTR subtypes have been detailed elsewhere (13,14). Cells were grown in T75 flasks in Hams F-12 medium containing 5% fetal calf serum and 400 U/ml G-418 and cultured for 3-5 days at 37°C in a humidified atmosphere with 5% CO₂.

Preparation of nuclear protein extract and determination of endonuclease activity. Nuclear protein extract was prepared according to Eastman (9) from CHO-K1 cells expressing individual hSSTR subtypes pre-incubated with 100 nM peptides for 24 h. Briefly, 2×10^6 cells were resuspended and allowed to swell for 20 min on ice in buffer 20 mM Hepes-KOH buffer, pH 7.4 containing 0.75 mM spermidine, 0.15 mM spermine, 0.1 mM EDTA and, 1 mM each of DTT and phenylmethylsulfonyl fluoride (HSSE buffer). Cells were homogenized after adding sucrose to a final concentration of 0.5 M. This mixture was centrifuged for 10 min at 150 g, and the pellet was resuspended in 0.75 ml of the buffer containing 0.5 M sucrose, layered on 1.5 M sucrose/HSSE buffer and centrifuged for 20 min at 13,000 g. The nuclei were then resuspended in a buffer containing 10 mM sodium acetate, 10 mM sodium phosphate, 10 mM bistris-propane, 1 mM DTT, 1 mM phenylmethylsulfonyl fluoride (APB buffer) and recentrifuged to remove residual spermine and spermidine. Nuclear protein extracts were prepared by resuspending the nuclei in APB buffer (pH 7) containing 0.5 M NaCl. After 1 h incubation on ice, the precipitated DNA was pelleted by centrifugation at 14,000 g for 10 min and the supernatant recovered.

The endonuclease assay was performed by incubating 100 ng of genomic DNA prepared from untransfected CHO-K1 cells as described previously (13) with 10 μ g of nuclear protein extract in APB buffer adjusted to pH 5, 7 or 8 in the absence or presence of 10 mM Ca²⁺/Mg²⁺. The mixtures were incubated at 37°C for 30 min and electrophoresed on a 1.2% agarose gel (w/v) containing ethidium bromide and visualized under UV light.

Measurement of intracellular pH and apoptosis. Intracellular pH measurements were performed in cells preloaded with carboxy-SNARF-1 AM according to Barry et al. (7). hSSTR3 expressing cells were loaded with 10 μ M acetoxymethyl ester derivative of SNARF-1 for during the final hour of the 24 h incubation in the absence or presence of 100 nM OCT at 37°C. The cells were then scraped, washed and resuspended in 2 ml of fresh medium and incubated for 1 min at 37°C with 1 μ g/ml Hoechst 33342, a DNA binding dye which is taken up preferentially by apoptotic cells due to their altered membrane permeability (16). Cells were maintained at 37°C in a Becton-Dickinson FACStar Vantage cytometer. Hoechst 33342 was excited at 355 nm and its emission was measured at 440 nm. Intracellular carboxy SNARF-1 was excited at 488 nm and emission was recorded at both 580 and 640 nm with 5 nm band pass filters with linear amplifiers. The ratio of the emissions at these wavelengths was electronically calculated and used as a parameter indicative of intracellular pH. The intracellular pH values in control and treated cells were

pH	5.0				7.0				8.0			
IONS	-	+	-	+	-	+	-	+	-	+	-	+
OCT	-	+	-	+	-	+	-	+	-	+	-	+



FIG. 1. Endonuclease activity in nuclear protein extracts of expressing hSSTR3 CHO-K1 cells incubated in the absence or presence of 100 nM OCT for 24 h was measured in vitro using the genomic DNA prepared from control CHO-K1. Following incubation for 15 min at 37°C at pH 5, 7 and 8 in the absence or presence of Ca²⁺ and Mg²⁺ as described under Methods, the samples were electrophoresed on 1.2% agarose gel, stained with ethidium bromide and visualized under UV light. Digestion of the DNA was observed only with nuclear protein extracts of OCT treated cells during incubation at pH 5 (lanes 2 and 4) but not in untreated cells (lanes 1 and 3). This enzyme activity was insensitive to divalent cations (compare lanes 2 and 4). By contrast, OCT did not induce Ca²⁺ and Mg²⁺ sensitive or insensitive endonucleases at pH 7 (lanes 5-8) or 8 (lanes 9-12). Data representative of 4 separate experiments.

estimated by comparison of the mean ratios of the samples to a calibration curve of intracellular pH generated by incubation of carboxy-SNARF-1 loaded hSSTR3 expressing CHO-K1 cells in buffers ranging in pH from 8.0 to 6.25 and containing the proton ionophore nigericin. Data was analyzed using the WinList software (Verity Software Inc., Topsham, ME). Cells with fluorescence of <50 units were excluded in the calculation of the ratio of the emissions at 580 nm and 640 nm.

RESULTS

Cytotoxic signaling of SST is selectively transduced through hSSTR3 and causes apoptosis characterized by the presence of oligonucleosome sized DNA fragments. In the present study we demonstrate that the DNA fragmentation in these cells is due to selective activation by OCT of a pH sensitive endonuclease which is active under acidic conditions (figure 1). The activity of this enzyme was not sensitive to Ca²⁺/Mg²⁺ since the extent of DNA digestion did not increase in the presence of the cations. As illustrated in this figure, OCT did not induce endonucleases exhibiting neutral or alkaline pH optima either in the absence or presence of Ca²⁺/Mg²⁺. This endonuclease was not active at or above neutral pH, but increased as the pH was lowered progressively over a range of 6.7- 4.9 (figure 2). Its activity was maximal at the lowest pH tested. Activation of this endonuclease in CHO-K1 cells was clearly hSSTR subtype selective and occurred only via hSSTR3 (figure 3).

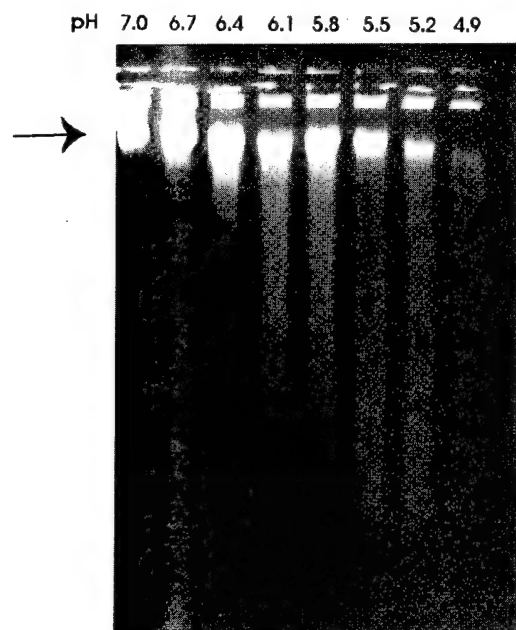


FIG. 2. Effect of pH on the activity of OCT induced acidic endonuclease. In vitro enzyme activity in nuclear protein extracts of OCT treated cells was measured in buffers ranging in pH from 7 to 5. Maximum activity was observed at the lowest pH tested. Data representative of 2 separate experiments.

In cells expressing hSSTR3, OCT induced pH dependent endonuclease activity increased in a time dependent manner. When tested for its ability digest DNA in vitro, its activity was detectable after 1 h during OCT treatment (figure 4A). This is evident from the decrease in the intensity of the labeling of intact DNA (which remains close to the origin, lane 2), the marked increase in the intensity of the digested DNA fragments at 4 h (lane 3) followed by

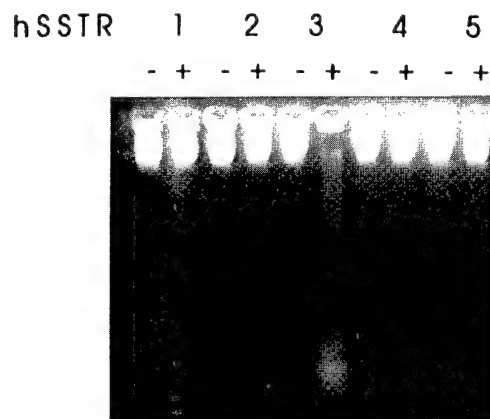


FIG. 3. Subtype selectivity of hSSTR signaled activation of endonuclease II. Cells were incubated in the absence or presence of 100 nM OCT (hSSTRs 2,3,5) or 100 nM D-Trp⁸ SST-14 (hSSTRs 1,4) for 24 h. The endonuclease activity in nuclear extracts was assessed at pH 5. Data representative of 4 separate experiments.

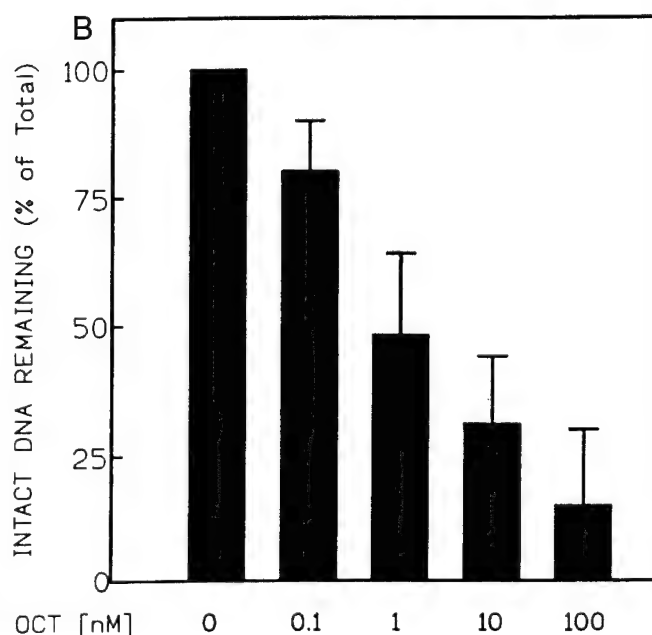
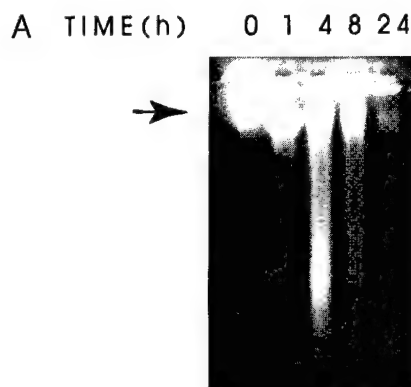


FIG. 4. Time dependent activation of acidic endonuclease by OCT (100 nM) in CHO-K1 cells expressing hSSTR3. **A.** Representative agarose gel electrophoresis demonstrating the time dependent decrease in the intensity of the intact DNA indicated by the arrow. Notice also that the intensity of ethidium bromide staining of DNA fragments increases initially reaching a maximum by 4 h, but decreases at later time points. **B.** Time dependent activation of this endonuclease by OCT was quantitated by densitometric measurement of intact DNA remaining at each time point and expressed as a percentage of the DNA in untreated cells (time 0). values represent mean \pm SE, $n=4$.

decrease in both the intact and fragmented DNA at longer time points of 8 and 24 h (lanes 4,5). The effect of OCT on the activity of this enzyme was quantitated densitometrically by measuring the decrease in the intensity of the labeling of the intact DNA. The decrease in the intensity of ethidium bromide staining of the intact DNA band at 1 h was $12 \pm 6\%$ and was $88 \pm 15\%$ at 24 h (figure 4B). hSSTR3 signaled activation of this endonuclease by OCT was dependent on its concentration over a range of 0.1-100 nM (figure 5 A,B). The loss of intensity of the intact DNA

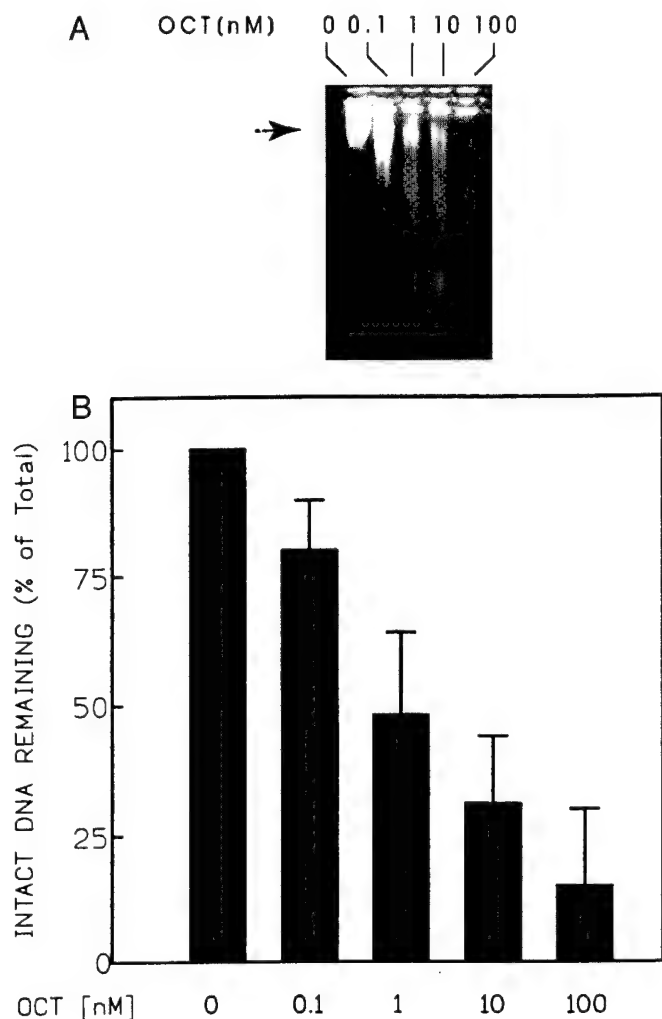


FIG. 5. Dose-dependent activation of acidic endonuclease by OCT in CHO-K1 cells expressing hSSTR3. **A.** Representative agarose gel electrophoresis showing the concentration dependent activation by OCT of the endonuclease activity. Arrow indicates the intact DNA. **B.** The intact DNA remaining at each OCT concentration was quantitated densitometrically and expressed as a percentage of intact DNA in untreated cells. Values represent mean \pm SE, $n=4$.

ranged from 20 ± 10 % to 82 ± 15 % respectively in cells treated with 0.1 and 100 nM OCT.

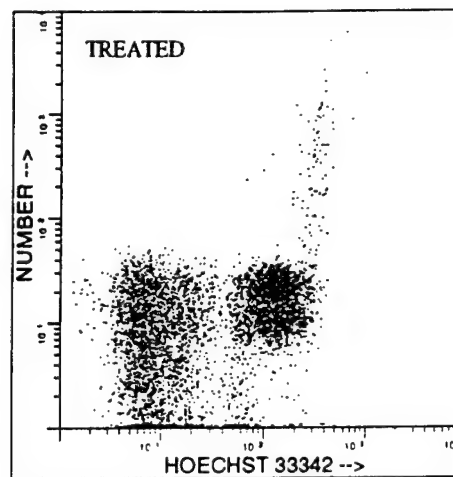
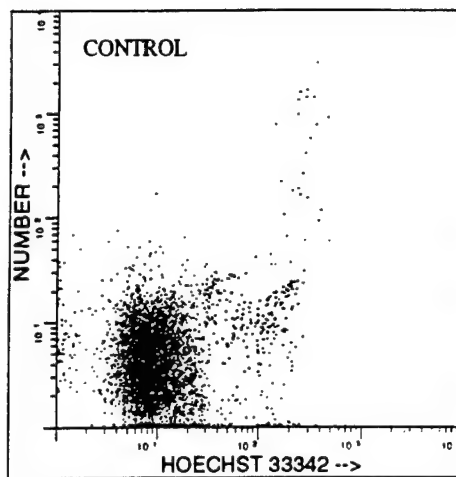
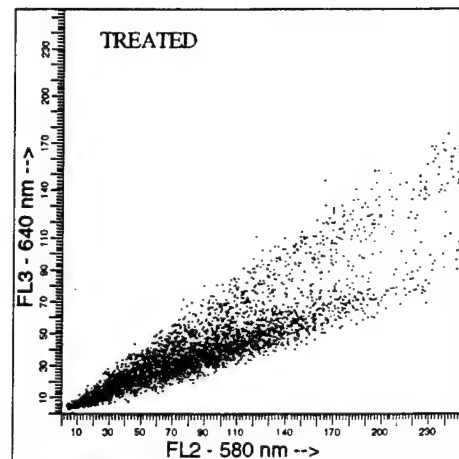
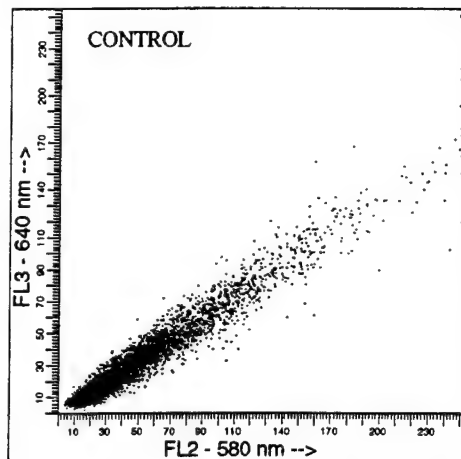
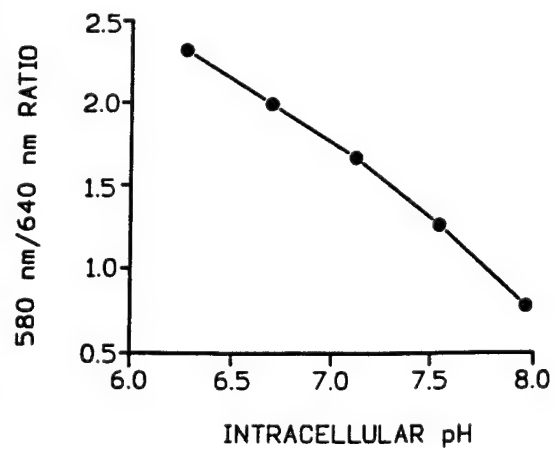
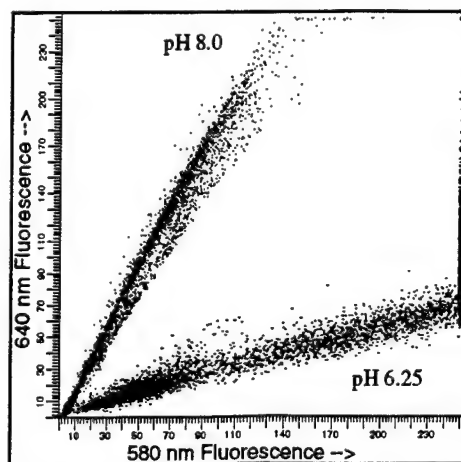
The above finding of involvement of a pH dependent acidic endonuclease in OCT signaled apoptosis suggested that intracellular acidification may underly cytotoxic signaling via hSSTR3. To test this, we measured the intracellular pH using the dye carboxy SNARF-1 in cells undergoing OCT induced apoptosis. Apoptotic cells were characterized by their increased Hoechst 33342 fluorescence following 24 h treatment with the peptide (figure 6A, right panel) while untreated control cells displayed low dye uptake (figure 6A, left panel). Apoptotic cells exhibiting increased Hoechst 33342 averaged $34 \pm 5\%$ ($n=3$). Intracellular pH was measured by analysing the carboxy-SNARF-1

fluorescence excited at 488 nm and the emission recorded at 585 vs 640 nm wavelengths. The data is presented as a two dimensional dot plot with 580 nm fluorescence on the abscissa and the 640 nm fluorescence on the ordinate. Control cells, not treated with the peptide, were found distributed along a single line out of the origin (figure 6B, left panel). Since the distance of each cell from the origin is directly proportional to the amount of carboxy-SNARF-1 loading, these cells possess the same intracellular pH. By contrast, OCT treatment led to the appearance of a distinct population of cells with a increased fluorescence at 580 nm and shifting to the right indicative of lower intracellular pH (figure 6B, right panel). The decrease in pH in these cells was determined by comparing the ratio of emissions at these wavelengths against a standard curve generated from the emission ratios at 580 and 640 nm in carboxy-SNARF-1 loaded cells which were incubated in buffers ranging in pH from 6.25 - 8.0 in the presence of the proton ionophore nigericin. The recordings obtained in cells incubated at buffers at pH 8 and 6.25 containing nigericin are compared in figure 6C (left panel). A calibration curve was generated from the ratios of emissions at 580 nm and 640 nm obtained in the different buffers containing nigericin (figure 7C, right panel). The intracellular pH was 6.5 ± 0.2 in OCT treated cells compared to 7.2 ± 0.1 in untreated, control cells ($n=3$) (figure 7). The intracellular pH was 6.3 ± 0.16 in cells exhibiting increased Hoechst 33342 fluorescence. The apoptotic cells were thus even more acidic. OCT induced decrease in cellular pH as well as the induction of the acidic endonuclease was inhibited by orthovanadate and abolished by pertussis toxin pretreatment (details not shown). In cells expressing other hSSTRs which did not signal apoptosis nor stimulate endonuclease activity, no change in intracellular pH occurred during agonist treatment.

DISCUSSION

In the present study, we demonstrate that hSSTR3 mediated cytotoxic signaling is associated with selective activation of a pH dependent endonuclease. This novel finding indicates that the endonuclease responsive to OCT is active under acidic conditions and is $\text{Ca}^{2+}/\text{Mg}^{2+}$ insensitive. This enzyme thus appears to be similar to DNase II previously implicated in CHO cell apoptosis induced by a variety of cytotoxic drugs (7-9). OCT did not induce cation sensitive endonucleases that are known to be active at neutral or alkaline pH and implicated in other models of apoptosis (3-6).

Activation of a pH dependent, cation insensitive endonuclease during hSSTR3 signaled apoptosis suggested that intracellular acidification may be an underlying cause. Using carboxy-SNARF-1 we demonstrate that OCT induced apoptosis is indeed associated with intracellular acidification. Such acidification was lim-

A**B****C**

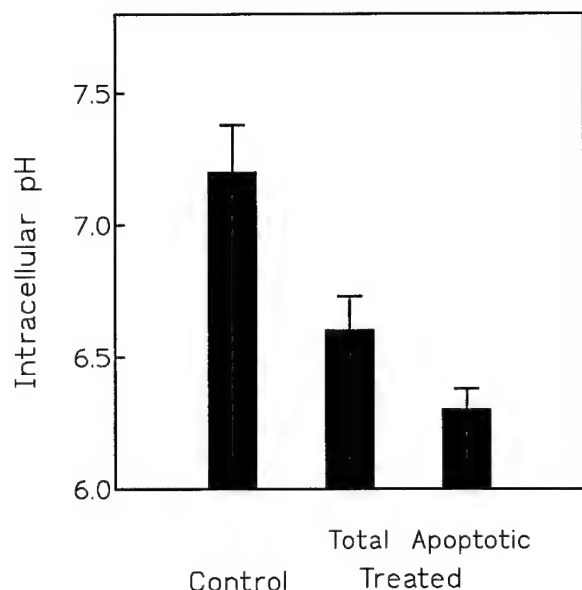


FIG. 7. OCT induced decrease in intracellular pH was greater in apoptotic (Hoechst 33342 positive) cells (6.3 ± 0.1) compared to the treated cells taken as a whole (6.5 ± 0.2). The pH of untreated cells was 7.2 ± 0.1 . (mean \pm SE, $n=3$)

ited to the cells that became Hoechst 33342 positive. This suggests that intracellular pH decrease may occur only in cells undergoing apoptosis induced by OCT. This is similar to the decrease in intracellular pH observed in other models of apoptosis involving activation of acidic endonuclease (7,10,11). The pH in these cells averaged 6.6 ± 0.2 , a pH at which the endonuclease activity is detectable, but not maximal, under in vitro conditions (figure 2). We have shown earlier that Bax but not Bcl-2 is induced during hSSTR3 signaled apoptosis (13). Bax as well as Bcl-2 can form pH-dependent channels but the intrinsic properties of channels formed by these proteins differ with respect to pH (16,17). In planar bilipid layers, Bax can form pH and voltage dependent ion-conducting channels at neutral and acidic pH whereas Bcl-2 is effective only at a pH <5.0 (17). The selective activation of Bax by OCT via hSSTR3 may therefore account, in part, for the decrease in intracellular pH in these cells. Additional

mechanisms involving Na^+/H^+ antiporter and H^+ -AT-Pase can also trigger cellular acidification. For instance, in HeLa cells and in murine hematopoietic cells, inhibition of Na^+/H^+ antiporter activity has been shown to decrease intracellular pH and activate acidic endonuclease (18,19). Furthermore, pharmacological induction of Na^+/H^+ antiporter can prevent acidification and endonuclease activation (19). The potential involvement of Na^+/H^+ antiporter in hSSTR3 initiated cytotoxic signaling needs to be assessed.

The present findings constitute, to our knowledge, the first instance of a G protein coupled receptor agonist induced intracellular acidification and activation of an acidic endonuclease leading to apoptosis. Furthermore, the cytotoxic effect is uniquely signaled via a single SSTR subtype, namely hSSTR3. Both PTx pretreatment and orthovanadate abolished OCT induced pH decrease and activation of the acidic endonuclease. Another G protein coupled receptor AT_2R has recently been reported to initiate apoptosis in neonatal ventricular myocytes (20). Angiotensin II acting via AT_2R appears to signal in a different manner in ventricular myocytes by elevating intracellular Ca^{2+} and activating a calcium dependent endonuclease, but not intracellular acidification (20).

In CHO-K1 cells expressing the other four hSSTRs agonist treatment did not alter intracellular pH. Additionally, no induction of endonuclease activity was observed in these cells during agonist treatment (details not shown). This is in accord with our earlier finding that these hSSTRs are incapable of eliciting a cytotoxic response, although agonist treatment inhibits cell growth via other human SSTR subtypes (13,21). How can hSSTR3 but not the other hSSTR subtypes transduce cytotoxic signaling? The five hSSTRs exhibit most homology in the transmembrane domains (55-70% sequence identity) and share considerable sequence identity (38-54%) in regions comprising the second and third intracellular loops, the putative G protein binding region in G protein coupled receptors (22). The cytoplasmic tail (C-tail) sequence of hSSTR3 however differs markedly from that of the four other subtypes (12-18% sequence identity, reviewed in 23) suggesting that the C-tail of hSSTR3 may be the functional domain

FIG. 6. hSSTR3 signaled apoptosis in CHO-K1 cells is associated with intracellular acidification. **A.** Apoptotic cells were identified by their increase uptake of Hoechst 33342. In control cells there is minimal uptake of the dye as indicated by the low fluorescence (left panel) whereas 40% of the cells become apoptotic following 24 h treatment with 100 nM OCT and display >10 fold higher Hoechst 33342 fluorescence (right panel, upper quadrant). **B.** Effect of OCT on carboxy-SNARF-1 fluorescence. Following incubation in the absence or presence of 100 nM OCT for 24 h, cells were loaded with carboxy-SNARF-1 and cells were excited at 488 nm and fluorescence measured at 585 and 640 nm in a Becton-Dickinson Vantage Plus flow cytometer as described under Methods. When the fluorescence at 580 nm is plotted against that at 640 nm, cells distributed along the same line out of the axis possess the same pH as seen in untreated cells since fluorescence intensity of the cells is directly proportional to the dye uptake (left panel). Following OCT treatment, $\sim 40\%$ of the cells display an increase in fluorescence at 580 nm relative to the fluorescence at 640 nm which is reflected by the downward shift in the distribution of the cells (right panel). **C.** Generation of a pH calibration curve. Carboxy-SNARF-1 loaded cells were incubated in the presence of the proton ionophore nigericin in buffers ranging in pH from 6.25 - 8. Representative plots of cells incubated at pH 8 and 6.25 are shown (left panel). A pH calibration curve was derived from the ratios of the emissions at 585 and 640 nm (right panel). The intracellular pH of CHO-K1 cells was 7.2 ± 0.1 ($n=3$). OCT induced acidification was reflected by the decrease in pH to 6.5 ± 0.2 ($n=3$), a loss of 0.7 pH units.

that confers specificity for apoptotic signaling. Studies to test this directly by mutagenesis are currently in progress.

The cytotoxic signaling via hSSTR3, which leads to intracellular acidification, activation of an acidic endonuclease and apoptosis, is PTx-sensitive G protein mediated. Other G protein coupled receptors such as the angiotensin type II receptor (AT₂R) and dopaminergic D₂ receptors (D₂R) also transduce antiproliferative signaling in PTx-sensitive G protein dependent manner (24,25). PTx-sensitive G protein dependent induction of apoptosis has also been observed with T cell and B cell receptors (TCR and BCR) which interact with distinct antigens and initiate cellular responses primarily by triggering tyrosine kinases (26,27). Additionally, activation-induced cell death mediated through simultaneous ligation of CD16/IL-2 receptor in human natural killer cells is prevented by PTx pretreatment (28). Only the negative consequences of TCR-mediated stimulation, namely apoptosis, is inhibited by PTx while the positive consequences including calcium mobilization, lymphokine secretion and proliferation remain unaffected (28,29). Whether these receptors which belong to different receptor family interact directly with G proteins and initiate cytotoxic signaling or require activation of a G protein coupled receptor during cytotoxic signaling is not known. In this context, it is of interest that induction of a putative G protein coupled receptor TDAG8 has been reported to be associated with T cell apoptosis signaled by TCR mediated activation as well as by glucocorticoids (30).

In summary, the present findings demonstrate that SST signaled apoptosis is associated with the activation of an acidic, cation insensitive endonuclease and intracellular acidification. These events are signaled in a subtype selective manner uniquely via hSSTR3.

ACKNOWLEDGMENTS

This work was supported by grants from the Medical Research Council of Canada (MT 12603) and the U.S. Department of Defence. We thank Dr. Y. C. Patel for providing the cell lines, J. Cai for technical assistance and K. McDonald for assistance with flow cytometry.

REFERENCES

1. Arends, M. J., and Wyllie, A. H. (1991) *Int. Rev. Exp. Pathol.* **32**, 223–254.
2. Wyllie, A. H., Arends, M. J., Morris, R. G., Walker, S. W., and Evan, G. (1992) *Seminars in Immunol.* **4**, 389–397.
3. Gaido, M. L., and Cidlowski, J. A. (1991) *J. Biol. Chem.* **266**, 18580–18585.
4. Nikonova, L. V., Beleski, I. P., and Umanski, S. R. (1993) *Eur. J. Biochem.* **215**, 893–901.
5. Shiokawa, D., Ohyama, H., Yamada, T., Takahashi, K., and Tanuma, S.-I. (1994) *Eur. J. Biochem.* **226**, 23–30.
6. Collins, M. K., Furlong, I. J., Malde, P., Ascaso, R., Oliver, J., Lopez Rivas, A. (1996) *J. Cell Sci.* **109**, 2393–2399.
7. Barry, M. A., Reynolds, J. E., and Eastman, A. (1993) *Cancer Res.* **53** (10 Suppl.), 2349–2357.
8. Barry, A., and Eastman, A. (1993) *Arch. Biochem. Biophys.* **300**, 440–450.
9. Eastman, A. (1995) *Meth. Cell. Biol.* **46**, 41–55.
10. Li, J., and Eastman, A. (1994) *J. Biol. Chem.* **270**, 3203–3211.
11. Gottlieb, R. A., Nordberg, J., Skowronski, E., and Babior, B. M. (1996) *Proc. Natl. Acad. Sci. U.S.A.* **93**, 654–658.
12. Srikant, C. B. (1995) *Biochem. Biophys. Res. Commun.* **209**, 400–407.
13. Sharma, K. S., Patel, Y. C., and Srikant, C. B. (1996) *Mol. Endocrinol.* **10**, 1688–1696.
14. Patel, Y. C., and Srikant, C. B. (1994) *Endocrinology* **135**, 2814–2817.
15. Ormerod, M. G., Sun, X.-M., Snowden, R. T., Davies, R., Fearnhead, H., and Cohen, G. M. (1993) *Cytometry* **14**, 595–602.
16. Schendel, S. L., Xie, Z., Montal, M. O., Matsuyama, S., Montal, M., and Reed, J. C. (1997) *Proc. Natl. Acad. Sci. U.S.A.* **94**, 5113–5118.
17. Antonsson, B., Conti, F., Ciavatta, A., Montessuit, S., Lewis, S., Martinou, I., Bernasconi, L., Bernard, A., Mermod, J.-J., Mazzei, G., Maundrell, K., Gambale, F., Sadoul, R., and Martinou, J.-C. (1997) *Science* **277**, 370–372.
18. Chen, Q., Benson, R. S., Whetton, A. D., Brant, S. R., Donowitz, M., Montrose, M. H., Dive, C., and Watson, A. J. (1997) *J. Cell. Sci.* **110**, 379–387.
19. Perez-Sala, D., Collado-Escobar, D., and Mollinedo, F. (1995) *J. Biol. Chem.* **270**, 6235–6232.
20. Cigola, E., Kajstura, J., Li, B., Meggs, L. G., and Anversa, P. (1997) *Exp. Cell Res.* **231**, 363–371.
21. Sharma, K., Patel, Y. C., and Srikant, C. B. (1997) Prog. of the 79th Annual Meeting of the Endocrine Society, Minneapolis. Abst # P1–152.
22. Taylor, J. M., and Neubig, R. R. (1994) *Cellular Signaling* **6**, 841–849.
23. Patel, Y. C., Greenwood, M. T., Panetta, R., Hukovic, N., Grigorakis, S. I., Robertson, L.-A., and Srikant, C. B. (1996) *Metabolism* **45** (suppl. 1), 31–38.
24. Yamada, T., Horiuchi, M., and Dzau, V. J. (1996) *Proc. Natl. Acad. Sci. U.S.A.* **93**, 156–160.
25. Florio, T., Pan, M. G., Newman, B., Hersherberger, R. E., Civelli, O., and Stork, P. J. S. (1992) *J. Biol. Chem.* **267**, 24169–24172.
26. Ramirez, R., Carracedo, J., Zamzami, N., Castedo, M., and Kroemer, G. (1994) *J. Exp. Med.* **180**, 1147–1152.
27. Weiss, A., and Littman, D. R. (1994) *Cell* **76**, 263–274.
28. Carracedo, J., Ramirez, R., Marchetti, P., Pintado, O. C., Baixeras, E., Martinez-A. C., and Kroemer, G. (1995) *Eur. J. Immunol.* **25**, 3094–3099.
29. Gonzalo, J. A., Gonzalez-Garcia, A., Baixeras, E., Zamzami, N., Tarazona, T., Rappouli, R., Martinez-A. C., Kroemer, G., and Terezzone, R. (1994) *J. Immunol.* **152**, 4291–4299.
30. Choi, J.-W., Lee, S. Y., and Choi, Y. (1996) *Cell. Immunol.* **68**, 78–84.

The Cytoplasmic Tail of the Human Somatostatin Receptor Type 5 Is Crucial for Interaction with Adenylyl Cyclase and in Mediating Desensitization and Internalization*

(Received for publication, March 12, 1997, and in revised form, May 26, 1998)

Nedim Hukovic‡§, Rosemarie Panetta‡¶, Ujendra Kumar‡, Magalie Rocheville¶, and Yogesh C. Patel||

From the Fraser Laboratories, Departments of Medicine, Neurology, and Neurosurgery and Pharmacology and Therapeutics, McGill University, Royal Victoria Hospital and the Montreal Neurological Institute, Montreal, Quebec H3A 1A1, Canada

We have investigated the role of the cytoplasmic tail (C-tail) of the human somatostatin receptor type 5 (hSSTR5) in regulating receptor coupling to adenylyl cyclase (AC) and in mediating agonist-dependent desensitization and internalization responses. Mutant receptors with progressive C-tail truncation ($\Delta 347$, $\Delta 338$, $\Delta 328$, $\Delta 318$), Cys³²⁰ → Ala substitution (to block palmitoylation), or Tyr³⁰⁴ → Ala substitution of a putative NPXXY internalization motif were stably expressed in Chinese hamster ovary K1 cells. Except for the Tyr³⁰⁴ → Ala mutant, which showed no binding, all other mutant receptors exhibited binding characteristics (K_d and B_{max}) and G protein coupling comparable with wild type (wt) hSSTR5. The C-tail truncation mutants displayed progressive reduction in coupling to AC, with the $\Delta 318$ mutant showing complete loss of effector coupling. Agonist pretreatment of wt hSSTR5 led to uncoupling of AC inhibition, whereas the desensitization response of the C-tail deletion mutants was variably impaired. Compared with internalization (66% at 60 min) of wt hSSTR5, truncation of the C-tail to 318, 328, and 338 residues reduced receptor internalization to 46, 46, and 23%, respectively, whereas truncation to 347 residues slightly improved internalization (72%). Mutation of Cys³²⁰ → Ala induced a reduction in AC coupling, desensitization, and internalization. These studies show that the C-tail of hSSTR5 serves a multifunctional role in mediating effector coupling, desensitization, and internalization. Whereas coupling to AC is dependent on the length of the C-tail, desensitization and internalization require specific structural domains. Furthermore, internalization is regulated through both positive and negative molecular signals in the C-tail and can be dissociated from the signaling and acute desensitization responses of the receptor.

* This work was supported by Medical Research Council of Canada Grant MT-10411 and grants from the National Institutes of Health, the U. S. Department of Defense, and the National Cancer Institute of Canada. The costs of publication of this article were defrayed in part by the payment of page charges. This article must therefore be hereby marked "advertisement" in accordance with 18 U.S.C. Section 1734 solely to indicate this fact.

‡ Contributed equally to this work.

§ Supported by a fellowship from the Fonds De La Recherche En Sante Du Quebec.

¶ Recipient of studentship support from the Royal Victoria Hospital Research Institute.

|| A Distinguished Scientist of the Canadian Medical Research Council. To whom correspondence should be addressed: Royal Victoria Hospital, Room M3-15, 687 Pine Avenue West, Montreal, Quebec H3A 1A1, Canada. Tel: 514-842-1231 (ext. 5042); Fax: 514-849-3681; E-mail: patel@rvhmed.lan.mcgill.ca.

The neurohormone somatostatin (SST)¹ is synthesized widely in the body and acts as a potent inhibitor of hormone and exocrine secretion as well as a modulator of neurotransmission and cell proliferation (1). These actions are mediated by a family of five G protein-coupled receptors (GPCRs) with seven α helical transmembrane segments termed SSTR1–5 (2). All five SSTRs inhibit adenylyl cyclase. Some of the receptor isotypes also modulate other effectors such as phosphotyrosine phosphatase, K⁺ and Ca²⁺ ion channels, a Na⁺/H⁺ exchanger, phospholipase C, phospholipase A2, and mitogen-activated protein kinase (2). The five SSTRs display an overlapping pattern of expression throughout the brain and in peripheral organs (2, 3). SSTR2 is the most widely expressed isoform (2, 3). SSTR5 is the predominant subtype in the pituitary and hypothalamus (2–5).

An important property of many GPCRs is their ability to regulate their responsiveness in the presence of continued agonist exposure (6). Such agonist-specific regulation by GPCRs involves a series of discrete cellular steps that include loss of binding affinity and signaling capability due to receptor uncoupling from G proteins (desensitization), receptor internalization, and receptor degradation. Like other GPCRs, SSTRs also appear to be dynamically regulated at the membrane by agonist treatment (2). For instance, during pharmacotherapy with SST analogs in man, the acute effects on pituitary islet and gastric functions subside with continued exposure to the peptide due to the development of tolerance (7). Agonist-dependent internalization of SSTRs occurs in rat pituitary and islet cells and in AtT-20 cells (8–10). In GH₄C₁ and Rin m5f cells, however, prolonged agonist treatment up-regulates SSTRs (11, 12). These differences may be explained by differential expression of SSTR subtypes since AtT-20 cells express predominantly the SSTR5 subtype, whereas GH₄C₁ cells are rich in the SSTR1 isotype (13, 14). Furthermore, because pituitary and islet cells or their tumor cell derivatives express multiple SSTR subtypes, it is difficult to determine subtype-selective responses in these systems (4, 5, 19, 20). To circumvent these problems, several recent studies have characterized agonist regulation of individual SSTRs using subtype-selective SST analogs or cell lines stably transfected with SSTR cDNAs (10, 15–18). These studies have shown differential internalization of SSTR2,3,4, and 5 but not of SSTR1 (15–18).

¹ The abbreviations used are: SST, somatostatin; LTT SST-28, Leu⁸-D-Trp²²-Tyr²⁵ SST-28; fluo-SST, α -fluoresceinyl-[D-Trp⁸] SST-14; SSTR, somatostatin receptor; wt hSSTR5, wild type human somatostatin receptor type 5; GPCR, G protein-coupled receptor; TM, transmembrane domain; C-tail, cytoplasmic carboxyl-terminal segment; PCR, polymerase chain reaction; CHO, Chinese hamster ovary; GTP γ S, guanosine 5'-O-(thiotriphosphate).

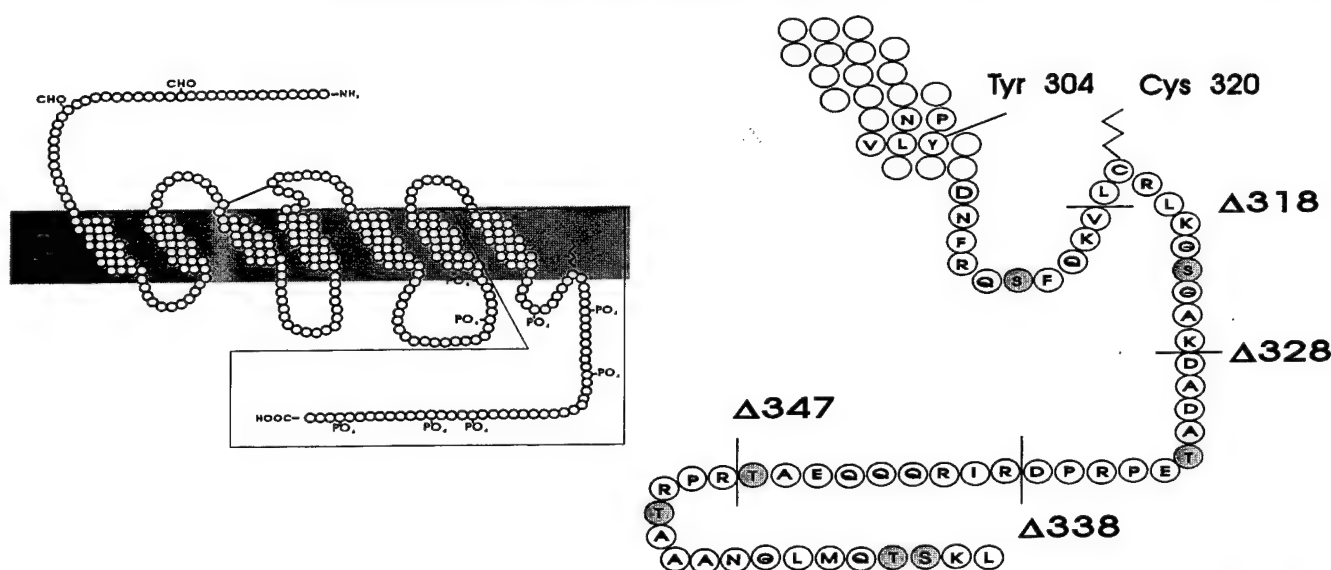


FIG. 1. Schematic depiction of the putative membrane topology of hSSTR5 (363 residues, *left panel*) and the C-tail (*right panel*) amplified to show the structure of the six mutant receptors that were constructed. Stop codons were introduced at residues 318, 328, 338, and 347 to create truncated receptors with variable length C-tail ($\Delta 318$, $\Delta 328$, $\Delta 338$, and $\Delta 347$). The Cys³²⁰ residue, a putative palmitoylation site, was mutated to Ala, and Tyr³⁰⁴ at the VIIth TM-C tail junction, which is part of a NPX_nY-type internalization motif, was mutated to Ala. Serine and threonine residues in the C-tail, which could serve as potential sites for phosphorylation, are shown as shaded circles. Additional phosphorylation sites in the third intracellular loop are also marked in the *left hand panel* (PO₄).

Very little is currently known about the molecular determinants of the desensitization and internalization responses of the SSTR family. For other GPCRs, the presence in the C-tail of Ser and Thr phosphorylation sites as well as Tyr internalization signals is critically important in these processes (6, 19). In the present study we have characterized by mutagenesis the structural domains in the C-tail of hSSTR5 necessary for agonist-dependent desensitization and internalization. We show that the C-tail of hSSTR5 is critical for internalization, receptor coupling to adenylyl cyclase, and acute desensitization responses. Although internalization and signaling both require the C-tail, they are independent functions of the receptor, which appear to be residue-specific in the case of internalization, or dependent on the length of the C-tail for coupling to adenylyl cyclase.

EXPERIMENTAL PROCEDURES

Materials—SST-28 and Leu⁸-D-Trp²²-Tyr²⁵ SST-28 (LTT SST-28) were from Bachem (Marina Del Rey, CA). The fluorescent SST ligand, α -fluoresceinyl-[D-Trp⁶] SST-14 (fluo-SST) was from Advanced Bioconcept, Montreal, Quebec. Phenylmethylsulfonyl fluoride, bacitracin, and GTP γ S were from Sigma. Pertussis toxin was from List Biological Laboratories. Ham's F-12 medium, fetal bovine serum, and G418 were from Life Technologies, Inc. Carrier-free Na¹²⁵I was obtained from Amersham Pharmacia Biotech. Rhodamine-conjugated goat antirabbit IgG was from Jackson ImmunoResearch Labs (West Grove, PA). Cyclic AMP radioimmunoassay kits were obtained from Diagnostic Products Corp. (Los Angeles, CA). All other reagents were of analytical grade and purchased from various suppliers.

Construction of Wild Type Cassette *sstr5* cDNA and Mutant *sstr5* cDNAs—A hSSTR5 cassette gene consisting of five cDNA fragments corresponding to consecutive segments of hSSTR5 was created as described previously by introducing silent mutations to generate unique restriction sites to facilitate the manipulation of the sequence as discrete restriction fragments (20). Using this construct, a series of point mutations in the C-tail of hSSTR5 were created to investigate the role of the length and of specific residues in the signaling, desensitization, and internalization properties of the receptor (Fig. 1). The wt hSSTR5 cytoplasmic tail (C-tail) contains 55 amino acid residues with 7 serine and threonine residues that could serve as putative phosphorylation sites. Stop codons were introduced at positions 318, 328, 338, and 347 to produce truncated receptors with variable length C-tail. The $\Delta 318$ truncation contains only 10 amino acid residues, with one serine residue at position 314. The $\Delta 328$ contains 20 amino acid residues in the C-tail and

incorporates the cAMP-dependent protein kinase phosphorylation site at Ser³²⁵. The $\Delta 338$ truncation contains 30 amino acid residues in the C-tail. The $\Delta 347$ mutant contains 39 amino acid residues and includes the ³⁴²QQQEAT³⁴⁷ motif, a putative G protein receptor kinase phosphorylation site. A palmitoylation site on a conserved Cys residue present in the C-tail of many GPCRs has been shown to be important for receptor sequestration. Such a site is present on Cys³²⁰ of hSSTR5 and was mutated to Ala. The Tyr residue in the NPX_nY motif located at the junction of the VIIth transmembrane (TM) helix and the C-tail acts as an internalization signal for a number of G protein-coupled receptors. This motif exists in hSSTR5 as NPVLY and was mutated at the Tyr³⁰⁴ position to Ala. Desired mutations were introduced into the *MluI-EcoRI* fragment of the cassette construct (20). Point mutations were created using the PCR overlap extension technique; for the C-tail-truncated mutants, oligonucleotide primers were used that contain an appropriately placed stop codon (20). Mutated DNA fragments were used to replace the corresponding wild type restriction fragment in the cassette construct in the expression vector pTEJ8. The structure of the cassette construct and the mutated cDNAs was confirmed by sequence analysis (University Core DNA Service, University of Calgary, Calgary, Alberta, Canada). CHO-K1 cells were transfected with cDNAs for wild type or mutant receptors by the Lipofectin method, and stable G418-resistant nonclonally selected cells were prepared for study.

Binding Assays—CHO-K1 cells expressing wild type and mutant hSSTR5 were cultured to ~70% confluency in D-75 flasks in Ham's F-12 medium containing 10% fetal calf serum and 700 μ g/ml G418. The cells were washed and pelleted by centrifugation, and membranes were prepared by homogenization. Binding studies were carried out for 30 min at 37 °C with 20–40 μ g of membrane protein and ¹²⁵I-LTT SST-28 radioligand as described previously (13, 20). To determine G protein coupling of the expressed receptors, the effect of treatment with 10⁻⁴ M GTP γ S for 30 min on ¹²⁵I-LTT SST-28 binding to membranes from cells expressing wild type and mutant SSTRs was evaluated. In addition, binding was analyzed after pretreatment of membranes with pertussis toxin (100 ng/ml) for 2 h at 37 °C to determine pertussis toxin sensitivity of the receptor-bound G proteins.

Receptor Coupling to Adenylyl Cyclase—Transfected cells were plated in Falcon 6-well dishes (2 \times 10⁵ cells/well) and used two days later at ~70% confluency. Receptor coupling to adenylyl cyclase was investigated by measuring the dose-dependent inhibitory effects of SST-28 on forskolin-stimulated cAMP accumulation. Cells were exposed to 1 μ M forskolin with or without SST-28 (10⁻⁶–10⁻¹⁰ M) for 30 min at 37 °C, scraped in 1 ml of ice-cold 0.1 N HCl, and assayed for cAMP by radioimmunoassay. To study agonist-dependent desensitization of adenylyl cyclase response, cells were preincubated for 1 h at 37 °C in binding buffer with or without 100 nM SST-28. The cells were

then washed twice with cold binding buffer to remove unbound SST-28. Receptor-bound SST-28 was then stripped by incubation for 10 min at 37 °C in Hanks' buffered saline acidified to pH 5.0 with 20 mM sodium acetate (acid wash). The cells were washed twice and analyzed along with control cells for receptor coupling to adenylyl cyclase.

Internalization Experiments—Cultured CHO-K1 cells expressing wild type and mutant SSTRs were incubated overnight at 4 °C in binding buffer with 125 I-LTT SST-28 (200,000 cpm) with or without 100 nM SST-28 (15). Cells were washed three times with ice-cold HEPES binding buffer containing 5% Ficoll to remove unbound ligand and then warmed to 37 °C for different times (0, 15, 30, and 60 min) to initiate internalization. Surface-bound radioligand was removed by treatment for 10 min with acid wash solution. Internalized radioligand was measured as acid-resistant counts in 0.1 N NaOH extracts of acid-washed cells. Internalization of receptor-bound ligand was also assessed using fluo-SST. This peptide binds with high affinity (IC_{50} 4.9 nM) to SSTRs in rat cortical homogenate and has been reported to undergo agonist-dependent internalization in COS-7 cells transfected with SSTR2A (16). CHO-K1 cells expressing wild type and mutant hSSTR5 receptors were grown to ~70% confluency. On the day of the experiment, the culture medium was removed, and the cells were washed and incubated in 1 ml of binding buffer containing 10 nM fluo-SST at 4 °C for 1–2 h. To examine internalization, sister cultures were incubated with fluo-SST under identical conditions for 45 min at 37 °C. At the end of each incubation, media were removed, and the cells were washed, mounted in immunofluor, and viewed under a Zeiss LSM 410 inverted confocal microscope (5, 20). All images were archived on a Bernoulli multidisc and printed on Kodak XLS8300 high resolution printer.

Immunocytochemistry—Confocal immunofluorescence studies were performed to confirm cell surface expression of the Tyr³⁰⁴ → Ala mutant in live unfixed transfected cells using a rabbit polyclonal antibody directed against the amino-terminal 4–11 peptide sequence of hSSTR5 as described previously (5, 20).

RESULTS

Binding Affinity—Table I shows the results of membrane binding analyses of CHO-K1 cells transfected with wt hSSTR5 cassette cDNA and the hSSTR5 C-tail mutant cDNAs. By saturation analysis, wt hSSTR5 displayed high affinity binding with a K_d of 0.31 nM and a B_{max} of 162 ± 42 fmol/mg of protein. The $\Delta 328$, $\Delta 338$, and the $\Delta 347$ C-tail truncation mutants as

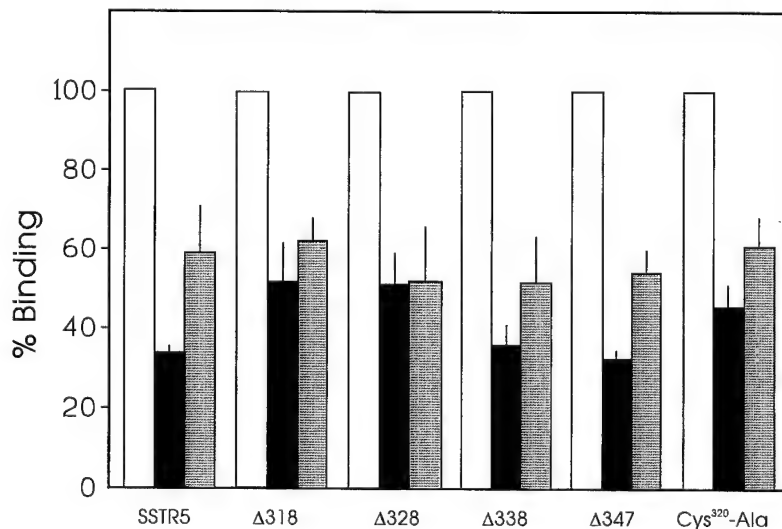
TABLE I
Binding characteristics of wild type and mutant hSSTR5

Receptor	K_d	B_{max}
	nM	fmol/mg of protein
wt hSSTR5	0.31 ± 0.01	162 ± 42
$\Delta 318$ hSSTR5	0.89 ± 0.07	262 ± 71
$\Delta 328$ hSSTR5	0.47 ± 0.16	298 ± 99
$\Delta 338$ hSSTR5	0.41 ± 0.18	247 ± 40
$\Delta 347$ hSSTR5	0.21 ± 0.07	352 ± 96
$\Delta Cys^{320} \rightarrow Ala$ hSSTR5	0.40 ± 0.12	179 ± 51

well as the Cys³²⁰ → Ala mutants displayed binding affinities of 0.21–0.47 nM, comparable with that of wt hSSTR5. The $\Delta 318$ truncation mutant also displayed high affinity ligand binding (K_d 0.89 nM), which, however, was 3-fold lower than that of the wild type receptor. B_{max} of the four C-tail deletion mutants ranged between 247 and 352 fmol/mg of protein, 1.5–2-fold higher than that of wt hSSTR5; the B_{max} of the Cys³²⁰ → Ala mutant (179 ± 51 fmol/mg of protein) was comparable with that of the wild type receptor. No specific binding was observed in membranes prepared from cells transfected with the Tyr³⁰⁴ → Ala mutant. The mutant protein, however, was expressed on the cell membrane as determined by immunocytochemistry using live unfixed cells. Using the hSSTR5 primary antibody, nonpermeabilized CHO-K1 cells expressing wt hSSTR5 showed rhodamine immunofluorescence localized to the cell surface (not shown). Cells transfected with the Tyr³⁰⁴ → Ala mutant also exhibited surface immunofluorescence with this antibody, indicating that the mutant receptor was properly targeted to the plasma membrane. No specific immunofluorescence was detected in nontransfected CHO-K1 cells or in transfected cells probed with preimmune serum or antigen-absorbed primary antibody. To exclude any breach of the plasma membrane and labeling of cytosolic structures beneath the plasmalemma during incubation with primary antibody, parallel immunocytochemistry was performed with antibody to vimentin, an intracellular protein. Under these conditions, vimentin immunoreactivity was detected only in cells permeabilized with 0.2% Triton X-100 but not in intact CHO-K1 cells. These findings suggest that the loss of binding of the Tyr³⁰⁴ → Ala mutant is not due to a failure of the mutant receptor to be localized to the plasma membrane but rather reflects an important structural requirement of the Tyr residue in maintaining a high affinity ligand binding conformation. Loss of agonist binding by this mutant precluded further analysis of the role of the Tyr³⁰⁴ residue as an internalization signal.

G Protein Coupling—To determine whether the hSSTR5 C-tail mutants were coupled to G proteins, the effect of 10^{-4} M GTP γ S on membrane binding was assessed in cells expressing wild type and mutant hSSTR5 receptors (Fig. 2). Pretreatment with GTP γ S reduced 125 I-LTT SST-28 binding of wt hSSTR5 to $67 \pm 2\%$ that of control. The four C-tail truncation mutants as well as the Cys³²⁰ → Ala mutant also displayed significant loss of radioligand binding of 50–70% that of control, comparable with that of the wild type receptor. This suggests that the mutant receptors are capable of associating with G proteins. Pretreatment of membranes with pertussis toxin also led to a significant 40–50% reduction of 125 I-LTT SST-28 binding to the

FIG. 2. Effect of pretreatment with GTP γ S (10^{-4} M) and pertussis toxin (100 ng/ml) on 125 I-LTT SST-28 binding to membranes prepared from cells expressing wt hSSTR5 and mutant hSSTR5 receptors. Total binding for the different receptors ranged between 7000–8000 cpm; nonspecific binding was in the range of 2400–3600 cpm. Both GTP γ S and pertussis toxin reduced radioligand binding in wild type and in all the mutant receptors (mean \pm S.E. of three separate experiments). Open bars, control; black bars, GTP γ S; shaded bars, PTX, pertussis toxin.



wild type and the C-tail mutant SSTRs, suggesting that the mutant receptors associate with pertussis toxin-sensitive G proteins.

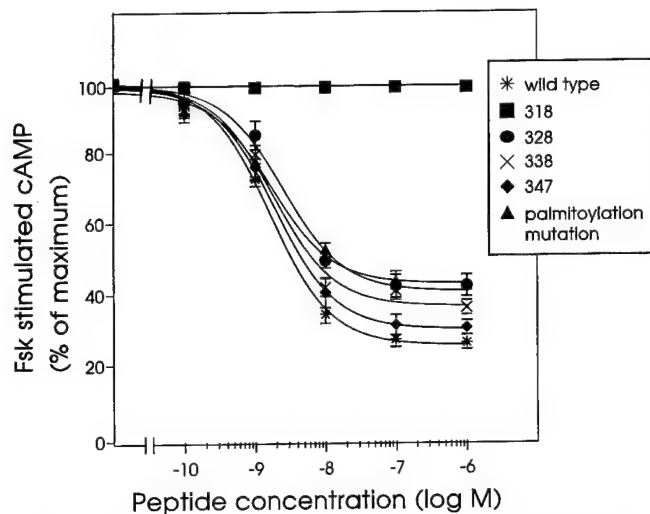


FIG. 3. Coupling of wild type and C-tail mutant hSSTR5 receptors to adenylyl cyclase. Compared with the wild type receptor, which showed a maximum 70% inhibition by SST-28 of forskolin (Fsk)-stimulated cAMP accumulation, the C-tail deletion mutants displayed a progressive loss of the ability to inhibit forskolin-stimulated cAMP. The coupling efficiency of the Cys³²⁰ → Ala mutant was also attenuated. Forskolin-induced 12–15-fold increase in cAMP levels to 138 ± 28 pmol/ 5×10^5 cells for wt hSSTR5, 134 ± 1.1 for $\Delta 318$, 155 ± 4.3 for $\Delta 328$, 92 ± 3 for $\Delta 338$, 70 ± 1.5 for $\Delta 347$, and 92 ± 2 for Cys³²⁰ → Ala mutants (mean \pm S.E., three complete experiments in triplicate).

Coupling to Adenylyl Cyclase and Desensitization Responses—Fig. 3 depicts the results of coupling of the C-tail mutants to adenylyl cyclase. Basal cAMP level in cells expressing the mutant receptors was comparable with that in cells transfected with wt hSSTR5. Compared with the wild type receptor, which showed a maximum of $70 \pm 6\%$ inhibition by SST-28 of forskolin-stimulated cAMP accumulation, the C-tail deletion mutants displayed a progressive loss of the ability to inhibit forskolin-stimulated cAMP from $69.8 \pm 2\%$ for the $\Delta 347$ mutant to $63 \pm 3.8\%$ for the $\Delta 338$ mutant to $60 \pm 3.1\%$ for the $\Delta 328$ mutant. The Cys³²⁰ → Ala mutant showed only $57 \pm 3.4\%$ maximum inhibition of forskolin-stimulated cAMP; the $\Delta 318$ showed complete loss of coupling to adenylyl cyclase.

To study agonist-dependent desensitization of adenylyl cyclase responses, parallel studies were carried out in sister cultures preincubated with 100 nM SST-28 for 1 h at 37 °C. Surface-bound SST-28 was then removed, and the cells were tested with different concentrations of SST-28 for their ability to inhibit forskolin-stimulated cAMP. Such agonist pretreatment induced a marked loss of the ability of wt hSSTR5 to inhibit forskolin-stimulated cAMP from $70 \pm 6\%$ in control nontreated cells to $21 \pm 5\%$ in treated cells (Fig. 4). The mutant receptors that displayed partial loss of efficiency for adenylyl cyclase coupling also showed variable impairment of their uncoupling responses. The $\Delta 328$ and $\Delta 347$ mutants both retained some ability to uncouple from adenylyl cyclase, although the range of responses for maximum forskolin-stimulated cAMP inhibition before and after agonist pretreatment ($60 \pm 3.1\%$ and $40 \pm 1.2\%$ for $\Delta 328$ mutant; $69.8 \pm 2\%$ and $45.4 \pm 3.3\%$ for $\Delta 347$ mutant) was markedly attenuated compared with the native receptor. The $\Delta 338$ mutant displayed virtually complete

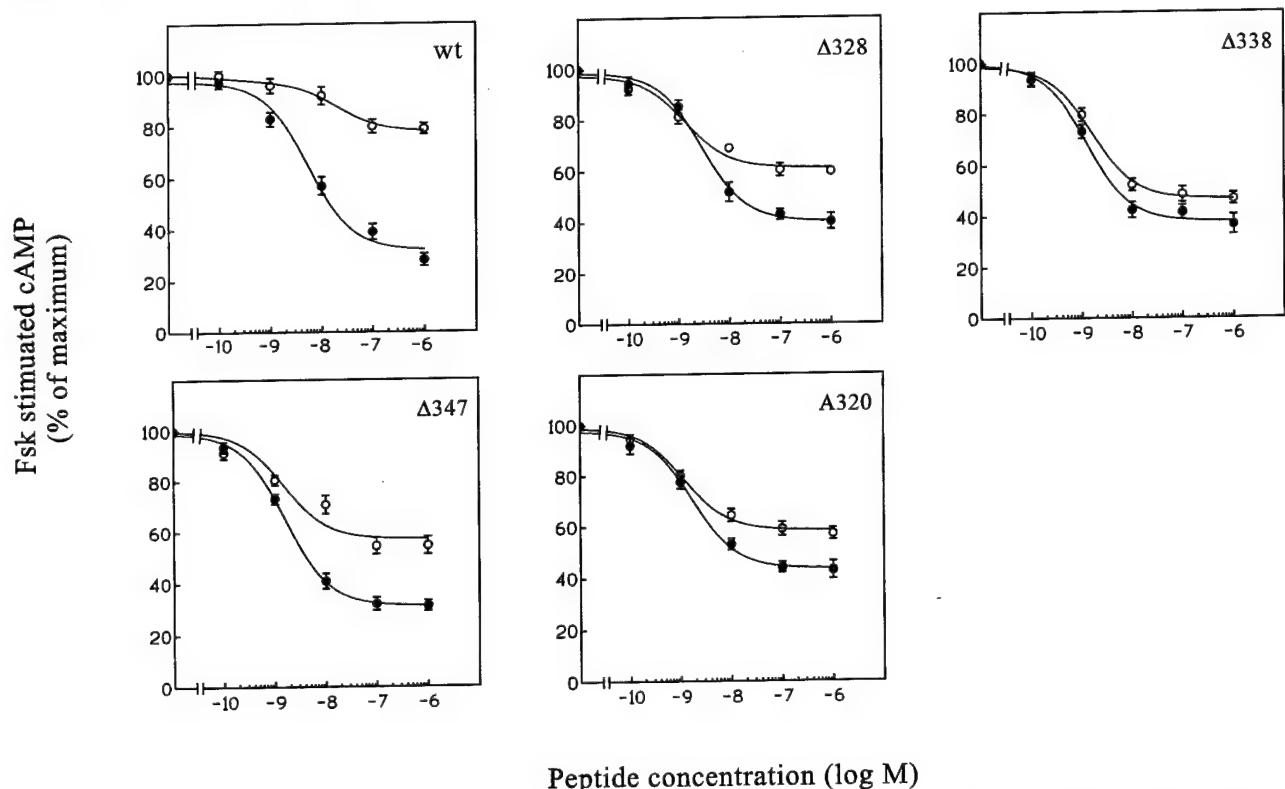


FIG. 4. Agonist-dependent desensitization of the inhibition of adenylyl cyclase by wild type and C-tail mutant hSSTR5 receptors. CHO-K1 cells expressing the receptors was preincubated with 100 nM SST-28 for 1 h at 37 °C. Surface-bound SST-28 was then removed, and the cells were tested with different concentrations of SST-28 for their ability to inhibit forskolin (Fsk)-stimulated cAMP. Such agonist pretreatment induced marked desensitization of the ability of wt hSSTR5 to inhibit adenylyl cyclase. The mutant receptors displayed variable loss of efficiency for adenylyl cyclase coupling, which in each case was only partial compared with that of wt hSSTR5. Maximum forskolin-stimulated cAMP levels (pmol/ 5×10^5 cells) after SST-28 pretreatment, were 109 ± 2.6 (wt hSSTR5), 88 ± 1.9 ($\Delta 328$), 93 ± 2 ($\Delta 338$), 74 ± 1.7 ($\Delta 347$), 78 ± 1.5 ($\Delta 320$) (mean \pm S.E. of three experiments in triplicate). ●, control; ○, pretreatment with 1×10^{-7} SST-28.

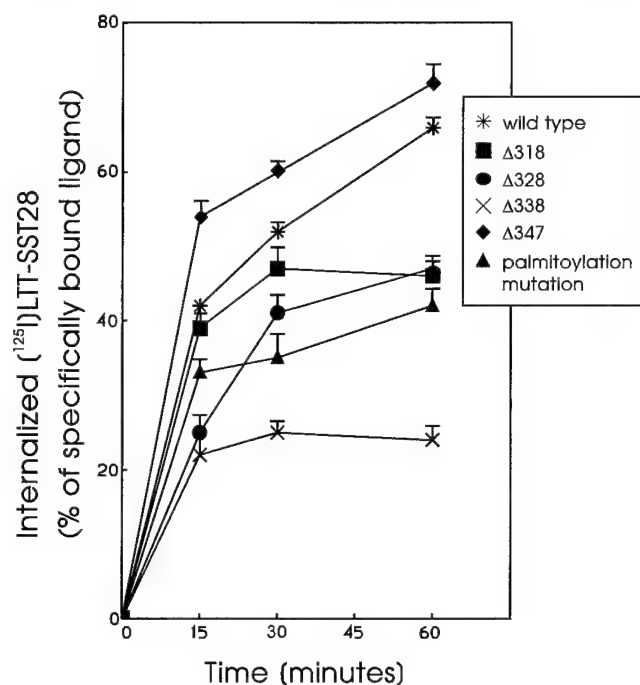


FIG. 5. Time-dependent internalization of ^{125}I -LTT SST-28 specifically bound to plasma membrane hSSTR5 and mutant hSSTR5 receptors stably expressed in CHO-K1 cells. Surface-bound radioligand was removed by acid wash, and internalized radioligand was measured as acid-resistant counts in 0.1 N NaOH extracts of acid-washed cells and expressed as a percent of specifically bound surface radioligand. Total binding for the various receptors ranged between 8200–11,000 cpm, and nonspecific binding ranged between 2600–3850 cpm (mean \pm S.E. of three independent experiments).

loss of the ability to uncouple from adenylyl cyclase with agonist preexposure ($63 \pm 4\%$ and $53 \pm 2.3\%$ maximum forskolin-stimulated cAMP inhibition). Like the $\Delta 328$ and $\Delta 347$ mutants, the $\text{Cys}^{320} \rightarrow \text{Ala}$ mutant retained some ability to uncouple from adenylyl cyclase inhibition with SST-28 pretreatment but with a blunted response ($57 \pm 3.4\%$ and $43 \pm 2.4\%$ maximum forskolin-stimulated cAMP inhibition) compared with the wild type receptor.

Internalization of Receptor Bound ^{125}I -LTT SST-28—Internalization of ^{125}I -LTT SST-28 ligand was studied in stably transfected CHO-K1 cells initially treated with ligand for 12 h at 4°C to allow for equilibrium binding but to limit internalization (Fig. 5). Switching from 4 to 37°C led to a rapid time-dependent internalization of radioligand that, in the case of wt hSSTR5, reached a maximum of $66 \pm 2\%$ at 60 min (Fig. 5). Truncation of the C-tail to 318 and 328 residues produced moderate decreases in receptor internalization to 46% at 60 min. Truncation to 338 residues led to a dramatic loss of radioligand internalization of only $23 \pm 3\%$ at 60 min. In contrast, truncation to 347 residues improved the efficiency of internalization even more than that of the wild type receptor ($72 \pm 3\%$ compared with 66%). This suggests the presence of a positive internalization signal between residues 338 and 347 and a negative signal between 347 and 364 residues and 328 and 338 residues. Mutation of the Cys^{320} palmitoylation site reduced ligand internalization to $42 \pm 3\%$ at 1 h. The extent of the loss of internalization of this mutant was comparable with that of the $\Delta 318$ mutant, which also lacked the Cys^{320} residue and suggests an important function of the palmitoylation anchor in producing the impaired internalization of both these mutant receptors.

The pattern of internalization obtained by radioligand binding was confirmed directly with fluo-SST-14 ligand, whose sur-

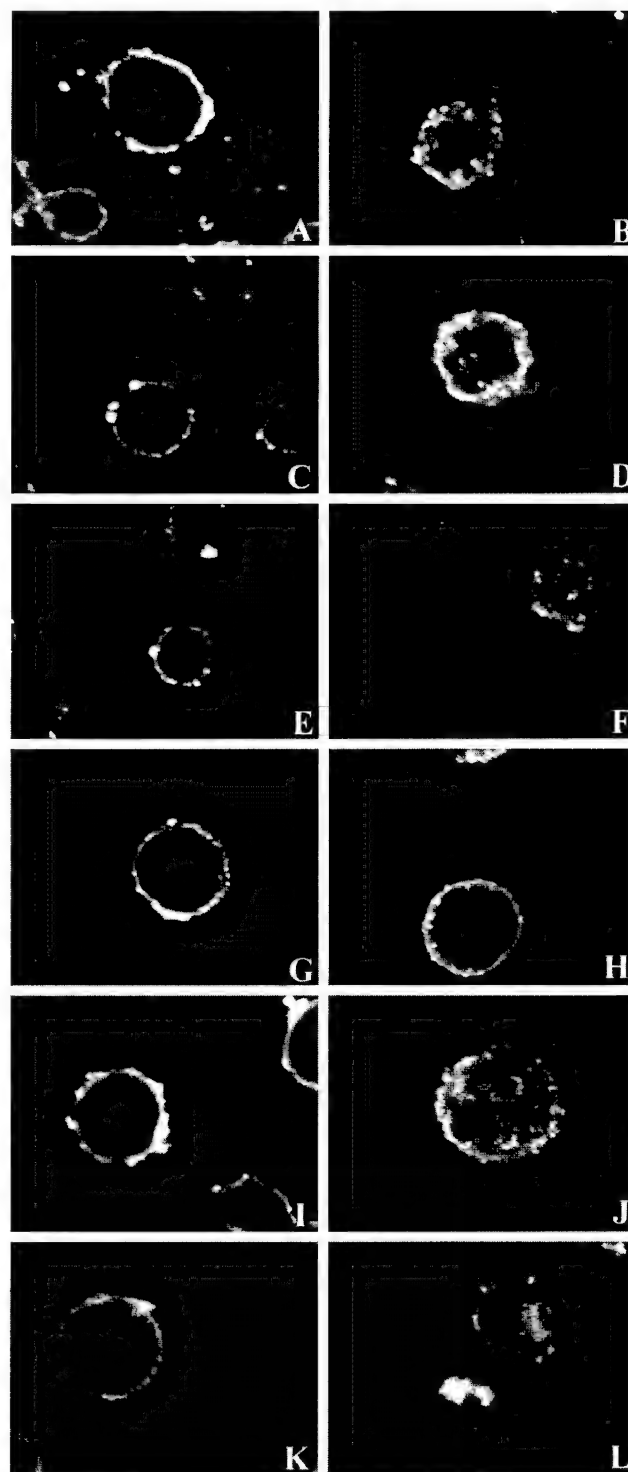


FIG. 6. Confocal fluorescent images of CHO-K1 cells expressing wild type and mutant hSSTR5 incubated with a fluorescent SST-14 ligand (fluo-SST) at either 4°C (left hand panels) or 37°C (right hand panels). Cells expressing wild type or mutant hSSTR5 displayed specific fluorescent labeling at 4°C , which was localized almost exclusively to the cell surface. Incubation at 37°C resulted in variable endocytosis of the fluorescent ligand to intracellular vesicular structures. Panels A and B, wild type hSSTR5; panels C and D, $\Delta 320$ hSSTR5 mutant; panels E and F, $\Delta 328$ hSSTR5 mutant; panels G and H, $\Delta 338$ hSSTR5 mutant; panels I and J, $\Delta 347$ hSSTR5 mutant; panels K and L, $\text{Cys}^{320} \rightarrow \text{Ala}$ mutant ($\times 250$).

face binding and endocytosis in transfected CHO-K1 cells was traced by confocal microscopy. Fig. 6 shows confocal fluorescent images of cells incubated with fluo-SST at either 4°C (left hand panels) to inhibit internalization or at 37°C (right hand panels)

to promote internalization. CHO-K1 cells expressing either the wild type or mutant hSSTRs displayed specific fluorescent labeling at 4 °C that was localized almost exclusively to the cell surface (*panel A*). Incubation of wt hSSTR5 with fluo-SST at 37 °C resulted in the transfer of the fluorescent ligand to intracellular vesicular structures (*panel B*). Temperature-dependent internalization of the fluorescent ligand was also observed for the $\Delta 320$ (*panels C and D*) and $\Delta 328$ (*panels E and F*) mutants, although the amount of intracellular labeling was reduced compared with the wild type receptor. In the case of the $\Delta 338$ mutant, there was minimal fluorescent labeling of a few intracellular vesicles directly beneath the plasma membrane. Overall, however, this mutant displayed marked inhibition of the ability to endocytose the surface-bound fluorescent ligand (*panels G and H*). In contrast, the $\Delta 347$ mutant exhibited pronounced internalization of fluo-SST-28 at 37 °C, with labeling distributed diffusely throughout the cytoplasm (*panel J*). Finally, the Cys³²⁰ → Ala mutant displayed the ability to internalize fluo-SST, but the overall efficiency of internalization was impaired compared with the wild type receptor (*panel L*).

DISCUSSION

Role of C-Tail in Ligand Binding and in Coupling to G Protein and Adenylyl Cyclase—Progressive deletion of the C-tail of hSSTR5 had no effect on high affinity ligand binding, indicating that the C-tail, like that of other GPCRs, does not influence receptor targeting or binding conformation (21). Mutation of the Tyr³⁰⁴ residue, however, produced a receptor protein that was correctly targeted to the plasma membrane but which showed complete loss of binding, suggesting a critical role of Tyr³⁰⁴ in ligand binding through either direct hydrophobic interaction with SST ligand or through an allosteric change in the receptor binding conformation. The C-tail as well as the second and third intracellular loops of several GPCRs have been implicated in G protein interaction (6, 22). Radioligand binding by all of the C-tail mutants of hSSTR5 was inhibited to the same degree as the wild type receptor by GTP γ S and pertussis toxin, indicating that the mutant receptors are capable of associating with pertussis toxin-sensitive G proteins and that the C-tail of hSSTR5 is not required for this interaction. Interestingly, despite the ability to associate with G proteins, the four C-tail deletion mutants as well as the Cys³²⁰ → Ala mutant displayed reduced efficiency for adenylyl cyclase coupling. This was most pronounced in the case of the $\Delta 318$ mutant, which showed a complete loss of the ability to inhibit adenylyl cyclase. Whether this mutant can signal through other effector pathways remains to be seen. There are two other examples of dissociated G protein and effector coupling by C-tail mutants of GPCRs. The first is the C-tail-truncated postaglandin EP3 receptor, which retains the ability to associate with G₁₂ but which shows no forskolin-induced inhibition of cAMP accumulation, identical to the $\Delta 318$ hSSTR5 mutant (23). The second is an Ala → Glu substitution in the distal third intracellular loop of the gastrin-releasing peptide receptor, which abrogates phospholipase C coupling while retaining full efficacy for G protein interaction (24). In contrast to the C-tail of hSSTR5, which is required for inhibitory regulation of adenylyl cyclase, the naturally occurring SSTR2B splice variant with a shorter C-tail length than SSTR2A is more efficiently coupled to adenylyl cyclase (25).

Role of C-Tail in Mediating Acute Desensitization—We found that hSSTR5 stably expressed in CHO-K1 cells was desensitized by agonist pretreatment. Phosphorylation of the rat SSTR2A receptor primarily on serine residues and of the rat SSTR3 receptor on both serine and threonine residues in the C-tail has been reported to be crucial for desensitization and

internalization of these two subtypes (17, 18). hSSTR5 features three serine (Ser³¹⁴, Ser³²⁵, Ser³⁶¹) and four threonine (Thr³³³, Thr³⁴⁷, Thr³⁵¹, Thr³⁶⁰) residues in the C-tail (Fig. 1). The Ser³²⁵ and Thr³⁶⁰ sites fit the consensus sequence for phosphorylation by protein kinase A and protein kinase C, respectively, and the Thr³⁴⁷ position qualifies as a putative G protein-coupled receptor kinase phosphorylation site (26). The third intracellular loop of this receptor displays three additional sites for phosphorylation by second messenger-activated kinases. The ability of the $\Delta 347$ mutant to be desensitized by agonist to the same degree as the wild type receptor suggests that the Thr³⁵¹, Thr³⁶⁰, and Ser³⁶¹ sites in the distal C-tail play a minimal role in the desensitization response. In contrast, the resistance of the $\Delta 338$ mutant to desensitization suggests an important role of Thr³⁴⁷ in the putative G protein receptor kinase phosphorylation site. This role, however, cannot be absolute since the $\Delta 328$ mutant, which also lacks the Thr³⁴⁷ residue, underwent significant desensitization. A conserved cysteine residue 11–12 amino acids downstream from the 7th TM is found in the C-tail of most GPCRs and serves as a palmitoylation membrane anchor for a fourth intracellular loop. Palmitoylation induces differential changes in G protein coupling, desensitization, intracellular trafficking, and internalization of different GPCRs (27, 28). In the case of hSSTR5, the Cys³²⁰ → Ala mutant displayed poor ability to uncouple from adenylyl cyclase, indicating an important role of C-tail palmitoylation in the desensitization response of this receptor. Overall, these studies suggest that the C-tail plays a prominent role in agonist-induced desensitization of hSSTR5 through both specific motifs, which may serve as sites for phosphorylation, as well as through conformational changes in the C-tail of the agonist-occupied receptor, which may determine its substrate specificity for phosphorylation.

Role of C-Tail in Mediating Receptor Internalization—The C-tail segment of hSSTR5 is not only critical for receptor coupling to adenylyl cyclase and in mediating acute desensitization responses but also plays an important role in regulating agonist-induced receptor internalization. This is in agreement with previous studies that have shown that the C-tail of many other GPCRs, *e.g.* receptors for angiotensin II_{1A} (29), β_2 adrenergic (30), m₂ muscarinic (31), luteinizing hormone/human chorionic gonadotrophin (32), parathyroid hormone (33), thyrotrophin releasing hormone (34), neurotensin (35), and cholecystokinin (36), is also involved in internalization. Our results indicate that mutant receptors with variable length C-tails are differentially internalized. Truncation of the C-tail at positions 318 and 328 attenuated receptor internalization only partially from 66 to 46% at 60 min. This suggests that the C-tail distal to position 318, which contains multiple phosphorylation sites including the putative G protein receptor kinase site on Thr³⁴⁷, although important, is not a critical determinant of endocytosis. Furthermore, the comparable rates of internalization of the $\Delta 328$ mutant, which contains the putative protein kinase A site at Ser³²⁵, and the $\Delta 318$ mutant, which does not, excludes a role of the protein kinase A site in agonist-induced hSSTR5 internalization. Truncation of the C-tail to 338 residues led to a dramatic loss of internalization. This mutant has 10 more residues than $\Delta 328$ that appear to contain potent negative endocytic signals. The $\Delta 347$ deletion mutant internalized slightly more than the wild type receptor, suggesting that the nine-amino acid residue stretch between positions 338 and 347 harbors a positive internalization signal, likely on Thr³⁴⁷ in the putative G protein receptor kinase phosphorylation site. Furthermore, the ability of the $\Delta 347$ mutant to internalize more than the wild type receptor argues for a second negative endocytic signal in the extreme C-tail segment distal to residue 347.

Negative endocytic signals have been postulated in the case of the luteinizing hormone/human chorionic gonadotrophin and parathyroid hormone/parathyroid hormone-related protein receptors (32, 33). The EVQ sequence in the membrane-proximal C-tail, which is highly conserved across members of the parathyroid hormone/secretin receptor family has been identified as a negative endocytic signal for this receptor subclass. Point mutations in the 328–338 and 347–363 segment of hSSTR5 C-tail will help to determine whether there are similar structural motifs in this receptor capable of acting as negative endocytic regulators. The palmitoylation-defective hSSTR5 mutant showed reduced internalization comparable with that reported for the thyrotrophin-releasing hormone (34) and vasopressin V2 (37) receptors but different from the palmitoylation-deficient luteinizing hormone/human chorionic gonadotrophin receptor, which displays enhanced internalization (38). Tyrosine-based internalization signals on NPXY-type motifs are common to many classes of membrane receptors (39). In the case of GPCRs, a conserved NPXXY sequence at the interface between the VIIth TM and the C-tail serves as an endocytic signal for some receptors (19). In other GPCRs such as the gastrin-releasing peptide and the angiotensin II receptors, however, an identical NPXXY motif has no effect on receptor sequestration, arguing against a general role for this sequence (40, 41). This motif is found in all members of the SSTR family, but since its mutation in the case of hSSTR5 abolished high affinity ligand binding, it will be difficult to characterize its function as an endocytic signal.

Relationship Between Receptor Signaling and Internalization—An important question concerning GPCRs is the relationship between receptor signaling and internalization. Although there has been some controversy in the past, many recent studies have suggested that the two events can be readily dissociated (24, 29, 36, 42, 43). For instance, receptor mutations that inhibit G protein coupling or signaling do not prevent endocytosis (24, 29, 36, 42, 43). The addition of second messengers such as phorbol 12-myristate 13-acetate, Ca^{2+} , and cAMP fails to stimulate internalization of mutant thyrotrophin-releasing hormone receptors or antagonist-blocked luteinizing hormone/human chorionic gonadotrophin receptors that cannot activate phospholipase C or adenylyl cyclase (34, 36). A cholecystokinin antagonist has been reported to induce receptor internalization independent of G protein coupling, signaling events, and receptor phosphorylation (36). The human muscarinic receptor subtype 1 has been shown to undergo internalization by interaction with antibody against an epitope tagged to the amino terminus, independent of exogenous ligand or second messenger activation (44). The dissociated effects of the hSSTR5 C-tail mutants on adenylyl cyclase coupling and internalization lend further support to these arguments. For instance, there was no correlation between the progressive loss of the ability of the C-tail deletion mutants of hSSTR5 to inhibit adenylyl cyclase and receptor internalization, which was both inhibited or accelerated. In particular, the $\Delta 318$ mutant, which was rendered inert with respect to its ability to inhibit adenylyl cyclase, nonetheless exhibited reduced internalization. Although activation of second messenger systems may exert a secondary influence on the internalization process, the collective findings from all of these studies suggest that internalization is an intrinsic property of most receptors, dependent on specific conformational changes rather than receptor signaling capability.

In conclusion, we have shown that the C-tail of hSSTR5 serves a multifunctional purpose in mediating effector coupling, agonist-dependent desensitization, and internalization. Receptor coupling to adenylyl cyclase is dependent on the

length of the C-tail, whereas desensitization and internalization require specific structural domains. Since SSTR5 is the principal SSTR subtype in tissues such as the pituitary, elucidation of the molecular signals underlying these processes will provide a better understanding of the function of this receptor during prolonged agonist treatment normally and in disease such as pituitary tumors.

Acknowledgments—We thank Dr. D. Laird for the vimentin antibody and M. Correia for secretarial help.

REFERENCES

- Reichlin, S. (1983) *N. Engl. J. Med.* **309**, 1495–1501 and 1556–1563
- Patel, Y. C., and Srikant, C. B. (1997) *Trends Endocrinol. Metab.* **8**, 398–405
- Bruno, J. F., and Berelowitz, M. (1994) *Biochem. Biophys. Res. Commun.* **202**, 1738–1743
- Day, R., Dong, W., Panetta, R., Kraicer, J., Greenwood, M. T., and Patel, Y. C. (1995) *Endocrinology* **136**, 5232–5235
- Kumar, U., Laird, D., Srikant, C. B., Escher, E., and Patel, Y. C. (1997) *Endocrinology* **138**, 4473–4476
- Dohlman, H. G., Thörner, J., Caron, M. G., and Lefkowitz, R. J. (1991) *Annu. Rev. Biochem.* **60**, 653–658
- Lamberts, S. W. J., Van Der Lely, A. J., and de Herder, W. W. (1996) *N. Engl. J. Med.* **334**, 246–254
- Morel, G., Leroux, P., and Pelletier, G. (1985) *Endocrinology* **116**, 1615–1620
- Amherdt, M., Patel, Y. C., and Orci, L. (1989) *J. Clin. Invest.* **84**, 412–417
- Hofland, L. J., Van Koetsveld, P. M., Waaijers, M., Zuyderwijk, J., Breeman, W. A. P., and Lamberts, S. W. J. (1995) *Endocrinology* **136**, 3698–3706
- Sullivan, S. J., and Schonbrunn, A. (1988) *Endocrinology* **122**, 1137–1145
- Presky, D. H., and Schonbrunn, A. (1988) *J. Biol. Chem.* **263**, 714–721
- Patel, Y. C., Panetta, R., Escher, E., Greenwood, M. T., and Srikant, C. B. (1994) *J. Biol. Chem.* **269**, 1506–1509
- Xu, Y., Berelowitz, M., and Bruno, J. F. (1995) *Endocrinology* **136**, 5070–5075
- Hukovic, N., Panetta, R., Kumar, U., and Patel, Y. C. (1996) *Endocrinology* **137**, 4046–4049
- Nouel, D., Gaudriault, G., Houle, M., Reisine, T., Vincent, J.-P., Mazella, J., and Beaudet, A. (1997) *Endocrinology* **138**, 296–306
- Hipkin, R. W., Friedman, J., Clark, R. B., Eppler, C. M., and Schonbrunn, A. (1997) *J. Biol. Chem.* **272**, 13869–13876
- Roth, A., Kreienkamp, H. J., Meyerhof, W., and Richter, D. (1997) *J. Biol. Chem.* **272**, 23769–23774
- Barak, L. S., Tiberi, M., Freedman, N. J., Kwatra, M. M., Lefkowitz, R. J., and Caron, M. G. (1994) *J. Biol. Chem.* **269**, 2790–2795
- Greenwood, M. T., Hukovic, N., Kumar, U., Panetta, R., Hjorth, S. A., Srikant, C. B., and Patel, Y. C. (1997) *Mol. Pharmacol.* **52**, 807–814
- Sugimoto, Y., Negishi, M., Hayashi, Y., Namba, T., Honda, A., Watane, A., Hirata, M., Narumiya, S., and Ichikawa, A. (1993) *J. Biol. Chem.* **268**, 2712–2718
- Baldwin, J. M. (1994) *Cell Biol.* **6**, 180–190
- Irie, A., Sugimoto, Y., Namba, T., Asano, T., Ichikawa, A., and Negishi, M. (1994) *Eur. J. Biochem.* **224**, 161–166
- Benya, R. V., Akeson, M., Mrozinski, J., Jensen, R. T., and Battey, J. F. (1994) *Mol. Pharmacol.* **46**, 495–501
- Vanetti, M., Vogt, G., and Hollt, V. (1993) *FEBS Lett* **331**, 260–266
- Premont, R. T., Inglese, J., and Lefkowitz, R. J. (1995) *FASEB J.* **9**, 175–182
- Bouvier, M., Loisel, T. P., and Hebert, T. (1995) *Biochem. Soc. Trans.* **23**, 577–581
- Tanaka, K., Nagayama, Y., Nishihara, E., Namba, H., Yamashita, S., and Niwa, M. (1998) *Endocrinology* **139**, 803–876
- Thomas, W. G., Thekkumkara, T. J., Motel, T. J., and Baker, K. M. (1995) *J. Biol. Chem.* **270**, 207–213
- Jockers, R., Da Silva, A., Strosberg, A. D., Bouvier, M., and Marullo, S. (1996) *J. Biol. Chem.* **271**, 9355–9362
- Goldman, P. S., and Nathanson, N. M. (1994) *J. Biol. Chem.* **269**, 15640–15645
- Rodriguez, M. C., Xie, Y.-B., Wang, H., Collison, K., and Segaloff, D. L. (1992) *Mol. Endocrinol.* **6**, 327–336
- Huang, Z., Chen, Y., and Nissenson, R. A. (1995) *J. Biol. Chem.* **270**, 151–156
- Nussenzweig, D. R., Heinfinkel, M., and Gershengorn, M. C. (1993) *J. Biol. Chem.* **268**, 2389–2392
- Chabry, J., Botto, J. M., Nouel, D., Beaudet, A., Vincent, J. P., and Mazella, J. (1995) *J. Biol. Chem.* **270**, 2439–2442
- Roettger, B. F., Ghanekar, D., Rao, R., Toledo, C., Yingling, J., Pinon, D., and Miller, L. J. (1997) *Mol. Pharmacol.* **51**, 357–362
- Schulein, R., Liebenhoff, U., Muller, H., Birnbaumer, M., and Rosenthal, W. (1996) *Biochem. J.* **313**, 611–616
- Kawato, N., and Menon, K. M. J. (1994) *J. Biol. Chem.* **269**, 30651–30658
- Bonifacio, J., Marks, M. S., Ohno, H., and Kirchhausen, T. (1996) *Proc. Assoc. Amer. Phys.* **108**, 285–295
- Slice, L. W., Wong, H. C., Sternini, C., Grady, E. F., Bunnett, N. W., and Walsh, J. H. (1994) *J. Biol. Chem.* **269**, 21755–21761
- Laporte, S. A., Servant, G., Richard, D. E., Escher, E., Guillemette, G., and Leduc, R. (1996) *Mol. Pharmacol.* **49**, 89–95
- Ng, G. Y., Trogadis, J., Stevens, J., Bouvier, M., O'Dowd, B. F., and George, S. R. (1995) *Proc. Natl. Acad. Sci. U. S. A.* **92**, 10157–10161
- Pals-Rylaarsdam, R., Xu, Y., Witt-Enderby, P., Benovic, J. L., and Hosey, M. M. (1995) *J. Biol. Chem.* **270**, 29004–29011
- Tolbert, L. M., and Lamch, J. (1998) *J. Neurochem.* **70**, 113–119

EXTENDED ABSTRACT (SINGLE SPACE).

**EXPRESSION AND ANTIPROLIFERATIVE FUNCTIONS OF SOMATOSTATIN
RECEPTORS IN BREAST CANCER**

**Yogesh C. Patel, Kamal Sharma, Ujendra Kumar, Stelios Grigorakis, Peter
Watson*, and Coimbatore B. Srikant**

**Fraser Laboratories, Departments of Medicine and Neurology and Neurosurgery, Royal
Victoria Hospital and Montreal Neurological Institute, Montreal, Quebec H3A 1A1, and
*Department of Pathology, University of Manitoba, Manitoba, Winnipeg, Canada**

The peptide hormone somatostatin (SST) acts via a family of five G protein coupled SST receptors (SSTRs) to regulate the secretion of hormones, growth factors, and neurotransmitter substances, and to modulate cell growth. SST also exerts significant anti-tumor activity in a number of *in vitro* and *in vivo* mammary cancer models. These effects are mediated both indirectly through inhibition of hormones and growth factors which promote tumor growth as well as directly via SSTRs present on tumor cells to inhibit mitogenic signalling of growth factor receptor kinases leading to growth arrest and induction of apoptosis. These findings have sparked enormous interest in the use of synthetic SST analogs as adjuvant therapy for breast cancer and led to the recent approval of multi-center clinical trials by the NSABP and the NCI Canada to look at the effect of SST alone or in combination with tamoxifen in stage I and stage II breast cancer. The longterm goal of our work is to elucidate the pattern of expression of the five individual SSTR subtypes in breast tumor, to determine which SSTR subtypes and signalling mechanisms mediate the antiproliferative effects of SST, whether the available SST analogs are effective in binding to these antiproliferative SSTR subtypes, and whether the pattern of SSTR expression in tumors can provide an independent prognostic marker. Towards these goals we have made significant progress in two areas since the initiation of the project in September 1996.

Expression of the Five SSTR Subtypes in Human Breast Cancer Tissue

Expression of mRNA for the five SSTR subtypes has been analysed by semiquantitative RT-PCR in 66 primary human ductal NOS breast tumors and in 9 primary tubular/lobular tumors.

LIST UP TO 5 KEYWORDS. TYPE "KEY WORDS:" FOLLOWED BY UP TO FIVE
Keywords: Somatostatin, Receptors, Antiproliferation, Apoptosis, p53.

BEGIN CONTRACT ACKNOWLEDGMENT HERE ON PAGE 1.

This work was supported by the U.S. Army Medical Research and Material Command under DAMD17-96-1-6189.

EXTENSION MUST NOT EXTEND BELOW THIS LINE.

INSERT PAGE NO. IN NONREPRO BLUE IN MIDDLE BOX.

Sample were received as 4x125 mm frozen sections/tumor from the Manitoba Breast Tumor Bank. mRNA for hSSTR1-5 was determined by RT-PCR followed by Southern blots. The relative abundance of SSTR mRNA was calculated as a ratio of the densitometric hybridization signal for SSTRs compared to actin. Adjacent tumor sections were characterized histologically for tumor grade (Nottingham Scale), invasiveness, and ER/PR status). Of the 66 ductal NOS tumors, 93% were positive for at least 1 SSTR subtype. 89% expressed multiple SSTR mRNAs; 32% were positive for all five SSTR mRNAs and 42% were positive for 3 or 4 SSTR mRNAs. hSSTR3 was expressed in 56/66 tumors (85%), hSSTR5 in 55/66 (83%), hSSTR2 in 44/66 (67%), hSSTR4 in 44/66 (67%), and hSSTR1 in 38/66 (58%). The relative amount of SSTR mRNA was highest for SSTR5 (8.3 fold vs actin), followed by SSTR1 (7.4), SSTR2 (7.2), SSTR3 (6.3), and SSTR4 (5.2). No correlation was found between SSTR expression, tumor size, lymph node status, or ER/PR status. However, there was a trend towards lower total SSTR expression in high grade tumors and higher expression in low grade tumors. The small group of tubular/lobular cancers generally expressed lower amounts of SSTR mRNAs, subtypes 4 and 5 being the predominant species. We have developed antipeptide rabbit polyclonal antibodies against the 5 hSSTRs and have begun to analyse a subgroup of tumor samples by immunocytochemistry. Initial results show abundant expression of SSTR proteins in tumor cells as well as in peritumoral structures especially the muscle layers of blood vessels and in immune cells. The presence of SSTR mRNA generally correlates well with receptor protein expression.

SSTR Subtype Selectivity For Antiproliferative Signalling

We have investigated subtype selectivity of SSTRs for cytotoxic (apoptosis) and cytostatic (growth arrest actions) and shown that the cytotoxic action is signalled uniquely via hSSTR3. hSSTR3 signalled apoptosis is associated with induction of wild type p53 (secondary to dephosphorylation dependent conformational change) and of Bax and endonuclease II. By contrast, the other 4 SSTR subtypes signal cell cycle arrest with the following rank order: hSSTR5 > hSSTR2 > hSSTR4 > hSSTR1. These changes are associated with induction of the retinoblastoma protein pRB and the cyclin-dependent kinase inhibitor p21. The subtype selective antiproliferative actions of SSTRs are dependent on pertussis toxin sensitive G proteins and are abolished by orthovanadate, an inhibitor of PTP. The structural and functional determinants which dictate hSSTR subtype selective antiproliferative signalling are currently under investigation. In parallel studies we have examined the nature of antiproliferative signalling by SST analogs in ER⁺ and ER⁻ human breast cancer cell lines and shown that apoptosis is dependent on ER expression. Studies are underway to investigate whether estrogens modulate the expression of SSTRs and whether it is subtype selective for hSSTR3.

TEXT MUST NOT EXTEND BELOW THIS LINE.

INSERT PAGE NO. IN NONREPRO BLUE IN MIDDLE BOX.

